**Forschungszentrum Karlsruhe**
in der Helmholtz-Gemeinschaft

**Wissenschaftliche Berichte**
FZKA 7070

# Humic Substances in Performance Assessment of Nuclear Waste Disposal: Actinide and Iodine Migration in the Far-Field

## Third Technical Progress Report

**G. Buckau**

**Institut für Nukleare Entsorgung**

**April 2005**

Forschungszentrum Karlsruhe

in der Helmholtz-Gemeinschaft

Wissenschaftliche Berichte

FZKA 7070

# Humic Substances in Performance Assessment of Nuclear Waste Disposal: Actinide and Iodine Migration in the Far-Field

Third Technical Progress Report

G. Buckau (Editor)

Institut für Nukleare Entsorgung

Forschungszentrum Karlsruhe GmbH, Karlsruhe
2005

**Impressum der Print-Ausgabe:**

**Als Manuskript gedruckt**


**Forschungszentrum Karlsruhe GmbH**
**Postfach 3640, 76021 Karlsruhe**

**Mitglied der Hermann von Helmholtz-Gemeinschaft**
**Deutscher Forschungszentren (HGF)**

**ISSN 0947-8620**

**urn:nbn:de:0005-070701**

# Foreword

The present report describes progress within the third and final year of the EC-project "Humic Substances in Performance Assessment of Nuclear Waste Disposal: Actinide and Iodine Migration in the Far-Field". The work conducted within the present project builds on a number of previous activities/project supported by the Commission. It finds its continuation within different EC FP 6 instruments and also provides for additional continued cooperation through network structures resulting from the broad cooperation within the project.

Without being a formal requirement of the Commission or co-funding bodies, this report documents results in great technical detail and makes the results available to a broad scientific community. The report contains an executive summary written by the coordinator. More detailed results are given as individual contributions in the form of 12 annexes. Not all results are discussed or referred to in the executive summary report and thus readers with a deeper interest also need to consult the annexes.

The report also reflects the successful integration of a temporary contributor via a Marie-Curie Fellowship (MCFI-2001-01983) (Annex 12). Involvement of this Marie-Curie grantee also successfully contributes to training. A broad European dimension has been achieved by involvement of two new EU member states.

Results of the first two project years of the project have been published in the same form, i.e. as open FZKA reports (FZKA 6800 and FZKA 6969).

**The consortium**

**Partner:**

**1: Forschungszentrum Karlsruhe GmbH (FZK/INE), D (Coordinator)**

**2: Forschungszentrum Rossendorf (FZR-IfR), D**

**3: GSF-National Research Center for Environment and Health (GSF), D**

**4: Commissariat à l'Energie Atomique (CEA-DPC), F**

**5: University of Nantes - Presidence (U-Nantes), F**

**6: University of Manchester (U-Manch), UK**

**7: Technical University of Prague (CTU), Cz**

**8: Fodor Joszef National Center of Public Health, Frederic Joliot-Curie National Research Institute of Radiobiology and Radiohygiene (FJC), HU**

**9: University of Cyprus (UCY), Cy**

- **Temporary reporting contribution by Francis Claret, FZK/INE through EC Marie-Curie Grant**

## Table of contents

# Executive Summary

**G. Buckau**
**(FZK/INE)**

**Content**

**Executive Summary**
**G. Buckau**

## Introduction

The overall objectives were to generate knowledge about the impact of humic substances on the migration of actinides and iodine in the far-field of a nuclear waste repository. In the beginning, focus was rather on the potential enhancement due to humic colloid mediated radionuclide transport. Thereby, sources, inventory, stability and mobility of dissolved humic substances in their colloidal form formed a key topic. Other key topics were the interaction with actinides and iodine, transport studies under near-natural conditions in the laboratory, rationalization of knowledge in models and application to three migration cases for visualization of the overall outcome. Changes relative to the original objectives were given by moving emphasis of natural chemical analogue studies from the question of kinetic exchange constants for different inventories in natural and laboratory systems to the study of anthropogenic actinide contaminants in the Irish Sea. Furthermore, by the involvement of a Marie-Curie grantee, the question of additional sources from the high alkaline natural clay near-field was brought into the project.

The objectives of the project cover (i) generation of relevant scientific-technical results, (ii) visualization of the concerned impact on performance assessment, (iii) provision for knowledge transfer, and (iv) provision of a European dimension and training, especially in view of the EU enlargement during the project implementation period. The present report refers to the third and final project reporting year. For the two foregoing reporting years, please make reference to the preceding Technical Project Reports (FZKA 6800 and 6969, below). General conclusions with respect to the overall outcome are also reported in this third and final technical progress report.

Buckau, G. (Editor) “Humic Substances in Performance Assessment of Nuclear Waste Disposal: Actinide and Iodine Migration in the Far-Field (First Technical Progress Report)”, Report FZKA 6800, Research Center Karlsruhe, 2003, and

Buckau, G. (Editor) “Humic Substances in Performance Assessment of Nuclear Waste Disposal: Actinide and Iodine Migration in the Far-Field (Second Technical Progress Report)”, Report FZKA 6969, Research Center Karlsruhe, 2004.

## 1. Summary of work and key conclusions

The project is finalized and all main objectives have been achieved. During the present third and final reporting period, work has continued on several work packages. Within work package 1, additional investigations have been conducted. These include additional work on experimental methods and testing of electrophoretic mobility for its application to determining the composition of ternary Th(IV) humic acid complexes. Some general observations are made with respect to the formation of different charged Th(IV)-humate species at different pH.

Within work package 2, characterization of humic substances has continued and provided data well beyond the standard level. In the present work period, the thermal stability and spectroscopic characterization of thermal processes have continued. These results provide the basis for thermodynamic complexation studies but may also provide important aspects for the thermal stability of humic material and its precursors in natural systems.

Within work package 3, studies on redox functions and processes with humic substances have continued. Synthetic humic acids with designed properties have been generated and used together with natural humic substances. The reduction of Np(V) to Np(IV) was followed by a number of analytical methods. It was shown that careful selection of analytical methods is required in order to obtain trustworthy results. Three different types of humic wafers (silica wafers with humic acid bound in, presumably covalent form) have been generated and a series of advanced analytical methods have been applied. An intercomparison study between the three humic wafers was conducted for the actinide interaction. Finally, the iodine humic acid interaction was characterized by three advanced analytical methods. Iodine is probably covalently bound to humic acid, the reason for the possible sensitivity of this binding to the electro-spray process still needs to be resolved.

Within work package 4, a number of prominent studies have been performed aiming at characterizing the coordinative environment of humate complexed actinide ions. Furthermore, the potential for intermolecular humic acid association induced by actinide complexation was studied. In the former case, new interpretation approaches for time-resolved laser-induced fluorescence spectroscopy and new data were obtained. These data provide important information potentially clarifying the coordinative environment of complexed Cm(III). It also provides for a further development in the general approach to interpretation of photodynamic processes of actinide-humate complexes. With respect to the potential for intermolecular humic acid association induced by actinide complexation, a combination on most prominent size and mass distribution methods were applied (AFFFF, ESI-MS and TOF-SIMS). The flocculation at high metal ion loading of humic acid is verified. A shift of the molecular mass distribution towards higher masses is found for high loading. To which extent this is related to variation in ionization efficiency or actually reflects the generation of associates is not fully clear. The question to which extent complexation induced association takes place already at low loading, i.e. is part of the complexation process irrespective of overall ligand loading, is also not yet fully clear. Final conclusions will require studies beyond the present project.

Within work package 5, work has been finalized and key conclusions for the main objectives of the project could be drawn. It is (i) verified that laboratory studies can provide the data required for long-term predictive modeling, and (ii) shown that the basic approaches apply to an anthropogenic several decades long contact time case, providing trust that data and approaches can be applied to PA relevant spatial and time scales.

Work package 6 has already been finalized and no additional results are reported from the present reporting period.

Within work package 7, model description of humic acid association has been refined. The kinetic approach applied predicts a distribution of associates. This is in good qualitative agreement with experimental observations and thus contributes to improvement of the overall humic system behavior.

Work package 8 was scheduled to be the focus for the present final reporting period. Three already defined and documented migration cases are used for visualization of the humic colloid mediated impact under different conditions. The migration cases represent (i) shallow sandy aquifer systems, (ii) deep sandy aquifer systems, and (iii) uranium mining and milling rock piles. For the definition of the three migration cases, considerable development had been done on geochemical and isotope-geochemical process analysis. The transport predictive calculation code k1d was applied to the three migration cases. General conclusions concerning the potential impact of humic colloid mediated actinide impact have been drawn and the application of the tools developed for PA has been described. In addition, reporting of results from a Marie Curie Grant through the project has added valuable information concerning clay organic matter as a potential additional source for humic colloids under chemically amended near-field conditions. Finalization of this work package concludes the project, providing all the scheduled main deliveries.

## 2. Progress within work packages

### *WP 1 (Critical assessment of experimental methods)*

The work contributions provide (i) a broadening of the experimental database for actinide/lanthanide humate interaction, (ii) additional information concerning limitations and restrictions for the use of different analytical methods, and (iii) new characterization data with the key information on the charge of complexes in course of progressive metal ion complexation.

Electrophoretic study of Th(IV) humate complexation can be complicated by a number of phenomena, such as sorption loss of thorium possibly accompanied by distortion of equilibrium, errors in measurement of electrophoretic mobility, and formation of mixed ternary complexes, polynuclear species, pseudocolloids and carbonate complexes. Occurrence and effect of the phenomena depends mainly on pH and concentration of thorium. In addition, the mutual effect of positively and negatively charged Th species on their mobility needs to be

considered. Nevertheless, appropriate interpretation of electrophoretic data enables obtaining important information on the abundance and charge of Th humate complexes, for example on changes due to progressive ligand loading by Th(IV).

First the behavior of Th(IV) without humic acid is investigated. Depending on the nature of the Th(IV) ions, i.e. accompanying hydroxyl and carbonate ions, the charge will vary with pH. At very low Th concentrations, positive mobility is lower and negative species are found also below the pH neutral range, indicating association with impurities. At higher Th(IV) concentrations (around $10^{-5}$ mol/L), impurity impact should be suppressed with the disadvantage of super-saturation in the non-acidic pH range. With increasing pH, carbonate complexes may also contribute to the formation of negative species, complicating study of Th humate complexes.

Addition of humic acid suppresses positive mobility of Th and enhances its negative mobility, which can be used for determination of abundance and mobility of Th humate complexes. In general, negative thorium humate species are found. The mean negative mobility of ThHA complexes increases with pH from 2 to 4 and does not strongly depend on thorium/humic acid molar concentration ratio unless the ratio increases close to 1. Incomplete neutralization of charge of dissociated ($COO^-$) groups of humic acid is observed even at this rather high ratio, when the amount of bound Th(IV) cations evidently exceeds exchange capacity of these groups.

The U(VI) humate complexation was studied by ion-exchange method as a function of pH, ionic strength and concentration of U(VI) and Aldrich humic acid. Preliminary evaluation indicates that the interaction constant depends not only on pH and ionic strength but also on metal ion concentration. Final evaluation will need to include the effect of possible formation of polymeric products of U(VI) hydrolysis.

***WP 2 (Generation and characterization of humic material)***

The objectives are to provide well characterized natural and designed humic material for the different project studies. Characterization includes deduction of various properties important for other studies and overall interpretation and process understanding..

The thermal stability of humic substances is investigated. This is important for the generation of thermodynamic data, i.e. entropy and enthalpy. The present findings may also form the basis for basic understanding of evolution of sediment organic carbon under thermal influence and the relation to the characteristic properties, including the tendency of release of/ conversion into aquatic mobile complexing humic and fulvic acid.

In previously reported results, release of water from humic acid was observed at increasing temperature by mass spectroscopy. Two distinct water releases were observed at around 60 °C and around 100 °C. Just above this temperature, carbon dioxid and carbon monoxide were

released showing thermal decomposition. The question was to which extent the first water release peak at around 60 °C is reversible, i.e. represent strongly associated water, or if irreversible decomposition/rearrangement takes place already at this temperature. Evaluation of previous data showed around 6 % of loss in mass via release of water at 100 °C, with the corresponding number being around 7 % at 130 °C. In the present study FTIR/DRIFTS was used in order to identify changes in IR absorbing functional group and water content.

It was verified that the water content is decreased between room temperature and 100 °C. In addition, the band at 1600 $cm^{-1}$ decreased. At higher temperatures the release of carbon dioxide is also verified by the strong IR absorption of gaseous $CO_2$. After the present verification of previous results by FTIR/DRIFTS data, further more detailed studies will be conducted in the lower temperature range (especially around 60 °C). These further studies will include resaturation of humic acid and testing of irreversibility criteria.

As already mentioned above, these studies may also be extended to the question of nature of natural Clay Organic Matter in light of the burial history (maximum temperature) and the possible impact of elevated temperature in the disposal near-field.

***WP 3 (Radionuclide humate interaction data by designed system investigations)***

The objectives are to provide data for the actinide and iodine interaction with humic substances of different types and systems. The studies are closely related to characterization of humic material, complex characterization and modeling. In the present third project year, investigations ere made on, (i) reduction processes of actinide ions with humic acid (ii) intercomparison study of An/Ln interaction with humic wafers, and (iii) iodine humate interaction.

The first topic is of key importance for the chemical state of actinide ions in the far-field. It has not yet been possible to directly relate the actinide reduction by humic substances to a single well identified process. The second topic reflects the delay in generation and characterization of humic wafers, relative to original planning. The unexpected difficulties in generating humic wafers led to a project amendment, as agreed upon with the Commission, already in the beginning of the project. At this stage of the project, wafers from different generation approaches are available and an actinide interaction intercomparison study between such wafers from different generation approaches and laboratories has been conducted. The third topic is related to the application of recent advanced analytical methods in addition to the originally planned activities on iodine humate interaction.

Studies have continued on the reduction of actinide ions by humic acid. Previous studies have shown that humic acid can reduce, amongst others Np(V) and U(VI). For studies of the processes involved, synthetic humic acids have been generated designed with high reducing strength and capacity. The strong reducing character of the designed synthetic humic acids is based on high phenolic OH group content. Comparison between different natural and designed humic acids shows a strong relation between the phenolic OH group content and

reducing strength/capacity. Another direct evidence for phenolic OH groups being key players in the reducing character of humic acids is that chemical blocking of the phenolic OH groups results in strong decrease in the reducing character. As a number of studies reported through the HUPA project have shown, however, the phenolic OH group content is not a sole parameter capable of directly describing the overall reducing function.

The present study also verified the need to use a spectrum of analytical methods for trustworthy interpretation of results. At high concentrations, the reduction of Np(V) to Np(IV) can be followed in UV/Vis/NIR spectroscopy by the disappearance of the Np(V) absorption. Laser-induced photoacoustic spectroscopy (LIPAS) was applied for direct spectroscopic detection on Np(IV) and Np(V) species in solution. At low concentrations, however, spectroscopic identification especially of the resulting tetravalent neptunium species, is not possible due to low extinction coefficients. At low neptunium concentrations, indirect methods need to be applied. The frequently used liquid-liquid extraction was shown to be hampered by the distribution behavior of the tetravalent neptunium humate complex. Contrary to this, ultrafiltration allows for determination of the non-humate complexed pentavalent form, not retained on the filter, with the humic acid associated tetravalent form retained on the filter.

Three types of humic coated silica wafers generated by different approaches were selected for studying the possibility to use surface bound humic acid in studies on the humate complexation behavior and application of surface specific methods making use of the high local ligand concentration in a defined surface layer. One wafer type is used where the entire generation process has been thoroughly characterized by TOF-SIMS and AFM studies on the starting wafer material and all intermediate as well as the final process products. Two silica wafers coated with humic acid by other approaches were also used. An adequate characterization also of these wafers is on the way aiming for inclusion in the final scientific-technical reporting. An interaction intercomparison study was also finalized by determining the Am(III)/Nd(III) interaction with the three different wafers. It was shown, that using two different approaches give very similar sorption isotherms. As expected, a deviating behavior is found where water is used during synthesis leading to undesired and uncontrolled hydrolysis.

In conjunction with the generation and characterization of wafers aimed for fixed covalent binding of humic acid via spacer molecules, analysis of complexation data for systems with actinide ions, mineral surfaces and humic acid distributing between solution and physico-sorption on the mineral surface is reported. The data do not allow distinction between the humate complexation behaviors of humic acid physico-sorbed on the surface and dissolved humic acid. More detailed complexation data and spectroscopic evidence would provide desired additional information on this important topic, eventually determining to which extent geochemical data-bases need to be extended by different complexation data for the sorbed and the dissolved humic acid or if the same set of numbers can be used for the two groups of humic substances.

The binding of iodine to humic acid has been studied in order to provide an answer to the question if there is a trustworthy basis for iodine retention by sediment humic substances.

Previous results showed the iodine does bind to humic acid under specific conditions. A natural humic acid with high iodine content also shows the potential relevance for iodine humic acid binding. One question that remained without a satisfactory answer was the nature of iodine humic acid binding. The character of humic acid bound iodine was studied by three different advanced analytical methods. These are XPS, ESI-MS and XAFS. Both XAFS and XPS indicate dominance of covalent binding. ESI-MS, however, showed separate mass spectroscopy peaks for iodine and humic acid. To which extent the latter is a consequence of the electro spray ionization process and the other two methods show the actual binding nature still needs verification.

In summary, work on this work package has continued with investigations using advanced analytical approaches in order to provide further process understanding required for trustworthy long-term predictions on the geochemical behavior of concerned radionuclides. These investigations will be carried over into future investigations within and outside the EC supported RTD activities.

***WP 4 (Characterization of radionuclide humate complexes):***

The objective of this work package is to provide structural information of the different systems and complexes. At the end, this is the key for providing trust in the overall outcome of the project, namely trustworthy long-term predictions on the impact of humic substances on the radionuclide migration

A key question in the characterization of actinide humate complexes is related to the direct coordinative complex environment (coordination) and the question to which extent humic acid molecules associate by the actinide complex via binding to functional groups of different humic acid molecules. The former question can be investigated by spectroscopic methods, however, so far not having delivered an unambiguous answer. The second question can be investigated by possible increase in mass/size of actinide complexes compared to individual humic acid molecules. The slow humate complex dissociation kinetics observed is frequently assumed to be related to intermolecular processes, especially because such slow dissociation kinetics is not reported for model organic ligands, including chelating ones. The idea that the slow dissociation kinetics is related to the formation of intermolecular complexes may be approached by studying the dissociation kinetics in the presence of simple acids, expected to provide for dissociation.

Time resolved laser induced fluorescence spectroscopy has been used for about two decades for studying the humate complexation using actinide and lanthanide ions with fluorescence life-times in the microsecond range. Especially the fluorescence behavior of the complexed ions has been characterized with respect to shift in transition energy (shift in peak position) relative to the aquo ion, or change in distribution between different transitions (shift in intensity distribution between different transitions/peaks), and the fluorescence life-time. A precondition for fluorescence is that part of absorbed energy is transferred to an excited state

from which light is emitted with time delay compared to prompt return to the starting point prior to absorption (the ground state). One specific issue with humic acid is energy transfer from the ligand to the complexed metal ion, providing for an enhancement of fluorescence intensity relative to direct excitation of /absorption by the complexed ion. Simultaneously, energy can be withdrawn from the excited state by transfer to the organic ligand. The latter is one of several processes diminishing the yield of emitted fluorescence light from the excited state ("(fluorescence) quenching"). One contribution deals with the energy transfer from the ligand to the complexed curium(III) ion and the magnitude of this curium fluorescence enhancement relative to the photodynamic properties of fulvic acids of different origins. Another contribution deals with clarification of the quench impact of humic acid, possibly resolving a long-standing question.

The topic of energy transfer from humic/fulvic acid to complexed curium(III) was investigated by varying the excitation wavelength over the range of the direct excitation of the curium itself using four different fulvic acids from different origin and with different specific absorption and fluorescence of the fulvic acids themselves. The latter differences are also related to differences in functional entity distribution as determined by C-XANES. Conditions are chosen so as to have basically all the curium complexed by the fulvic acids. Varying the excitation wavelength over the range where there is one of the Cm(III) absorption peaks, the total Cm(III) humate complex fluorescence becomes the sum of (i) direct excitation (via absorption of the complexed curium), and (ii) curium fluorescence enhancement via energy transfer form the fulvate ligand. Delineating the two contributions it is found that (i) the fluorescence contribution from direct excitation is independent of the nature of the fulvic acid used, whereas (ii) the contribution by the energy transfer is strongly dependent of the photodynamic properties of the fulvic acids.

As an immediate outcome this means that measurement of the complexation constants by TRLFS can be done irrespective of the nature of the fulvic acid by evaluation of the fluorescence contribution from the direct excitation. By this approach, the variation in total fluorescence due to different contributions from energy transfer, i.e. due to differences in the nature/ photodynamic properties of the humic/fulvic acids is removed. This approach still needs to be verified by studies on further substances, especially different humic acids. A second aspect is the desire to understand the nature of energy transfer. Present investigations indicate that the frequency of fluorescent states of the humic and fulvic acids populated for a specific excitation wavelength used is the precondition for energy transfer. These follow-up investigations will be conducted after the HUPA project, requiring networking of several institutions also from outside the HUPA consortium.

The second aspect, namely the quench impact of humic and fulvic acids has been puzzling the community of involved researchers for around two decades. The fluorescence life-time of complexed curium(III) has four components. These are the measured emission of fluorescence light, quenching (removal of excited states by processes that diminish/drain the emission of fluorescence light) by coordinated water molecules and two components originating from the energy exchange with the humate/fulvate ligands. By measurement in both water and

heavy water media, the two different life-time quench components of the humate ligand could be subtracted and the difference allocated to quenching by water. The quenching by heavy water is much lower than that of water and thus the difference can be set to be the quench influence of water. The quench rate for water is equivalent to three water molecules in the inner coordination sphere. The total coordination number at room temperature is set to nine, leaving a six-fold coordination by humic acid functional groups. The key to this new approach in interpreting time-resolved fluorescence is that the two different life-time quench components from humic acid represent one complex and can be subtracted by comparison of water and heavy water media. This is a great step forward in interpretation of time-resolved fluorescence data where the key point is showing that the two quench components of the humic acid is not related to different species and remains sufficiently constant when changing medium from water to heavy water. Use of the basic approach for other related questions, such as resolution of kinetic components and formation of ternary complexes, is under discussion for investigations beyond the HUPA project.

The second key topic is related to the humate complexation process, namely to the possible intermolecular complexation of multivalent metal ions. This topic is tackled by studying the impact of complexation with $Eu^{3+}$ ions on the size and the mass distribution.

Size distribution measurements are conducted by AFFFF with different humic and fulvic acids at different degrees of ligand loading with $Eu^{3+}$, as well as impact of contact time in order to regard possible rearrangements along with progressive occupation of kinetically more stable complexation modes. In the case of fulvic acid, no impact was found on the size distribution, including different ligand loadings and contact times. For humic acid, a slight increase in size distribution and broadening of the elution peak was found. This modest effect was not observed except for upon approaching humate ligand saturation. Also a slightly larger size is observed with 7 days contact time. The modest impact observed at high loading and with long contact time for humic acid may indicate complexation mediated humic-humic association, i.e. an intermolecular complex formation. The lack of such an observation in fulvic acid, however, makes conclusions difficult. In addition, if the complexation is followed by dehydration of ligand functional groups and the relatively bulky humic and fulvic acids associate in a favorable fashion, a large impact on the size distribution is not expected. The fluid medium used for AFFFF measurements is 10 mmol/L ammonium acetate without $Eu^{3+}$. Therefore, decomplexation at least of fast dissociation modes during measurement may also be important. Last but not least, previous investigations within the HUPA project with AFFFF fractionation into what is expected to be different size fractions followed by mass distribution of these fractions by TOF-SIMS showed no significant correlation between the size distribution obtained by AFFFF and their humic acid mass distribution.

In summary, the AFFFF results are difficult to interpret, but may indicate generation of larger entities with complexation at high metal ion ligand loading. This is also expected because of the known flocculation of humic acid for ligand saturation with multivalent metal ions. The lack of such an observation for fulvic acid is in qualitative agreement with the lack of flocculation of fulvic acid at high metal ion ligand loading. Nevertheless, changes in size distribu-

tion could be expected also for fulvic acid reflecting observations on sharp increase in scatter light under such conditions.

Mass spectrometry shows a strong impact of complexation on the mass distribution of humic acid. ESI-MS and TOF-SIMS show a decrease in overall signal with increasing Eu(III) humate loading. Thereby, the relative peak at high masses increased. To which extent ionization of europium complexed molecules with lower masses was preferentially suppressed or if the abundance of higher masses increases due to complexation induced humic acid molecule association is not fully clear. The impact is lower on fulvic acid than on humic acid. In addition, longer contact times enhance the impact on humic acid.

Bringing together the results of size fractionation by AFFFF, and mass distribution by TOF-SIMS and ESI-MS it is clear that the impact of europium(III) complexation (i) is very low on fulvic acid, (ii) becomes significant on humic acid when approaching ligand saturation, and (iii) increases with increasing contact time, where this impact is increased in size and presumably also mass distribution. The results agree with solubility behavior of humic and fulvic acids under progressive metal ion complexation with multivalent metal ions, namely that (i) humic acid flocculates whereas fulvic acid does not, and (ii) a significant increase in size/mass of humic acid is not seen by dynamic light scattering until the humate ligand approaches saturation. The results may support the assumption of complexation mediated humic acid association as supported by modeling (cf. below, WP 7) and the occupation of six coordination sites by humate ligands (cf. above), difficult but not impossible to arrange with one molecule alone with the functional groups density of humic and fulvic acids.

The assumption that humic acid associates are responsible for the slow dissociation kinetics of multivalent humate complexes was investigated by addition of simple acids reported to dissociate humate associates. There was no significant impact on the dissociation kinetics by addition of reactants presumable dissociating humic acid associates. Intermolecular complexation, thus is not expected to be responsible for the gradual population of slow dissociation modes. The question remaining is to which extent intermolecular complexation by multivalent metal ions is very strong compared to the weak hydrophobic associative forces where the added simple acids are reported to lead to humic acid dissociation. A final conclusion is still pending.

***WP 5 (Natural chemical analogue studies):***

Reflecting project amendment, as accepted by the Commission, emphasis of work was shifted relative to original intentions and studies focused of anthropogenic actinide contaminant behavior. The objectives are to demonstrate the validity of findings on comparably large spatial and time scales.

Some additional rounding-up investigations were conducted beyond the scheduled project contribution period. The overall results may be summarized as follows:

(i) The anthropogenic actinides are about 10 times more concentrated in the humic acid fraction than in the overall top-soil,
(ii) The differences in dissociation rates observed between anthropogenic actinides and actinide ions added in the laboratory are related to the actinide concentrations but there is no additional impact of the decades of contact time for the anthropogenic ones, and
(iii) There is, however, an impact of the decades long contact time for the anthropogenic actinides, namely a higher population of the slow dissociation mode.

The results are extremely important because they provide an answer to one of the key questions of the HUPA project. This key question is related to the observed differences in dissociation kinetics between actinide ions added in the laboratory and the natural multivalent trace metal ion inventory in natural humic acid. Contrary to the former one, the latter shows a large fraction of especially tetravalent trace metal ions with basically irreversible association to humic acid. If there is a simple contact between humic acid and actinide ions, the population distribution between different slow but not basically irreversible dissociation rates can be used for long-term predictive transport modeling. Only if actinide ions are built into mobile humic substances in a quasi irreversible mode under geochemical conditions different than the present ones, a non-retarded humic colloid mediated transport is expected to occur. Focus on the anthropogenic actinides instead of the original intention of providing more precise data for the difference between added and natural inventory actinides thus has proven to contribute the delivering desired key information.

***WP 6 (Radionuclide transport experiments):***

No work was done on this work package during the third and final reporting year.

***WP 7 (Model development):***

The objectives of this work package are to rationalize findings and bringing them into consistent mathematical descriptions. These descriptions serve the basis for predictive modeling, but also for testing and feed-back to experimental work providing the knowledge base.

Models developed and associated accessible input data provide the basis for migration case modeling during the final reporting period as reported under WP 8. Nevertheless, modeling of humic acid self-association has continued due to (i) the great interest in the potential for intermolecular humic acid complexation of multivalent actinide ions, as supported by numerous experimental observations (cf. above), and (ii) the complexation process suggested in the Second Technical Progress Report where the total ligand concentration is described as the concentration of humic acid molecules, and the actual humic acid ligand concentration at given pH is a function of deactivation of molecules with respect to complexation through sequential protonation of molecules.

The previous state of model development was hampered by the use of flat wall surface approach. The present development is using a more realistic curved surface approach and results agree much better with different experimental observations. The formation of associates is a kinetic process where the association and dissociation depends also on the size of the entities. Diffusion-controlled association, counteracted by Coulomb repulsion, drives this process. For a specific charge density, the coulomb repulsion increases with increasing mass. The reversed reaction, namely the dissociation is also size/mass dependent. The dissociation rate increases with increasing size/mass of associates. The overall results show qualitative agreement with experimental observations. An exact prediction still requires understanding of the shape and density (mass to effective hydrodynamic size) of individual molecules and associates. This is especially true when calculating the effective charge density. It may be expected that work will continue beyond the HUPA project, aiming at providing the required process understanding. For this purpose additional fundamental understanding of basic parameters will be required and thus depends also on a general development of the field.

***WP 8 (PA):***

The objectives of this work package are to summarize the overall outcome with respect to the impact of humic colloid mediated actinide transport on the radionuclide migration in the far-field, and to visualize this by three migration cases. The overall outcome is discussed under section 3.

Work in this reporting period has focused on providing the overall outcome of the HUPA project by predictive modeling of the migration cases. The focus is on showing basic features of predictive modeling requirements for the impact of humic substances on the actinide transport. In addition, a work is reported on the nature of aquatic humic acid fulvic acids originating from clay organic matter as well as the potential impact of radiation damage in the near-field. This work is related to potential additional humic colloid sources in the clay near-field.

Humic and fulvic acids from clay organic matter were characterized with respect to the clay mineral origin and the solubilization process. For this purpose, spatially resolved C-XANES was used on clay samples and C-XANES on isolated aquatic humic and fulvic acids originating from the clay. It is shown that humic and fulvic acid precursors are present in clay organic matter. The fulvic acid precursors are covalently bound to mineral surfaces whereas humic acid precursors are mainly sorbed. Consequently, more humic acid dissolves than fulvic acid when clay is contacted with alkaline solution. The main difference between the clay organic humic and fulvic acid precursors and the aquatic humic and fulvic acids resulting from dissolution in alkaline solution is that the aquatic humic substances have higher concentration of carboxylic groups. This on one hand explains the selective dissolution of these acids, but it also raises the question concerning the complexation behavior of the precursors and the aquatic substances. It will need thorough future investigations in order to quantify the complexation capacity and overall behavior of clay organic matter relative to that of aquatic humic substances. The presently frequently argued for approach that the properties of aquatic

humic substances can be applied to the precursor material in the clay organic matter may need revision.

The three migration cases defined for the HUPA project are (i) Gorleben, (ii) Dukovany, and (III) uranium mining and milling rock pile Schlema-Alberoda. The outcome of the Gorleben and Dukovany migration cases may be summarized as:

(i) Equilibrium approaches are insufficient and underestimate the humic colloid mediated actinide transport,

(ii) The "quasi irreversible" transport is not relevant if not specific near-field conditions result in such inclusion of actinide ions into humic colloids,

(iii) The interaction with humic colloids will increase the mean residence time of actinides in the mobile state and thus enhance the actinide transport,

(iv) Even if there is a contribution of humic colloid sorption (not verified in isotope-geochemical real site analysis), this will only have a marginal impact,

(v) In all groundwater systems investigated, the humic colloid concentrations are found to be sufficiently high and thus the absolute concentration of humic colloids is not critical, and

(vi) There are considerable but quantifiable uncertainty ranges for the impact of humic colloid mediated actinide transport, depending on the specific conditions and uncertainty ranges of dissociation constants.

The uranium mining and milling case is very different compared to the other two cases. The humic colloid mediated uranium transport is well described by two kinetic humate complex dissociation constants with the other parameters set to equilibrium. The uranium transport is enhanced by the humic colloids with a strong influence of the slow dissociation mode. The overall outcome of the uranium transport is determined by the uranium distribution in the pile. In the beginning there is a wash-out phase of an easily accessible uranium inventory, followed by an about one order of magnitude lower elution rate. This wash-out takes only one or few years. These results are in agreement with observations from comparison of uranium concentrations in water in medieval and recent uranium mines. Both mines have been subject to wash-out of the easily accessible inventory, and despite the long difference in time span between the two, after this first wash-out the uranium concentrations in contacted water are similar.

The overall result of the mining and milling residue pile migration case is that the main factors are given by the distribution and accessibility of uranium in the pile material and that the humic colloid mediated transport enhances the initial uranium wash-out process as well as the mobility in the later phase.

## 3. Overall outcome of the HUPA project with respect to PA

Below the overall outcome with respect to application to PA is briefly discussed in the form of different topics.

### *3.1. Generalization of humic substances properties*

In a first approximation, characteristic properties of humic substances can be generalized. Despite individual differences, definition of humic substances over a large number of common characteristics, varying within limits, is possible. If more detailed results are required, however, knowledge about specific properties is needed.
The complexation properties are shown to partly depend on the specific nature of humic and fulvic acids of different origin. More problematic, however, is that a correlation between different properties and the interaction kinetics is still an open issue. This specifically refers to the question of the relatively large basically irreversibly bound part of the inventory of trace metal ions found in natural humic colloids. Contrary to this, only a small fraction of actinide ions added under near-natural laboratory conditions and time-scales show dissociation kinetics so slow that it cannot be quantified by laboratory column transport experiments. In this context, especially the potential role of inorganic/mineral constituents has not yet been clarified.
Another issue is the question of mobility of dissolved humic substances in its natural colloidal form. Investigations in real systems ((isotope-)geochemical analysis of groundwater systems) show that humic colloids in general are stable (directly shown for up to 15.000 years) and mobile like ideal tracers. One exception is the Gorleben aquifer system, where fulvic acid from deep groundwater in-situ generation is not mobile into high ionic strength groundwater near the salt dome, whereas fulvic acid from recharge is. For the recently identified potential additional source of dissolved humic substance from high pH influence in the clay near-field, prediction of their mobility over relevant time and spatial scales is not yet possible (no natural chemical analogue available).

### *3.2. Applicability of laboratory data*

The principle agreement between laboratory transport studies and the anthropogenic actinide contaminant studies in the Irish Sea shows, that there is an agreement between laboratory and large scale anthropogenic systems. However, the short-term laboratory studies and the chemical environment in the Sea may not adequately reflect natural groundwater conditions and the time-scales involved. This may be specifically true for chemically amended near-field conditions and the potential for actinides to become built into humic colloids in a comparable fashion as found for the natural trace element inventory, presumable in mineral inclusion form. When it comes to prediction of mobility in the aqueous phase, only real system analysis provides trustworthy information, presently missing for the clay near-field and other additional sources (cf. above).

### *3.3. Impact of humic colloid mediated transport versus mineral bound humics/organics*

The kinetics of radionuclide interaction with the aqueous humic inventory (humic colloids) is comparably well known. The slow dissociation kinetic mode leads to an enhanced actinide transport irrespective of the presence of other sinks. The magnitude of the impact is determined by the groundwater flow rate relative to the magnitude of the slow dissociation kinetics, and may be negligible especially in diffusion controlled systems.
Corresponding radionuclide interaction data for the stationary organic/humic inventory is not known. Characterization of clay organic matter shows that humics and humic precursors are present. The solubilization and release of humic matter from this source is very much associated with formation of carboxylic groups. This means that distinction between the two inventories (mobile and stationary organics/humics) is not the result of sorption/desorption equilibrium exchange but reflects structural differences, especially the lower content of complexing carboxylic groups in the stationary inventory. Furthermore, solubilization is associated with breaking of strong bonds to the mineral surfaces (not only sorption through the less hydrophilic nature). This clear distinction in the two inventories by their very different nature is also reflected in the capability to perform $^{14}C$ groundwater dating by dissolved fulvic acids.
In summary, adequate knowledge about the stationary humic/organic inventory is still missing, especially the radionuclide interaction kinetics required for application to PA.

### *3.4 Amendment of mineral surface properties*

As mentioned above, organic/humic substances are bound to mineral surfaces. This leads to an amendment of mineral radionuclide sorption properties. Organic coating may be found on less active surfaces, changing the chemical properties, but will have a more specific impact by sorption on otherwise active sites. Determination of this impact of organic substances on the mineral surface properties is still at an infant stage.

### *3.5 Overall importance of humic substances*

With respect to humic colloid mediated transport enhancement, humic substances appear to be important for the long-term assessment of a repository in many systems. With respect to the interaction with stationary organic/humic substances, the situation is not yet clear, however, the radionuclide retention by minerals will be strongly influenced by the organic coating and sorption on active sites. Consequently, for a large number of systems, as a minimum the impact of humic substances should be considered and brought into comparison with other possibly more important impacts.

### *3.6. Availability of knowledge, data and models*

Actinide humate interaction data is available with exception for the tetravalent ions in the relevant pH range, some other mixed/ternary complexes and description of the competition

impact by other cations. Ranges of kinetic radionuclide humic colloid interaction data are available.
With reference to the HUPA project, interaction of iodine with humic substances gives partly contradicting results, and thus the potential retention via the stationary humic/organic substances is still not resolved.
To some extent, models and associated data are available for trustworthy prediction of the humic colloid mediated actinide transport. This especially refers to the agreement between the "several decades long migration case" with anthropogenic contaminants at the shore of the Irish Sea and other sources of knowledge and data. Transport codes for the modeling of column experiments under near-natural conditions are available, correctly predicting the magnitude of the "ideal tracer mobile fraction". The capability to predict the transport of the residual inventory still is not fully demonstrated. This especially refers to decoupling of the unknown dissociation kinetics from the stationary phase and the transport enhancement in the mobile phase.

### *3.7. Implementation in PA*

For the purpose of application to PA, a broad basis of data and knowledge is available, reaching from progress in detailed complex coordination to large scale real system analysis. At the end, however, data that will enter into PA will probably be restricted to overall description of humic colloid sources and their mobility, and the radionuclide interaction kinetics with both humic colloids and the stationary inventory. The sorption on/ coating of mineral surfaces will probably be included via the sorption behavior of the minerals. Introduction of the kinetics in the exchange of radionuclides between different compartments in an element along a potential flow path is possible in PA codes. The underlying mechanisms, however, are still unclear and trustworthy data for stationary organic/humic substances are missing. Therefore, confidence in long-term predictions over many thousands of years remains hampered.

## 4. Remaining main uncertainties

Uncertainties are still given with respect to:
- Lack in process understanding resulting in lack in trust in long-term predictions,
- The problem of selecting processes observed in different types of experiments under different types of conditions and by different systems investigated, for their regard or disregard in the predictive long-term modeling,
- The potential for especially near-field processes that may incorporate actinides in a comparable fashion as found for the natural trace element inventory,
- The magnitude of some interaction data is still unsatisfactorily, especially (i) the lack in trustworthy data for the tetravalent actinide ions forming ternary complexes under relevant conditions, and (ii) lack of adequate data for some other ternary complexes,

- The impact and treatment of cation competition is unclear, especially with metal ions abundant in natural groundwater systems,
- The potential differences between the frequently studied aquatic humic and fulvic acids, and the basically unknown properties of their sediment organic carbon precursors of aquatic humic substances, key substances for actinide retention, still needs to be resolved,
- Potential additional sources need to be quantified, especially under non-natural near-field conditions,
- Stability and mobility of humic substances depending on their properties/origin, especially in view of potential additional sources for which no natural chemical analogues are available, and
- Stationary humic/organic substances as a potential source for retention of iodine is still not clear.

Based on the great progress within the HUPA project, including the established knowledge network(s) where the foundations have been laid also during earlier EC supported RTD activities/programs, these topics will be subject to further studies beyond the present project, especially the Integrated Project "Fundamental processes of radionuclide migration" (IP FUNMIG), starting January 2005 with a duration of four years.

**Annex 1:**

**Coordination of trivalent actinides by humic acids: A TRLFS study**

Stumpf Th., Buckau G., Fanghänel Th.

# Coordination of trivalent actinides by humic acids: A TRLFS study

Thorsten Stumpf[1], Gunnar Buckau[2], Thomas Fanghänel[1,2]

[1]Ruprecht-Karls-Universität Heidelberg, Angewandte Physikalische Chemie am Physikalisch-Chemischen Institut, Im Neuenheimer Feld 253, 69120 Heidelberg, Germany

[2]Forschungszentrum Karlsruhe, Institut für Nukleare Entsorgung, P.O. Box 3640, D-76021 Karlsruhe, Germany

## Summary

The fluorescence lifetime of humate complexed Cm(III) is studied in water and $D_2O$ media. The fluorescence decay function is a combination of the impact of the humic acid ligand backbone and quenching by hydration water in the coordination sphere of the complexed Cm(III) ion. The energy transfer between the complexed Cm(III) ion and the humic acid backbone results in a bi-exponential fluorescence decay function. The additional quench impact of water molecules in the inner coordination sphere of the complexed Cm(III) ion is evaluated by the difference in water and $D_2O$ medium. The outcome is that three water molecules are found in the inner coordination sphere, presumably with the residual six coordination sites occupied by functional groups of the humic acid.

## Introduction

Besides sorption and desorption processes on mineral surfaces, organic ligands in natural water are well known to have significant impact on metal ion bioavailability and mobility in aquifer systems. In natural water, toxic heavy metals, rare earth elements and radionuclides such as actinides are frequently found to be attached to natural organic matter as humic/fulvic acids. These complexes are known to be of high kinetic and thermodynamic stability under given geochemical conditions and therefore may control trace metal transfer to bioorganisms and their transport in soil and groundwater systems. For those reasons the interaction of metal ions with humic matter is a major issue in a number of research fields such as environmental monitoring, risk assessment of contaminated sites and nuclear waste disposal. In order to understand and to assess the impact of humic/fulvic acids on the behaviour of trace metals we need to know the interaction mechanisms and associated complexation kinetic and thermodynamic data that can be implemented into geochemical speciation and transport codes.

Cm(III) is a representative of the trivalent actinides which are common in nuclear wastes. It is chosen as because its fluorescence spectroscopic sensitivity allowing studied on a molecular level at nano-molar concentrations. **T**ime **r**esolved **l**aser **f**luorescence **s**pectroscopy (TRLFS) has been proven to be a versatile tool for Cm(III) speciation studies (e.g.[1,2,3,4,5]). It is capable of identifying different species as well as determining their hydration status ([6,7]). TRLFS enables the speciation of Cm(III) in solution and suspension. Investigations of complexation reactions as well as sorption reactions at mineral surfaces are possible with this method. The characterization of the different Cm(III) species is performed by the interpretation of excitation and emission spectra. The record of the Cm(III) fluorescence emission lifetime gives information about the number of O-H ligands in the first coordination sphere of the metal ion ([8]). Moreover it is possible to deduce the kinetic of complexation reactions from these measurements ([9]).

## Material and Methods

### Humic Acid

The purified natural humic acid investigated, Gohy-573(HA), originates from a 139 m deep groundwater of the Gorleben aquifer system in Northern Germany. The isolation, purification and detailed characterization of this humic acid is described elsewhere ([10]). The proton exchange capacity (PEC) determined by pH titration under Ar atmosphere is 5.38 ± 0.20 meq/g ([10]). Stock solutions of the purified humic material are prepared by dissolving a known amount of humic acid in 0.1 M $NaOH/H_2O$ or $NaOD/D_2O$, respectively. After about ten minutes the pH is adjusted to 6.0 by addition of $HClO_4$ (0.1 M) or $DClO_4$.

### **TRLFS** (**t**ime **r**esolved **l**aser **f**luorescence **s**pectroscopy)

TRLFS measurements were performed using a dye laser (Lambda Physics, scanmate) pumped by a XeCl-eximer laser (Lambda Physics, EMG, 308 nm, 24ns) for excitation. Emission spectra were recorded from 580 nm to 620 nm. The fluorescence emission is detected by an optical multichannel analyzer consisting of a polychromator (Jobin Yvon, HR 320) with a

300/600/12000 lines/ mm grating and a photodiode array (Spectroscopy instruments, ST 180, IRY 700G). The Cm(III) was excited at 396.6 nm. The emission spectra of Cm(III) were recorded in the 580 – 620 nm range (1200 lines/mm grating). For measuring the time dependent emission decay (300 lines/mm grating), the delay time between laser pulse and camera gating was scanned with time intervals between 5 and 10 μs. For measuring the decay time of the fluorescence emission the delay time was shifted in steps between 15 (in $H_2O$) and 20 μs (in $D_2O$) using a constant time window of 1 μs and 10 μs, respectively.

**Lifetime (fluorescence decay) of Cm(III).**

The fluorescence emission lifetime provides information on the composition of the first coordination sphere. According to the method developed by Horrocks Jr. & Sudnick ([11]) and Barthelemy & Choppin ([12]) for Eu(III) and later applied to Cm(III) by Kimura & Choppin ([7]), there is a linear correlation between the observed decay rate and the number of $H_2O$ or $OH^-$ molecules in the first coordination sphere. In the case of Cm(III) this linear correlation takes the form of:

$$n(H_2O/OH^-) = 0.65k_{obs} - 0.88 \quad (1)$$

where $k_{obs}$ is the observed decay rate (reciprocal lifetime) of the excited state [$ms^{-1}$] and $n(H_2O/OH^-)$ is the number of coordinated water molecules or hydroxyl ions. $Cm(H_2O)_9^{3+}$ corresponds to a lifetime of 68 ± 3 μs ([13,14]). When all water molecules are removed from the first coordination sphere, the lifetime is calculated to be 1250 ± 80 μs ([15]). The decay rate is obtained by measuring the fluorescence signal at different delay times after the laser pulse.

**Results and Discussion**

Figure 1 shows the emission decay in logarithmic scale of $2x10^{-7}$ mol/L Cm(III) in 10 mg/L humate solution at pH 6. The curium shows a bi-exponential fluorescence emission decay behavior, indicating two different Cm-humic acid complexes. The emission lifetimes are calculated to be $\tau_1$=76 μs and $\tau_2$=145 μs. According to equation 1, a lifetime of 76 ± 3 μs corresponds to 8 water/$OH^-$ molecules in the first coordination sphere of Cm(III) whereas a lifetime of 145 ± 15 μs indicates the loss of more than half of the $Cm^{3+}$ aquo ion hydration sphere by formation of the second Cm(III)-humate species. Two Cm-humate species with a different curium hydration sphere should differ significantly in their emission spectra. Figure 2 shows emission spectra of Cm(III)-humate at pH 6 measured at different delay times. The spectra are scaled to the same peak area and show no differences, neither in peak maximum nor in the peak shape. Therefore, the emission decay behaviour can be explained only under the assumption that the humic acid is responsible for the bi-exponential Cm(III) fluorescence quenching and not a variation in the curium hydration sphere. To verify this suggestion the fluorescence emission of Cm(III) in humate $D_2O$ suspension was investigated by TRLFS.

Figure 3 shows the fluorescence emission decay behaviour of $10^{-7}$ mol/L Cm(III) in 20 mg/L humic acid in $D_2O$ at pH 6. The decay behaviour is bi-exponential again with lifetimes of $\tau_3$=129 ± 5 μs and $\tau_4$=570 ± 7 μs. A quench influence of OH vibronics can be ruled out because exclusively $D_2O$, NaOD and $DClO_4$ were used. The quench impact of $D_2O$ and $OD^-$

is negligible compared to the water counterparts. Hence, the humic acid itself is responsible for the Cm(III) fluorescence quenching and for the bi-exponential emission decay.

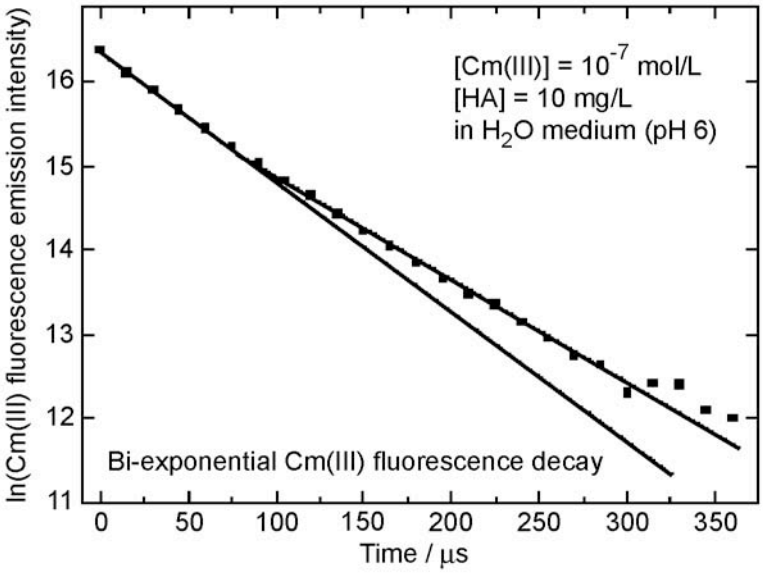


Figure1: Cm(III) humate fluorescence decay.

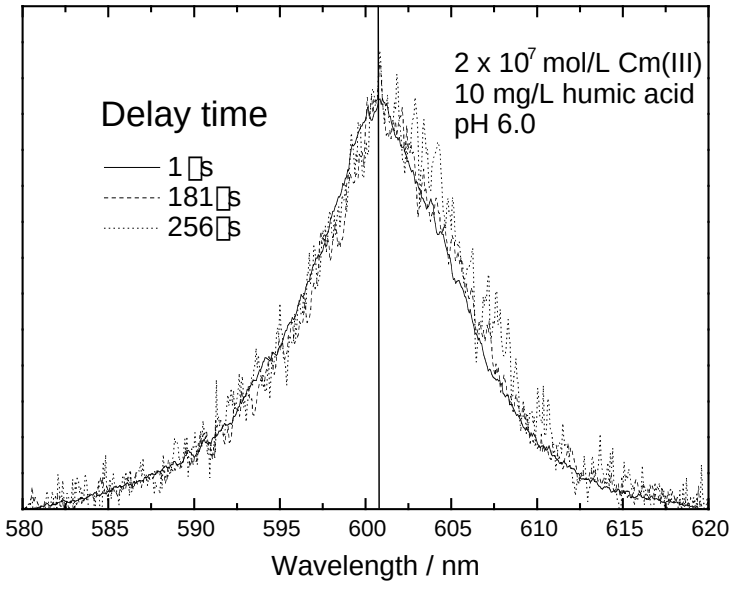


Figure 2: Cm(III) emission spectra along with fluorescence decay

In literature it is shown, that the experimental lifetime depends on the sum of the rates of the fluorescent, radiative processes $k_f$ and the rates of non-radiative processes $k_a$ ([16]).

$$1/\tau = k_f + k_a \qquad (2)$$

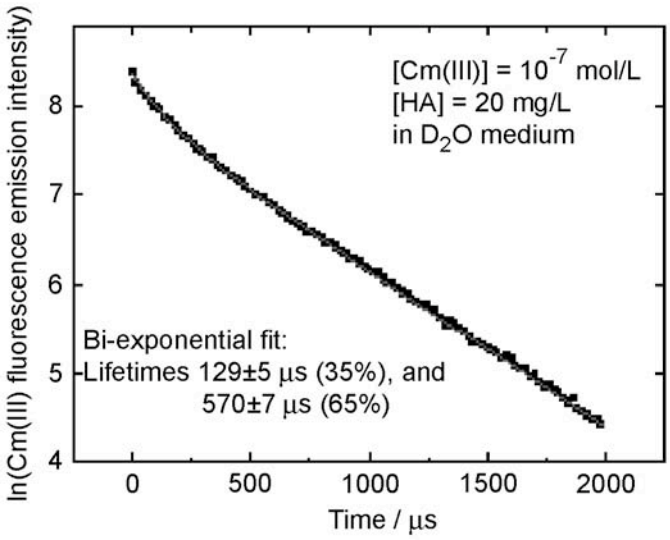


Figure 3: Cm(III) humate fluorescence decay in $D_2O$ medium.

In order to calculate the proportion of OH vibronics on the Cm(III) emission quenching the quenching in $D_2O$ have to be subtracted from the quenching measured in $H_2O$.

$$1/\tau_{(OH)} = (k_f + k_a)(H_2O) - (k_f + k_a)(D_2O) \qquad (3)$$

From that follows for Cm(III)/humic species 1 $1/\tau_{1(OH)} = 0.0054$ and for Cm/humic species 2 $1/\tau_{2(OH)} = 0.0052$, corresponding to the lifetimes $\tau_1$=185 µs and $\tau_2$=192 µs. The quenching rate and the emission lifetime of Cm(III)-humate species 1 and Cm(III)-humate species 2 show the same value within the uncertainty. Hence, the "two" curium species have the same hydration sphere and the same ligand field, indicating that ONLY ONE Cm(III)-humate complex exists at pH 6. This finding is in good agreement with the delay spectra presented in figure 2, which show only one Cm(III) spectrum independent of the delay time.

The lifetimes $\tau_1$ and $\tau_2$ correspond to ~ 3 water molecules in the first hydration sphere of the Cm(III) after Cm(III)/humic complex formation at pH 6. Hence, we conclude that one Cm(III)/humic complex predominate the speciation at pH 6 and that curium is six-fold coordinated by the humic acid.

## References


[1] Wimmer, H., Kim, J. I., Klenze, R., Radiochim: Acta, 58 / 59, 165 (1992).

[2] Moulin, V., Tits, J., Moulin, C., Decambox, P., Mauchien, P., De Ruty, O., Radiochim. Acta, 58 / 59, 121 (1992).

[3] Fanghänel, T., Kim, J. I., Paviet, P., Klenze, R., Hauser, W., Radiochim. Acta, 66/67, 81 (1994).

[4] Fanghänel, T., Weger, H. T., Könnecke, T., Neck, V., Paviet-Hartmann, P., Steinle, E., Kim, J. I., Radiochim. Acta, 82, 47 (1998).

[5] Fanghänel, T., Kim, J. I., J. Alloys Comp., 271-273, 728 (1998).

[6] Horrocks, W. DeW., Sudnick, D. R., J. Am. Chem. Soc. 101, 334 (1979)

[7] Kimura, T., Choppin, G. R., J. Alloys Comp., 213/214, 313 (1994).

[8] Supkowski RM, Horrocks W. DeW., Inorg. Chim. Acta, 340, 44 (2002).

[9] Stumpf, T., Fanghänel, T., Grenthe, I., J. Chem. Soc., Dalton Trans. 3799, (2002).

[10] Kim, J. I., Buckau, G., Li, G. H., Duschner, H., Psarros, N., Fresenius J. Anal. Chem. 338, 245 (1990).

[11] Horrocks Jr., W. D., Sudnick, D. R., J. Am. Chem. Soc., 101, 334 (1979).

[12] Barthelemy, P. P., Choppin, G. R., Inorg. Chem., 28, 3354 (1989).

[13] Beitz, J. V., Hessler, J. P., Nuclear Technology, 51, 169 (1980).

[14] Beitz, J. V., Bowers, D. L., Doxtader, M. M., Maroni, V. A., Reed, D. T., Radiochimica Acta, 44/45, 87 (1988).

[15] Carnall, W. T., Crosswhite, H. M., Report ANL, 84 (1995).

[16] Stein, G., Würzberg, E., J. Chem. Phys., 62, 208 (1975)

## Annex 2:

**Study of the Redox Stability of Uranium(VI) in Presence of Humic Substances**

Sachs S., Geipel G., Bernhard G.

**Study of the Redox Stability of Uranium(VI) in Presence of Humic Substances**

S. Sachs, G. Geipel, G. Bernhard

Forschungszentrum Rossendorf e.V., Institute of Radiochemistry, P.O. Box 510 119, 01314 Dresden, Germany
(FZR-IfR)

## Abstract

We studied the stability of the oxidation state of U(VI) in the presence of natural humic acid from Aldrich and synthetic acids Hyd-Glu and Cat-Gly representing humic acid model substances with pronounced redox functionalities. Using laser-induced photoacoustic spectroscopy, we obtained the first spectroscopic proof for the reduction of U(VI) to U(IV) by synthetic humic acids. In contrast to that, no spectroscopic indications were found for an Aldrich humic acid-mediated reduction of U(VI). Therefore, we concluded that both humic acid-like products show higher U(VI) redox capacities compared to Aldrich humic acid.

## 1 Introduction

Humic acids play an important role for the mobilization of radioactive and non-radioactive toxic substances in the environment which is attributed to their strong ability for complex and colloid formation. In addition to that, humic acids are characterized by redox properties that can influence the oxidation state of metal ions which also effects their speciation and therefore, their migration in natural aquifers. Thus, the trustworthy modeling of the migration of radioactive and toxic metal ions in the environment requires knowledge on the influence of humic acids on the oxidation state of metal ions in addition to the understanding of the humic acid-metal ion-complexation.

From literature it is known that humic acids are able to reduce actinide ions. For instance, in the presence of humic acids, Pu(VI) is reduced to Pu(IV), Np(VI) to Np(V) (Choppin, 1999) as well as Np(V) to Np(IV) (Zeh et al. 1999, Schmeide and Bernhard, 2005). The stability of the oxidation state of U(VI) in the presence of lignin, wood degradation products and natural humic acid was investigated by Abraham (2002). For the first time, it was shown that these organic materials are able to reduce U(VI) to U(IV). Using laser-induced photoacoustic spectroscopy, the direct spectroscopic proof for the occurrence of U(IV) after equilibration of U(VI) solutions with lignin and wood degradation products at pH 9 and pH 8, respectively, was obtained.

Based on the oxidation of diphenolic compounds, we developed synthetic humic acid model substances with pronounced redox functionalities (Sachs et al., 2003 and 2004) in order to study the redox behavior of humic acids and the redox stability of actinide humate complexes in more detail. In the present work we investigated the redox stability of U(VI) in the presence of these synthetic humic acids in comparison to one natural humic acid. Before use, these synthetic products were characterized with regard to their elemental, structural, functional and redox properties in comparison to natural humic acids.

## 2 Experimental

*Humic acids*

Our studies were performed using synthetic humic acid Hyd-Glu (oxidation product of hydroquinone synthesized in the presence of glutamic acid) and Cat-Gly (oxidation product of catechol synthesized in the presence of glycine) with distinct redox properties (Sachs et al., 2003 and 2004). These model substances were synthesized in alkaline solution at 60 °C using potassium peroxodisulfate as oxidizing agent. The humic acid-like fractions of the oxidation products were separated by precipitation with HCl, purified by dialysis against purified water (MWCO <1000), and lyophilized (Sachs et al., 2004). For comparison, we used the commercially available natural humic acid from Aldrich (AHA) after purification (Kim and Buckau, 1998).

The applied humic materials were characterized for their elemental composition, functional group content, and structure. In order to characterize the redox properties of these substances, we de-

termined their formal redox potentials according to Österberg and Shirshova (1997) and Mack (2002) as well as their Fe(III) redox capacities at pH 3.0 and pH 9.2 according to Mack (2002) and Matthiessen (1995), respectively.

*Redox studies*

The redox stability of U(VI) in the presence of the synthetic humic acids Hyd-Glu and Cat-Gly as well as of natural humic acid AHA was studied at pH 6, 8, and 9 in 0.1 M $NaClO_4$ solutions according to Abraham (2002). U(VI) humic acid solutions with initial U(VI) and humic acid concentrations of $1 \cdot 10^{-4}$ M and 0.4 g/L, respectively, were prepared applying $CO_2$-free solutions under nitrogen atmosphere and exclusion of light. The pH values were adjusted using NaOH and $HClO_4$ solutions. In order to keep the pH values of the solutions constant, they were periodically checked and reset.
Laser-induced photoacoustic spectroscopy (LIPAS) was applied for the direct spectroscopic detection of U(IV) in the test solutions. For this a tunable laser system, that is described in detail by Geipel et al. (1998), was used. The wavelength range between 600 and 675 nm was studied. Contrary to U(VI), U(IV) shows characteristic absorption bands in this wavelength range. For sample preparation, 1 mL 6 M $H_2SO_4$ was added to 5 mL of the sample solution in order to precipitate the humic acid, to decompose U(IV) humate complexes and to stabilize U(IV) in solution in form of its sulfate complex. After acidification, the humic acid precipitate was separated by centrifugation and the supernatant was studied by LIPAS.

## 3 Results and discussion

*Characterization of humic acids*

Table 1 summarizes results of the humic acid characterization. Synthetic humic acid Hyd-Glu and Cat-Gly show elemental compositions that are close to those of AHA and other natural humic acids cited in the literature. Due to the use of nitrogen-containing precursors, both synthetic products show higher nitrogen contents than AHA.
The carboxyl group contents of both humic acid-like oxidation products of diphenolic compounds are comparable to those of natural humic acids. However, due to the use of phenolic starting materials the synthetic products show significantly higher phenolic/acidic OH group contents than AHA.
From FTIR results (not shown) it was concluded that synthetic humic acid Hyd-Glu and Cat-Gly exhibit structural components which are also found for natural humic acids (Sachs et al., 2004).
The formal redox potentials of humic acid AHA and Hyd-Glu agree with those of Aldrich humic acid (578 ± 16 mV, -(57 ± 10) mV/pH) and lignin (579 ± 6 mV, -(54 ± 1) mV/pH) determined by Mack (2002). The formal redox potential of humic acid Cat-Gly was found to be slightly lower. However, it shows a similar pH dependence compared to those of the other humic materials.

**Table 1:** Characterization of the studied humic acids.

| Elemental composition | C (%) | H [a] (%) | N (%) | S (%) | O [b] (%) | Ash (%) | Moisture (%) |
|---|---|---|---|---|---|---|---|
| Hyd-Glu (batch R13/02) | 53.7 ± 0.1 | 2.3 ± 0.1 | 2.0 ± 0.1 | 0.2 ± 0.1 | 28.2 ± 0.1 | 1.6 | 11.9 |
| Cat-Gly (batch R18/02) | 48.8 ± 0.1 | 2.8 ± 0.2 | 5.1 ± 0.1 | 0.9 ± 0.1 | 31.1 ± 0.2 | 1.7 | 9.5 |
| AHA (batch A2/98) | 58.6 ± 0.1 | 3.0 ± 0.1 | 0.8 ± 0.1 | 3.8 ± 0.1 | 23.5 ± 0.1 | 2.4 | 7.9 |
| Natural HA (Stevenson, 1994) | 53.8 – 58.7 | 3.2 – 6.2 | 0.8 – 4.3 | 0.1 – 1.5 | 32.8 – 38.3 | | |

| Functional groups | COOH [c] (meq/g) | Phenolic/acidic OH [d] (meq/g) |
|---|---|---|
| Hyd-Glu (batch R13/02) | 3.65 ± 0.14 | 5.8 ± 0.2 |
| Cat-Gly (batch R18/02) | 4.16 ± 0.04 | 6.6 ± 0.7 |
| AHA (batch A2/98) | 4.49 ± 0.14 | 3.1 ± 0.1 |
| Natural HA (Stevenson, 1994) | 1.5 – 5.7 | 2.1 – 5.7 |

| Redox properties | $E^{0*}$ [e] (mV) | ΔE/ΔpH (mV/pH) | Fe(III) Redox capacity [f] (meq/g) | |
|---|---|---|---|---|
| | | | pH 3.0 | pH 9.2 |
| AHA (batch A2/98) | 570 ± 9 | -65 ± 1 | 1.2 ± 0.1 | 7.2 ± 1.9 |
| Hyd-Glu (batch R13/02) | 565 ± 12 | -64 ± 12 | 10.7 ± 0.2 | 33.6 ± 4.0 |
| Cat-Gly (batch R18/02) | 517 ± 12 | -57 ± 12 | 14.5 ± 1.6 | 36.9 ± 0.2 |

[a] Corrected for the water content of the humic acid. [b] The oxygen content was calculated from the difference to 100 % under consideration of the ash and moisture content of the humic acid. [c] Determined by calcium acetate exchange (Schnitzer and Khan, 1972). [d] Radiometrically determined (Bubner and Heise, 1994). [e] Formal redox potential. [f] After ~3 weeks reaction time.

The redox potentials of humic acids are deciding for their ability to influence the oxidation state of metal ions. Comparing the redox potentials of the redox couple U(IV)/U(VI) (Fig. 1) with those of the humic acids it becomes clear that these are close together in the studied pH range between pH 6 and 9. Therefore, it can be concluded that a humic acid-mediated reduction of U(VI) to U(IV), especially by synthetic humic acid Cat-Gly, becomes possible.

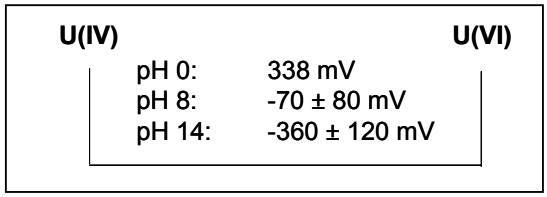


**Fig.1:** Redox potentials for U(IV)/U(VI) (according to Choppin, 1983).

The comparison of the Fe(III) redox capacities of all studied humic acids shows that the humic acid alike products Hyd-Glu and Cat-Gly exhibit a significantly more pronounced redox behavior

towards Fe(III) ions than AHA. Due to the fact that phenolic/acidic OH groups play a significant role for the redox properties of humic substances (Sachs et al., 2003 and 2004), this results can be basically ascribed to the higher phenolic/acidic OH group content of both synthetic products compared to AHA.

*LIPAS results*

Figure 2 shows the photoacoustic spectra of the uranium solutions that were equilibrated with humic acids at pH 9 after humic acid separation including their peak deconvolutions.

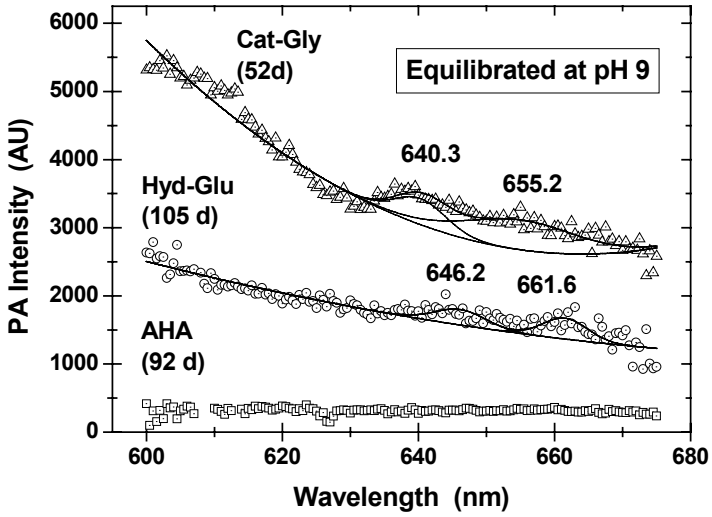


**Fig. 2:** LIPAS spectra of the uranium solutions equilibrated with humic acids at pH 9 after humic acid separation. Numbers in brackets indicate the contact time of humic acid with uranium.

In contrast to the spectrum of the AHA sample, the spectra of the synthetic humic acid test solutions show high background absorption intensities. This fact is due to an incomplete humic acid exclusion from the solutions resulting in a humic acid contribution to the absorption signal. However, from the spectra it becomes clear that no absorption signals were detected for the uranium solution of the AHA sample. In contrast to that, the uranium solutions of the Hyd-Glu and Cat-Gly samples show absorption bands at 646.2 and 661.6 nm and at 640.3 and 655.2 nm, respectively. Thus, we conclude that after 93 days contact time no detectable U(IV) (detection limit $10^{-6}$ mol/L; Abraham, 2002) was formed by an AHA-mediated U(VI) reduction. In absence of humic acid the solvated U(IV) ion shows characteristic absorption maxima at 629.5 nm, 649.1 nm and 671.7 nm (Table 2). These are close to those observed in the uranium solutions of the Hyd-Glu and Cat-Gly samples. This result points to the occurrence of U(IV) in the uranium solutions of the synthetic humic acids with pronounced redox functionality. Furthermore, the spectra of both synthetic humic acid test solutions are similar to that of a uranium solution after equilibration of U(VI) with wood degradation products, where the spectroscopic evidence for the reduction of

U(VI) to U(IV) by these substances was given (Abraham, 2002). From this it can be concluded that U(VI) was reduced to U(IV) by both synthetic humic materials.
Figure 3 depicts the LIPAS spectra of the uranium solutions equilibrated with synthetic humic acid Cat-Gly for 52 days at pH 6, 8, and 9. In case of this humic acid, which shows the lowest formal redox potential and the highest Fe(III) redox capacity among the considered materials, U(IV) absorption bands were detected in all studied solutions. Therefore, we conclude that this humic acid-like product is able to reduce U(VI) to U(IV) already at pH 6.

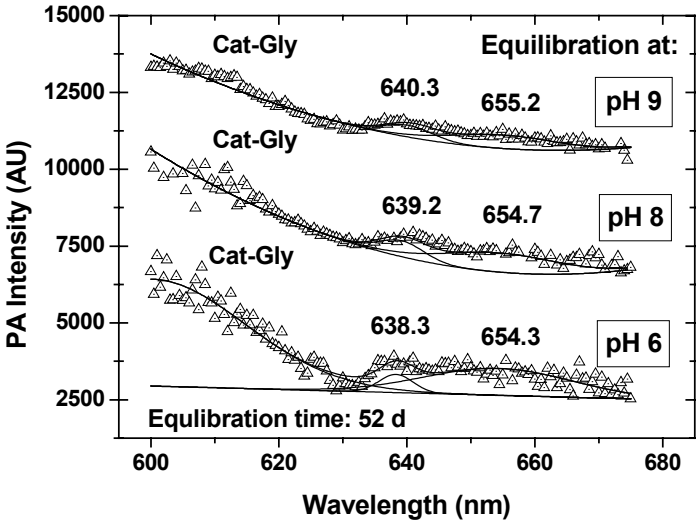


**Fig. 3:** LIPAS spectra of the uranium solutions of humic acid Cat-Gly equilibrated at pH 6, 8, and 9 after humic acid separation. The spectra are shifted along the y-axis for clarity.

In all LIPAS spectra the observed absorption bands are shifted compared to those of the solvated U(IV) ion. Similar peak shifts were already identified for the U(IV) complexation by arsenate, phosphate and sulfate (Table 2).We attribute the observed shifts of the absorption maxima to the formation of U(IV) sulfate complexes. Sulfuric acid was added for sample preparation. The final $H_2SO_4$ concentration was 1 mol/L. The deviations of the observed peak maxima compared to those of U(IV) in 1.2 M $H_2SO_4$ given in Table 2 could be explained by an additional complexation of U(IV) by not completely removed humic acid molecules.

**Table 2:** Absorption maxima of U(IV) reference substances.

| U(IV) Species | Absorption maxima (nm) | | | Reference |
|---|---|---|---|---|
| $U(H_2O)_n^{4+}$ | 629.5 | 649.1 | 671.7 | Geipel et al., 2002 |
| $U(H_2PO_4)^{3+}$ | 645.0 | 656.6 | 667.0 | Geipel et al., 2002 |
| $U(H_2AsO_4)^{3+}$ | 645.1 | 662.9 | | Geipel et al., 2002 |
| U(IV) in 1.2 M $H_2SO_4$ | 634.6 | 652.8 | 670.0 | this work |

From our studies we conclude that synthetic humic acids Hyd-Glu and Cat-Gly with pronounced redox functionalities are able to reduce U(VI) to U(IV). Both substances show higher Fe(III) and U(VI) redox capacities than AHA. Similar results were also observed for the reduction of Np(V) to Np(IV) (Schmeide and Bernhard, 2005) and can be expected for other heavy metal and actinide ions. The higher redox capacities of the synthetic materials compared to Aldrich humic acid can be attributed to their higher phenolic/acidic OH group. From our former studies it is known that phenolic/acidic OH groups play a significant role for the redox behavior of humic acids (Sachs et al., 2003 and 2004). The obtained results represent a first spectroscopic proof for the reduction of U(VI) by humic acids. Further studies are in progress in order to quantify the U(VI) redox capacity of the studied humic acid alike substances.

## Acknowledgments

This study was supported by the EC Commission under contract No. FIKW-CT-2001-00128 and by the German Federal Ministry of Economics and Labor (BMWA) under contract No. 02 E 9299. The authors thank R. Ruske and M. Meyer for their help in humic acid preparation and characterization as well as in the performance of the redox studies.

## References

Abraham, A. (2002) "*Einfluß von Huminstoffen und Holzabbauprodukten auf den Valenzzustand von Uran*", PhD Thesis, TU Dresden.

Bubner M., Heise K.H. (1994) "Characterization of Humic Acids. II. Characterization by Radioreagent-Derivatization with [$^{14}$C]Diazomethane", In: *FZR-43, Annual Report 1993* (Nitsche, H., Bernhard, G., eds.), Forschungszentrum Rossendorf, Institute of Radiochemistry, Rossendorf, Germany, 22.

Choppin, G.R. (1983) "Solution Chemistry of the Actinides", *Radiochim. Acta*, 32, 43.

Choppin, G.R. (1999) "Role of Humics in Actinide Behavior in Ecosystems", In: *Chemical Separation Technologies and Related Methods of Nuclear Waste Management* (Choppin, G.R., Khankhasayev, M.Kh., eds.), Kluwer Academic Publishers, 247.

Geipel, G., Bernhard, G., Brendler, V., Nitsche, H. (1998) "Complex Formation between $UO_2^{2+}$ and $CO_3^{2-}$: Studied by Laser-Induced Photoacoustic Spectroscopy (LIPAS)", *Radiochim. Acta*, 82, 59.

Geipel, G., Bernhard, G., Brendler, V. (2002) "Complex Formation of Uranium(IV) with Phosphate and Arsenate", In: *Uranium in the Aquatic Environment* (Merkel, B.J., Planer-Friedrich, B., Wolkersdorfer, C., eds.), Springer Verlag, Berlin, 373.

Kim J.I., Buckau G. (1988) "*Characterization of Reference and Site Specific Humic Acids*", RCM-Report 02188, TU München.

Mack, B. (2002) "*Redoxeigenschaften von Lignin und Huminsäuren und deren Wechselwirkung mit Eisen*", PhD Thesis, TU Dresden.

Matthiessen, A. (1995) “Determining the Redox Capacity of Humic Substances as a Function of pH”, *Vom Wasser*, 84, 229.

Österberg, R., Shirshova, L. (1997) “Oscillating, Nonequilibrium Redox Properties of Humic Acids“, *Geoch. Cosmochim. Acta* 61, 4599.

Sachs, S., Heise, K.H., Bernhard, G. (2003) “Synthetic Humic Acid Model Substances with Specific Functional Properties for the Use in Complexation and Sorption Experiments with Actinides”. In: *Humic Substances in Performance Assessment of Nuclear Waste Disposal: Actinide and Iodine Migration in the Far-Field. First Technical Progress Report* (G. Buckau, ed.), Forschungszentrum Karlsruhe, Wissenschaftliche Berichte, FZKA 6800, Karlsruhe, 51.

Sachs, S., Schmeide, K., Brendler, V., Křepelová, A., Mibus, J., Geipel, G., Heise, K.H., Bernhard, G. (2004) “*Investigation of the Complexation and the Migration of Actinides and Non-radioactive Substances with Humic Acids under Geogenic Conditions. Complexation of Humic Acids with Actinides in the Oxidation State IV Th, U, Np*”, Forschungszentrum Rossendorf, Wissenschaftlich-Technische Berichte, FZR-399, Rossendorf, Germany.

Schmeide, K., Bernhard, G. (2005) “Study of the Neptunium(V) Reduction by Various Natural and Synthetic Humic Substances”, this report.

Schnitzer M., Khan S.U. (1972) “*Humic Substances in the Environment*” (A.D. McLaren, ed.), Marcel Dekker, Inc., New York.

Stevenson, F.J. (1994) “*Humus Chemistry*”, 2nd ed., John Wiley&Sons, New York.

Zeh, P., Kim, J.I., Marquardt, C.M., Artinger, R. (1999) “The Reduction of Np(V) in Groundwater Rich in Humic Substances”, *Radiochim. Acta,* 87, 23.

## Annex 3:

**Study of the Neptunium(V) Reduction by Various Natural and Synthetic Humic Substances**

Schmeide K., Geipel G., Bernhard G.

# Study of the Neptunium(V) Reduction by Various Natural and Synthetic Humic Substances

K. Schmeide, G. Geipel, G. Bernhard

Forschungszentrum Rossendorf e.V., Institute of Radiochemistry, P.O. Box 510119, 01314 Dresden, Germany (FZR-IfR)

## Abstract

The time dependence of the reduction of Np(V) to Np(IV) by various natural and synthetic humic substances was studied under anaerobic conditions between pH 3.5 and pH 9. For Np speciation in solution liquid-liquid extraction, NIR absorption spectroscopy, laser-induced photoacoustic spectroscopy (LIPAS) and ultrafiltration were applied. In comparison to natural humic substances, synthetic humic acids lead to a stronger reduction of Np(V) to Np(IV). The Np(IV) formed in the course of the experiments is stabilized in form of Np(IV) humate complexes, whereas the remaining Np(V) occurs as $NpO_2^+$ ion or Np(V) humate depending on pH. The higher reduction potential of the synthetic humic acids can be attributed to their higher phenolic/acidic OH group contents compared to natural humic substances. The influence of phenolic/acidic OH groups on the redox behavior of humic substances was verified applying a synthetic humic acid with blocked phenolic/acidic OH groups.

# 1 Introduction

The migration behavior of actinide contaminants in natural aquatic systems can be effected by humic substances (humic acid (HA) and fulvic acid (FA)) due to their strong complexing and redox properties and their ability for colloid formation. Therefore, risk assessments, predicting the fate and transport of actinides in the environment, require basic knowledge of the interaction of humic substances with metal ions. The complexation of Np(V) by humic substances has been studied in a number of publications (e.g., [1-4]). In a study of Np(IV) complexation by fulvic acid at pH 1 and 1.5, first values for conditional complexation constants were estimated [5]. The redox behavior of humic substances of different origin towards Np and Pu in higher oxidation states (mostly hexa- or pentavalent) was reported in [6-14].

Due to reduction of Np(V) to Np(IV), the migration behavior of the actinide changes strongly. Compared to Np(V), which shows a relatively weak interaction with HA, Np(IV) is generally stronger complexed by HA [13]. The humic colloid-borne Np(IV) species is known to remain stable in groundwater and to be easily mobile in porous aquifer systems [10,13].

Recently, synthetic HA with distinct redox properties were synthesized by oxidation of diphenolic compounds in the presence of amino acids in alkaline solution by Sachs et al. [15]. The most promising synthetic HA were the HA type Cat-Gly, which is an oxidation product of catechol and glycine, and the HA type Hyd-Glu, which is an oxidation product of hydroquinone and glutamic acid. These synthetic HA have shown significantly higher Fe(III) redox capacities [15] and also higher U(VI) redox capacities than the natural Aldrich HA [16]. In this work, the stability of Np(V) in contact with various natural and synthetic aqueous humic substances was studied. For redox speciation liquid-liquid extraction, NIR absorption spectroscopy, laser-induced photoacoustic spectroscopy (LIPAS) and ultrafiltration were applied.

# 2 Experimental

## 2.1 Humic substances

Two natural humic substances and three synthetic humic acids were used in this study: The natural Kranichsee fulvic acid (KFA) was isolated from surface water of the mountain bog ‘Kleiner Kranichsee’ (Saxony, Germany) [17]. The commercial Aldrich humic acid (AHA, charge A2/98) (Aldrich, Steinheim, Germany) was purified before use according to the procedure described in [18]. The synthetic products were the humic acids type Cat-Gly (charge R1/03) and type Hyd-Glu (charge R13/02), as well as the humic acid with blocked phenolic/acidic OH groups type Hyd-Glu-PB (charge R20/02). Details to the synthesis and characterization of the synthetic humic acids are given in [15]. The functional group contents of the humic substances are compiled in Tab. 1.

## 2.2 Sample preparation

The Np(V) stock solution was obtained by dissolving solid $^{237}NpO_2NO_3$ in 0.1 M $HNO_3$. The pentavalent oxidation state of Np in the stock solution was verified by NIR absorption

spectroscopy and liquid-liquid extraction. Prior to the preparation of the various humic substance stock solutions, the humic material (50 mg each) was suspended in about 4 mL 0.1 M $NaClO_4$ and degassed under vacuum. The Np(V) humate samples were prepared in a glove box under nitrogen atmosphere using carbonate-free solutions. The initial Np(V) and humic substance concentration was $1 \cdot 10^{-4}$ M and 100 mg/L, respectively. The ionic strength of the solutions was 0.1 M $NaClO_4$. The pH value of the samples (pH 3.5, 5, 7, 9) was adjusted applying diluted NaOH and $HClO_4$ solutions, no buffers were added. During the experiment, the pH value of the solutions was checked and readjusted repeatedly. Blanks without Np were prepared from each humic substance at pH 3.5 to pH 9. All samples were stored in the dark to minimize degradation of the organic material.

Tab. 1: Functional group contents of humic substances

| Humic substance | COOH [a] (meq/g) | Phenolic/acidic OH [b] (meq/g) |
|---|---|---|
| Cat-Gly (batch R1/03) | 4.39 ± 0.13 | 6.6 ± 0.9 |
| Hyd-Glu (batch R13/02) | 3.65 ± 0.14 | 5.8 ± 0.2 |
| Hyd-Glu-PB (batch R20/02) | 2.67 ± 0.03 | 1.4 ± 0.1 |
| AHA (batch A2/98) | 4.49 ± 0.14 | 3.1 ± 0.1 |
| KFA | 6.05 ± 0.31 | 4.8 ± 0.7 |

[a] Determined by calcium acetate exchange [19].
[b] Radiometrically determined [20].

### 2.3 Methods for Np speciation

The Np(V) reduction was determined by monitoring the Np(V) and Np(IV) concentrations in solution over time. For this, samples were taken after different time intervals and characterized by the redox speciation methods described in the following.

Liquid-liquid extraction

The separation of Np(V) and Np(IV) was performed by liquid-liquid extraction using 2-thenoyltrifluoroacetone (TTA) as complexing agent [21]. For this, 1.5 mL of the Np(V,IV) sample solution (pH 1) were shaken vigorously with 2 mL of 0.5 M TTA in xylole for 15 min, and separated by centrifugation. By this method, Np(IV) is extracted into the organic phase, while Np(V) remains in the aqueous phase. The Np concentration was determined by liquid scintillation counting (Wallac system 1414, Perkin Elmer) using $\alpha$-$\beta$ discrimination. For this, 200 µL aliquots were mixed with 15 mL of a Ultima Gold™ scintillation cocktail (Packard BioScience Company).

NIR absorption spectroscopy and laser-induced photoacoustic spectroscopy (LIPAS)

For the direct spectroscopic detection of Np species in the sample solutions, NIR absorption spectroscopy (CARY-5G, Varian) and LIPAS were applied. For LIPAS, a tunable laser system was used which is described in detail in [22]. Quartz cuvettes with 1 cm pathlength (Hellma) were used and thermostated at 20°C. The sample solutions were measured directly, without any further preparations, in the spectral range from 920 nm to 1050 nm. For

quantitative determination of uncomplexed $Np^{4+}$ and $NpO_2^+$ aquo ions, the absorption bands at 960 nm and 980.4 nm with molar absorption coefficients of 162 L $mol^{-1}$ $cm^{-1}$ [23] and 395±5 L $mol^{-1}$ $cm^{-1}$ [2], respectively, were used. For Np(IV) and Np(V) humate complexes, the absorption bands at 967.5 nm and 990 nm with molar absorption coefficients of 63±8 L $mol^{-1}$ $cm^{-1}$ [5] and 230±8 L $mol^{-1}$ $cm^{-1}$ [2], respectively, were used.

Ultrafiltration

For ultrafiltration experiments, MicroSep™ centrifugal concentrators (PallGelman Laboratory) of different pore sizes were used: 1 kDa, 10 kDa, 30 kDa, 100 kDa, 300 kDa, 1000 kDa.

## 3 Results and discussion

In Fig. 1, the Np(V) speciation in the starting solutions is shown for the experimental conditions applied in this study. It was calculated with the geochemical computer code EQ3/6 [24] applying the Np(V) hydrolysis constants compiled in the NEA data base [25], the Np(V) humate complexation constant log $\beta$ = 3.6 and the pH function of the loading capacity (LC) with LC = -0.589 + 0.101 • pH [15]. The results show that the free neptunyl ion predominates the Np speciation in aqueous solution. The $NpO_2HA(I)$ species is formed increasingly in solution between pH 6 and pH 10. For the pH region higher than 9, the formation of the mixed complex $(NpO_2(OH)HA)_{coll.}$ is suggested by Marquardt et al. [2]. However, presently, this complex cannot be quantified thermodynamically. The formation of the neptunyl hydroxyl species $NpO_2OH_{(aq)}$ can be neglected in the considered pH range.

The Np(IV) which is produced in the course of the experiments, occurs either as Np(IV) hydrolysis species or their mixed hydroxo fulvate/humate complex species ($Np(OH)_2FA(II)$ and Np(OH)FA(III)) as was proposed by Marquardt et al. [5].

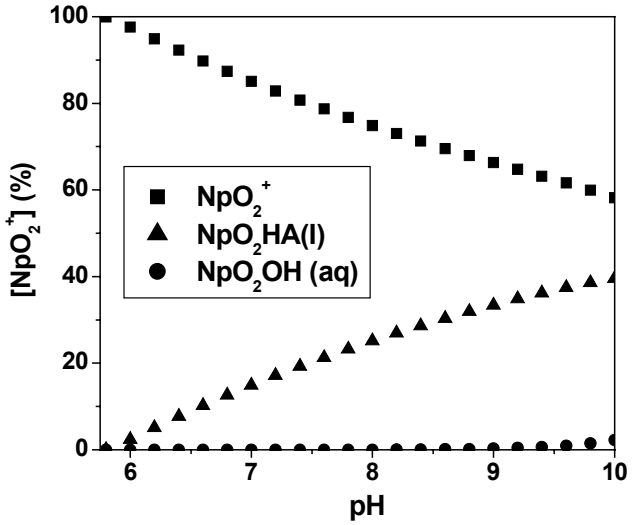


**Fig. 1:** Np(V) speciation at start of equilibration of the Np humic substance solutions. ($[NpO_2^+] = 1\times10^{-4}$ M; [HA] = 100 mg/L; I = 0.1 M $NaClO_4$; $N_2$ atmosphere).

The reduction of Np(V), determined by TTA extraction, is shown in Figs. 2 and 3 as plot of the ratio of pentavalent Np to total Np versus equilibration time. It is obvious, that the Np(V) reduction is dependent on equilibration time, on the type of humic substances as well as on pH value of the sample solutions. In the initial phase of the equilibration of the Np humic substance solutions, the formation of Np(IV) is fast. With increasing equilibration time the rate of Np(IV) formation slows down. The synthetic HA type Cat-Gly and Hyd-Glu show a stronger Np(V) reduction in comparison to the natural humic substances AHA and KFA.

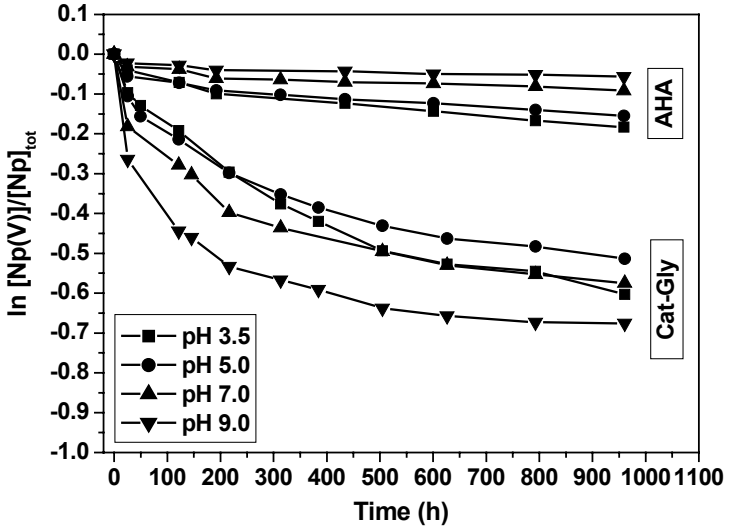


**Fig. 2:** Reduction of Np(V) to Np(IV) by HA type Cat-Gly and AHA between pH 3.5 to pH 9.0. Determination of Np(V) by TTA extraction.

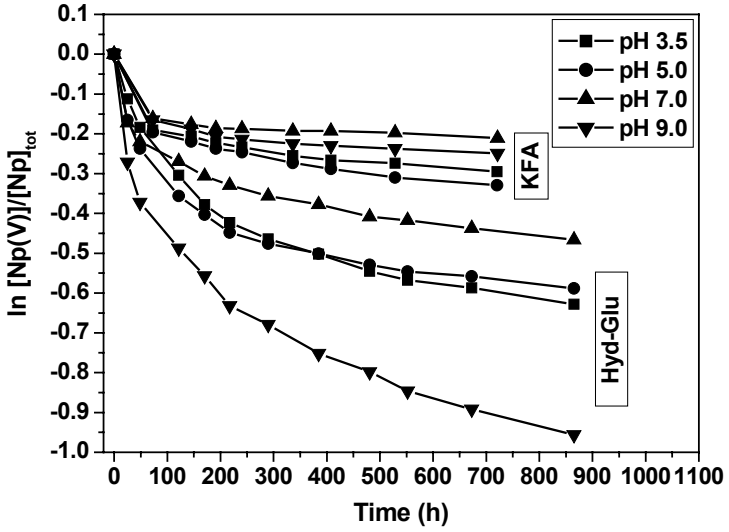


**Fig. 3:** Reduction of Np(V) to Np(IV) by HA type Hyd-Glu and KFA between pH 3.5 to pH 9.0. Determination of Np(V) by TTA extraction.

The strongest Np(V) reduction is found for the HA type Hyd-Glu at pH 9. After 865 h (36 d) 62% of the Np(V) is converted to Np(IV). Also in case of HA type Cat-Gly, the strongest Np(V) reduction is found at pH 9 (961 h (40 d), 49% Np(IV)). The pH dependency

determined for the Np(V) reduction by AHA correlates with that found by Marquardt et al. [1] for the same HA. Generally, however, no trend is observable for the pH dependency of the Np(V) reduction for the various humic substances.
The redox capacity, which decreases in the sequence synthetic HA > KFA > AHA, can be correlated to the phenolic/acidic OH group contents of the humic substances (cf. Tab. 1). A comparable correlation between the phenolic/acidic OH group content of various synthetic and natural HA and their Fe(III) and U(VI) redox capacities was observed in [15,16].
Contrary to the partial reduction of Np(V) under the experimental conditions applied in this work, a nearly complete reduction of Np(V) was found in experiments applying the same Np concentration but the fourfold HA concentration (400 mg/L HA type Cat-Gly).

As already mentioned, by liquid-liquid extraction with TTA as complexing agent, Np(IV) is extracted into the organic phase, while Np(V) remains in the aqueous phase. However, in case of the humic substance solutions studied here, the Np(IV) could not be extracted quantitatively into the organic phase but partly remained bound in the humic substance precipitate. Exemplary this is shown for HA type Hyd-Glu in Fig. 4. With increasing equilibration time, the amount of Np(V) determined in the aqueous phase decreases but the amount of Np(IV) determined in the organic phase does not increase to the same extent. This results in a decreasing Np recovery during TTA extraction. The part of Np that cannot be extracted represents a fraction of tetravalent Np which is strongly bound to the HA and which is not released from the HA even at pH 1. Np(V), however, would decomplex from the HA under these pH conditions and remain in aqueous solution as $NpO_2^+$ ion. This effect was even more pronounced in experiments applying the fourfold HA concentration (not shown here) which confirms again the strong complexation of Np(IV) by HA. Too low activity recoveries were also reported for liquid-liquid extraction of Pu species [26].
The total amount of Np in the sample solutions remains constant in the course of the experiments (cf. Fig. 4), i.e., Np adsorption onto the vial walls is negligible, even at pH 9.0.

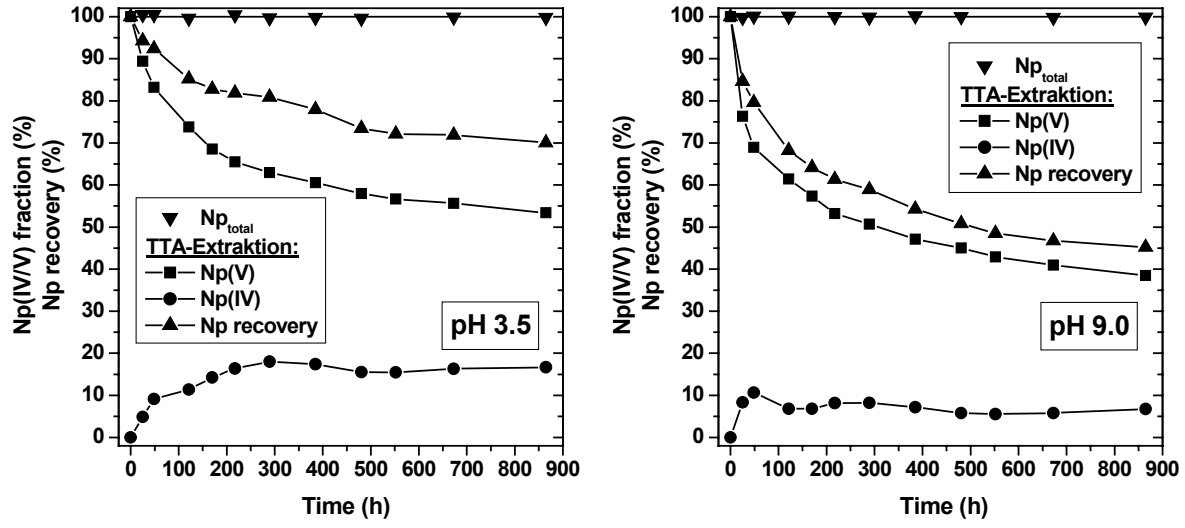


**Fig. 4:** Recovery of Np during TTA extractions in comparison to the total Np content for HA type Hyd-Glu equilibrated at pH 3.5 and pH 9.0.

To study influence of phenolic/acidic OH groups on the redox behavior of humic substances further, the synthetic HA with blocked phenolic/acidic OH groups of type Hyd-Glu-PB was equilibrated with Np(V) under the same experimental conditions as described above. Due to methylation with diazomethane [27,28], the phenolic/acidic OH group content of HA type Hyd-Glu-PB is 76% lower than that of HA type Hyd-Glu (cf. Tab. 1), which was used as starting material. The carboxylic group content of HA type Hyd-Glu-PB is also somewhat lower than that of HA type Hyd-Glu. Possible reasons are a partial decomposition of HA molecules in acid-soluble components and/or leaching of smaller HA molecules with a higher carboxylic group content from the HA mixture [27] or an incomplete hydrolysis of the methyl ester groups that were previously formed during methylation with diazomethane. Nevertheless, Table 1 shows that the molar ratio of phenolic OH to carboxylic groups becomes significantly smaller due to the modification process.

The amount of Np(IV) formed by the modified HA with blocked phenolic/acidic OH groups type Hyd-Glu-PB is very small compared to the strong Np reduction by the unmodified HA type Hyd-Glu (Fig. 5). After 865 h (36 d) the amount of Np(IV) formed by HA type Hyd-Glu-PB is about 55% lower than the amount of Np(IV) formed by HA type Hyd-Glu (pH 9). This again shows that the phenolic/acidic OH groups play a major role for the redox behavior of humic substances. The slight Np reduction in the initial phase of the experiment can be attributed to the small amount of phenolic/acidic OH groups that could not be blocked by methylation (1.4 ± 0.1 meq/g).

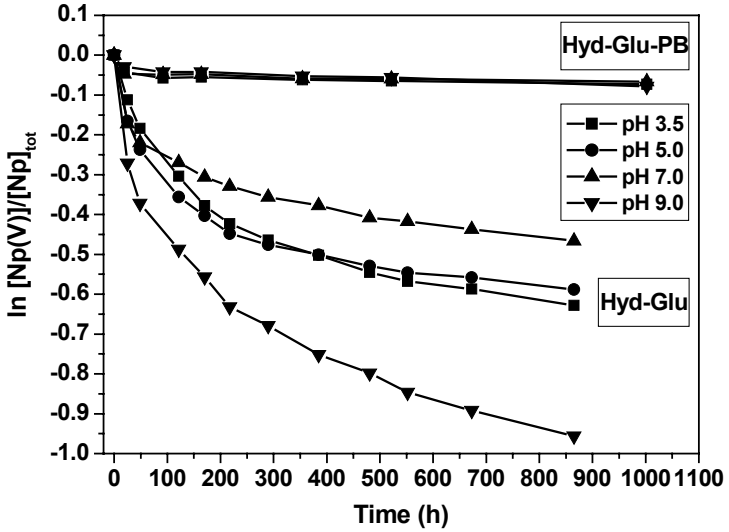


**Fig. 5:** Reduction of Np(V) to Np(IV) by HA type Hyd-Glu and HA type Hyd-Glu-PB between pH 3.5 to pH 9.0. Determination of Np(V) by TTA extraction.

By NIR absorption spectroscopy the gradual decrease of the Np(V) absorption peaks is observed, while the total Np concentration in the sample solutions remains constant in the course of the experiments (cf. Fig. 4).

Because of the higher sensitivity of LIPAS compared to absorption spectroscopy [29,30], LIPAS was applied for direct spectroscopic detection of the Np species in the sample solutions. Exemplary for all sample solutions the photoacoustic spectra of Np(IV,V)/HA type

Cat-Gly equilibrated at pH 3.5 and pH 7 is shown in Fig. 6 together with the peak deconvolution of the spectra. As expected, at pH 3.5, the LIPAS spectrum shows the Np(IV) humate complex at 967 nm together with the $NpO_2^+$ aquo ion at 980 nm. At pH 7, the spectrum shows both the Np(IV) humate complex at 967 nm and the Np(V) humate complex at 990 nm. In addition, in all LIPAS spectra obtained from solutions equilibrated between pH 3.5 and pH 9, a further peak at about 1018 nm is observed which cannot be assigned to a certain Np species so far.

The formation of Np(IV) hydrolysis products besides the formation of Np(IV) humate cannot be excluded completely by these methods since the various Np(IV) hydrolysis species and their mixed hydroxo fulvate or humate complex species cannot be distinguished by NIR absorption spectroscopy [5] or EXAFS [31].

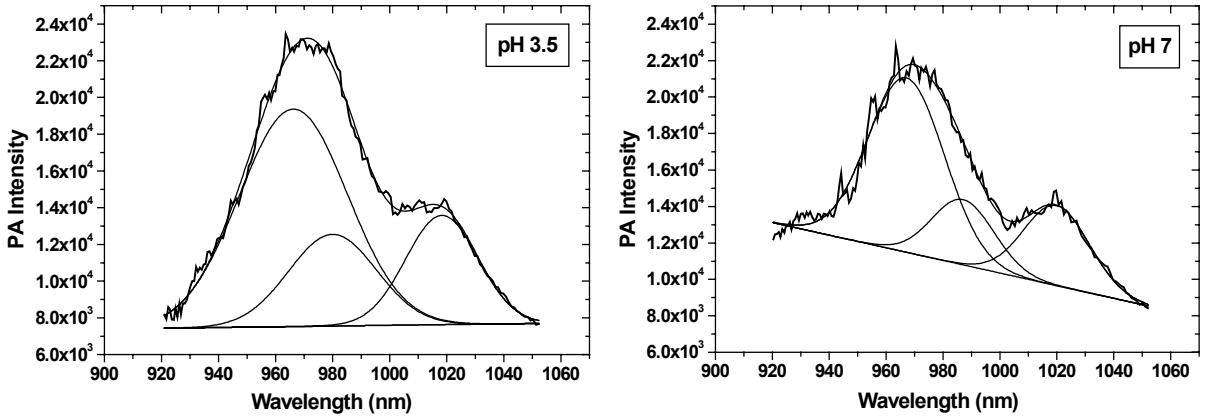


**Fig. 6:** Photoacoustic spectrum of Np(IV,V)/HA type Cat-Gly equilibrated at pH 3.5 and pH 7.

The results of ultrafiltration of the Np(IV,V)/HA type Hyd-Glu sample solutions with membrane filters of pore sizes between 1 kDa and 1000 kDa are shown in Fig. 7. At pH 7 and pH 9, where 36% and 64% Np(IV) are detected by TTA extraction, a Np fraction of 43.1% and 86.6%, respectively, is found to be retained on a 1 kDa filter, whereas at 1000 kDa, Np passes quantitatively through the filter. That means, that a fraction of about 43.1% or 86.6% of the Np is bound onto HA colloids, mostly as Np(IV) and but also as Np(V) (especially at pH 9, cf. Np(V) speciation given in Fig. 1). At pH 3.5 and pH 5, where 47.4% and 43% Np(IV) are detected by TTA extraction, a Np fraction of 49.2% and 45.8%, respectively, is found to be retained on a 1 kDa filter, showing the fraction of humic colloid-bound Np(IV). In this pH range, no Np(V) humate is formed (cf. Fig. 1), and the $NpO_2^+$ ion, detected by LIPAS, passes through the filter. The Np humate solution at pH 3.5 shows the peculiarity that the amount of Np retained on the filters of pore sizes between 1 kDa and 1000 kDa is nearly constant. This is attributed to the precipitate and/or large aggregates that are formed by the humic colloid-bound Np(IV) in the sample solution at pH 3.5.

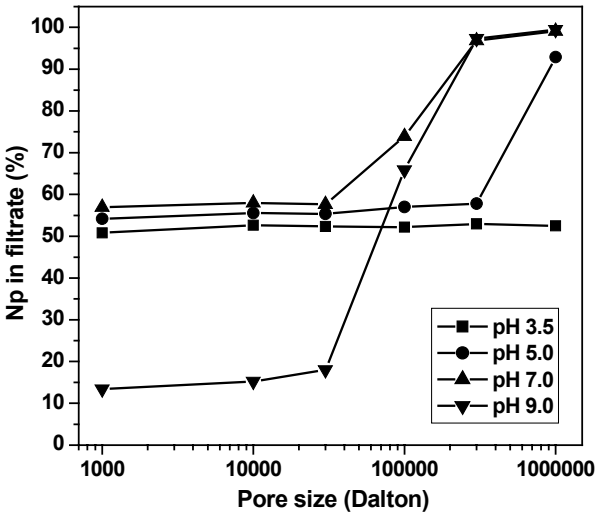


**Fig. 7:** Ultrafiltration of Np(IV,V)/HA type Hyd-Glu equilibrated at pH 3.5 to pH 9.0 for 1543 h (~64 d).

## 4 Conclusions

The redox properties of various natural and synthetic humic substances towards Np(V) were determined. In comparison to the natural humic substances (AHA, KFA), the synthetic HA (type Hyd-Glu and Cat-Gly) lead to a stronger reduction of Np(V) to Np(IV) and to a stabilization of the tetravalent oxidation state in form of Np(IV) humate complexes. The various Np species in solution (uncomplexed $NpO_2^+$ ions as well as Np(IV) and Np(V) humate complexes) could be identified spectroscopically by LIPAS and NIR absorption spectroscopy. The stronger reduction behavior of the synthetic HA in comparison to the natural humic substances can be attributed to their higher amount of phenolic/acidic OH groups. The reduction rates also depend on the concentration of humic substances. However, attempts to derive correlations between the reduction strength and pH value for the various humic substances did not yield any strong relationships. By application of the synthetic HA with distinct redox properties actinides can be stabilized in lower oxidation states, e.g. in complexation and sorption studies.

*Acknowledgment.* This work was partly supported by the EC Commission under contract No. FIKW-CT-2001-00128 and by the German Federal Ministry of Economics and Labour (BMWA) under contract No. 02E9673. We would like to thank S. Sachs for providing the synthetic humic acids and V. Brendler for Np speciation calculations.

## References

1. Marquardt, C., Herrmann, G., Trautmann, N.: Complexation of Neptunium(V) with Humic Acids at Very Low Metal Concentrations. Radiochim. Acta 73, 119 (1996).

2. Marquardt, C., Kim, J.I.: Complexation of Np(V) with Humic Acid: Intercomparison of Results from Different Laboratories. Radiochim. Acta 80, 129 (1998).

3. Seibert, A., Mansel, A., Marquardt, C.M., Keller, H., Kratz, J.V., Trautmann, N.: Complexation Behaviour of Neptunium with Humic Acid. Radiochim. Acta 89, 505 (2001).

4. Sachs, S., Bernhard, G.: NIR Spectroscopic Study of the Complexation of Neptunium(V) with Humic Acids: Influence of Phenolic OH Groups on the Complex Formation. Radiochim. Acta, accepted.

5. Marquardt, C.M., Pirlet, V., Kim, J.I.: Initial Studies on the Complexation of Tetravalent Neptunium with Fulvic Acid. In: FZKA 6524, Wissenschaftliche Berichte (G. Buckau, ed.). Forschungszentrum Karlsruhe, Karlsruhe 2000, p. 45.

6. Nash, K., Fried, S., Friedman, A.M., Sullivan, J.C.: Redox Behavior, Complexing, and Adsorption of Hexavalent Actinides by Humic Acid and Selected Clays. Environ. Sci. Technol. 15, 834 (1981).

7. Choppin, G.R.: Humics and Radionuclide Migration. Radiochim. Acta 44/45, 23 (1988).

8. Chen, Y.Z., Tan, B.M., Lin, Z.J.: A Kinetic Study of the Reduction of Np(VI) with Humic Acid. Radiochim. Acta 62, 199 (1993).

9. Tan, J.X., Chen, Y.Z., Lin, Z.J.: A Kinetic Study of the Reduction of Plutonium with Humic Acid. Radiochim. Acta 61, 73 (1993).

10. Zeh, P., Kim, J.I., Marquardt, C.M., Artinger, R.: The Reduction of Np(V) in Groundwater Rich in Humic Substances. Radiochim. Acta 87, 23 (1999).

11. Marquardt, C., Artinger, R., Zeh, P., Kim, J.I.: Redoxchemistry of Neptunium in a Humic Rich Groundwater. In: FZKA 6324, Wissenschaftliche Berichte (G. Buckau, ed.). Forschungszentrum Karlsruhe, Karlsruhe 1999, p. 21.

12. André, C., Choppin, G.R.: Reduction of Pu(V) by Humic Acid. Radiochim. Acta 88, 613 (2000).

13. Artinger, R., Marquardt, C.M., Kim, J.I., Seibert, A., Trautmann, N., Kratz, J.V.: Humic Colloid-borne Np Migration: Influence of the Oxidation State. Radiochim. Acta 88, 609 (2000).

14. Marquardt, C.M., Seibert, A., Artinger, R., Denecke, M.A., Kuczewski, B., Schild, D., Fanghänel, Th.: The Redox Behaviour of Plutonium in Humic Rich Groundwater. Radiochim. Acta, in press.

15. Sachs, S., Schmeide, K., Brendler, V., Krepelová, A., Mibus, J., Geipel, G., Heise, K.H., Bernhard, G.: Investigation of the Complexation and the Migration of Actinides and Non-radioactive Substances with Humic Acids under Geogenic Conditions. Complexation of Humic Acids with Actinides in the Oxidation State IV Th, U, Np. FZR-399, Wissenschaftlich-Technische Berichte, Forschungszentrum Rossendorf, Dresden 2004.

16. Sachs, S., Geipel, G., Bernhard, G.: Study of the Redox Stability of Uranium(VI) in the Presence of Humic Substances. This report (2005).

17. Schmeide, K., Zänker, H., Heise, K.H., Nitsche, H.: Isolation and Characterization of Aquatic Humic Substances from the Bog 'Kleiner Kranichsee'. In: FZKA 6124, Wissenschaftliche Berichte (G. Buckau, ed.). Forschungszentrum Karlsruhe, Karlsruhe 1998, p. 161.

18. Kim, J.I., Buckau, G.: Characterization of Reference and Site Specific Humic Acids. RCM-Report 02188, TU München, Institute of Radiochemistry, München 1988.

19. Schnitzer, M., Khan, S.U.: Humic Substances in the Environment (A.D. McLaren, ed.). Marcel Dekker, New York 1972.

20. Bubner, M., Heise, K.H.: Characterization of Humic Acids. II. Characterization by Radioreagent-Derivatization with [$^{14}$C]Diazomethane. In: FZR 43, Annual Report 1993 (H.

Nitsche and G. Bernhard, eds.). Forschungszentrum Rossendorf, Institute of Radiochemistry, Dresden 1994, p. 22.

21. Bertrand, P.A., Choppin, G.R.: Separation of Actinides in Different Oxidation States by Solvent Extraction. Radiochim. Acta 31, 135 (1982).

22. Geipel, G., Bernhard, G., Brendler, V., Nitsche, H.: Complex Formation Between $UO_2^{2+}$ and $CO_3^{2-}$: Studied by Laser-Induced Photoacoustic Spectroscopy (LIPAS). Radiochim. Acta 82, 59 (1998).

23. Keller, C.: The Chemistry of the Transuranium Elements (K.H. Lieser, ed.). Verlag Chemie GmbH, Weinheim 1971, p. 294.

24. Wolery, T.J.: EQ3/6. A Software Package for the Geochemical Modeling of Aqueous Systems. Report UCRL-MA-110662 Part I. Lawrence Livermore National Laboratory, California, USA, 1992.

25. Guillaumont, R., Fanghänel, Th., Fuger, J., Grenthe, I., Neck, V., Palmer, D.A., Rand, M.H.: Update on the Chemical Thermodynamics of Uranium, Neptunium, Plutonium, Americium and Technetium. NEA Chemical Thermodynamics Vol. 5, Elsevier, Amsterdam 2003.

26. Artinger, R., Kuczewski, B., Marquardt, C.M., Schäfer, Th., Seibert, A., Fanghänel, Th.: Comparison of Humic Colloid Mediated Transport of Plutonium Studied by Column Experiments with Tri- and Tetravalent Actinide Experiments. In: FZKA 6969, Wissenschaftliche Berichte (G. Buckau, ed.). Forschungszentrum Karlsruhe, Karlsruhe 2004, p. 47.

27. Pompe, S., Schmeide, K., Bubner, M., Geipel, G., Heise, K.H., Bernhard, G., Nitsche, H.: Investigation of Humic Acid Complexation Behavior with Uranyl Ions Using Modified Synthetic and Natural Humic Acids. Radiochim. Acta 88, 553 (2000).

28. Schmeide, K., Sachs, S., Bubner, M., Reich, T., Heise, K.H., Bernhard, G.: Interaction of Uranium(VI) with Various Modified and Unmodified Natural and Synthetic Humic Substances Studied by EXAFS and FTIR Spectroscopy. Inorg. Chim. Acta 351, 133 (2003).

29. Geipel, G., Bernhard, G., Grambole, G.: Laser-Induced Photoacoustic Spectroscopic Studies of Neptunium. In: FZR-285, Annual Report 1999 (H. Nitsche and G. Bernhard, eds.). Forschungszentrum Rossendorf, Institute of Radiochemistry, Dresden 2000, p. 8.

30. Mesmin, C., Roudil, D., Hanssens, A., Madic, C.: New Laser Induced Photoacoustic Signal Measurement Method. Example of Application: Identification of the Uranium(IV)-dioxalato Complex in Solution. Radiochim. Acta 91, 385 (2003).

31. Schmeide, K., Reich, T., Sachs, S., Brendler, V., Heise, K.H., Bernhard, G.: Neptunium(IV) Complexation by Humic Substances Studied by X-ray Absorption Fine Structure Spectroscopy. Radiochim. Acta, accepted.

## Annex 4:

**Molecular Mass and Size Distributions and of Europium Complexed Humic Substances Measured by TOF-SIMS and AFFFF**

Szymczak W., Wolf M., Chanel V., Buckau G.

# Molecular mass and size distributions of europium complexed humic substances measured by TOF-SIMS and AFFFF

Szymczak W.[1], Wolf M.[2], Chanel V.[2], Buckau G.[3]

[1] GSF-National Research Center for Environment and Health, Institute of Radiation Protection, 85764 Neuherberg, Germany

[2] GSF-National Research Center for Environment and Health, Institute of Groundwater Ecology, 85764 Neuherberg, Germany

[3] Forschungszentrum Karlsruhe, Institut für nukleare Entsorgung, 76021 Karlsruhe, Germany

## 1. Introduction

Humic substances (HSs) are very complex mixtures of organic acids with only partly known structures, can be subdivided in fulvic acid (FA), humic acid (HA) and humin and are ubiquitous in the terrestrial and aquatic environment. The chemical properties of HSs to form relatively stable complexes with heavy metals and radionuclides have a strong influence on the migration of these pollutants in groundwater. To get a better knowledge of the type of HS complexes formed characterization of these complexes is necessary. The aim of this paper is the determination of the mass and size distribution of Eu-HS complexes with the methods time-of-flight secondary ion mass spectrometry (TOF-SIMS) and asymmetrical flow field-flow fractionation (AFFFF) to get a better understanding of the physical/chemical interactions of HSs with radionuclides. For this purpose different HSs (Gohy-573 FA and HA, Aldrich HA) loaded with europium (1%, 10% and 50% PEC/3, reaction time 1 day and 7-8 days) were investigated.

## 2. Materials and Methods

### 2.1 Materials

***2.1.1 Humic Substances.*** Natural aquatic humic and fulvic acids (Gohy-573 HA and FA) were isolated from groundwater of the deep borehole Gohy-573 in the Gorleben aquifer (Wolf et al. 2004a). Purified Aldrich humic acid (Aldrich HA) was obtained from Dr. Mizera (CTU Prague).

***2.1.2 Other Materials.*** Eu(III) acetate (purity 99.9 %) was obtained from Aldrich; ammonium acetate (purity > 98 %) was obtained from Merck. All substances were used as delivered and all aqueous solutions were prepared with high purity water (Milli-$Q_{PLUS}$, Millipore).

### 2.2 Methods

***2.2.1 Time-of-Flight Secondary Ion Mass Spectrometry (TOF-SIMS).*** Time-of-flight secondary ion mass spectrometry (TOF-SIMS) in combination with oblique 30 keV $SF_5^+$ ion bombardment produces highly reproducible mass spectra of HSs which cover up to five

orders of magnitude in dynamic range without background subtraction (Szymczak et al. 2000). The recorded spectra were highly reproducible, not just with respect to characteristic spectral features but also in absolute terms. Usually the measured yields were the same to within 10% or better. Spectra in the negative ionization mode are less affected by fragmentation than in the positive mode. Therefore, spectra are presented in the negative mode.

The time-of-flight secondary ion mass spectrometer used in this work has been described elsewhere (Szymczak and Wittmaack 2002). The bombardment parameters were as follows: primary ions $SF_5^+$, ion source terminal voltage 30 kV, target bias -6 kV (for negative secondary ions), ion impact energy 36 kV, stationary beam current 1–2 nA, pulse width about 3 ns, repetition rate 19 kHz, $1–3 \times 10^7$ pulses per spectrum, channel width 0.5 ns/bin. The nominal angle between the primary ion beam line and the surface normal of the sample is 60°. The area of ion bombardment was ~ $0.3 \times 0.4$ $mm^2$. The corresponding upper limit of detectable mass was m/z 6000. Neutrals generated along the first half of the beam line were removed by tilting the second half of the drift tube by a few degrees (both sections straight). The secondary ions were directed to the detector electrostatically. Postacceleration by biasing the detector was not applied.

Solid samples for TOF-SIMS analysis were prepared by spray-deposition on cleaned silicon substrates with a hydrophilic character (Szymczak et al. 2000). Solutions of 30 mg/L of HSs were dissolved in a dilute aqueous solution of $NH_4OH$. Typically 400 µL of solution were sprayed at a nozzle-to-substrate spacing of at least 35 mm. The area covered by the spray was a factor of about three to four larger than the area spanned by the silicon substrates (8x8 $mm^2$). The total amount of sprayed HSs was about 12 µg. This converts to areal densities of roughly 4.7 – 6.2 µg/$cm^2$.

***2.2.2 Asymmetrical Flow Field-Flow Fractionation (AFFFF).*** Field-flow fractionation is a technique for size fractionation of macromolecules and colloids. It was first proposed in 1966 by Giddings (Giddings 1966) and later also applied for humic substances (e.g. Ngo Manh Thang 2001). In this method the analyte, dissolved in a carrier medium, is pumped with constant velocity through a thin ribbon-like channel equipped with a membrane permeable for the carrier. The flow-field is established by a cross-flow perpendicular to the channel flow and the size fractionation is a function of the diffusion coefficient of the analyte. Two types of equipments are available: a) the first developed symmetrical flow field-flow fractionation (FFFF) using a symmetrical channel with constant width and two permeable walls and b) the more recently developed asymmetrical flow field-flow fractionation (AFFFF) using an asymmetrical channel with continuously reduced channel width and one permeable wall (Wahlund and Giddings 1987).

The AFFFF measurements were carried out at room temperature with a system delivered from Wyatt Technology using an asymmetrical fractionation channel from ConSenxus (Germany) with a length of 286 mm and a spacer thickness of 0.54 mm. The used regenerated cellulose membrane has a cut-off of 1 kDa (related to globular proteins). As eluent 10 mM ammonium acetate with a pH of ~6.8 at room temperature was used at a channel flow of 0.6 mL/min and a cross-flow of 3.0 mL/min. The absorbance of the effluent was recorded with an UV/Vis detector (K-2500, Knauer, Germany) at 210 nm. The fractionated sample volume was 20 µL.

Eu-HS complexes were prepared with HSs (30 mg/L) dissolved in 10 mM ammonium acetate and different Eu loads (1, 10 and 50 % PEC/3).

## 3. Results and Discussion

### 3.1 Molecular mass distribution of Eu-HS complexes

The measured molecular mass distributions by TOF-SIMS of the Eu-HSs complexes change with the amount of Eu-loading. In comparison to the pure HSs the overall outcome is that a higher mass region appears to grow with europium complexation at the expense of a decrease in lower mass region (Fig. 1).
The absolute yields are influenced by the topographic features of the Eu-HS deposit. With

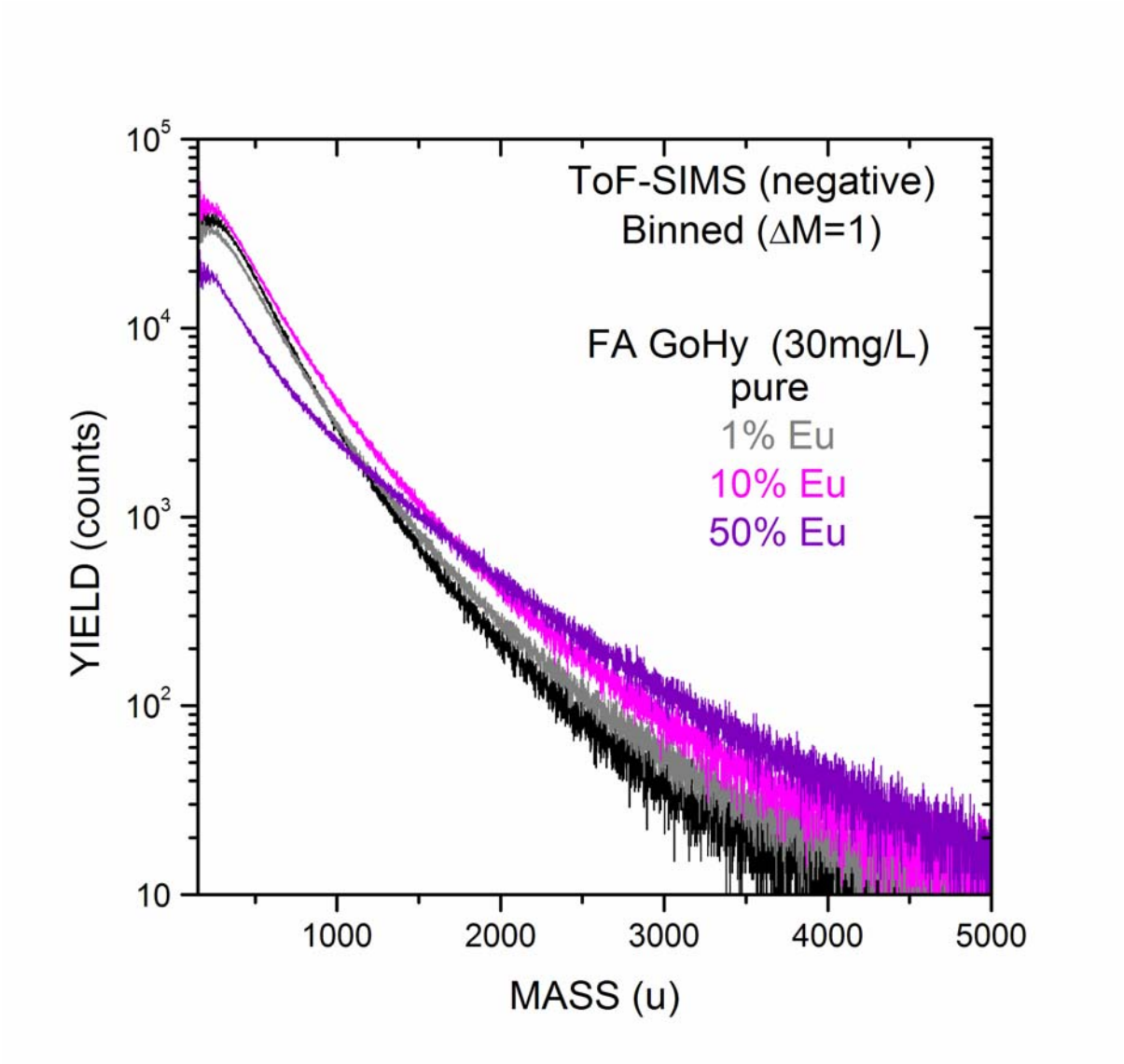


Fig. 1: Molecular mass distributions of pure and Eu-loaded (1, 10 and 50 % PEC/3) Gohy-573 FA measured from a deposit of an 1 d aged solution.

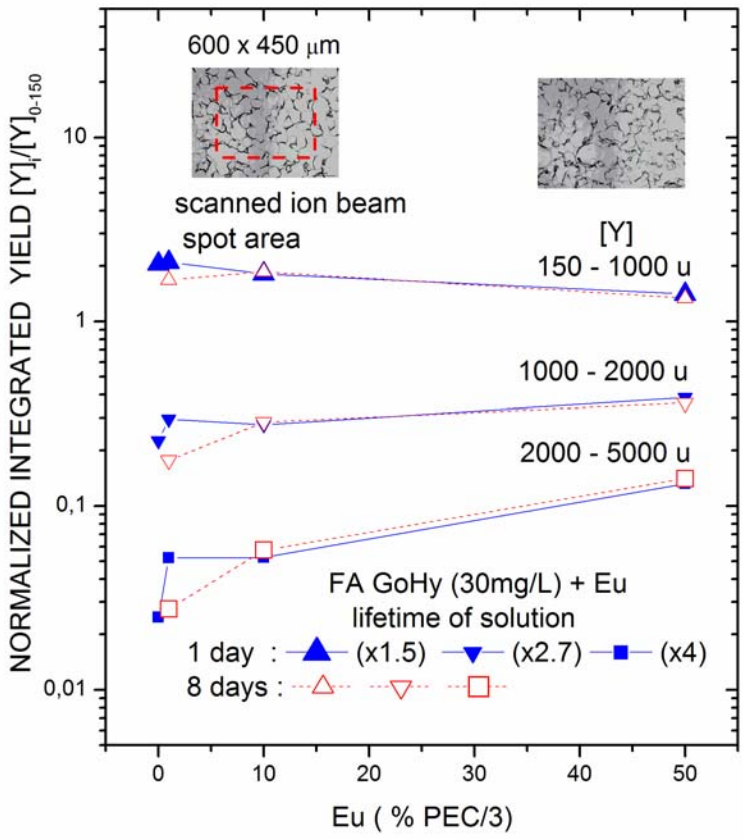


Fig. 2: Normalized integrated yields of molecular mass distributions of pure and Eu-loaded (1, 10 and 50 % PEC/3) Gohy-573 FA measured from deposits of 1 and 8 d aged solution. The microscopic picture insets depict the Eu-loaded FA spray deposit on Si-wafer.

increasing Eu-loading the topography becomes more jagged (cp. insets in Fig. 2). By normalizing the summed yield [Y] over broad mass ranges to the summed yield $[Y]_{0\text{-}150}$ of the lowest mass region below 100 u the effect of topographic induced changes in the absolute yield can be included. The normalized integrated yield around the broad maximum $[Y]_{150\text{-}1000}$ decreases slightly with the Eu-loading whereas in the mass region of the tail $[Y]_{2000\ \text{-}5000}$ increases with Eu-loading. The same tendency is seen with the deposits from a 8 day aged Eu-HS solution (Fig. 2).

From the analysis in the positive mode the $EuOH^+$ peak intensity increases roughly proportional with the Eu-loading. Compared to the spectrum of the pure Eu-acetate deposit where the $Eu^+$ signal is as high as the $EuOH^+$ signal the $Eu^+$ peak is strongly suppressed. This may indicate, that the $EuOH^+$ is rather cleaved from an Eu-HS complex than from segregated Eu.

The ratios of the pure HSs to the europium loaded samples calculated at integrated mass intervals ($\Delta M$ = 5 u) depict the affected mass regions in more detail (Fig. 3). With the Gohy-573 FA the ratio have a common peak maximum around 385 u roughly independent of the europium content and with increasing europium complexation the grow at masses above the ratio peak maximum becomes more pronounced.

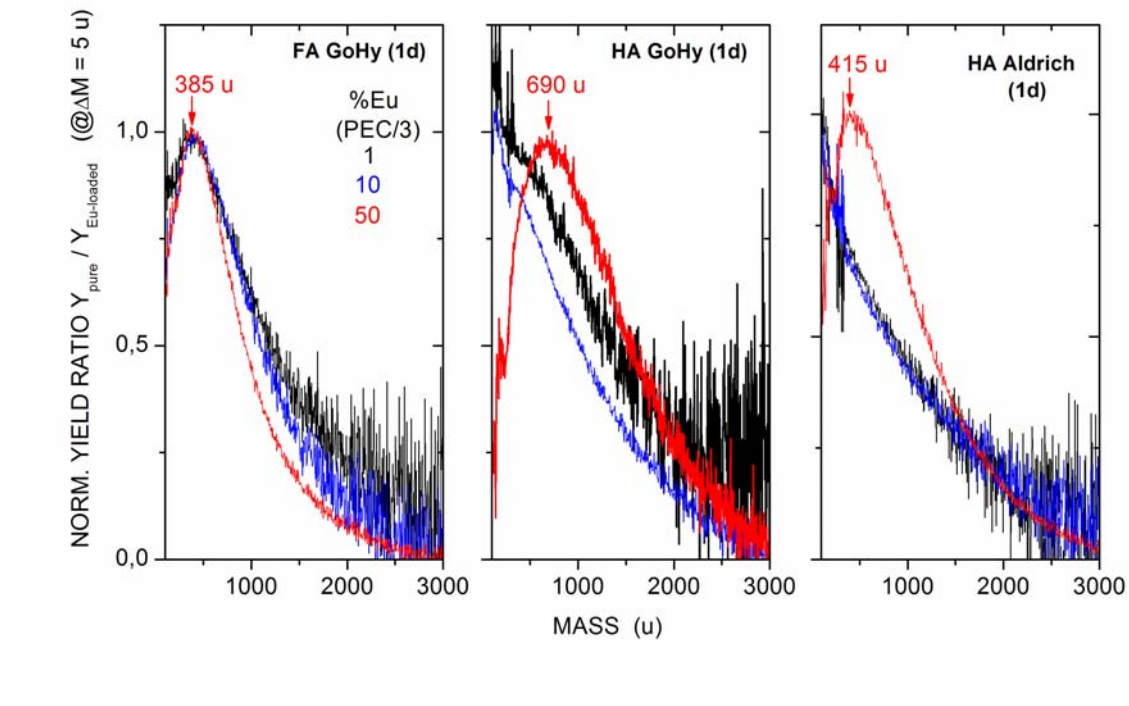


Fig. 3: Normalized yield ratios of molecular mass distribution of pure and Eu-loaded (1, 10 and 50 % PEC/3) Gohy-573 FA, HA and Aldrich HA from deposits of an 1 d aged solution.

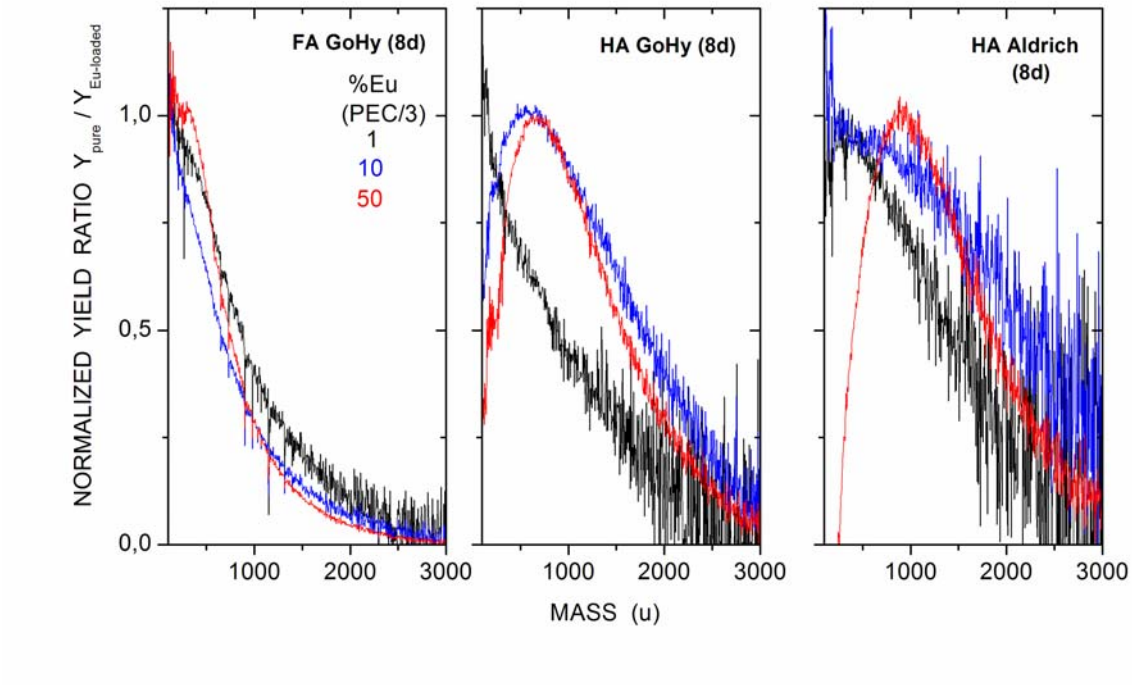


Fig. 4: Normalized yield ratios of molecular mass distribution of pure and Eu-loaded (1, 10 and 50 % PEC/3) Gohy-573 FA, HA and Aldrich HA from deposits of an 8 d aged solution.

With the Gohy-573 HA and the Aldrich HA there is only a peak maximum of the ratio at the highest europium load (50% PEC/3) which is roughly twice the FA value in the case of the Gohy-573 HA (690 u) and only slightly shifted in the case of the Aldrich HA (415 u). Aging of the solution add to the change of the mass distributions of the Gohy-573 HA and the Aldrich HA at already lower europium loading (10% PEC/3), cp. Fig. 4.

### 3.2 Molecular size distribution of Eu-HS complexes

The transformation of the AFFFF fractograms into the size distribution (relative mass concentration related to the mass of the used standards) plotted on a logarithmic mass scale was done after Wolf et al. (2004b). The derived molecular size distributions of the analyzed HSs are plotted in Fig. 5-7. The molecular size distributions of the pure Gohy-573 FA and the Eu-loaded (1, 10 and 50 % PEC/3) Gohy-573 FA measured 1 d (Fig. 5) or 7 d (Fig. 6) after preparation show no detectable differences. The reasons for these results may be that 1) the formed Eu-FA complexes have probably similar size than the pure FA and no further aggregation between Eu-FA complexes, between Eu-FA complexes and FA or between different FA molecules happens by Eu loads up to 50 % PEC/3 or 2) during the measurements existing Eu-HS complexes are dissociating very fast. On the other side show size distributions of Eu-HA complexes of Gohy-573 (Fig. 7) in comparison to the size distributions of the pure HA small differences with a tendency to slightly larger molecular sizes (particularly the complexes with the highest Eu load). Contrary to FA also the size distributions of the pure HA show after 7 days a tendency to larger size distributions probably caused by small changes in the aggregation state.

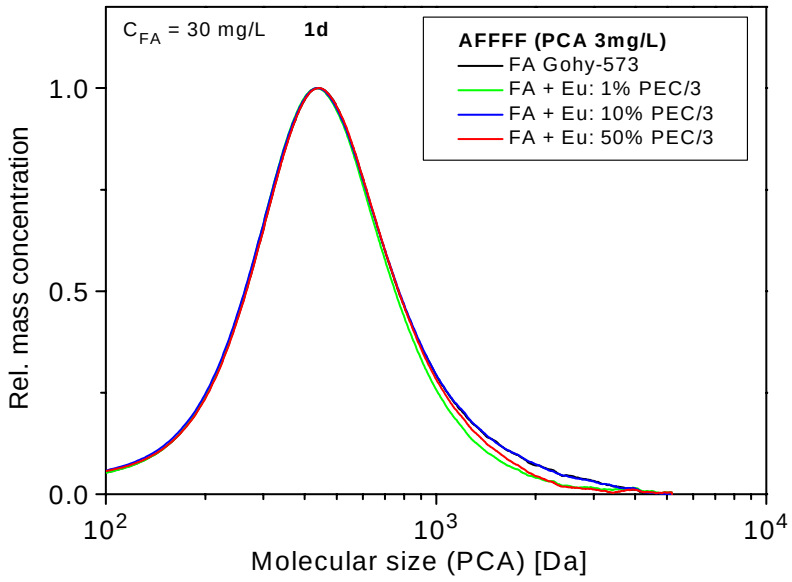


Fig. 5: Molecular size distribution of pure and Eu-loaded (1, 10 and 50 % PEC/3) Gohy-573 FA measured 1 d after preparation.

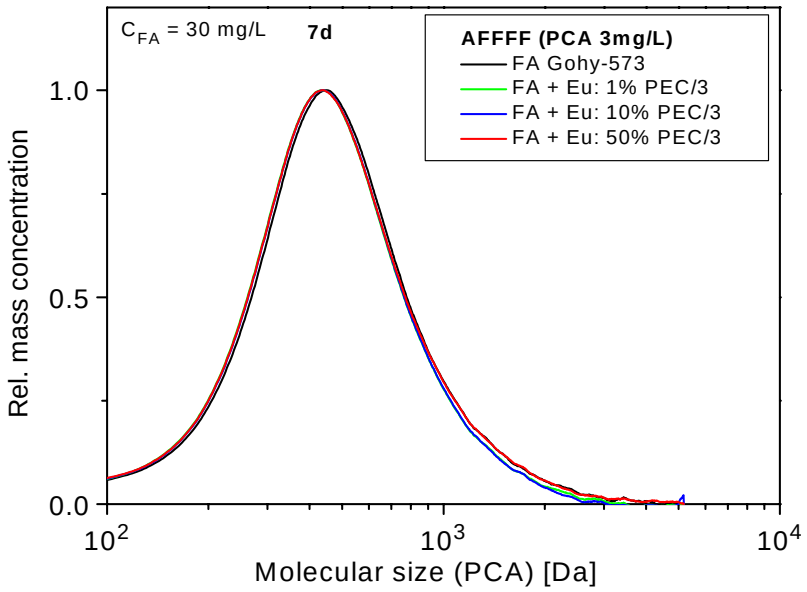


Fig. 6: Molecular size distribution of pure and Eu-loaded (1, 10 and 50 % PEC/3) Gohy-573 FA measured 7 d after preparation.

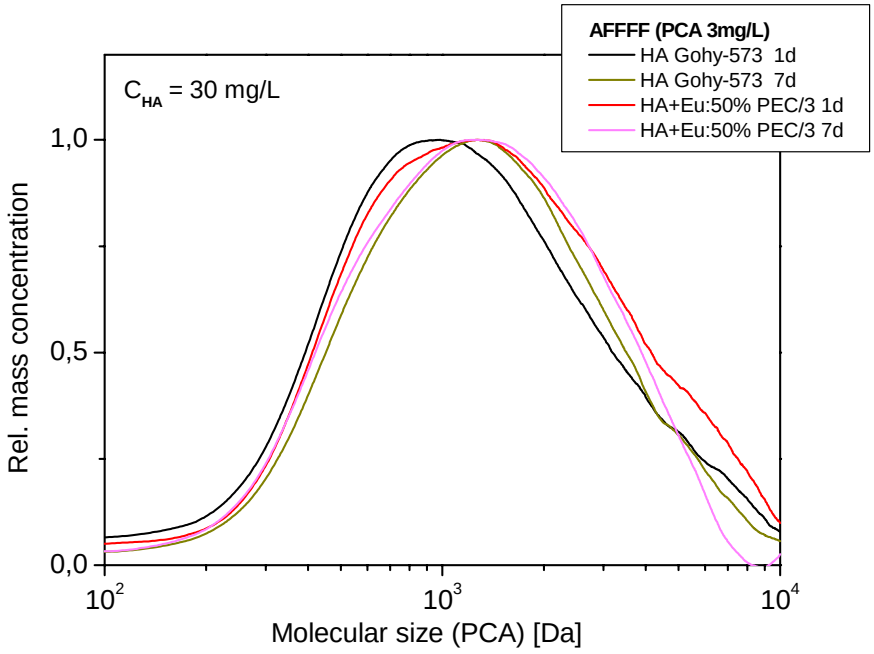


Fig. 7: Molecular size distribution of pure and Eu-loaded (50 % PEC/3) Gohy-573 HA measured 1 and 7 d after preparation.

## 4. Conclusions

The spectral changes in the mass distribution of the Eu-loaded samples with its displacement of species frequency from low to higher mass regions support the formation of Eu-HS complexes. But the distinct changes in the mass of Eu-HSs complexes are not significantly related to the size of europium loaded HSs as measured by AFFFF. Mass spectrometry shows a strong impact of complexation on the mass distribution of HSs, e.g. higher mass region appears to grow with europium complexation at the expense of a decrease in lower mass region. The impact is lower on fulvic acid than on humic acid and in addition longer contact times enhance the impact on humic acids. Topographic changes in the deposit from the Eu-HS solutions onto the Si-wafer modify the absolute intensities of the TOF-SIMS yield and inhibit the evaluation on an absolute scale.

## 5. Acknowledgements

The authors thank Dr. J. Mizera (CTU Prague) for making the purified Aldrich HA available and D. Jurrat and G. Teichmann for technical support in the laboratory.

## References

Giddings J.C. (1966) A new separation concept based on a coupling of concentration and flow uniformities. *Sep. Sci.* **1**, 123-125.

Ngo Manh Thang, Geckeis H., Kim J.I., Beck H.P. (2001) Application of the flow field flow fractionation (FFFF) to the characterization of aquatic humic colloids: evaluation and optimization of the method. *Colloids Surf. A* **181**, 289-301.

Szymczak W., Wolf M., Wittmaack K. (2000) Characterization of Fulvic Acids and Glycyrrizic Acid by Time-of-Flight Secondary Ion Mass Spectrometry. Acta hydrochim. hydrobiol. **28**, 350-358.

Szymczak W., Wittmaack K. (2002) Effect of water treatment on analyte and matrix ion yields in matrix-assisted time-of-flight secondary ion mass spectrometry: the case insulin in and on hydroxycinnamic acid. Rapid Commun. Mass Spectrom. **16**, 2025-2033.

Szymczak W., Wolf M., Wittmaack K. (2004) Comparison of as-delivered and AFFFF-size-fractionated Suwannee River fulvic acid by time-of-flight mass spectrometry, In: Humic Substances: Nature's Most Versatile Materials (Eds. E.A. Ghabbour and G. Davies), Taylor & Francis, New York, 31-38.

Wahlund K.-G., Giddings J.C. (1987) Properties of an asymmetrical flow field-flow fractionation channel having one permeable wall. *Anal. Chem.* **59**, 1332-1339.

Wolf M., Buckau G., Geyer S. (2004a) Isolation and characterization of new batches of Gohy-573 humic and fulvic acids. In: Buckau G. (ed.) *Humic substances in performance assessment of nuclear waste disposal: Actinide and iodine migration in the far-field.* Second Technical Progress Report, FZK/INE, Karlsruhe, 111-124.

Wolf M., Szymczak W., Chanel V., Buckau G. (2004b) Molecular size and mass distributions of humic substances measured by AFFFF and TOF-SIMS. In: Buckau G. (ed.) *Humic substances in performance assessment of nuclear waste disposal: Actinide and iodine migration in the far-field.* Second Technical Progress Report, FZK/INE, Karlsruhe, 95-110.

## Annex 5:

**Iodination of the Humic Samples from HUPA Project**

Reiller P., Mercier-Bion F., Gimenez N., Barré N., Miserque F.

# Iodination of the humic samples from HUPA project

*Pascal Reiller,[1] Florence Mercier-Bion,[2] Nicolas Gimenez,[1,2] Nicole Barré[2] and Frédéric Miserque[3]*

[1] CEA/DEN/DPC/SECR/Laboratoire de Spéciation des Radionucléides et des Molécules, CE Saclay, Bâtiment 391, BP 11, F-91191 Gif-sur-Yvette CEDEX, FRANCE

[2] UMR 8587 «Analyse et Environnement» (CEA/CNRS/Université d'Evry Val-d'Essonne) CE Saclay, F-91191 Gif-sur-Yvette Cedex, FRANCE.

[3] CEA/DEN/DPC/SCP/Laboratoire de Réactivité des Surfaces et Interfaces, CE Saclay, Bâtiment 391, BP 11, F-91191 Gif-sur-Yvette CEDEX, FRANCE.

## Introduction

The interaction of iodine with natural organic matter in general and with humic substances (HS) in particular, has been the subject of numerous studies. It has come to a consensus that in soils as well as in aquatic systems, the speciation of iodine is closely related to the redox potential of the medium. In oxidizing media, as in sea water or upper horizons, the major part of iodine is found in iodate form $IO_3^-$, whereas in reducing media, iodide $I^-$ is the major specie. Nevertheless, it has been shown that in some cases, organically bound iodine can dominate the speciation either as methyl iodide [1] or bounded to humic substances [2-6].

It is now also clear that this reactivity is closely related to the occurrence of molecular iodine $I_2$(aq) and its disproportionation to HIO and $I^-$. The reaction scheme can be viewed as an electrophilic substitution of an hydrogen to an iodine atom on a phenolic ring [7]:

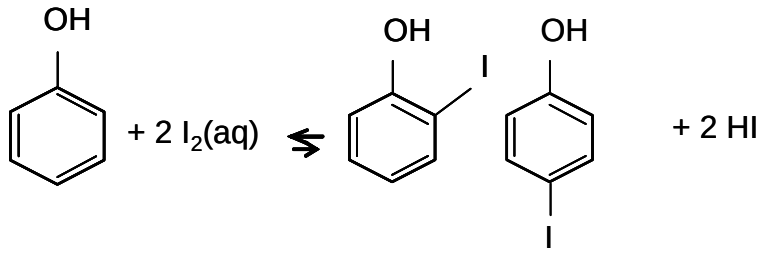


This reaction is well known in water treatment with HOCl to lead to trihalomethane [8, 9]. This scheme has been validated in the case of HS on different samples including HUPA [10-12], and the covalent character of this interaction has been shown using electrospray ionization mass spectroscopy (ESI-MS) [13], X-ray photoelectron spectroscopy [14-16].

Nevertheless, in some of the latter studies, the characterization of the final reaction products did not satisfied the authors completely as total separation from $I^-$ could not be achieved. Thus, further studies were led using HUPA samples: natural humic and fulvic extract from Gorleben and synthetic samples obtained from FZ Rossendorf. Dialysis procedures were envisaged to improve the incomplete separation between the colloidal humic matter and the iodide ions either unreacted or produced by the reaction [12].

## Materials

Humic and fulvic acids from Gorleben deep borehole Gohy-573 was obtained from GSF [17], and synthetic samples were obtained from FZ Rossendorf [18]. Weighted samples were dissolved in $10^{-4}$ NaOH (pH ≈ 10) in order to attain a thorough dissolution of HA and to have the samples in the same conditions before iodination procedure.

The stock saturated solutions of $I_2$(aq) was prepared from bisublimed iodine (Prolabo), at a concentration of $10^{-3}$ mol/L [19]. NaI was obtained from Merck.

UV-Visible absorption spectra were obtained using a Cary 1 spectrophotometer.

As in previous studies [10, 12], kinetics of consumption of iodine by HS was monitored through the decrease in UV-Visible absorbance of triiodide complex (351 nm).

The XPS experiments were carried out at the "Surfaces and Interfaces Laboratory" of the CEA (Saclay, France), with a VG Instruments® 220i spectrometer by using an monochromated $AlK_\alpha$ X-ray source (incident energy: 1486.6 eV). A source power of 15 kV and of 20 mA was used. The dimensions of the X-ray beam were approximately 8 mm per 7 mm. The analysis chamber pressure was in the range of $10^{-8}$ Torr. The BE resolution of the spectrometer was estimated to 0.2 eV. No charge effect compensation was achieved during the XPS analyses and so all the BE values were corrected using the $C_{1s}$ signal of contamination carbon at 285 eV.

## Results and discussion

*UV-Visible spectrosocopy*

Firstly, the reaction pattern was verified on the samples. The kinetics of the triiodide consumptions by Gohy HA and FA are reported in figure 1. The decreases in absorbance are somewhat faster than in the previous studies on Mol and Aldrich samples. As in the previous cases, the kinetics cannot be linearalised.

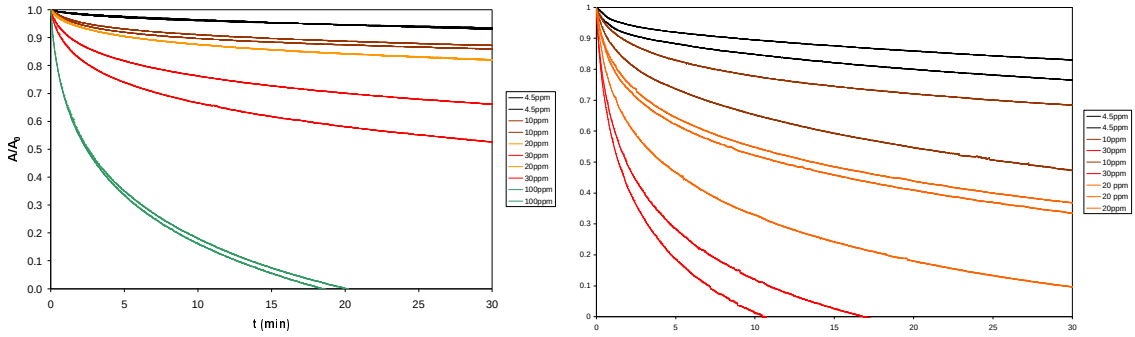


**Figure 1 : Kinetics of consumption of triiodide complex by HA and FA Gohy-573 at pH = 5 and *I* = 0.1 M $NaClO_4$.**

The same experiments were performed on the synthetic samples M1 and M42 from Rossendorf. The kinetic patterns are even faster than the natural humic samples as it can be seen in figure 2.

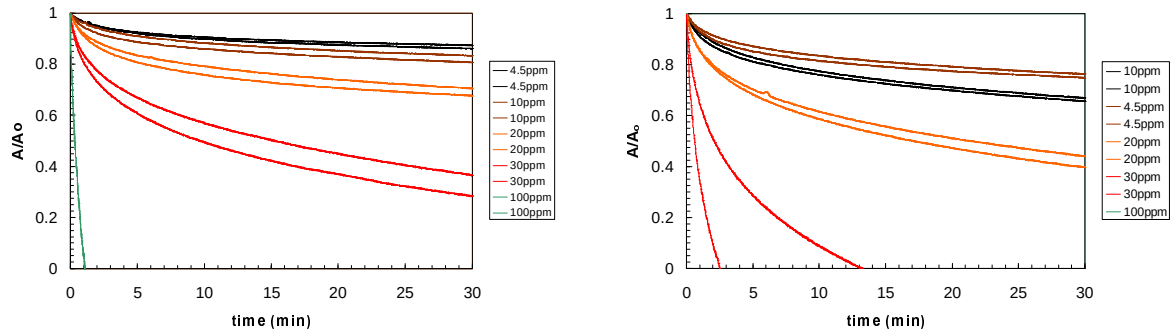


**M1** **M42**

**Figure 2 : : Kinetics of consumption of triiodide complex by synthetic HA at pH = 5 and *I* = 0.1 M $NaClO_4$.**

The kinetics of the different samples can be compared in figure 3 as they were acquired in comparable conditions at pH = 5, except for the Mol sample (pH = 6). It can be seen in figure 3 that the kinetics increases from Aldrich to M42 samples. This behaviour can be related to the elementary ration H/C, which in turn can be related to the aromaticity of the humic sample. The H/C ratios calculated from the elementary compositions of these samples are reported in table 1. Hence, the increase of the iodination kinetics can clearly be related to the decrease of the H/C ratio, *i.e.* to the increasing aromaticity of the samples. The case of Mol 15B sample, which appears to be faster than Aldrich whereas its H/C value is somewhat higher is not surprising knowing that the kinetics has a negative order in $[H^+]$, *i.e.* it increases with pH [10, 12].

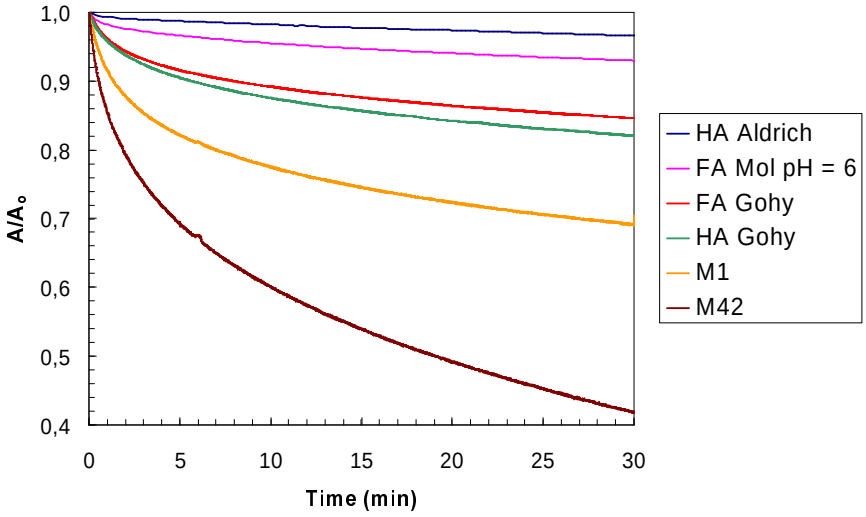


**Figure 3 : Kinetics of triiodide complex consumption by humic samples at pH = 5.**

**Table 1: Elementary ratio for the different iodinated samples.**

| Sample | H/C |
|---|---|
| Mol 15B | 0.98 [20] |
| Aldrich | 0.97 [21] |
| FA Gohy | 0.93 [17] |
| HA Gohy | 0.92 [17] |
| M1 | 0.89 [18] |
| M42 | 0.87 [18] |

Warner *et al.* [10] and Reiller & Moulin [12] already identified the decrease of the $I_3^-$ absorption bands in the near UV region. The release of $I^-$ due to the halogenation can also be evidenced in the UV region when $\lambda \leq 250$ nm. The same experiment was performed with Gohy-573 HA (20 ppm) and $I_2$(aq) ($10^{-4}$ M). The absorption spectra were acquired in the range 190-260 nm every 1.25 minutes (

Figure 4).

The initial absorption represents the cumulative spectrum of $I_2$(aq), $I^-$, $I_3^-$ and HA. With time, absorbance at $\lambda \approx 230$ nm representing the first UV band of $I^-$ increases, shifted by the addition of HA absorption. The second iodide UV-band at $\lambda \approx 190$ nm also increases as the broad absorption band of $I_2$(aq) at $\lambda \approx 205$ nm decreases resulting in two isobestic points.

The different contributions of iodide and molecular iodine are reported in figure 5.

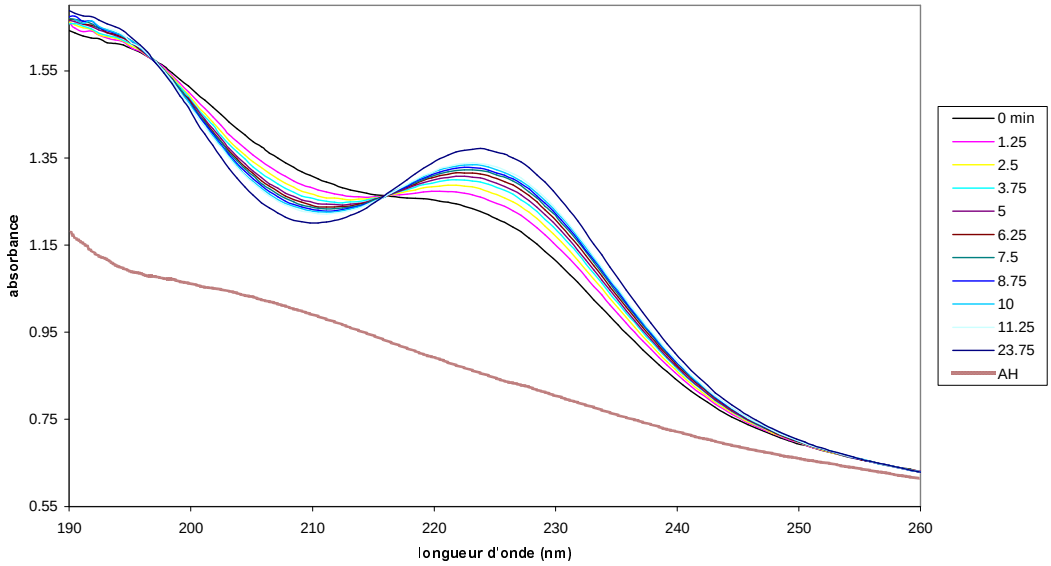


**Figure 4 : UV-visible Spectra resulting from the reaction between Gohy-573 HA and $I_2$(aq): [HA] = 20 ppm ; [$I_2$(aq)] = $10^{-4}$ M.**

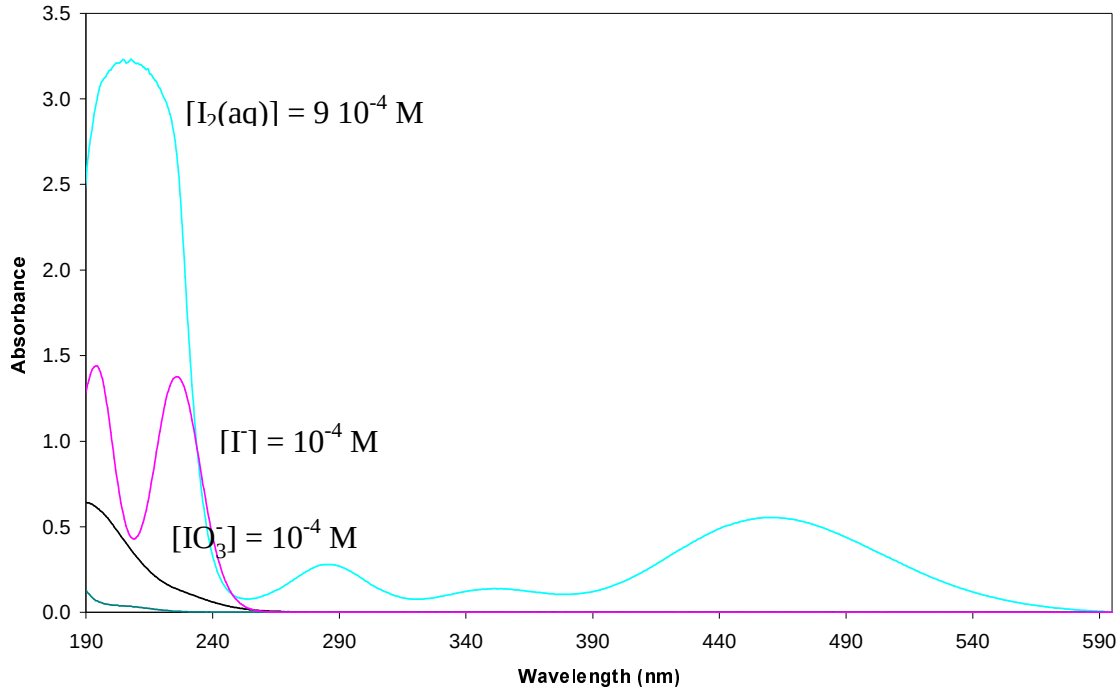


**Figure 5: Absorption spectra of iodide, molecular iodine and iodate.**

*X-ray Photoelectron Spectroscopy results*

XPS spectroscopy is a surface analysis technique (the analyzed depth is of some nanometers under the sample surface), well adapted to derive information on the chemical environment of one atom. The principle of the technique lies in measuring the binding energy (BE) of core electrons ejected from this atom under photoionization. The measured BE enables to determine the nature of the chemical bonds in which the atom is implied (ionic or covalent character, nature of associated ligands).

Before XPS analyses, the powdered humic substances were fixed on double-sided carbon tape.

To determine the chemical environment of iodine, the BE position of the core-level region $I_{3d5/2}$ of iodine was followed for all the humic substances, such as natural humic substances *"GOHY 573"* (Fulvic Acid FA) extracted from the Gorleben groundwaters, and synthetic humic acids *"M1"* and *"M42"* obtained from FZ Rossendorf contacted to diiodine solutions. The $I_{3d5/2}$ XPS spectra were deconvoluted by using the VG Instruments® software "AVANTAGE".

The preparation of the binary system "humic substances/diiodine consists in the contact of 50 mL of HS (stock solution : HS powder dissolved in NaOH and prepared in pH = 5 solution of concentration 2 g/L) with 50 mL of a diiodine solution of concentration $10^{-3}$ mol.L$^{-1}$. The solutions were then dialysed against pure water. The outer compartment was renewed until no $I^-$ could be detected in UV-Visible spectrophotometry (LoD = $10^{-5}$ M)

The four humic substances samples contacted with diiodine were analyzed by XPS (humic and fulvic acids "GOHY 573" and synthetic humic acids M1 and M42). As XPS is a solid investigation technique, a drop of the solution was set on a glass slide and dried under hood until the solvent evaporation.

All the samples revealed the presence of iodine, as showed by the obvious $I_{3d5/2}$ signal (Figure 6 to 9), and so relatively to the same samples non contacted with diiodine solutions (see Figure 8

for M1 and Figure 9 for the comparison of the survey spectra of M42 without and with contact to the $I_2$ solution).

The deconvolution of the $I_{3d5/2}$ peak of all the samples indicates a major contribution at 620.8 eV, corresponding to iodine atoms attached by covalent bonds to the organic matter, as already evidenced in our previous studies by XPS and XANES on natural humic substances of different geological media [15, 16, 22].

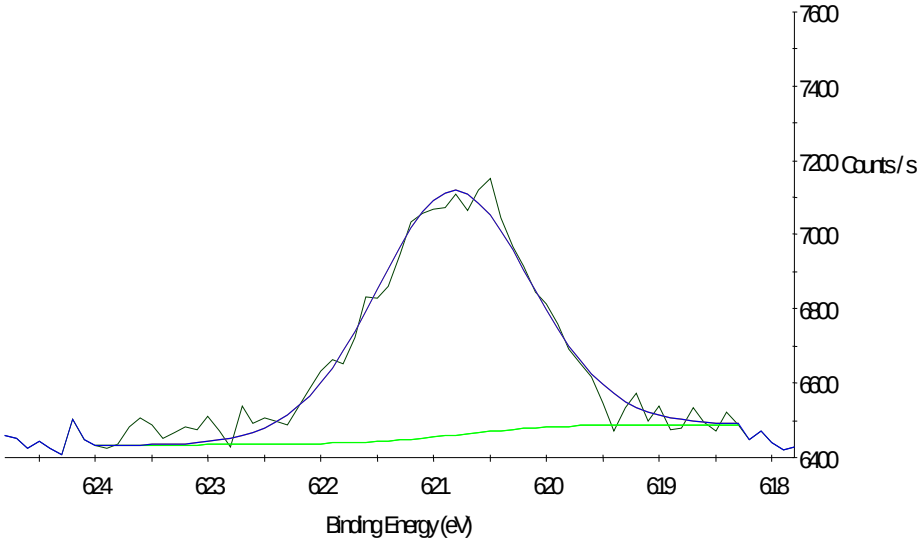


**Figure 6: $I_{3d5/2}$ region of the fulvic acid GOHY 573 contacted to diiodine**

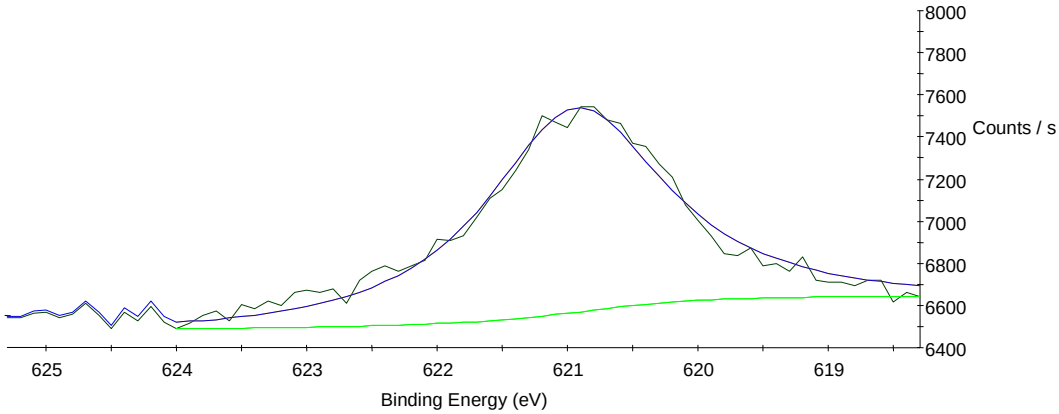


**Figure 7: $I_{3d5/2}$ region of the humic acid GOHY 573 contacted to diiodine**

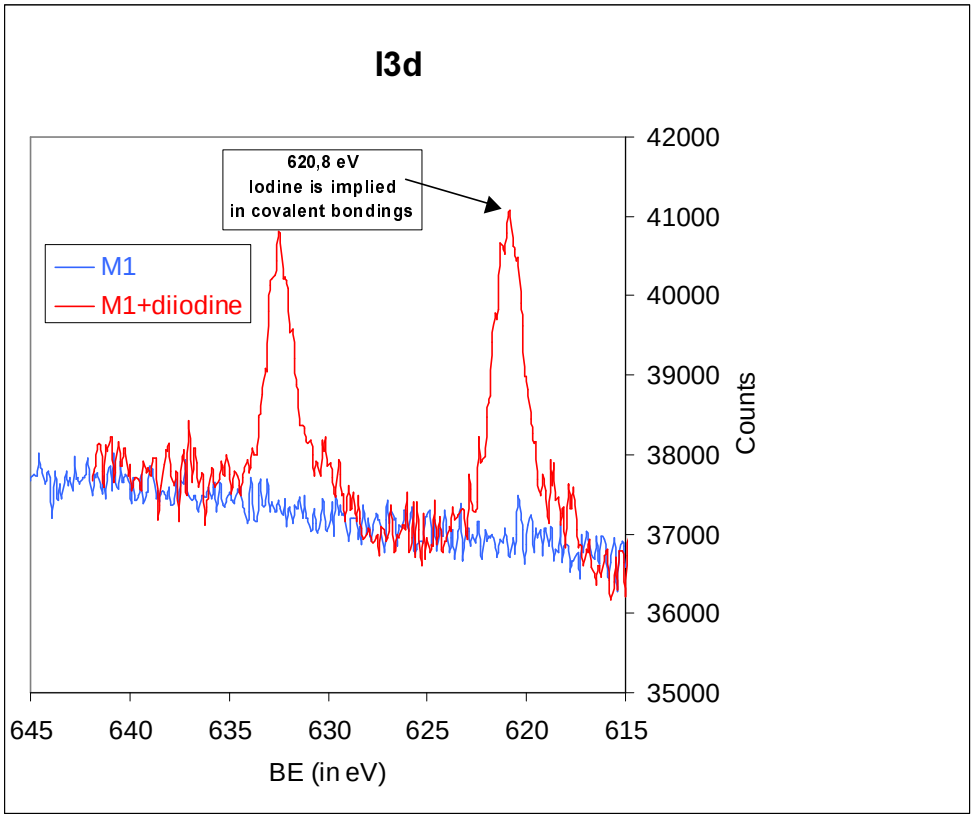


**Figure 8: $I_{3d5/2}$ region of the humic acid M1 contacted to diiodine**

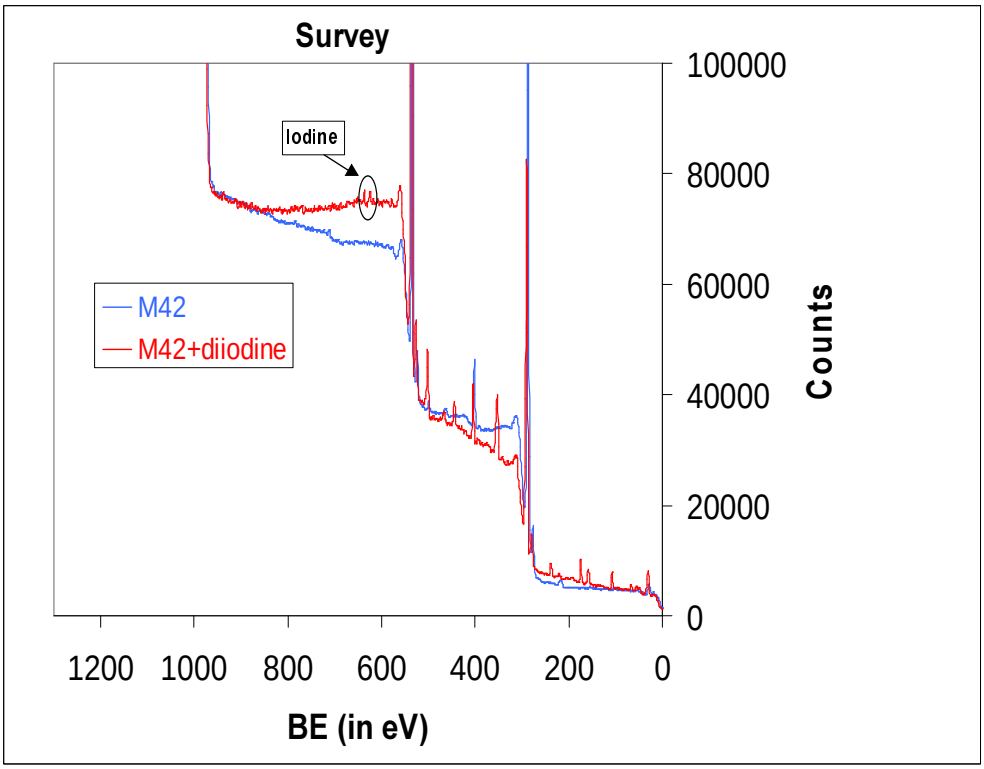


**Figure 9: Survey spectra of the humic acid M42 and of the humic acid contacted to diiodine**

## References


1. Tessier, E., Amouroux, D., Abril, G., Lemaire, E., Donard, O. F. X.: Formation and volatilisation of alkyl-iodides and -selenides in macrotidal estuaries. Biogeochemistry **59**, 183 (2002).
2. Yamada, H., Hisamori, I., Yonebayashi, K.: Identification of organically bound iodine in soil humic substances by size exclusion chromatography/inductively coupled plasma mass spectrometry (SEC/ICP-MS). Soil Sci. Plant Nutr. **48**, 379 (2002).
3. Yamada, H., Kiriyama, T., Onagawa, Y., Hisamori, I., Miyazaki, C., Yonebayashi, K.: Speciation of iodine in soils. Soil Sci. Plant Nutr. **45**, 563 (1999).
4. Andersen, S., Petersen, S. B., Laurberg, P.: Iodine in drinking water in Denmark is bound in humic substances. Eur. J. Endocrinol. **147**, 663 (2002).
5. Pedersen, K. M., Laurberg, P., Nohr, S., Jorgensen, A., Andersen, S.: Iodine in drinking water varies by more than 100-fold in Denmark. Importance for iodine content of infant formulas. Eur. J. Endocrinol. **140**, 400 (1999).
6. Bostock, A. C., Shaw, G., Bell, J. N. B.: The volatilisation and sorption of I-129 in coniferous forest, grassland and frozen soils. J. Environ. Rad. **70**, 29 (2003).
7. Lee, C. F.: Kinetics of reactions between chlorine and phenolic compounds. Principles and Applications of water chemistry proceedings. In: (Faust, S. D. and Hunter, J. V. eds.). Wiley, (1967) p. 54.
8. Gallard, H., Von Gunten, U.: Chlorination of phenols: Kinetics and formation of chloroform. Environ. Sci. Technol. **36**, 884 (2002).
9. Bichsel, Y., von Gunten, U.: Formation of iodo-trihalomethanes during disinfection and oxidation of iodide-containing waters. Environ. Sci. Technol. **34**, 2784 (2000).
10. Warner, J. A., Casey, W. H., Dahlgren, R. A.: Interaction kinetics of $I_2$(aq) with substituted phenols and humic substances. Environ. Sci. Technol. **34**, 3180 (2000).
11. Reiller, P., Moulin, V.: Influence of organic matter in the prediction of iodine migration in natural environment. Mat. Res. Soc. Symp. Proc. **757**, 565 (2003).
12. Reiller, P., Moulin, V.: Chemical data on iodine-natural organic mater interaction. In: *Humic substances in performance assessment of nuclear waste disposal: Actinide and iodine migration in the far-field. First technical report* (Buckau, G. ed.). INE, Report FZKA 6800, Karlsruhe (2003) p. 99.
13. Moulin, V., Reiller, P., Amekraz, B., Moulin, C.: Direct characterization of iodine covalently bound to fulvic acids by electrospray mass spectrometry. Rapid Commun. Mass Spectrom. **15**, 2488 (2001).
14. Mercier, F., Moulin, V., Barré, N., Trocellier, P., Toulhoat, P.: Study of a ternary system silica/humic acids/iodine: capabilities of the nuclear microprobe. Nuclear Instruments and Methods in Physics Research B **181**, 628 (2001).
15. Mercier, F., Moulin, V., Guittet, M. J., Barré, N., Toulhoat, N., Gautier-Soyer, M., Toulhoat, P.: Applications of NAA, PIXE and XPS for the quantification and characterization of the humic substances/iodine associations. Radiochim. Acta **88**, 779 (2000).
16. Mercier, F., Moulin, V., Guittet, M. J., Barre, N., Gautier-Soyer, M., Trocellier, P., Toulhoat, P.: Applications of new surface analysis techniques (NMA and XPS) to humic substances. Org. Geochem. **33**, 247 (2002).
17. Wolf, M., Buckau, G., Geyer, S.: Isolation and characterization of new batches of Gohy-573 humic and fulvic acids. In: *Humic Substances in Performance Assessment of Nuclear Waste Disposal: Actinide and Iodine Migration in the Far-Field. Second Technical Progress Report* (Buckau, G. ed.). FZK-INE, Report FZKA 6969, Karlsruhe (2004) p. 111.

18. Sachs, S., Heise, K. H., Bernhard, G.: Synthetic humic acid model substances with specific functional porperties for the use in complexation and sorption experiments with actinides. In: *Humic Substances in Performance Assessment of Nuclear Waste Disposal: Actinide and Iodine Migration in the Far-Field (First Technical Progress Report)* (Buckau, G. ed.). FZK-INE, Report FZKA 68000, Karlsruhe (2003) p. 51.

19. Ramette, R. W., Sandford, R. W.: Thermodynamics of iodine solubility and triiodide ion formation in water and in deuterium oxide. J. Am. Chem. Soc. **87**, 5001 (1965).

20. Montjotin, C.: Isolation, caractérisation et mesures des teneurs en $^{14}C$ de substances humiques aquatiques: application à la datation des eaux souterraines. Université d'Orsay, Paris Sud, Orsay (1996).

21. Kim, J. I., Buckau, G., Klenze, R., Rhee, D. S., Wimmer, H.: Characterisation and complexation of humic acids. Commission of the European Communities, Report EUR 13181, Brussels (1991).

22. Mercier-Bion, F., Barré, N., Moulin, V., Jeanvoine, Y., Cartailler, T.: Study of the interactions between iodine and humic substances: coupling of experimental and theoretical approaches. Radiochim. Acta (submitted).

## Annex 6:

**Accounting for Chemical Kinetics in Field Scale Transport Calculations.**
Bryan N.D.

# Accounting for Chemical Kinetics in Field Scale Transport Calculations.

Bryan N.D.

Department of Chemistry, The University of Manchester, Oxford Rd., Manchester, UK.

## Abstract

The modelling of column experiments has shown that the humic acid mediated transport of metal ions is dominated by the non-exchangeable fraction. Metal ions enter this fraction via the exchangeable fraction, and may transfer back again. However, in both directions these chemical reactions are slow. Whether or not a kinetic description of these processes is required during transport calculations, or an assumption of local equilibrium will suffice, will depend upon the ratio of the reaction half-time to the residence time of species within the groundwater column. If the flow rate is sufficiently slow or the reaction sufficiently fast then the assumption of local equilibrium is acceptable. Alternatively, if the reaction is sufficiently slow (or the flow rate fast), then the reaction may be 'decoupled', i.e. removed from the calculation. These distinctions are important, because calculations involving chemical kinetics are computationally very expensive, and should be avoided wherever possible. In addition, column experiments have shown that the sorption of humic substances and metal-humate complexes may be significant, and that these reactions may also be slow. In this work, a set of rules is presented that dictate when the local equilibrium and decoupled assumptions may be used. In addition, it is shown that in all cases to a first approximation, the behaviour of a kinetically controlled species, and in particular its final distribution against distance at the end of a calculation, depends only upon the ratio of the reaction first order rate to the residence time, and hence, even in the region where the simplifications may not be used, the behaviour is predictable. In this way, it is possible to obtain an estimate of the migration of these species, without the need for a complex transport calculation.

## Introduction

Over the last 6 years models have been developed that are able to predict the humate mediated transport of metal ions in laboratory column experiments (e.g. Warwick et al 2000, Bryan et al 2003). At the same time, there have been a number of batch experimental studies that have improved our knowledge of the metal ion-humate system. All of these studies have shown that humic substances bind metal ions in two different modes. The initial uptake is to the exchangeable fraction, where the metal ion is bound very strongly, but it may be removed instantaneously if a stronger competing sink is encountered. Over time, the metal may transfer to the non-exchangeable fraction. In this state, the metal is not necessarily more strongly bound, but may not desorb instantaneously, rather its release is kinetically controlled. It is effectively isolated from all direct contact with solution and mineral surface chemistry, and the rate at which it desorbs from the humic is fixed and independent of the concentration or strength of any competing sink. This fraction is not irreversibly bound, and will desorb from its humic complex, but the process is slow.

While it is effectively 'trapped' within the non-exchangeable fraction, the metal ion (or radionuclide) takes on the characteristics of the humic itself. Recent column experiments and associated modelling have shown that the interaction of humic material, and hence also metal-humic non-exchangeable complexes, with mineral surfaces may significantly affect transport (Bryan et al 2003). Moreover, the interaction between the humic and surface may be slow.

It has been demonstrated that chemical kinetics may have implications for field scale migration studies (Bryan et al 2003). However, calculations that include chemical kinetics are computationally expensive, and hence, should be avoided if at all possible. Further, all approaches to Performance Assessment calculations assume equilibrium, and, to include kinetics directly would not be feasible immediately. Therefore, it is important to identify exactly when it is necessary to include them explicitly in mathematical calculations.

The aim of this work is to examine the relationship between chemical rate constants, and the groundwater column residence time. Rules have been developed that predict when, and in what manner, chemical kinetics should be considered in field scale studies, and when other approximations may be used. Here, humic kinetics have been examined, but clearly the approach is equally applicable to other slow chemical processes. In this report the general problems of accounting for chemical kinetics in field scale calculations are considered. However, the specific implications of humic substances for radionuclide migration and radiological performance assessment calculations are discussed elsewhere (Bryan et al 2005).

## The System

The very complexity of the humic/metal ion/surface ternary system makes it an ideal choice for a study of the effects of chemical kinetics, because it would be hard envisage a more complex system of reactions, since in this system we have the potential for multiple simultaneous kinetic chemical reactions.

**Metal ion humic acid interactions**

Batch experiments have shown that metal ions do not bind to humics via a single mode: there are exchangeable and non-exchangeable interactions. However, it is important to appreciate that even this two fraction model is a simplification of the true system. The true complexity is shown in Figure 1.

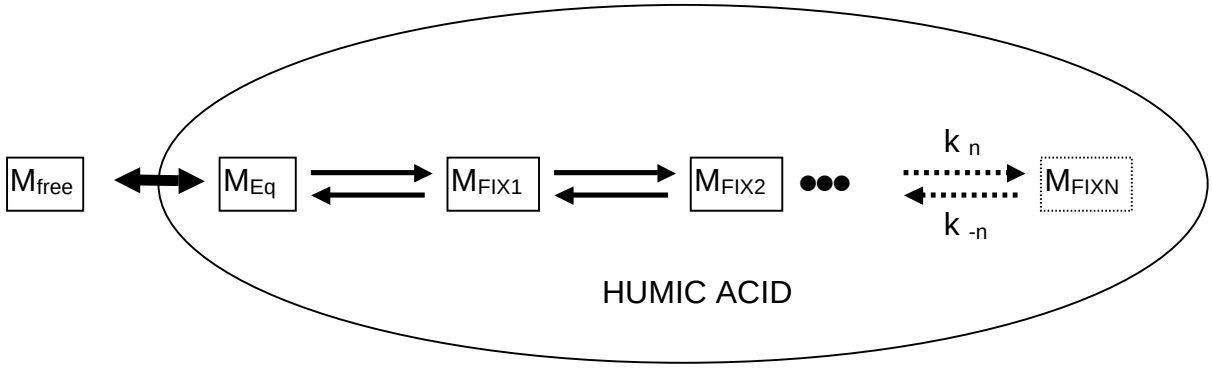


**FIGURE 1: The conceptual model metal ion/humic interactions, $M_{free}$ represents uncomplexed metal ion, $M_{Eq}$ exchangeably bound metal ion, and $M_{FIX1,\ 2\ ..N}$ successively more slowly desorbing non-exchangeably bound metal fractions.**

Initial uptake is to an exchangeable site ($M_{Eq}$). With time, metal ions may transfer to a number of non-exchangeable fractions, which have a spectrum of first order desorption rates ($M_{FIX,1}$ → $M_{FIX,N}$). However, it is clear that there is a distinct, most long lived fraction (most slowly desorbing) fraction that accounts for a significant amount of the non-exchangeable metal (between 10 and 80%). Column modelling over the last few years has shown that in order to simulate transport adequately, it is necessary to consider only two fractions: the exchangeable and this distinct non-exchangeable fraction. All the intermediate ($M_{FIX,1}$ → $M_{FIX,N-1}$) fractions effectively behave as if they were exchangeable. Many authors have found that even for the exchangeable fraction, there is a wide spectrum of binding strengths. However, it seems that this too need not be included in order to simulate transport. These simplifications work for lab column experiments, and we would expect them to hold true for field-scale cases.

**Mineral surface humic acid interactions**

It has been known for many years that humic substances may sorb to inorganic surfaces (e.g. Gu et al 1995), and recent column modelling (Bryan et al 2003) has shown that these processes may affect the transport of metal ions. However, there is some uncertainty about the correct description of the system, since some column experiments can be simulated using a simple equilibrium approach, whilst others require a full kinetic description, and in some cases it is not necessary to include humic sorption at all. It is important to consider the effect of humic sorption, because metal 'trapped' in the non-exchangeable fraction will behave with the characteristics of the humic until such time as it has had chance to leave the humate complex.

**The Full ternary system: metal ion/humic/surface**

Potentially, the full ternary system is very complex. The humic has multiple bound fractions, and these will be present in both humics in solution and sorbed to surfaces. The reaction between the humic and mineral surface is no less complex than the metal humic system, and is less well understood. However, it is necessary to make some simplifications in order to make the problem soluble even for short term migration predictions, let alone full field scale calculations. Therefore, we define a simplified model. Figure 2 shows the system of processes and equations that have been used here.

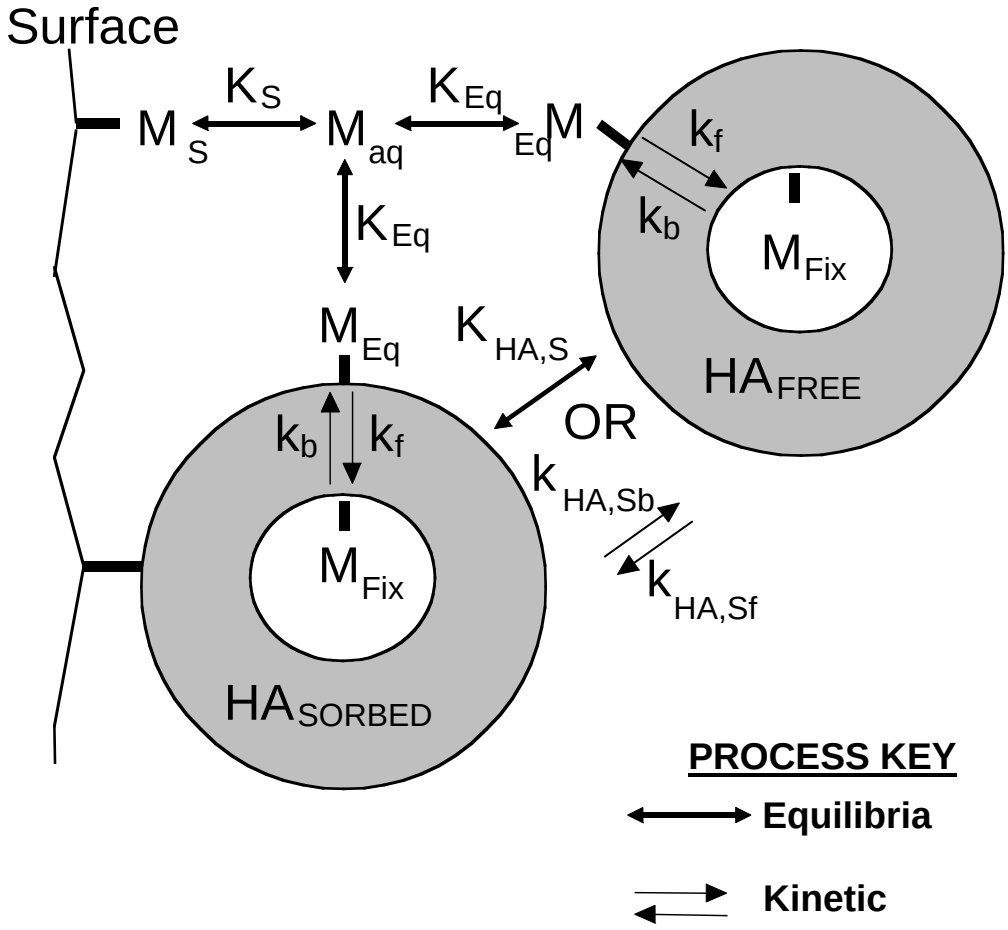


**FIGURE 2: Chemical processes used in the Dukovany and Gorleben calculations. Maq represents uncomplexed metal ion, $M_S$ metal bound to the surface, $M_{Eq}$ exchangeably bound metal ion, and $M_{FIX}$ the non-exchangeable fraction, whilst $HA_{FREE}$ and $HA_{SORBED}$ represent humic free in solution and sorbed to the mineral surface, respectively; $K_S$ and $K_{Eq}$ are the equilibrium constants used to describe the interaction of the metal ion with the mineral surface and humic exchangeable fraction, respectively, and $k_f$ and $k_b$ are the rate constants that describe the transfer of metal to and from the non-exchangeable fraction. The treatment of the sorption of humic and humic-radionuclide complex is uncertain, and may be described either with an equilibrium constant, $K_{HA,S}$, or a pair of forward and backward rate constants $k_{HA,Sf}$ and $k_{HA,Sb}$. The corresponding mathematical equations are given in full in Bryan et al (2005).**

Even with these simplifications, this is still a complex system of reactions and equations. Therefore, we will start with a simpler system with only one kinetic component, and this is shown in Figure 3. This simpler system contains no humic sorption onto the surface. We will return to the more complex full ternary system in Figure 2 later.

## The Binary (humic/metal ion) System (no humic sorption).

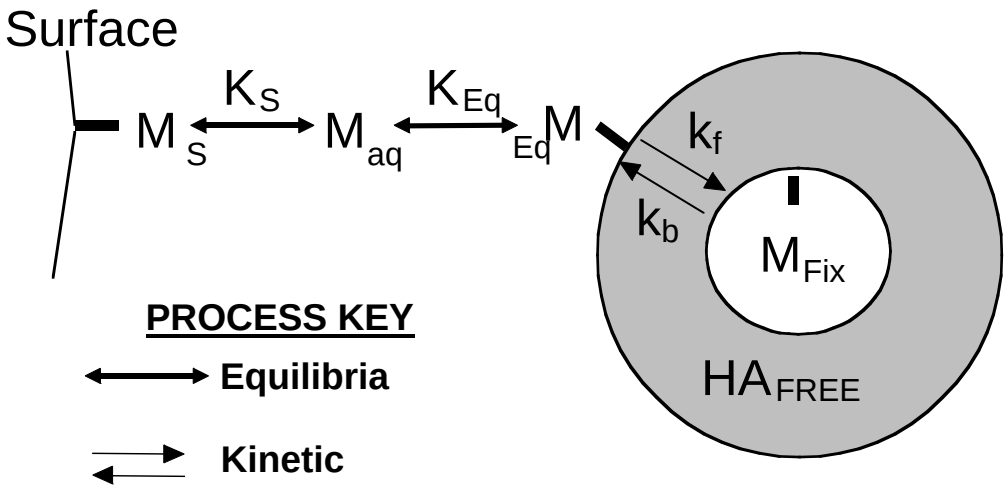


**FIGURE 3: The processes and parameters included in the binary model, which excludes humic sorption (symbols defined in caption to Figure 2).**

### Are reactions equilibria or kinetic?

The distinction between equilibrium and kinetic reactions is always artificial, since it depends upon the time scale of the observation. A reaction which is 'equilibrium' over periods of hours, may well be 'slow' on the time scale of seconds. Given the conditions of the transport calculation, for example, flow rate, distance travelled and total time of interest, it is possible to reduce any series of reactions to just three classes:

1. Those reactions that are sufficiently fast to be treated as equilibria.
2. Those that are sufficiently slow that they effectively do not take place.
3. Those reactions that can only accurately be described by the use of rate equations.

This will be true for all processes, regardless of origin or chemistry. Approximations are common in science, but there is a special requirement here that any approximations must lead to **conservative** estimates, that is, they must over-estimate radionuclide migration, because this methodology is being developed for radiological performance assessment.

### Exchangeable and Non-exchangeable Metal Ion Binding

Although the humic exchangeable interaction shows a high affinity for metal ions, the vast excess of surface sites means that any exchangeably bound radionuclide would not be expected to travel very far before being sorbed onto a surface. Experiments have shown that the non-exchangeable fraction is not particularly more strongly bound, at least in terms of the free energy difference between the bound state and the free metal ion. However, the desorption of the metal from the humic site is kinetically controlled, and the number or affinity of surface sites is no longer sufficient to prevent the movement of the radionuclide. The critical factor becomes the time available for transfer from the non-exchangeable to the exchangeable to take place. If there is time for the metal to transfer, then it will not migrate, but, for example, if the flow rate is sufficiently fast, then it will.

The best way to demonstrate the difference between the exchangeable and non-exchangeable fractions is with an example calculation. Figure 4 shows the results of a calculation using the simple system of reactions shown in Figure 3.

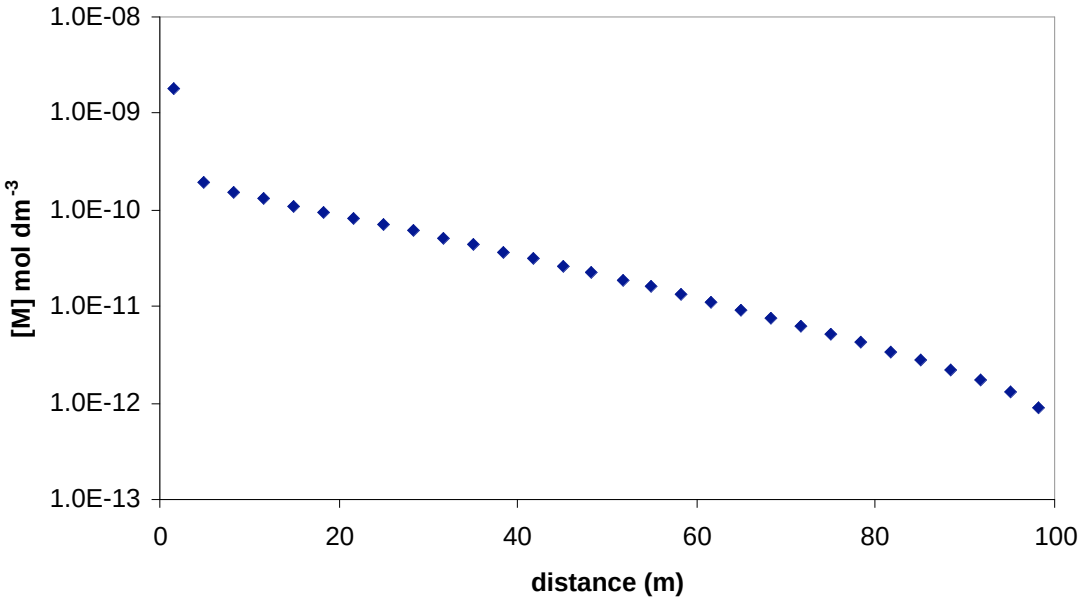


**FIGURE 4: Metal ion profile obtained using column modelling parameters from Bryan et al (2003); $K_{Eq}$ = $5x10^{8}$ $dm^3$ $mol^{-1}$, $K_S$ = $1x10^{7}$ $dm^3$ $mol^{-1}$, $k_f$ = $2.4x10^{-7}$ $s^{-1}$, $k_b$ = $5x10^{-7}$ $s^{-1}$, flow rate = $1x10^{-5}$ $ms^{-1}$, [S] = 1.0 mol $dm^{-3}$, [HA] = $6.8x10^{-6}$ mol $dm^{-3}$, total simulation time = $5x10^{6}$ s.**

The values of the constants are those typically found in batch experiments (King et al 1999, Monsallier et al 2003). The two distinct types of metal ion behaviour are discernible. The metal held in the exchangeable site is very easily removed by the mineral surface, and this is responsible for the sharp fall in concentration at short distances. The majority of the metal has not moved past the top of the column. Beyond the sharp initial fall, there is a long, shallow curve at medium to long distances. This is metal from the non-exchangeable fraction ($M_{FIX}$) that has been transported much further down the column. Clearly, the two fractions are behaving very differently. For the purposes of their migration, it is possible to treat the two fractions as essentially independent, once they are exposed to a surface. Kinetics are having an effect, but how does this depend upon the specific values of the rate constants?

Figure 5 shows the effect of changing the rate constants, $k_f$ and $k_b$, whilst keeping all other parameters fixed. The ratio between them (i.e. $k_f/k_b$) has been kept constant during these calculations.

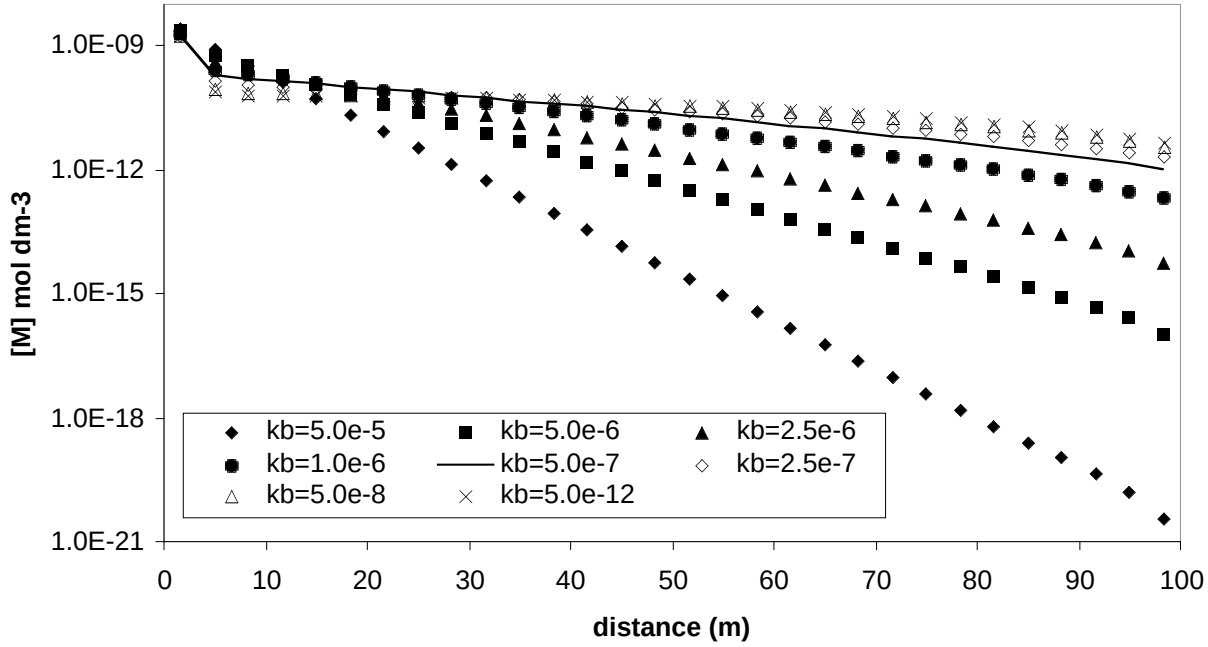


**FIGURE 5: Effect of changing metal ion desorption constant ($k_b$) on the metal ion profile (same general conditions as Figure 4).**

As the rate constant, $k_b$ (Figure 3) for the desorption reaction increases, the extent of metal migration decreases, and as $k_b$ falls, the behaviour seems to tend to some limit. For example, $k_b = 5x10^{-8}$ $s^{-1}$ produces virtually identical behaviour to that with $k_b= 5x10^{-12}$ $s^{-1}$. The behaviour of the exchangeable fraction is completely unaffected by the changes in $k_b$. In order to understand the behaviour of the non-exchangeable fraction, it is necessary to separate out its contribution from that of the exchangeable. Figure 6 shows a ratio plot for the same values of $k_b$ as in Figure 5: in a ratio plot the distribution of the non-exchangeable down the column is expressed as a ratio of its concentration at the top of the column. The advantage of this type of plot is that it allows direct comparison with other species regardless of absolute concentration. In addition to the non-exchangeable fractions, the behaviours of a conservative tracer and the exchangeable fraction are also shown in Figure 5. These are the limiting behaviours that are useful when considering the behaviour of the non-exchangeable fraction.

As the rate constant, kb, increases, the non-exchangeable metal fraction migrates less effectively, because it transfers from the non-exchangeable to the exchangeable increasingly quickly, and as soon as it does, it is instantaneously removed to the mineral surface. It is clear that as $k_b$ increases, the non-exchangeable fraction behaves increasingly like the exchangeable, and for $k_b > 5x10^{-5}$ $s^{-1}$, the non-exchangeable can be considered virtually identical to the exchangeable fraction. Conversely, as $k_b$ decreases, its behaviour tends towards that of a conservative tracer, and for $k_b=5x10^{-12}$ $s^{-1}$, the behaviour is identical: it can never migrate faster than the conservative tracer, the behaviour of its host humic acid.

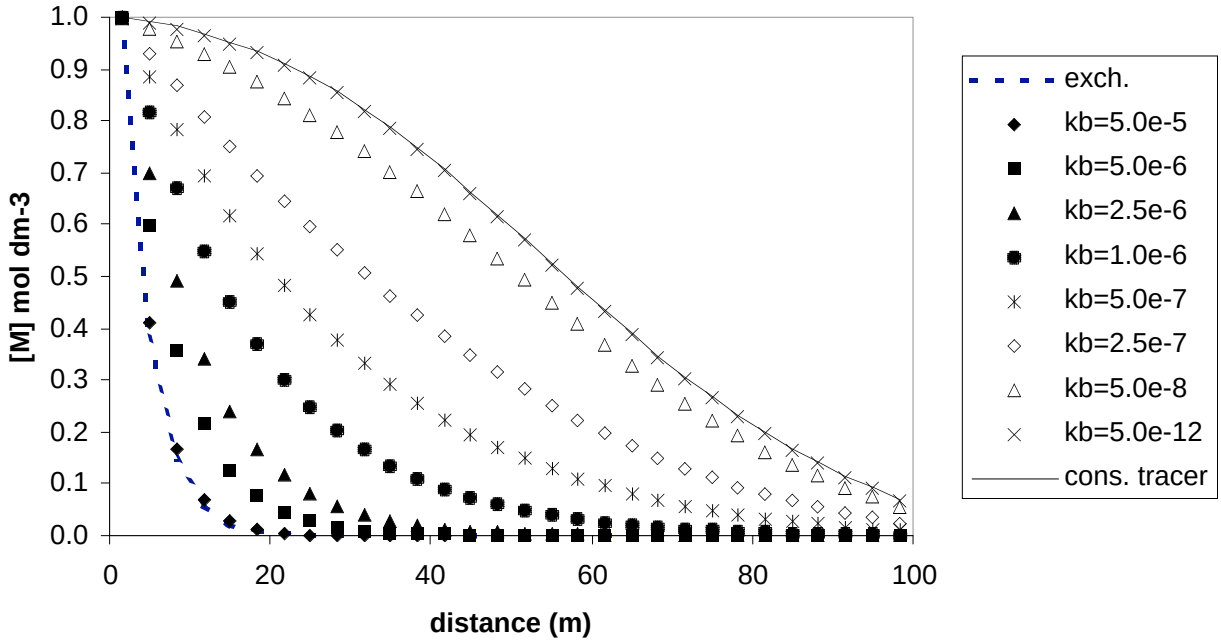


**FIGURE 6: Ratio plot showing the dependence of the behaviour of the non-exchangeable fraction upon metal ion desorption rate constant ($k_b$); conservative tracer (cons. tracer) and exchangeable fraction (exch.) behaviour also shown. Same general conditions as Figure 4.**

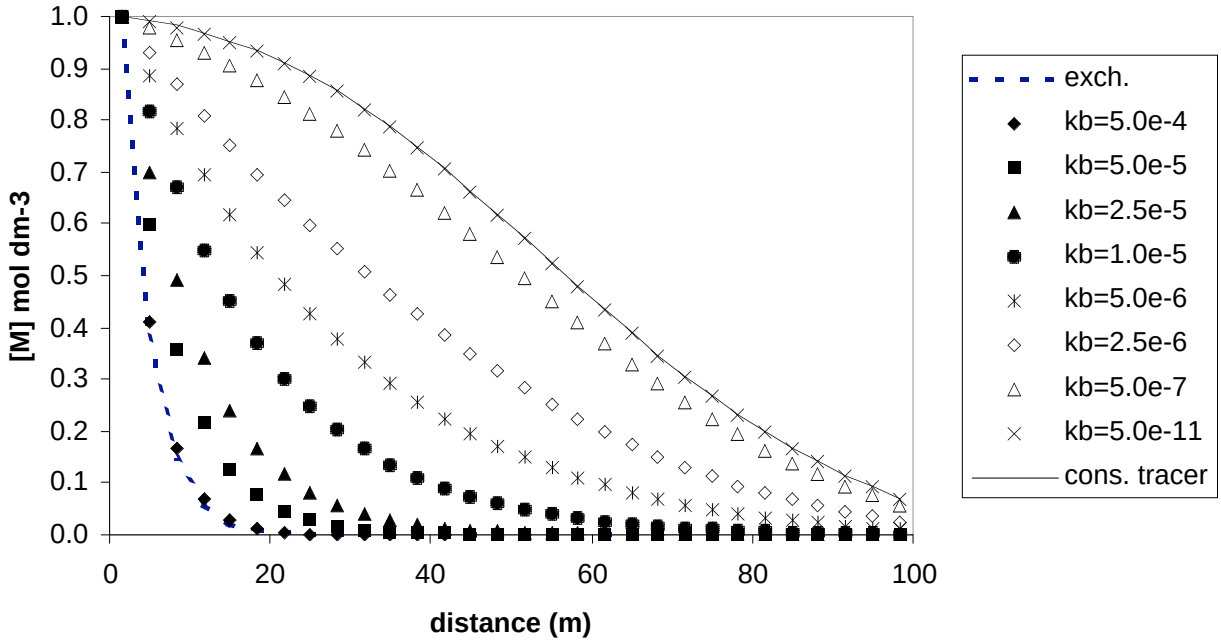


**FIGURE 7: Ratio plot showing behaviour of the non-exchangeable fraction at a flow rate 10 times greater than that for the calculations in Figure 6, and a total simulation time 10 times smaller.**

These observations are significant, since the exchangeable may be described by an equilibrium constant. Hence, for this case, humic desorption rate constants greater than $5x10^{-5}$ $s^{-1}$ may be estimated via the exchangeable equilibrium constant, whilst those with $k_b$ less than approximately $1x10^{-9}$ $s^{-1}$ can be modelled as a conservative tracer. In between these values

though a kinetic description is required. It is useful to repeat the calculation shown in Figure 6, but with the flow rate increased by a factor of 10 and the simulation time reduced by a factor of 10. The results are shown in Figure 7.

It is immediately obvious that the plots in Figures 6 and 7 have exactly the same shapes. The difference is that to get a plot in the same position in Figure 7 has required a rate constant a factor of 10 higher. If the flow rate had been reduced by a factor of 10 and the simulation time increased by a factor 10, then the rate constants would also need to be reduced by the same factor in order to achieve the same result. Hence, whether a kinetic description is required or the equilibrium or conservative tracer approximations will suffice depends upon the ratio between the first order desorption rate (kb) and the groundwater flow rate. Further, for the same column, systems with the same ratio of rate constant to flow rate behave in the same way.

At this point it is useful to introduce the concept of Damkohler numbers (Jennings and Kirkner 1984). The dimensionless Damkohler number for the non-exchangeable fraction, D(M), is defined by:

$$D(M) = \frac{L}{V_H} k_b$$

where, L is the length of the column, $k_b$ is the chemical (first order) rate constant and $V_H$ is the **effective linear velocity** of the metal containing species through the water column. In the current system defined by Figure 2, there is no humic sorption, and so the effective velocity of the non-exchangeable fraction is identical to the flow rate of the groundwater. In this work, a second dimensionless number, T has been defined:

$$T = \frac{t V_H}{L}$$

where, t is the total elapsed (simulation) time.

If we examine the plots for $k_b = 2.5 \times 10^{-7}$ ($s^{-1}$) in Figure 6 and $k_b = 2.5 \times 10^{-6}$ ($s^{-1}$) in Figure 7, then they lie in exactly the same position, and if we calculate the Damkohler numbers for these two systems, then we find that they both have D(M) = 2.5. Also, the calculations in Figures 6 and 7 have the same T number, since the product of simulation time and flow rate is the same. This is no coincidence: in the binary system, calculations with the same D(M) and T numbers always give the same shape plots.

The combination of D(M) and T numbers are sufficient to define uniquely the behaviour of these systems. Any system with the same D(M) and T numbers will show the same profile along a column. The term ‘column’ here is used to define the distance over which any calculation is based, whether in the laboratory (real column) or the field (hypothetical column). Figure 8 shows the results of a series of calculations with different values of $k_b$ (plotted again as ratio plots), but this time the results are expressed in terms of Damkohler

number. The plots in this figure again have the same shape as those in Figures 6 and 7. The advantage is that this figure serves for all the systems in both Figures 6 and 7, and indeed for any combination of rate constant, simulation time, length and flow rate that give the same D(M) and T values.

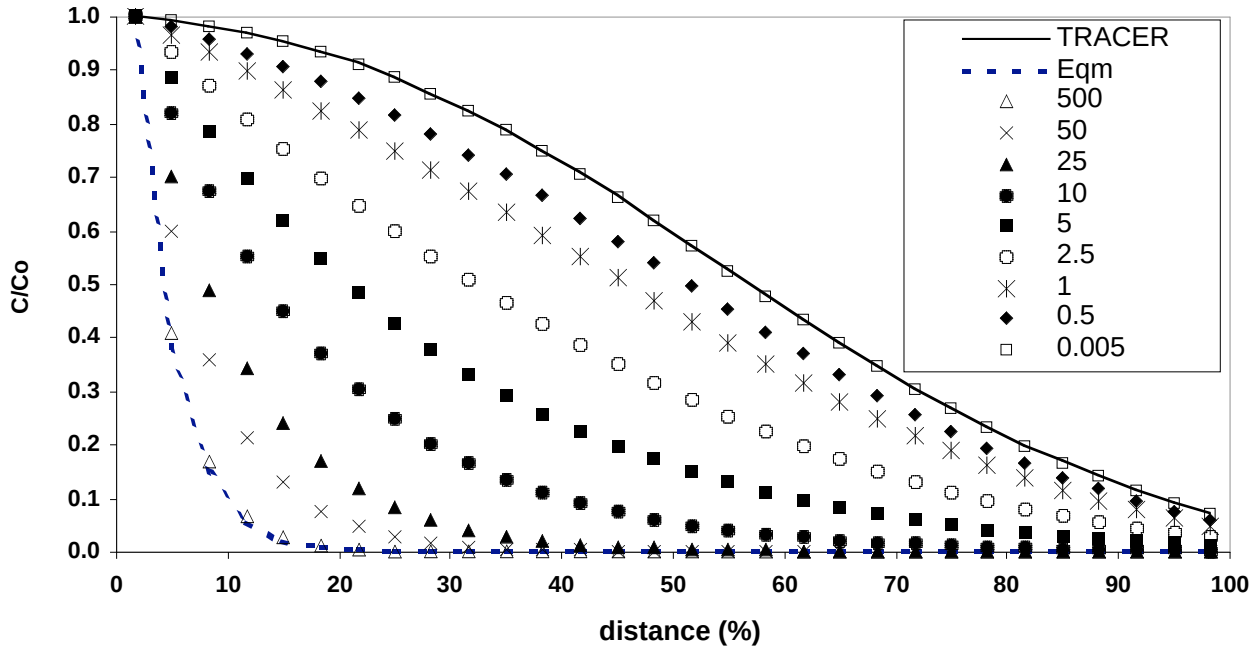


**FIGURE 8: The variation in non-exchangeable fraction transport with Damkohler number, D(M), shown with exchangeable (Eqm) and conservative tracer (TRACER) behaviours.**

Given that all systems with the same D(M) number behave in exactly the same way, we may use D(M) to judge the impact of chemical kinetics, and hence to judge when it is necessary to include chemical kinetics explicitly in transport calculations. As the value of D(M) increases, the non-exchangeably bound metal tends towards the behaviour of a conservative tracer. In fact, for any system with D(M) <0.02, the behaviour is virtually the same. This gives us our first approximation method, or alternative to including chemical kinetics in the transport calaculations, the '***decoupled***' **approximation**.

**Decoupled Approximation**

If the value of D(M) is sufficiently small, then the value of $k_b$ is so small, that virtually no metal ion can leave the non-exchangeable fraction in the time it takes to traverse the column. Therefore, we merely need to calculate the distribution of metal between exchangeable and non-exchangeable at the start of the column, but from that time on, we delete the reaction that connects the exchangeable and non-exchangeable from the calculation and treat them as independent species. Given that the exchangeable may be simulated with an equilibrium constant, and the non-exchangeable is to be treated as a conservative tracer, we have removed all the inconvenient kinetic calculations. Beyond the fact that it drastically reduces the mathematical complexity of the system, the great advantage of this technique is that it is inherently conservative. The non-exchangeable metal only tends towards the behaviour of a

conservative tracer. Therefore, if we assume that it moves as a conservative tracer, then we will always tend to overestimate its migration.

**Equilibrium Approximation**

At the other extreme of high D(M) values, the behaviour of the non-exchangeable tends towards that of the exchangeable. Therefore, the alternative approximation, the equilibrium approximation, assumes that the non-exchangeable may be treated in exactly the same way as the exchangeable. Therefore, at the start of the column, all humic bound metal is 'moved' (within the calculation) into the exchangeable fraction, and the non-exchangeable fraction and the kinetic reaction linking it to the exchangeable is deleted. Again, this will remove the kinetics from the calculation. However, it is clear from Figure 8 that although the behaviour of the non-exchangeable does tend towards that of the exchangeable, it always moves slightly further that the exchangeable, i.e., the approximation is no longer guaranteed to be conservative. The size of the error will decrease as D(M) increases, but it will always be there. The importance and implications of the error will depend upon many factors, such as the absolute concentration of the radionuclide in the non-exchangeable at the start of the column and the properties of the radionuclide, such as half-life, radiotoxicity etc. Therefore, we must exercise care when using the equilibrium approximation.

**Dimensionless approach**

At the limits we have the two approximations. However, in the region around D(M) = 1, no approximations will produce accurate predictions, and we must include kinetics in the calculations to produce an accurate result. However, there is a potential method that would allow an estimate of migration without the need actually to perform a costly calculation. For example, suppose we have the following system: rate constant, $k_b$ = $1x10^{-7}$ ($s^{-1}$); column length = 300 m; linear flow rate = $6x10^{-6}$ ($ms^{-1}$). The Damkohler number for this system is D(M) = 5, and in Figure 8 we already have a prediction for that D(M) value. Therefore, it would be possible to produce a library of calculation results by performing a series of these calculations for a range of these intermediate D(M) values, and a series of T values, giving a matrix of results. If one were to calculate the D(M) and T values for a unknown problem case, then the closest appropriate library calculation with the nearest D(M) and T values could be used as an 'instant' estimate. If the library result with lower D(M) and higher T values than for the real migration case where used as an estimate, then the result would be conservative.

An interesting observation is that the change in the plots in Figure 8 with D is gradual and steady. Therefore, it is possible to fit the plots to produce a series of approximations: Figure 9 shows a series of approximations to the correct result shown in Figure 8 (the lines are the approximations and the symbols show the exact results, copied from Figure 8).

All of the plots (curves) in Figure 9 were produced using the simple polynomial function,

$$(C/Co) = ax^3 + bx^2 + cx + k$$

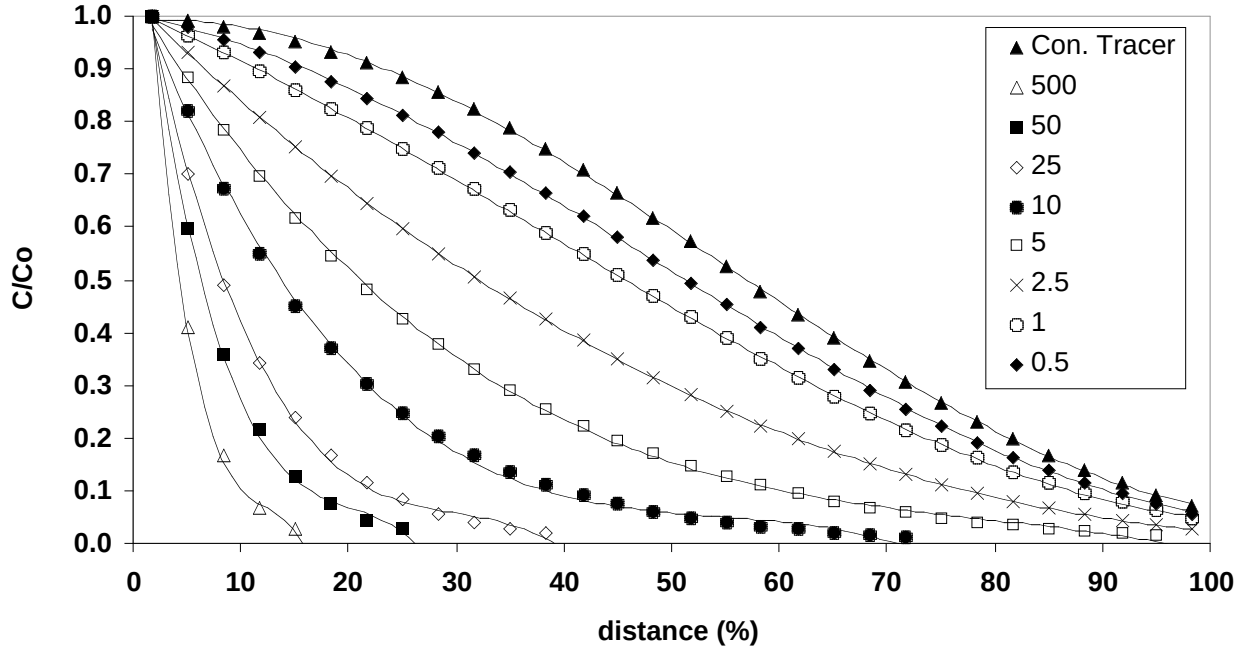


**FIGURE 9: Approximations (lines) to exact ratio plot results (symbols), as shown in Figure 8.**

where x is the distance from the start of the column expressed as a percentage of the total column length, L. The useful fact is that the parameters, a, b, c, and k, change consistently with, D(M). As an example, Figure 10 shows the variation in the parameter a with D(M).

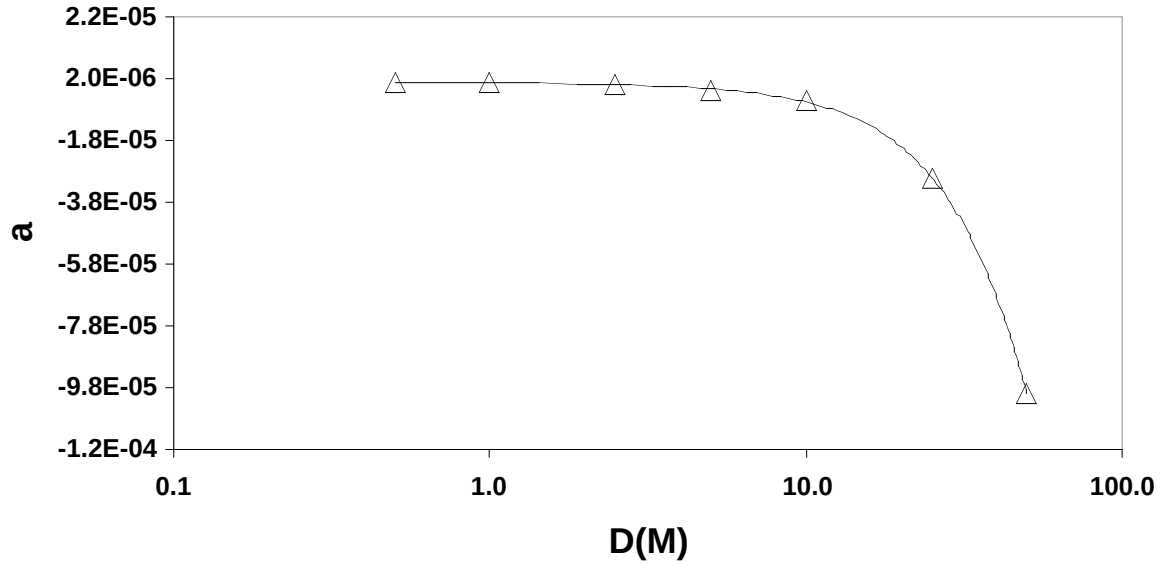


**FIGURE 10: variation in fitting parameter, a, with D(M)**

Therefore, it is possible to fit the change in a with D(M) (curve in Figure 10) with the polynomial,

$$a = 1.87\times10^{-10}D(M)^3 - 4.55\times10^{-8}D(M)^2 - 2.11\times10^{-7}D(M) + 8.89\times10^{-7}$$

In the same way, the other parameters may also be fitted:

$k = 7.28\times10^{-7}D(M)^3 - 9.18\times10^{-5}D(M)^2 + 7.24\times10^{-3}D(M) + 1.00$
$c = -1.57\times10^{-6}D(M)^3 + 1.52\times10^{-4}D(M)^2 - 6.68\times10^{-3}D(M) - 1.09\times10^{-3}$
$b = -4.35\times10^{-9}D(M)^3 + 7.14\times10^{-7}D(M)^2 + 1.14\times10^{-4}D(M) - 2.41\times10^{-4}$

Now, these equations are valid for only one value of T, but if the procedure were repeated for other T values, then it might be possible to produce estimates of migration that take account of chemical kinetics, but which may be obtained with only a spreadsheet, and with no need for a direct transport calculation.

Therefore, whether a calculation library method or fitting procedure is adopted, the dimensionless approach, using the D(M) and T numbers, can provide estimates in the intermediate region not covered by the decoupled and equilibrium approximations.

**Ranges of Validity**

Using the fact that humic first order desorption rates from the non-exchangeable fraction have a fairly narrow range, we can define regions of flow rate and calculation distance where the three different approaches should be used, Figure 11.

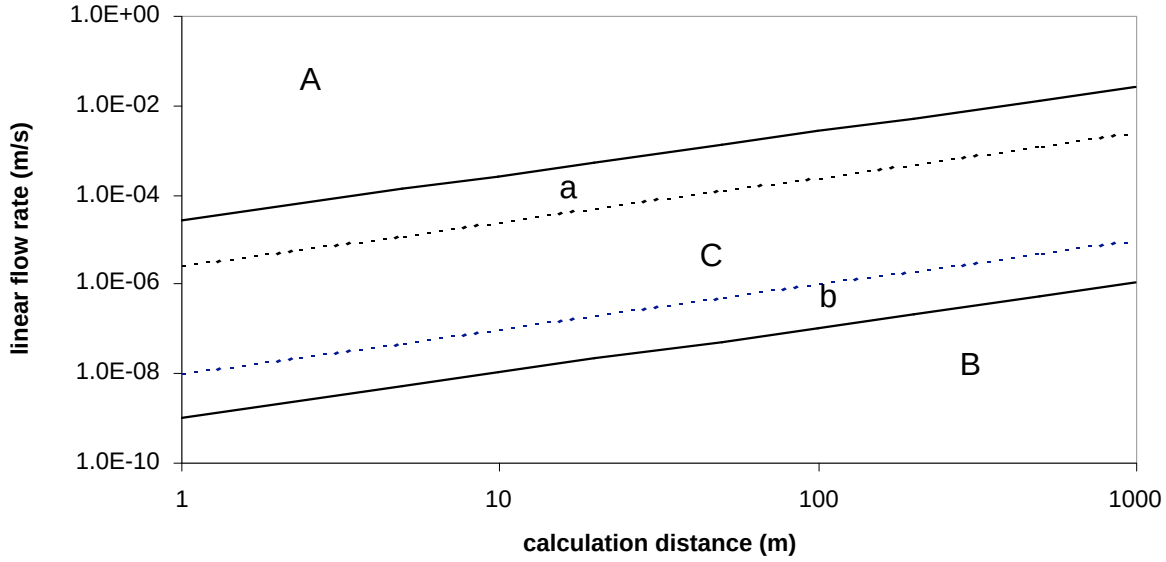


**FIGURE 11: Ranges of validity for approximation methods (labels explained in text).**

In the figure, the plot area is divided into a series of regions. In region A, the decoupled approximation is appropriate, and this will be still be true moving into the slice labelled 'a', but as we move down and right, the error introduced with the decoupled approximation will get larger and larger, although the prediction will always be conservative. In the bottom right hand corner (region B): the equilibrium approximation will be more appropriate, although as we move up and to the left towards slice b, the error incurred will become larger, and this time it will not be conservative. Therefore, care is required when using the equilibrium

approximation. In region C, the dimensionless approach is best. Since the decoupled approach is always conservative, it might be tempting to adopt it in all cases, the problem is that assuming that the radionuclide moves as a conservative tracer would lead to a gross overestimation of transport in many cases.

Of course one does not have to use an approximation, a full coupled chemical transport calculation including the kinetic equation will always give the correct answer, but it may be computationally expensive.

## The implications of kinetics in the full ternary system

Thus far, we have been studying the simpler binary system (shown in Figure 2), ie., we have assumed that the humic and metal humic complexes do not sorb, but transport as conservative tracers. If we allow them to sorb then we have a 'full' ternary system, as shown in Figure 2. An added complication is that the humic sorption reaction may also be slow on the time scale of the column residence time. Hence, it may be more appropriate to describe the humic sorption process as an equilibrium with equilibrium constant $K_{HA.S}$ or as a kinetic process with forward and backward rate constants, $k_{HA,Sf}$ and $k_{HA,Sb}$, respectively. Hence, each system will now have two Damkohler numbers, one for the metal, D(M), as defined above, and the other for the humic, D(hum),

$$D(hum) = \frac{L}{V_H} k_{HA,Sb}$$

The same value of T will be valid for both metal and humic. Once again, the best way to demonstrate the effect is with an example calculation. Figure 12 shows the results for a range of D(M) values.

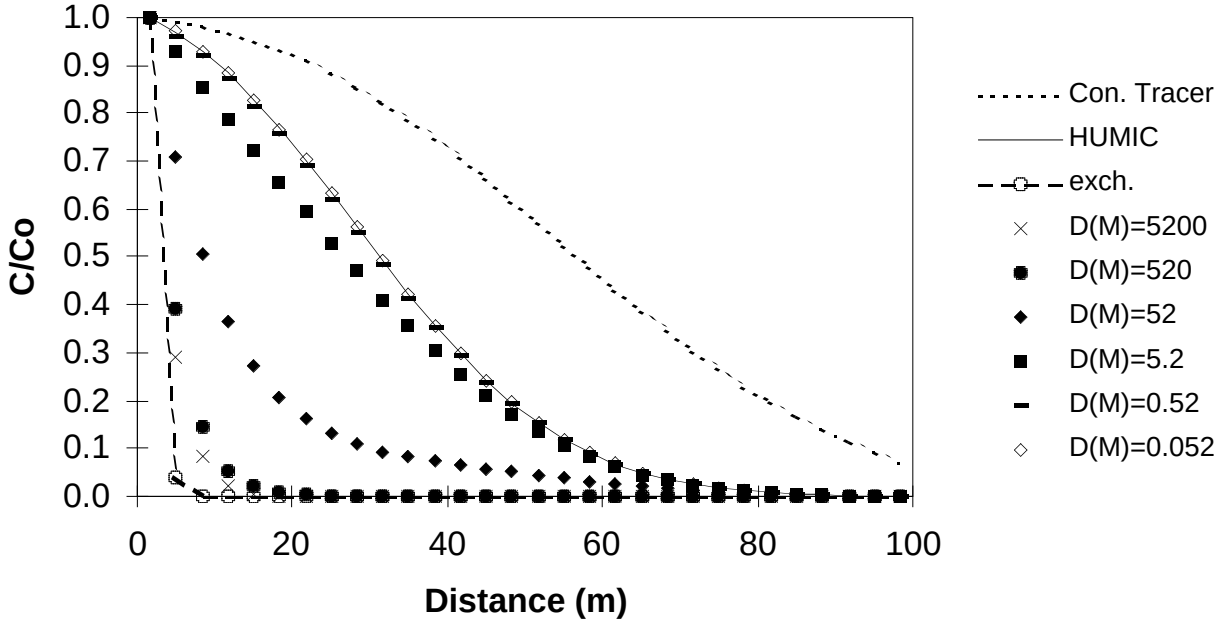


**FIGURE 12: Variation in migration of non-exchangeable fraction with D(M) for a system where humic and humic-metal complexes may sorb to the mineral surfaces; behaviour of conservative tracer (Con. Tracer), humic and exchangeable fraction (exch.) also shown.**

The most obvious difference, is that, although the behaviour of the non-exchangeable still tends towards that of the exchangeable as D(M) increases, it no longer tends towards the conservative tracer in the other direction. Instead, the non-exchangeable now tends towards the behaviour of the humic itself. This is no surprise, since this metal fraction is increasingly fixed within the humic as D(M) falls, and so it increasingly takes on the behaviour of the humic itself. Most importantly, the radionuclide cannot transport faster than its host humic acid. For all of the calculations represented in Figure 12, the behaviour of the humic is fixed, and so it provides the limiting behaviour.

If we perform a series of calculations where the behaviour of the metal ion is fixed, whilst the rate constants for the humic sorption reaction ($k_{HA,Sf}$ and $k_{HA,Sb}$) change, then similar behaviour is observed (Figure 13). As for the calculations where $k_b$ varied, the ratio between the humic forward and backward rate constants has been kept constant.

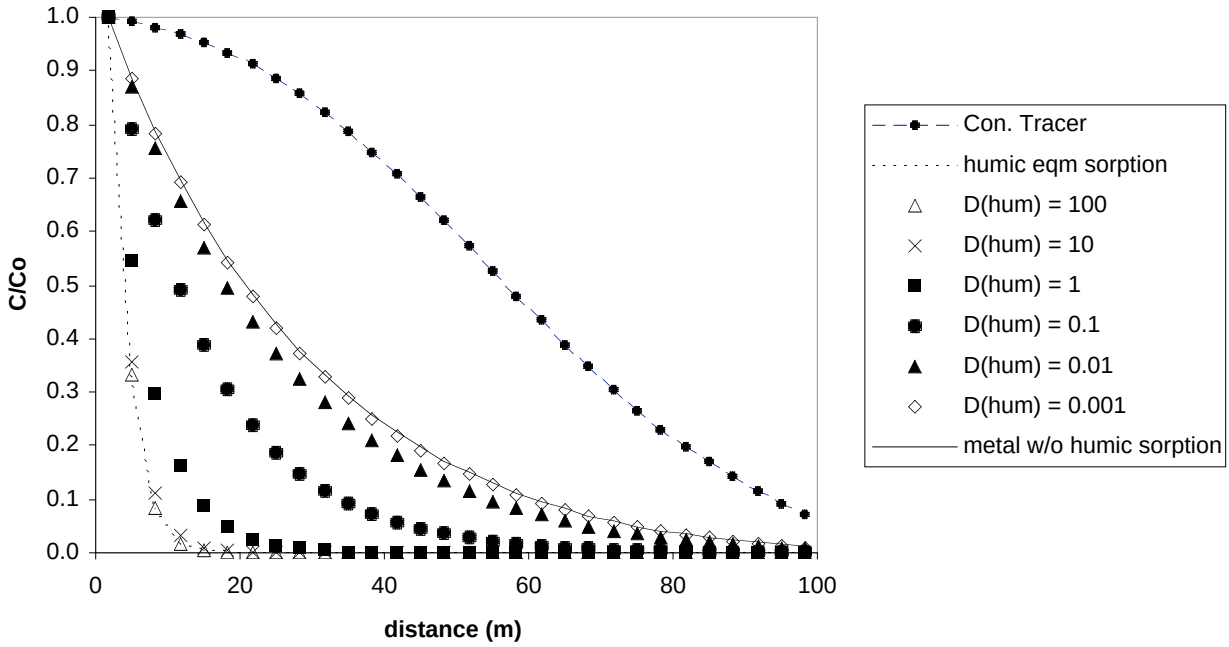


**FIGURE 13: Variation in transport of non-exchangeable fraction with D(hum); conservative tracer (Con. Tracer), humic fast sorption (humic eqm sorption) and behaviour with no humic sorption at all (full line) also shown.**

In these systems, the first order rate constants for the transfer of metal between exchangeable and non-exchangeable, $k_f$ and $k_b$, have been fixed at $2.4 \times 10^{-7}$ ($s^{-1}$) and $5.0 \times 10^{-7}$ ($s^{-1}$), respectively. As the humic rate constants and hence D(hum) fall, the metal ion travels further, because less and less humic-metal non-exchangeable complex sticks to the surface in any given time period (and distance travelled), and so more is free to migrate down the column. This time the behaviour tends towards that which those non-exchangeable fraction constants would produce if there were no humic sorption at all, i.e. if the humic moved as a conservative tracer. Here, the metal cannot travel more than its own rate constants ($k_f$ and $k_b$) will allow it to. At the other extreme, there is another limiting behaviour, as the rate constants

and D(hum) increase, the behaviour tends towards that shown by the humic itself if its sorption is described by an equilibrium constant, i.e. sorption is fast. As the humic sorption rate constants increase, more humic and humic-metal complex sorbs per time period, and hence the humic bound metal travels less far, but as the constants increase, the humic/surface interaction tends towards equilibrium behaviour, such that if the rate constants are sufficiently high, then the amount sorbing depends only upon the ratio of the forward and backward rates, and is independent of the absolute values. Once again, the non-exchangeable metal transport is limited by the fact that it cannot travel faster than the host humic.

Hence, for a fixed value of D(hum), the result is controlled by D(M), whilst for fixed D(M), it is D(hum) that determines the behaviour. In the case of the simpler binary system (Figure 3), it was shown that even for systems where kinetics played a significant role, the behaviour was surprisingly predictable, and depended only upon D(M) and T. In the case of the ternary system, the situation is much more complex. For example, we may not define ranges of D(M) where different approximations and approaches will be best. For example, for the calculations in Figure 13, D(M) = 5, which in a binary system would imply that kinetics were important. However, if the humic sorption reaction is fast then, even though D(M) = 5, kinetics need not be included, and the behaviour of the non-exchangeable may be described with the humic sorption equilibrium constant, $K_{HA,S}$. Hence, it is the combination of D(M) with D(hum) which is important, and we may not have a set of simple, rigid rules.

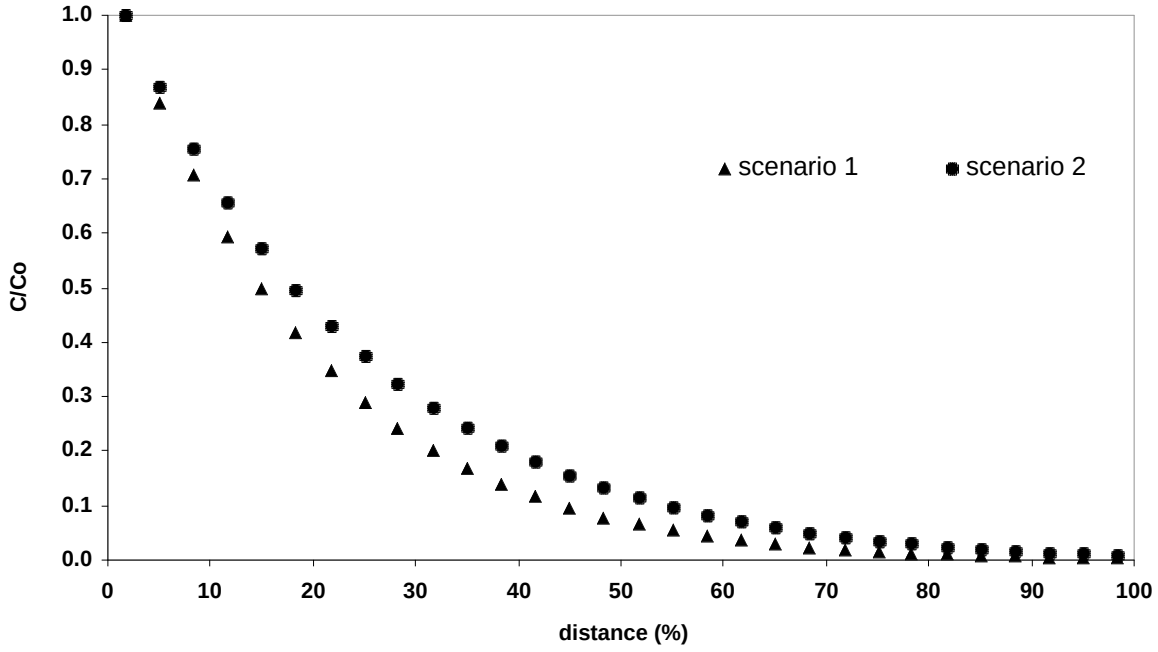


**FIGURE 14: behaviour of two different systems with the same D(M) and D(hum) numbers.**

However, systems with the same Damkohler numbers do seem to behave in similar ways. For example, consider two quite different calculation scenarios. In scenario 1, the linear flow rate is $1x10^{-4}$ $ms^{-1}$, $k_b = 5x10^{-7}$ $s^{-1}$ and $k_{HA,Sb}(HA) = 1x10^{-6}$ $s^{-1}$;, whilst in scenario2, linear flow rate is $1x10^{-05}$ $ms^{-1}$, $k_b = 5x10^{-8}$ $s^{-1}$ and $k_{HA,Sb}(HA) = 1x10^{-7}$ $s^{-1}$. The results for these two scenarios

(at constant T) are shown in Figure 14. The two scenarios have the same values of D(M) and D(hum). Now, in the binary system with only one kinetic reaction, two systems with the same D value would give identical results. However, for the ternary system, the two results are very close, but not quite identical. Therefore, although we still have some predictability, there is less certainty.

Figures 15 and 16 show the results of two calculations with the same value of D(hum), but with different D(M). In both figures, the limiting behaviour at low D(hum), is shown for comparison. Not surprisingly, the two results are different, because they have different D(M).

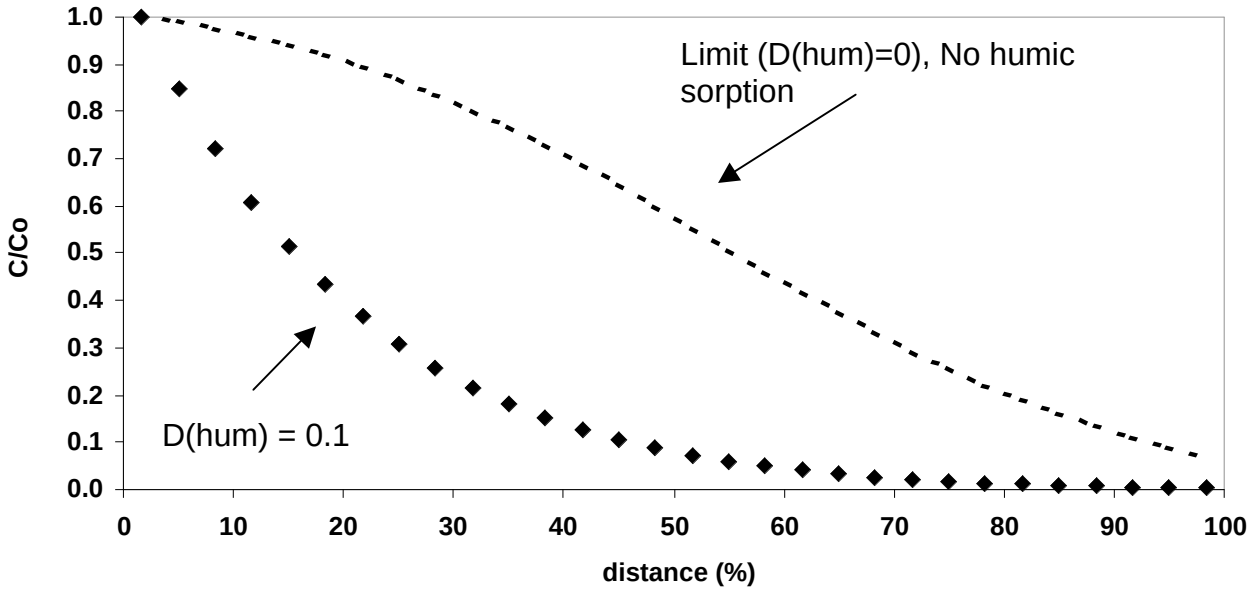


**FIGURE 15: Behaviour in system with D(M) = $5x10^{-5}$.**

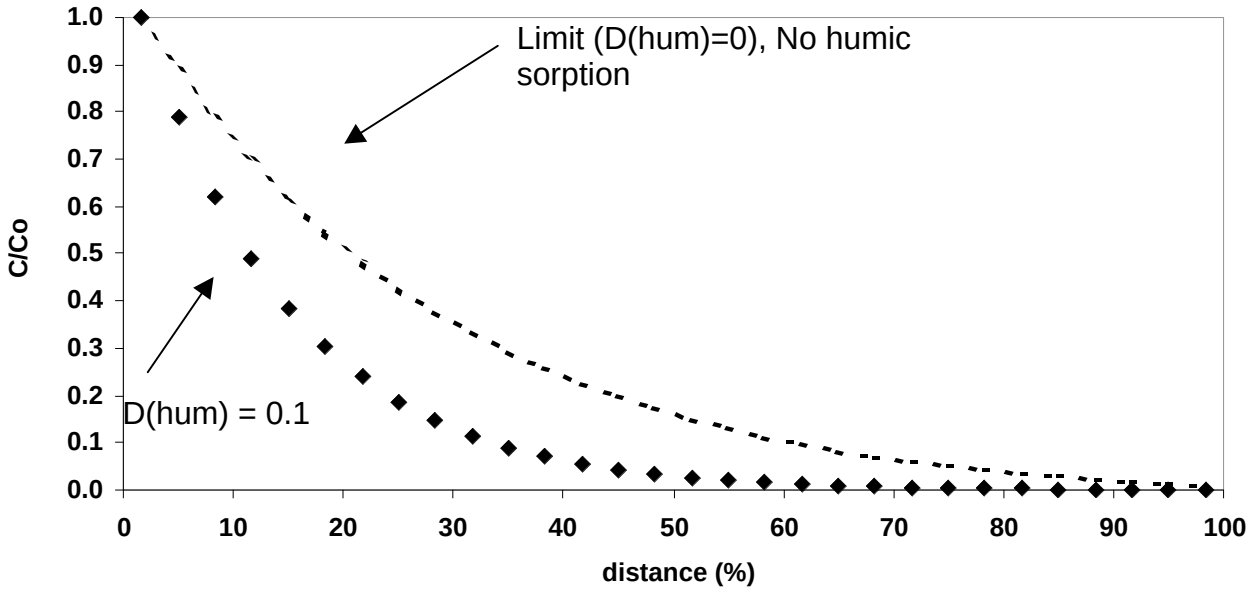


**FIGURE 16: Behaviour in system with D(M) = 5.**

However, it is found that in many cases, the ratio between the C/Co value for a calculation and the limiting (D(hum) → 0, no humic sorption) value is surprisingly constant for given values of D(hum). Figures 17 and 18 show examples, four different scenarios each, for D(hum) = 0.1 and D(hum)=1, respectively.

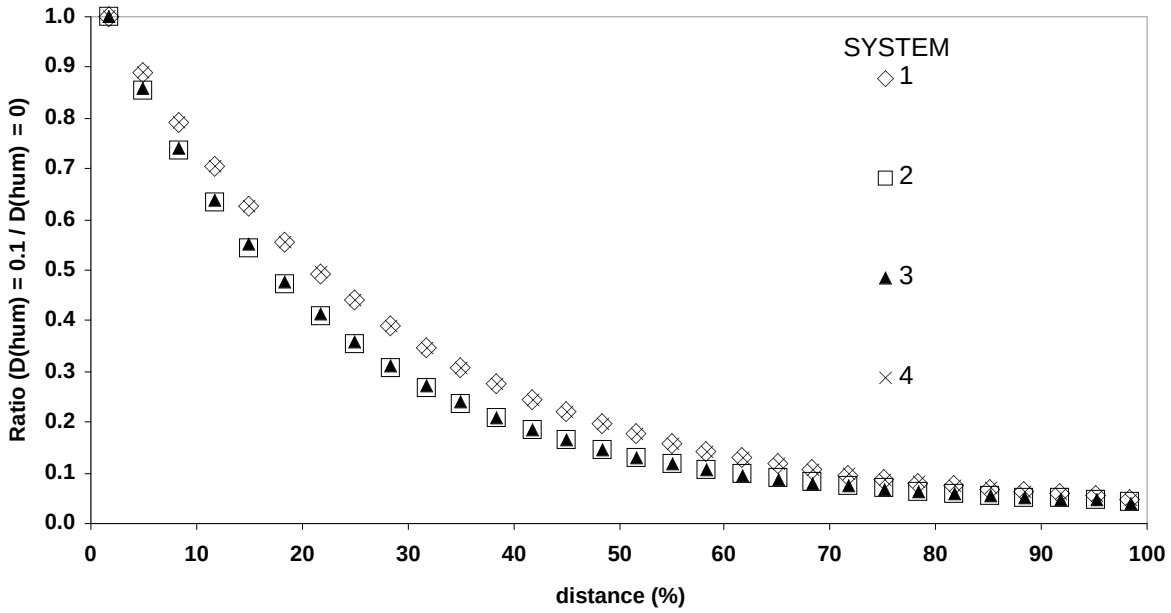


**FIGURE 17: Plot of ratio of C/Co for D(hum)=0.1 to that for D(hum)=0 for 4 different systems.**

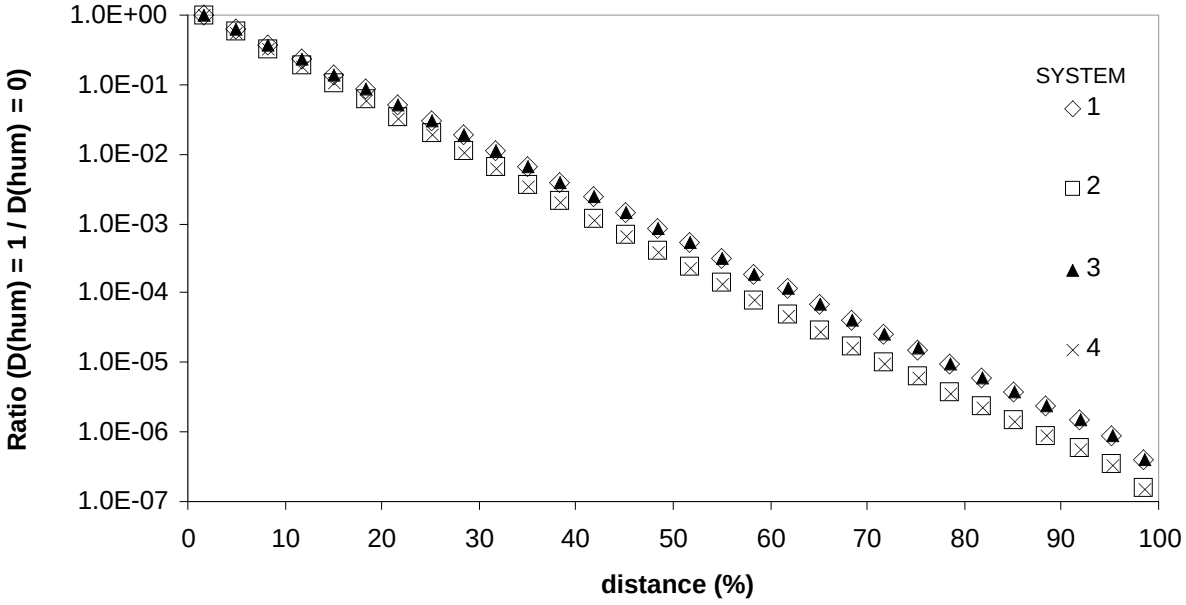


**FIGURE 18: Plot of ratio of C/Co for D(hum)=1 to that for D(hum)=0 for 4 different systems.**

Now, the plots in Figures 17 and 18 are not in exactly the same place, but the variation is really quite small considering the complexity of the system.

## Conclusions

For a system where there is no humic sorption, we now have a set of rules that allow us to determine when humic non-exchangeable metal binding will have a significant effect upon the results of migration calculations. A combination of the Damkohler, D(M), and T dimensionless numbers are sufficient to define the behaviour of the system.

At low D(M) numbers, the decoupled approximation, where the exchangeable and non-exchangeable are treated as independent species, and the reaction between them is removed, provides a reasonable and conservative estimate. At higher values, the equilibrium approximation, where the non-exchangeable behaviour may be approximated with an equilibrium constant, will provide an estimate, although it will not be conservative. At intermediate D(M) values, the dimensionless approach, which makes use of the fact that the value of D(M) serves to define the behaviour of the non-exchangeable fraction, can provide an estimate of the behaviour.

For the full ternary system, the general behaviour is still easy to understand, and the results in Figures 14 - 18 show that the system is still behaving in a predictable way, although estimates will be harder to obtain. Further, it is not possible to define a set of rigid rules to define when kinetics will have an effect.

This report has concerned the general problems of coping with chemical kinetics in transport calculations. The likely effects of humic substances upon radionuclide migration and the implications of humic substances for Radiological Performance Assessment are discussed elsewhere (Bryan et al 2005).

**References**

Bryan N.D., Jones D.M., Keepax R., Warwick P., Stephens S., Higgo J.J.W. (2003) "An Experimental and Modelling Study of Metal Ion/Humate Non-Exchangeable Binding." In: Buckau, G. (Editor) “Humic Substances in Performance Assessment of Nuclear Waste Disposal: Actinide and Iodine Migration in the Far-Field (First Technical Progress Report)”, Report FZKA 6800, Research Center Karlsruhe.

Bryan N.D., Buckau G., Bernhard G., Geipel G. , Heise K.H. and Schmeide K. (2005) "Migration Case Studies And The Implications Of Humic Substances For The Radiological Performance Assessment Of Radioactive Waste Repositories." In: Buckau, G. (Editor) “Humic Substances in Performance Assessment of Nuclear Waste Disposal: Actinide and Iodine Migration in the Far-Field (Third Technical Progress Report)”, Report FZKA, Research Center Karlsruhe.

Gu, B., Schmitt, J., Chen, Z., Liang L. and McCarthy J.F. (1995) Adsorption and desorption of different organic matter fractions on iron oxide. Geochimica et Cosmochimica Acta, 59, 219-229.

Jennings A.A. and Kirkner D.J. Instantaneous Equilibrium Approximation Analysis. *Journal of Hydraulic Engineering (A.S.C.E.)*, 1984, **110**, 1700 – 1717.

King, S.J., Warwick, P., Hall, A., Bryan, N.D. (2001) The dissociation kinetics of dissolved metal-humate complexes. Physical Chemistry Chemical Physics, 3, 2080-2085.

Monsallier J.M., Schussler W., Buckau G., Rabung T., Kim J.I., Jones D., Keepax R., Bryan N. Kinetic investigation of Eu(III)-humate interactions by ion exchange resins. *Anal. Chem.*, (2003), 75,3168-3174.

Warwick, P., Hall, A., Pashley, V., Bryan, N.D., Griffin, D. (2000) Modelling the effect of humic substances on the transport of europium through porous media: a comparison of equilibrium and equilibrium/kinetic models. Journal of Contaminant Hydrology, 42, 19-34.

## Annex 7:

**Migration Case Studies And The Implications Of Humic Substances For The Radiological Performance Assessment Of Radioactive Waste Repositories.**

Bryan N.D., Bernhard G., Geipel G., Heise K.H., Schmeide K., Benes P.

# Migration Case Studies And The Implications Of Humic Substances For The Radiological Performance Assessment Of Radioactive Waste Repositories.

Bryan N.D.[1], Bernhard G.[2], Geipel G.[2], Heise K.H.[2], Schmeide K.[2] , Benes P.[3]

1 Department of Chemistry, The University of Manchester, Oxford Rd., Manchester, UK.
2 Forschungszentrum Rossendorf, Institute of Radiochemistry, Dresden, Germany.
3 Czech Technical University, Department of Nuclear Chemistry, Brehova 7, 115 19 Praha 1, Czech Republic

## Abstract

Using the information obtained during the experimental and modelling tasks a series of migration case studies have been performed. These are not full performance assessment studies, but are merely intended to demonstrate the likely impact of humic substances upon the migration of radionuclides in the environment. Three separate sties have been investigated: (i) a shallow waste repository site at Dukovany in the Czech Republic; (ii) the formerly proposed, but now withdrawn, waste repository site at Gorleben in Germany; (iii) a large rock pile, consisting of tailings from a uranium mine, Schlema Alberode, near Dresden, Germany. To provide the maximum information, a variety of 'release scenarios' have been defined: continuous leakage in the Dukovany case study; a short pulsed release at Gorleben, and steady leaching in the case of the rock pile. The effects of the magnitudes of the chemical rate constants have been studied along with the effects of the initial distribution between exchangeable and non-exchangeable. Further, modelling during the HUPA project has shown that in certain lab column experiments the sorption of humic and humic-radionuclide complexes onto mineral surfaces could have an impact upon migration. Therefore, the likely impact of these processes on the field scale was investigated. In each of the three cases, humics are predicted to have a significant impact upon migration. However, whereas for the repository cases, it is the presence of the non-exchangeable fraction that results in migration, and the exchangeable fraction plays no significant part in transport, for the rock pile, the model predicts that the humic should promote migration even with the exchangeable interaction alone. Humic sorption may affect the degree of migration, but even in the case of maximum impact, the net effect of humic substances is still to enhance migration significantly. In fact, the initial distribution of radionuclide upon entry to the far-field is much more significant. Finally, conclusions are drawn about the likely impact of humic substances upon radiological performance assessment. Although there are still uncertainties and the underlying processes are not understood, all the evidence suggests that humic substances should have an impact, and their effects should at least be considered in performance assessment calculations.

## Introduction

This work describes migration test cases to demonstrate the effects of humic substances upon the transport of radionuclides in the environment. There are 3 specific case studies: (i) a shallow waste repository site at Dukovany in the Czech Republic; (ii) the formerly proposed, but now withdrawn, waste repository site at Gorleben in Germany; (iii) a large rock pile, consisting of tailings from a uranium mine, Schlema Alberode, near Dresden, Germany. The aim is to demonstrate how the models, codes and information generated as part of the HUPA project might be used in the context of a Radiological Performance Assessment (RPA) exercise, and to determine the likely implications of humic substances for the migration of radionuclides in the environment.

It is important to emphasise that the case studies are **not** full, post-closure radiological performance assessment studies. They are merely intended to be examples that illustrate the application of the methodology, which has been developed during this project. For this reason, the model predictions described within should **not** be taken as a definitive prediction of the movement of radionuclides in the environment at any site.

During the HUMICS and HUPA projects, models have been developed that can describe the influence of humic substances upon the transport of metals. Column experiments have shown that the interactions of metal ions with humic substances are dominated by chemical kinetics. A coupled chemical transport code, k-1D, has been produced, which is able to perform transport calculations, taking chemical kinetics into account. All calculations presented in this report were made using k1D. The model and code have been presented and described elsewhere (Bryan et al 2003; Warwick et al 2000), and hence, they will not be discussed again here.

### Humics and RPA

Experiments have shown that in column experiments humic substances may promote the migration of radionuclides (Bryan et al 2003 etc.). Further, it is known that it is the ability of the humic to bind metal ions non-exchangeably that is responsible for this effect.

Metal ions bind to humics via two distinct modes, the exchangeable, where the metal ion is bound strongly, but may be removed instantaneously by a stronger competing sink; and the non-exchangeable, where the netal is no more strongly bound, but the desorption process is slow. The situation is made more complex by the fact that both modes exhibit heterogeneity. Many authors have found a distributon of binding strengths for the exchangeable fraction, whilst a range of first order dissociation rates are found for the non-exchangeable. However, in the case of the non-exchangeable, there is a distinct, most long-lived fraction that may be described with a single first order rate constant, and which accounts for a substantial percentage of the bound metal (King et al 1999; Monsallier et al 2003).

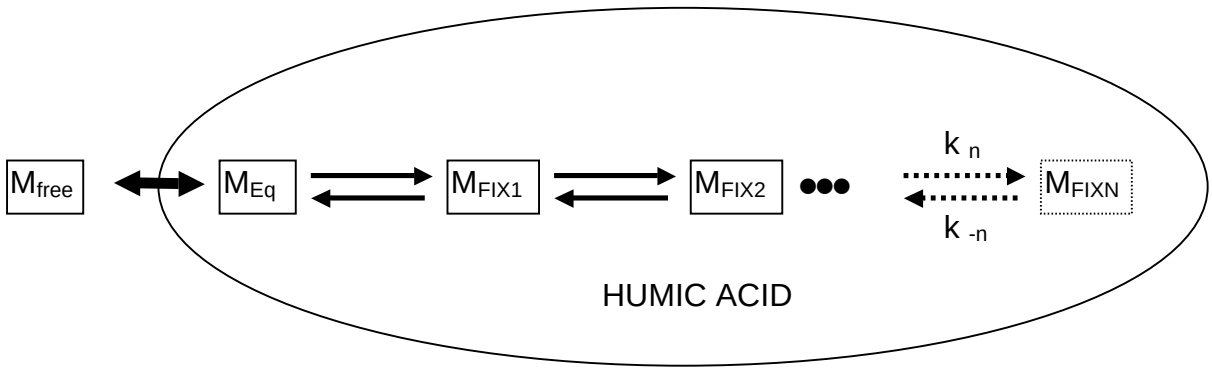


**FIGURE 1: The conceptual model metal ion/humic interactions, $M_{free}$ represents uncomplexed metal ion, $M_{Eq}$ exchangeably bound metal ion, and $M_{FIX1,\ 2\ ..N}$ successively more slowly desorbing non-exchangeably bound metal fractions.**

Figure 1 shows the conceptual model of humic substance metal ion binding developed over the last few years. Although there is evidence for heterogeneity, it has been found that adequate descriptions of column transport may be obtained by models that contain single exchangeable and single non-exchangeable binding sites, and so this is the approach adopted here.

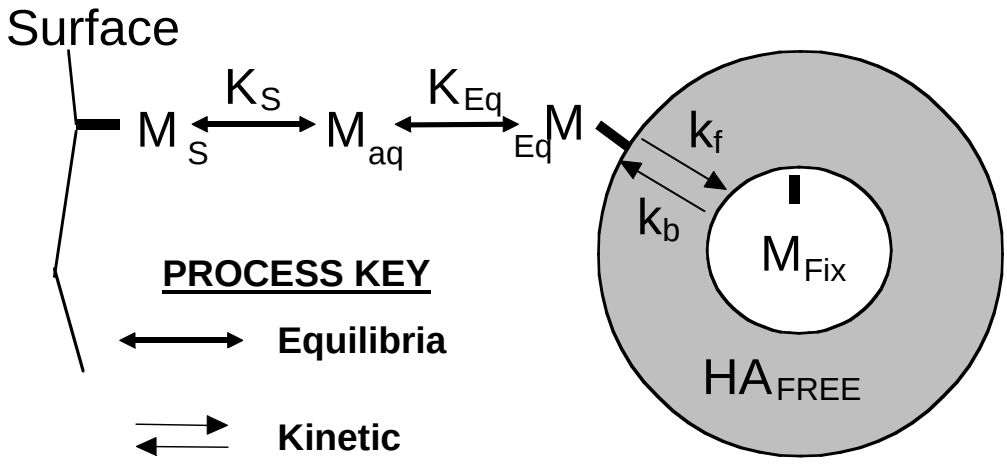


**FIGURE 2: The mathematical model of metal ion/humic interactions used in transport modelling, Maq represents uncomplexed metal ion, $M_S$ metal bound to the surface, $M_{Eq}$ exchangeably bound metal ion, and $M_{FIX}$ the non-exchangeable fraction; $K_S$ and $K_{Eq}$ are the equilibrium constants used to describe the interaction of the metal ion with the mineral surface and humic exchangeable fraction, respectively, and $k_f$ and $k_b$ are the rate constants that describe the transfer of metal to and from the non-exchangeable fraction.**

Hence, the complex conceptual model in Fig. 1 may be simplified to that shown in Figure 2, where a single equilibrium constant, $K_{Eq}$, describes initial, exchangeable binding, and a pair of rate constants, $k_f$ and $k_b$, describe the gradual transfer to the non-exchangeable, itself a slow process, and any subsequent removal of metal back to the exchangeable. This is the approach that has been applied in this work.

The Dukovany and Gorleben migration case studies comprise 'standard' medium to large distance and long-term migration calculations, i.e., they are essentially the type of calculations that might be required in the RPA of a waste repository (although they are not intended as full RPA studies; see above). The calculations for the U-tailings pile on the other hand are more distinct, and are very much specific to their individual test case. More than this, the chemistry for this study is quite different to that of the deep and shallow (Gorleben and Dukovany) repository type cases. Thus, while it has been possible to adopt a common general approach to the Gorleben and Dukovany cases, the U-tailings case study is treated separately here.

From the results of the case studies, we make conclusions about the impact of humic substances upon the migration of radionuclides and the implications for RPA, and these are discussed following the migration case studies.

## U-tailings Plie Case Study

The first migration case study concerns a pile of waste rock (tailings) from a mine in Schlema-Alberode, near Dresden, Germany. The pile was large (300m long by 30m high). The past tense is used, because since its selection as a study site, the pile has been removed by the authorities. The pile has been described in detail elsewhere (Schmeide et al 2003).

This case study presented more of a problem than the others, because the chemistry at the site is quite unique. Experiments were performed at CTU, Prague and the results modelled at Manchester (Bryan et al 2004). It was this work that provided the chemical equations to describe the dissolution of the uranium from the rock surface into the solution.

The water flowing through the pile contains significant concentrations of inorganic components. Those that have an effect upon uranium speciation are listed in Table 1. Given that these concentrations are large compared to the concentrations of uranium within the pile, it was found that these components had a 'constant' effect, and so conditional constants were defined, which took their effects into account implicitly. This allowed simplification of the migration calculations.

**Table 1: Composition of simulated Schlema-Alberode Water, SAW.**

| **Component** | **Concentration mol dm$^{-3}$** |
|---|---|
| $MgSO_4$ | 0.0175 |
| $CaSO_4$ | 0.0091 |
| $NaHCO_3$ | 0.00258 |

If these conditional surface sorption parameters are used to make transport predictions, then the effects of the background speciation will be included, but without making the calculations very 'expensive'. In effect, this approach treats all of the non-humic, solution phase uranium as $UO_2^{2+}{}_{(aq)}$. This approach and the derivation of the chemical model has been discussed elsewhere (Bryan et al 2004). To summarise, the following reactions, equations and

parameters were used to describe the interaction of U with the mineral surface in the migration case study. Two components were required, fast and slow.

The *Fast component,*

$$M + S \rightleftharpoons MS_{FAST} \qquad \text{[Eqn 1]}$$

$$K_{FAST} = \frac{[MS_{FAST}]}{[M].[S]} = 1.42x10^{5}\ dm^{3}\ mol^{-1} \qquad \text{[Eqn 2]}$$

where $[MS_{FAST}]$ [M] and [S] represent metal ion bound in the fast surface component, free metal ion, and free surface site concentrations, respectively, and $K_{FAST}$ is the equilibrium constant that describes sorption to the fast site.

The *Slow component,*

$$M + S \rightleftharpoons MS_{SLOW} \qquad \text{[Eqn 3]}$$

$$\frac{d[MS_{SLOW}]}{dt} = k_{slow,f}[M][S] - k_{slow,b}[MS_{SLOW}] \qquad \text{[Eqn 4]}$$

where $k_{slow,f} = 2x10^{-2}$ $mol^{-1}$ $dm^{3}$ $s^{-1}$; $k_{slow,b} = 1x10^{-7}$ $s^{-1}$, where $[MS_{SLOW}]$ represents metal ion bound in the slow surface component, and $k_{slow,f}$ and $k_{slow,b}$ are the rate constants that describe sorption to the slow surface site. A single surface site concentration for both components,

$$S_T = S + MS_{FAST} + MS_{SLOW} = 2.38x10^{-7}\ mol\ g^{-1} \qquad \text{[Eqn 5]}$$

This system of equations and parameters provided the best possible fit to the batch experimental data (Bryan et al 2004). The parameters to describe the interaction of $UO_2^{2+}$ with the humic substance were determined previously (during the HUMICS project). Note, these calculations have assumed that the U within the pile behaves as $UO_2^{2+}$ rather than "$U^{4+}$". The exchangeable is described using,

$$K_{Eq} = \frac{[M_{Eq}]}{[M_{aq}].[HA]} \qquad \text{[Eqn 6]}$$

and the non-exchangeable with,

$$\frac{d[M_{FIX}]}{dt} = k_f[M_{Eq}] - k_b[M_{FIX}]. \qquad \text{[Eqn 7]}$$

The parameters $K_{Eq}$, $k_f$ and $k_b$ are as defined in Figure 2, and their values are $2.24x10^{6}$ $dm^{3}$ $mol^{-1}$, $2.2x10^{-7}$ $s^{-1}$, $2.0x10^{-6}$ $s^{-1}$, respectively.

Ternary system experiments to study the desorption of U in the presence of humic acid were inconclusive, and no systematic or dramatic effect was observed. Therefore, in this case study, the sorption of humic or humic-metal ion complex has not been included, since there

was no evidence that this behaviour was significant. The effects of humic sorption are considered during the other two migration cases.

It is important to point out that the calculations for this case are limited by the available information. In a three year project, the time available to observe desorption is quite limited. It is clear that there will be two types of U present within such a rock pile: firstly, that which forms part of the mineral lattice, and then that which is sorbed onto the rock surfaces. The U within the lattice will be very strongly held, and will only desorb very slowly, particularly under the relatively mild conditions within the pile. Hence, the dissolution of this fraction was not observed during the experiments. Instead, only the desorption of the surface sorbed U was observed. Hence, the parameters ($K_{FAST}$, $k_{slow,f}$ and $k_{slow,b}$ above) describe the behaviour of this part of the U only. The net result is that the predictions for this case study represent the fate of this fraction only and **not** the lattice bound fraction.

Unfortunately, the distribution between lattice and (weakly) sorbed U within the pile itself is unknown (the pile had been removed before the migration case study started). Hence, for this calculation, it was assumed that all of the uranium was available for desorption. Hence, the concentrations eluting and migrating in these caculations represent an over estimate, although the results are scalable to the starting concentrations, so for example, if the sorbed fraction actually accounted for 50% of the total, then all of the concentrations in the results (Figs. 3 to 7) should be divided by 2.

The calculation scenario is very simple: simple linear flow from the top of the pile straight to the bottom is assumed. The linear flow rate is $9.5 \times 10^{-7}$ $ms^{-1}$ taken from measurements made at the site. The dispersivity is not known, and so an arbitrary value of 3m over a total column distance of 30m was selected. The k1-D code used to make the calculations is a simple 1-D advection-dispersion model, which is clearly suited to saturated systems. It is highly unlikely that the pile itself was saturated, but there was no scope within the project to produce a transport model for an unsaturated system that could cope with chemical equilibria and kinetics simultaneously. Hence, the k1-D model was used with a very low porosity (0.003) in order to achieve the correct linear flow rate. This was acceptable, because:
1. This is not a RPA study, and it is not the intention for any of the migration case studies to generate a credible prediction, rather, the aim was to determine the impact of humic substances upon migration in general;
2. This project was not concerned with the modelling or the interpretation of transport phenomena.

Despite the problems with the transport model, all of the relevant chemistry is included in the model, and so the general conclusions from the calculations will be valid, although for this reason the absolute predicted concentrations should be treated with caution.

The chemical composition of the seepage water is given in Table 1. As explained above, these species were included in the batch experiments from which the conditional constants $K_{FAST}$,

$k_{slow,f}$ and $k_{slow,b}$ were derived. Therefore, there was no need to include these in the calculations: indeed, it would have been wrong to do so. The humic acid concentration measured in the seepage water is ~5 mg DOC $dm^3$, which equates to an effective binding site concentration, [HA], of $3x10^{-5}$ mol $dm^{-3}$.

Separate hypothetical vertical columns were defined at two positions in the pile, labelled 1 and 2. This was to make sure that the conclusions were not dependent upon the initial distribution of U in the column. The pile is quite heterogeneous, and the U concentration varies with depth. The initial distribution of uranium down each of these columns is shown in Figure 3

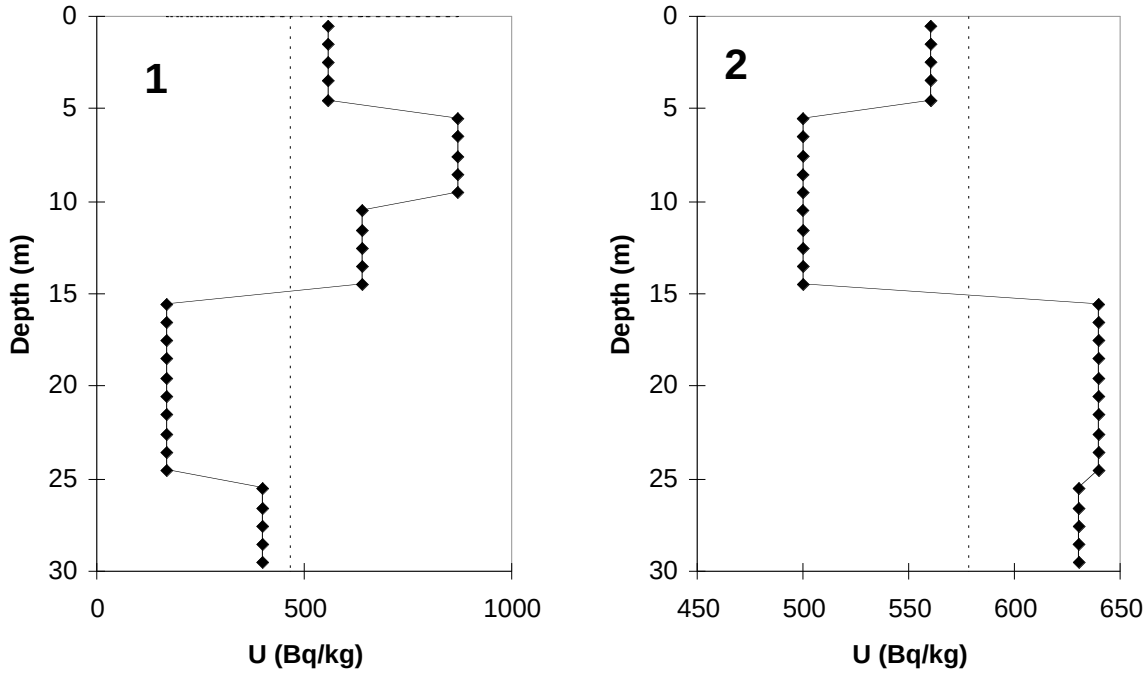


**FIGURE 3: Initial distribution of uranium in hypothetical columns 1 and 2.**

For each column 3 calculation types were performed:
1. including humic substances with both the exchangeable and non-exchangeable fractions present, i.e., using all of the chemical equations (1 to 7), and labelled "*with humic*" in the figures.
2. including humic substances with the exchangeable fraction, but with the non-exchangeable **excluded**, i.e., in these calculations the humics were not 'permitted' to bind metal ions non-exchangeably (equation 7 was removed). These results are labelled "*humic (exch only)*" in the figures.
3. excluding the humic substances completely, i.e. [HA] was set to zero. These results are labelled "*no humic*" in the figures.

The results of these calculations are shown in Figures 4 to 7.

Figures 4 and 5 show the predicted variation in the uranium concentration of the effluent seeping from the bottom of the pile with time for hypothetical columns 1 and 2, respectively.

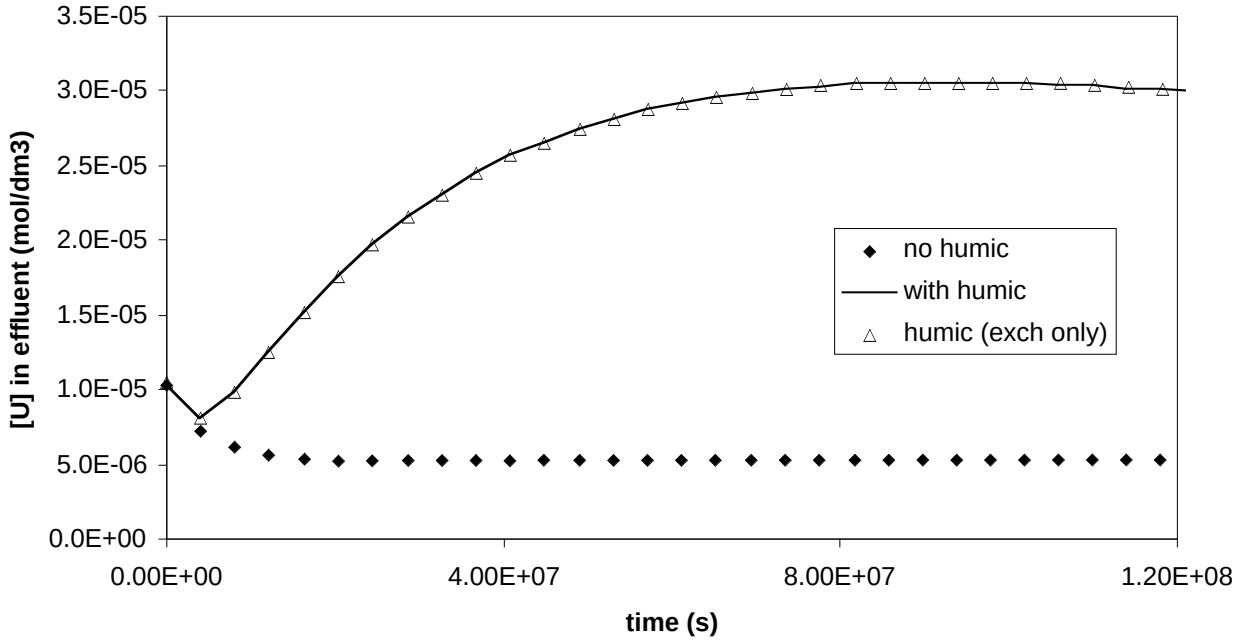


**FIGURE 4: predicted uranium effluent from hypothetical column1**

The variation in elution concentration clearly differs between the two columns; number 1 (with humic) climbs to a steady value after a small, initial dip, whilst number 2 falls steadily. This difference is a direct result of the different initial uranium distributions.

For column 1, initially the majority of the uranium sits at the start, and this slowly shifts towards the bottom with time, and hence the increasing effluent concentration represents the movement of U towards the bottom. Obviously, given long enough, the elution concentration starts to decrease, as the column becomes depleted in U. Column 2 is much less heterogeneous then number 1 (note the difference in the x-axis scales in Figure 3. The steady drop in effluent concentration with time here represents the gradual depletion of the column, which leaves less U to elute as time increases.

Both figures indicate that the humic is predicted to have an effect, and the effluent concentration is significantly higher than in the absence of humic. The surprise is that the humic is predicted to have an effect purely as a normal ligand, even in the absence of the non-exchangeable interaction. The model predicts that the exchangeable on its own is sufficient to prevent, or at least reduce, readsorption of U once it has left the surface. This result is unique. All real column experiments require the non-exchangeable interaction in order to explain migration, and the exchangeable is thought to play a negligible part in transport. The observation is also at odds with the other migration case studies in this project (see below), and other transport calculations (e.g. Bryan 2005, Bryan et al 2003, Warwick et al 2000).

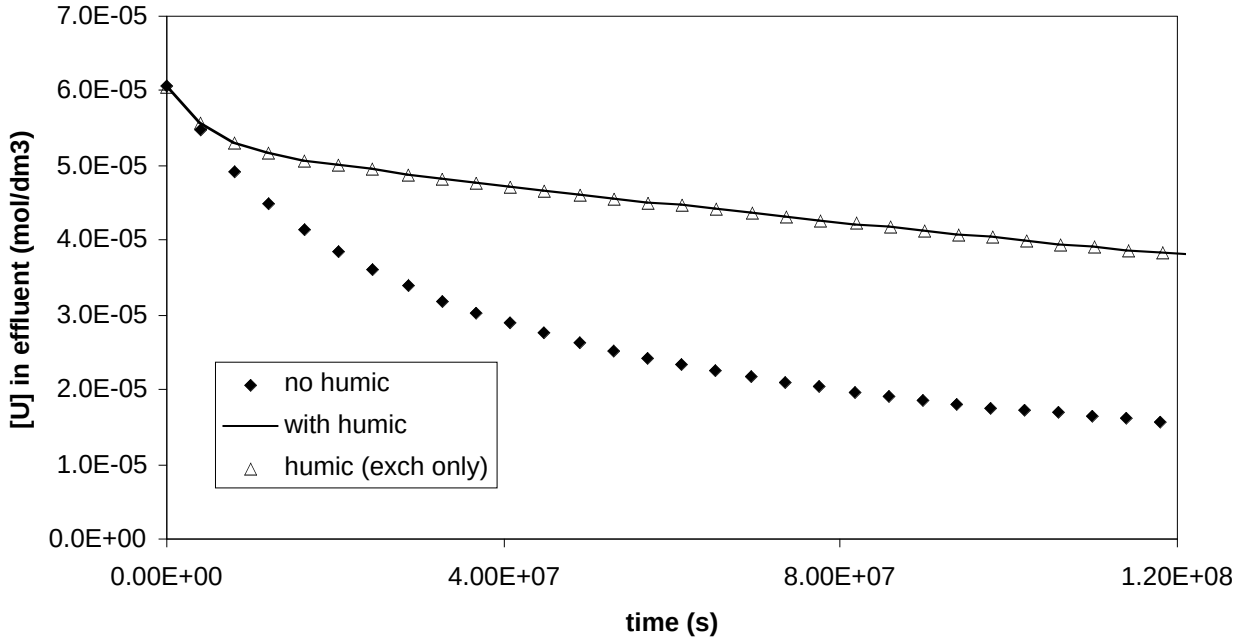


**FIGURE 5: predicted uranium effluent from hypothetical column 2**

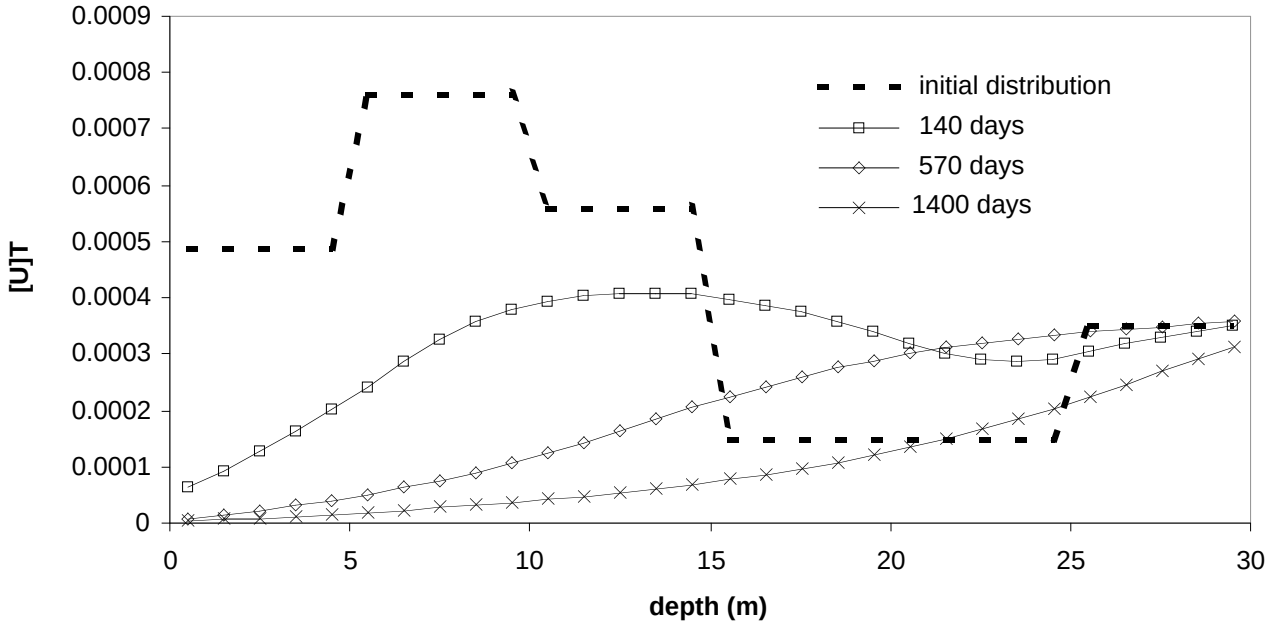


**FIGURE 6 variation in uranium concetration profile in column 1 with time for 'with humic' calculation, [U]T represents total uranium concentration, solution and surface phases together.**

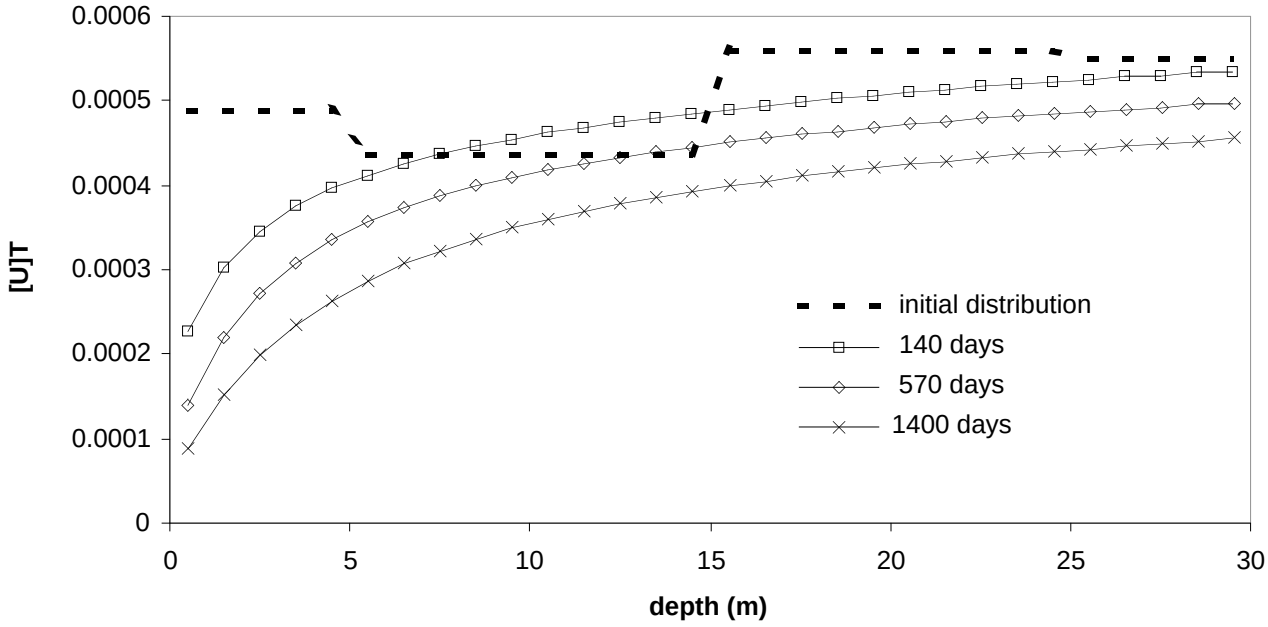


**FIGURE 7: variation in uranium concetration profile in column 2 with time for 'with humic' calculation, [U]T represents total uranium concentration, solution and surface phases together.**

Figures 6 and 7 show the variation in the column profiles with time for columns 1 and 2, respectively. The total uranium concentrations (effective mol $dm^{-3}$), regardless of chemical form and whether solution or solid is plotted vs distance from the top of the column. Not surprisingly, the area under the profile decreases steadily with time as U is removed from each of the columns. In column 1 (Figure 6) a transient peak moves down the column as the high initial concentration at the top is flushed towards the bottom. This behaviour matches that in Figure 4.

The more homogeneous column 2 shows much simpler behaviour: the same general profile shape is retained over time as the U is removed. At all times, there is a dip in concentration at the top of the column, which rises to a fairly steady level further down. This is due to the in flow of 'clean' seepage water at the top of the column that scours U from the surface there: further down the column, the arriving pore water will already be U-loaded, and there will be more of a balance between desorption from the surface and readsorption.

**U-Tailings Pile Summary**

In this migration case the humic is predicted to promote migration significantly, which is not particularly surprising. However, the calculations suggest that the presence of the non-exchangeable binding mode does not make a significant difference. This second result is at odds with all other studies. In mathematical terms, the origin of the effect is easy to identify. The reason that the exchangeable is not able to compete with the surface in real column experiments and in other modelling work is that it is unable to compete with the strong and numerous surface sites, and any metal ion in the exchangeable is immediately removed onto the surface at first contact. Here though, the exchangeable is able to compete, hold on to metal and pull metal off the surface, promoting migration. It seems highly unlikely that this

modelling result has application beyond this specific study, since it is so at odds with experiment: even in column experiments using relatively high humic concentrations and acid washed sand packing (not a particularly effective metal ion sink), none of the exchangeably bound metal fraction transports.

Either there is something very special about the material in this tailings pile, which seems unlikely, or the origin lies in the definition of the surface-uranium interaction (Eqns 1 to 5). The chemical parameters $K_{FAST}$, $k_{slow,f}$ and $k_{slow,b}$ were determined from batch desorption experiments only, and no sorption studies were performed. Hence, it may be that the parameters give a faithful description of the desorption process, but that they do not fully represent the sorption step.

It is worth remembering that the k1-D computer code is here being used for a purpose for which it was not intended, and for this reason alone, we should treat these predictions with caution. Whatever the origin of the effect, we should not draw the conclusion that the non-exchangeable fraction may not be important in some circumstances. Beyond the riddle of the non-exchangeable effect, this case study does represent a unique and esoteric scenario, which probably has limited application to the more usual RPA scenarios.

## The Repository Cases (Gorleben and Dukovany)

Although the Gorleben and Dukovany case studies have their own scenarios and conditions, there is sufficient similarity that we may describe many aspects together. The system of chemical equations used to describe the two cases is the same, and these are illustrated in Figure 8.

Mathematical equations were defined to describe each of the chemical processes in Figure 8. The interactions of the metal ions with the humic exchangeable site and the mineral surface were defined with equilibrium constants, $K_{Eq}$ and $K_S$, respectively,

$$K_{Eq} = \frac{[M_{Eq}]}{[M_{aq}].[HA]}, \qquad \text{[Eqn 8]}$$

$$K_S = \frac{[M_S]}{[M_{aq}].[S]}, \qquad \text{[Eqn 9]}$$

whilst the transfer between the exchangeable and non-exchangeable fractions was described with rate constants, $k_f$ and $k_b$,

$$\frac{d[M_{FIX}]}{dt} = k_f[M_{Eq}] - k_b[M_{FIX}]. \qquad \text{[Eqn 10]}$$

where $[M_{aq}]$ is the concentration of free metal; [S] is the effective concentration of surface sites; [HA] is the concentration of humic exchangeable sites; $[M_{Eq}]$ is the concentration of metal in the exchangeable site; $[M_{FIX}]$ is the concentration of metal in the non-exchangeable site.

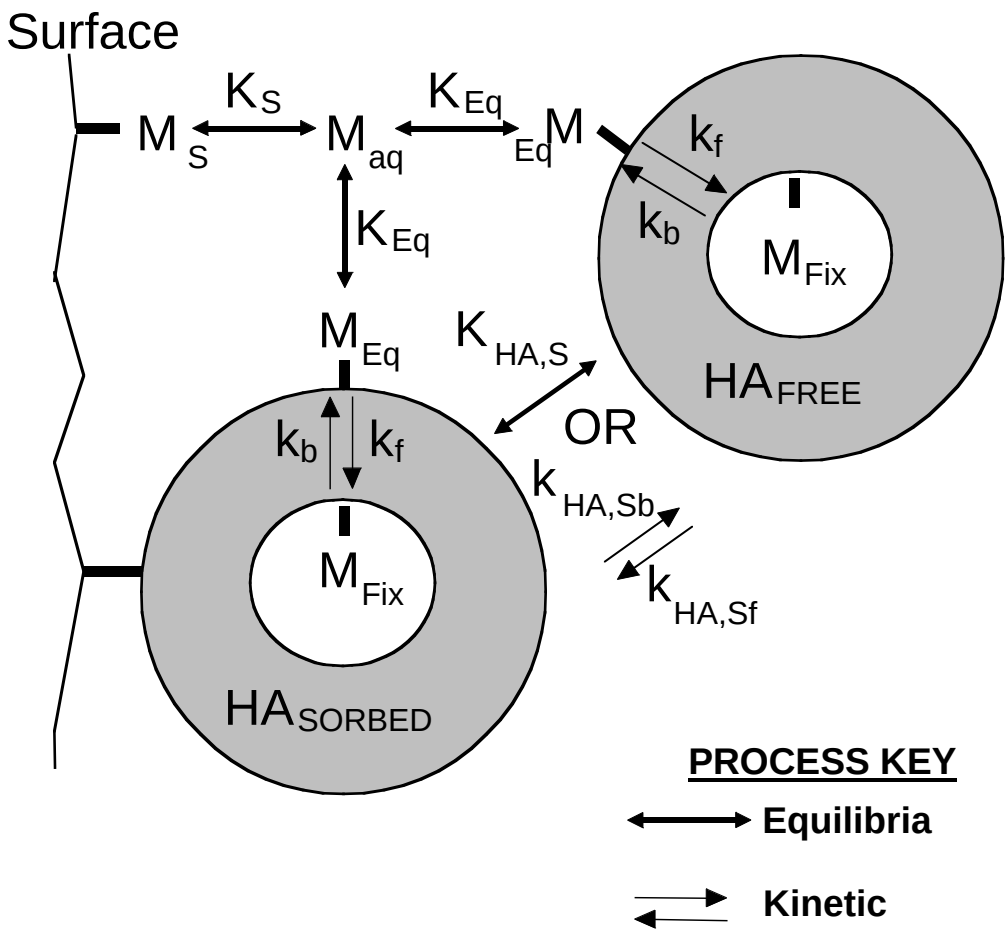


**Figure 8 Chemical processes used in the Dukovany and Gorleben calculations. Maq represents uncomplexed metal ion, $M_S$ metal bound to the surface, $M_{Eq}$ exchangeably bound metal ion, and $M_{FIX}$ the non-exchangeable fraction, whilst $HA_{FREE}$ and $HA_{SORBED}$ represent humic free in solution and sorbed to the mineral surface, respectively; $K_S$ and $K_{Eq}$ are the equilibrium constants used to describe the interaction of the metal ion with the mineral surface and humic exchangeable fraction, respectively, and $k_f$ and $k_b$ are the rate constants that describe the transfer of metal to and from the non-exchangeable fraction. The treatment of the sorption of humic and humic-radionuclide complex is uncertain, and may be described either with an equilibrium constant, $K_{HA,S}$, or a pair of forward and backward rate constants $k_{HA,Sf}$ and $k_{HA,Sb}$.**

In the case of the interaction of the humic substance (and humic/metal ion complexes) with the mineral surface, there was some uncertainty about whether the interaction should be described with an equilibrium or kinetic equation. Therefore, two alternatives were adopted: either,

$$K_{HA,S} = \frac{[HA_{SORBED}]}{[HA_{FREE}]} \qquad \text{[Eqn 11]}$$

where $K_{HA.S} = 60$, or,

$$\frac{d[HA_{SORBED}]}{dt} = k_{HA,Sf}[HA_{FREE}] - k_{HA,Sb}[HA_{SORBED}] \qquad \text{[Eqn 12]}$$

where $k_{HA,Sf}$=6.0x10$^{-6}$ s$^{-1}$ and $k_{HA,Sb}$=1.0x10$^{-7}$ s$^{-1}$, and [$HA_{FREE}$] and [$HA_{SORBED}$] represent the (effective, $HA_{SORBED}$) concentrations of free and sorbed humic or humic metal complex, respectively. These parameter values ($K_{HA.S}$, $k_{HA,Sf}$ and $k_{HA,Sb}$) are derived from column experiments (Bryan et al 2003).

In a repository there will be a very large number of isotopes. This study, however, has been limited to the study of the three actinide elements: Np, Am and Pu. In the case of Am the choice of oxidation state is clear, since it has only one stable state under realistic far field conditions. In the case of Pu, there will be some uncertainty. However, the +IV state was selected, since it is more likely to be transported by humics, and hence, is a conservative choice. For Np, the $NpO_2^+$ ion, oxidation state V, was selected as a contrast to the Pu calculations.

Both of these sites were studied very briefly during the previous HUMICS project. At that time, the non-exchangeable interaction was less clearly understood. In particular, many rate constants had been determined in the laboratory, but these were derived from experiments where the humic and metal ion had only equilibrated for a period of several weeks, and there was some uncertainty regarding the rate constants that might be observed on a larger, field time scale, and indeed whether the percentage of metal entering the non-exchangeable would also be different. It was not clear that the data determined under short time scale artificial lab conditions were applicable to the environment. Indeed, some had even suggested that under the long time scales of a waste repository scenario, metal ions might become pseudo-irreversibly bound to their humic. Such a position would have a profound impact upon migration, because any pseudo-irreversibly bound metal ion would remain isolated from the mineral surface indefinitely, and in the absence of the sorption of the humic itself, would transport as a conservative tracer. This was one of the scenarios adopted during the original Gorleben calculations during the HUMICS project. However, during this (HUPA) project, the kinetic parameters ($k_f$ and $k_b$) for a series of radionuclides have been determined from a soil sample naturally labelled with anthropogenic radionuclides over the last several decades. Table 2 shows the values that were obtained.

**Table 2: Desorption rate constants and amounts of isotopes in the non-exchangeable fraction for the sample from the Esk Estuary, U.K. A range for $^{239,\ 240}$Pu concentrations is given, as the proportion of each isotope is unknown.**

| Isotope | Experiment Type | Equilibration Time | $Log_{10}$ (Rate Constant) /$s^{-1}$ ± Log (Error) | Amount in non-exch. Fraction ± Error % | Metal Concn. (mol $dm^{-3}$) |
|---|---|---|---|---|---|
| $^{237}$Np | natural | 25 – 30 a | -7.4 (1.17) | 60 (40) | 1.1 x 10$^{-12}$ |
| $^{239, 240}$Pu | natural | 25 – 30 a | -7.4 (0.06) | 44 (4) | 7.3 x 10$^{-15}$ – 1.89 x 10$^{-11}$ |
| $^{241}$Am | natural | 25 – 30 a | -7.2 (0.09) | 28 (3) | 1.8 x 10$^{-12}$ |

Clearly, in any series of calculations such as this, there will be some uncertainty regarding precisely which values of the various chemical parameters are the most suitable. However, these are not intended as 'full' RPA studies, and the calculations are not intended to provide predictions for the behaviour at each site. Rather, our aim is to demonstrate the general effects of humic substances. Therefore, values for the chemical parameters were selected (arbitrarily) as those determined for Gorleben and used for both sites. Table 3 shows the common parameters and associated values.

**Table 3: equilibrium and rate constants used in the Dukovany and Gorleben case studies. The values of kf and kb are taken from HUPA Work Package 5 (Table 2). values for $K_{EQ}$ and $K_S$ are standard values for the Gorleben site**

| | $K_{Eq}$ (l $mol^{-1}$) | $K_S$ (l $mol^{-1}$) | $k_f$ ($s^{-1}$) | $k_b$ ($s^{-1}$) |
|---|---|---|---|---|
| $NpO_2^+$ | 597 | $4.35x10^3$ | $5.97x10^{-8}$ | $3.98x10^{-8}$ |
| Am (III) | $4.80x10^5$ | $3.50x10^6$ | $2.45x10^{-8}$ | $6.31x10^{-8}$ |
| Pu (IV) | $2.50x10^9$ | $1.82x10^{10}$ | $3.13x10^{-8}$ | $3.98x10^{-8}$ |

In order to calculate the migration of the radionuclides in the far-field, it is necessary to define an input concentration from the waste repository, i.e. an upper boundary concentration or $C_o$. A value of $1x10^{-10}$ mol $l^{-1}$ was chosen, since this would prevent any of the metal binding fractions from becoming saturated. The limiting factor is the concentration of humic substance. The fraction of metal that ends up in the non-exchangeable fraction is independent of humic concentration until a threshold concentration is reached (King et al 1999). The metal ion concentration representing the saturation point, $[M]_{SAT}$ (mol $l^{-1}$), is related to the DOC (mg $l^{-1}$) via,

$$[M]_{SAT} \propto DOC(1x10^{-7}).$$

For both Dukovany and Gorleben, the $1x10^{-10}$ mol $l^{-1}$ input concentration is below the limit. The advantage of choosing a concentration below the limit is that, if the results are presented as concentrations divided by the input concentration (i.e. $C/C_o$), then they will be the same for all input concentrations below the limit. Hence, although calculations were made with $C_o$ = $1.0x10^{-10}$ mol $l^{-1}$, they are equally valid for all values of $C_o$ less than approximately $3.1x10^{-7}$ mol $l^{-1}$ for Dukovany and $1x10^{-6}$ mol $l^{-1}$ for Gorleben.

Another significant source of uncertainty in these types of calculations is the initial chemical state of the humic/radionuclide complex. Metal may be bound either in the exchangeable or non-exchangeable states. Initially, metals bind at the exchangeable site and then transfer, with rate constant $k_f$, to the non-exchangeable. Hence, some time is required to populate the non-exchangeable fraction. In a real situation, it is unclear how much time the metal will have to interact with the humic before migration commences. This uncertainty is problematic, since the non-exchangeable fraction is responsible for long distance migration. The answer to the problem will depend largely upon whether humic materials penetrate the near or local fields. In the absence of any evidence to the contrary, the only conservative approach must be to assume that population of the non-exchangeable site is complete prior to the onset of migration.

Beyond this point the conditions, scenarios and calculations for the two sites will be discussed separately.

## The Dukovany Case Study

The Dukovany site in the Czech Republic contains a power station and low level waste repository all within the same complex. The site was considered originally because it was used for field studies as part of the CARESS Framework IV, E.U. project, which studied the role of inorganic colloids in the transport of the actinides.

The geology at the site is complex. However, it has been characterised as a sandy deposit with some silt and clay. The groundwater flow at the site runs from North to South with an average flow rate of $1x10^{-6}$ m $s^{-1}$. The CARESS borehole (HV3) lies to the South of the complex. It was found that the transmissivity at the borehole was $2x10^{-6}$ $m^2s^{-1}$, and the linear dispersion was 0.1m over a distance of 3m. The CARESS and other work were not 'humic specific' and so there are no in situ data from borehole experiments. The pumping studies using the inert, and notionally conservative, tracers Rhodamine, Fluorescein and $SF_6$, plus silica colloids found that there was significant spatial heterogeneity.

**The Scenarios**

The calculations described here use a scenario based (loosely) upon the Dukovany site. However, the purpose is merely to demonstrate the likely effect of humic substances at this sort of site. If this were a rigorous performance assessment exercise, then very much more information would be required, in particular, detailed knowledge of geochemistry, geology and hydrology. The scenario is based upon the notional transport of radionuclides away from the low level waste repository at Dukovany. However, the results are applicable to any shallow, sandy site.

The scenario assumes that the repository near field containment has failed, allowing radionuclides to enter the far field (geosphere). The leak of contamination is assumed to be constant over time. Calculations have been performed over a 300m distance. A linear flow rate of $1x10^{-6}$ $ms^{-1}$ was used. The linear dispersion observed in the CARESS experiments was scaled to give a value of 10m over the 300m hypothetical column. A porosity of 0.3 (30%) was used. However, provided the linear velocity was constant, the calculations were found to be extremely insensitive to this parameter. Molecular Diffusion was assumed insignificant. Calculations were routinely performed on a time scale of 100 years from the onset of repository failure.

The *in situ* concentration of humic substances at the Dukovany site is 3.1 mg DOC $l^{-1}$. The value of [HA] ($3.1x10^{-5}$ mol $l^{-1}$) was obtained by analogy with the standard Gorleben humic values, allowing for the different humic concentrations. [S] was set at $5.7x10^{-2}$ mol $l^{-1}$, again by analogy with Gorleben. Other chemical parameters are shown in Table 3.

Calculations were performed using the k1D code. A hypothetical column cross-sectional area of 1 $m^2$ was used, although this has no effect upon the results, provided that a constant linear flow rate is maintained. The 300m column was split into 50 subdivisions, and 0.1 year time steps were used.

Using the information and parameters from this HUPA project, 4 calculation scenarios (A - D) were used for each radionuclide:

**A**: Including humic sorption on the mineral surface described with a kinetic reaction, with the exchangeable and non-exchangeable metal fractions in equilibrium, i.e. non-exchangeable full at the point of entry to far field;

**B**: No humic sorption at all: i.e. the humic and humic/radionuclide complexes move as conservative tracers, humic exchangeable and non-exchangeable metal fractions in equilibrium;

**C**: Including humic sorption on the mineral surface described with an equilibrium reaction, and with the humic exchangeable and non-exchangeable metal fractions in equilibrium;

**D**: Including humic sorption on the mineral surface described with a kinetic reaction, but with exchangeable and non-exchangeable metal fractions **not** in equilibrium, i.e. non-exchangeable fraction empty at the point of entry to far field.

All of these scenarios used the values of the parameters given in Table 3.

In addition to these four new calculations, some other calculation results are shown in the figures.

The results of the calculations from the previous HUMICS project are labelled as '**old kinetics**'. These calculations did not include humic (or humic radionuclide complex) sorption to the mineral surfaces, i.e. neither equations 11 or 12 were used. Also, the first order desorption rates were larger than those in Table 3, since they were determined from short term synthetic laboratory batch experiments: the values are shown in Table 4 The values that were used for $K_S$ and $K_{Eq}$ were the same as those in Table3

**Table 4 values of rate constants used in calculations during the humics project (To produce plots labelled 'old kinetics').**

| | $k_f$ ($s^{-1}$) | $k_b$ ($s^{-1}$) |
|---|---|---|
| $NpO_2^{2+}$ | $2.22 \times 10^{-7}$ | $2.00 \times 10^{-6}$ |
| Am (III) | $4.03 \times 10^{-7}$ | $9.30 \times 10^{-7}$ |
| Pu (IV) | $2.44 \times 10^{-7}$ | $2.00 \times 10^{-7}$ |

In the next set of calculations the non-exchangeable interaction is excluded completely from the calculation, i.e. equation 10 excluded (humic sorption is still excluded). These results are labelled '**No kinetics at all**'.

In the final set of calculations, the humic is removed completely from the scenario (eqn 8 also removed). These are labelled '**no humic**'.

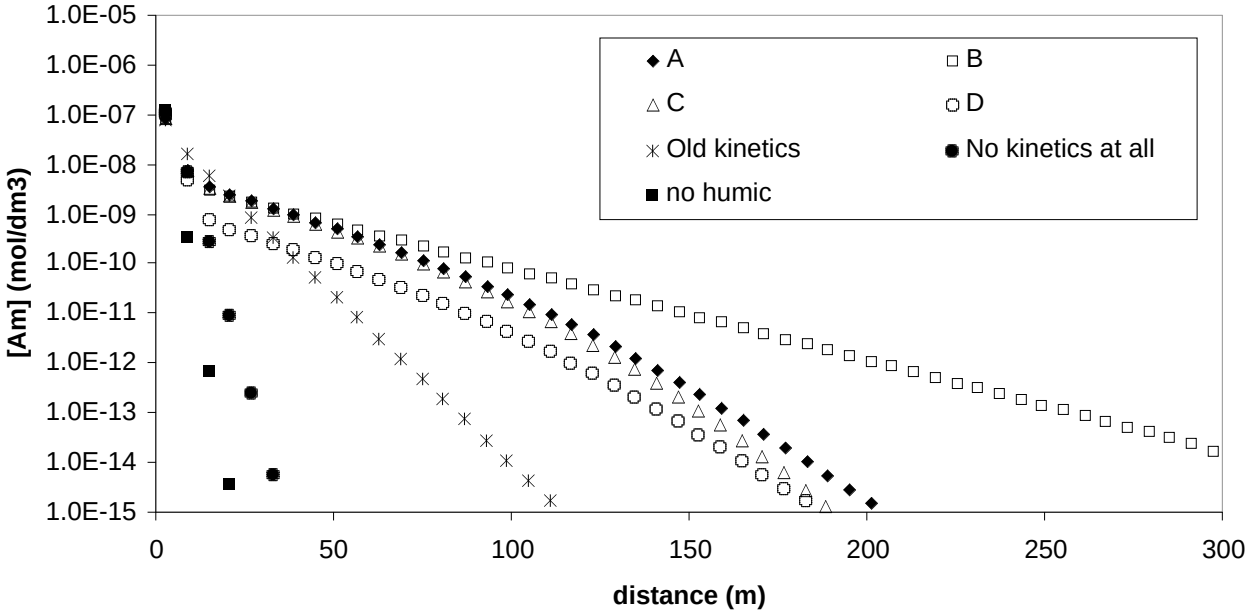


**FIGURE 6: Dukovany 100 year Am migration predictions, y-axis = total radionuclide concentration, all species, solution and sorbed.**

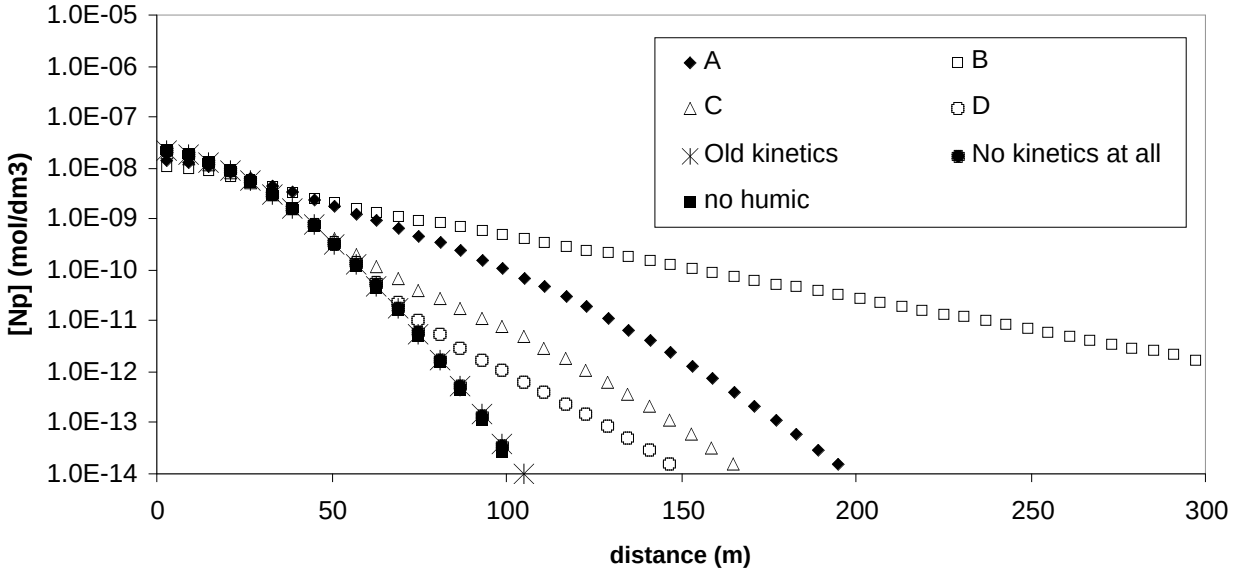


**FIGURE 7 Dukovany 100 year Np migration predictions, y-axis = total radionuclide concentration, all species, solution and sorbed**

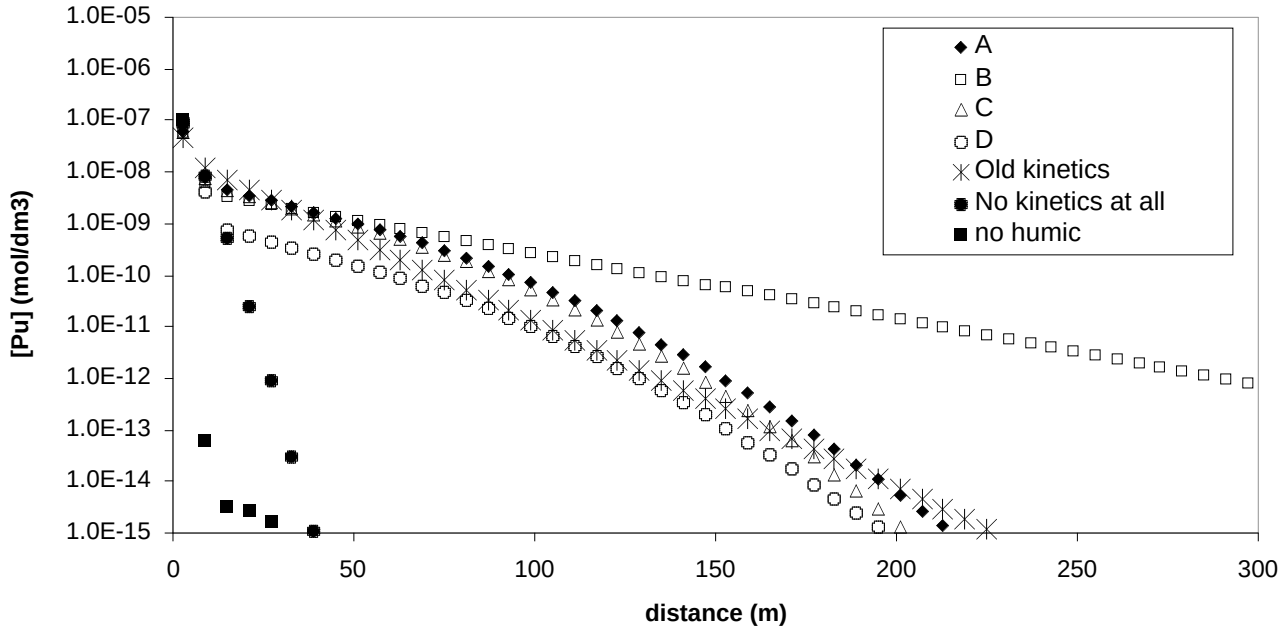


**FIGURE 8 Dukovany 100 year Pu migration predictions, y-axis = total radionuclide concentration, all species, solution and sorbed**

Figures 6, 7 and 8 show 100 year migration predictions for Am, Np and Pu, respectively. In each case, the data are plotted as the sum of the radionuclide concentrations, regardless of chemical form, and whether in solution or sorbed, versus distance from the point that the radionuclide enters the far field. In all three cases, there is little difference between the 'no humic' and 'no kinetics at all' plots. Hence, these calculations confirm that in the absence of the non-exchangeable interaction, humic substances are predicted to have very little effect upon the migration of radionuclides. The predictions using the values of $k_f$ and $k_b$ from short term lab systems ('old kinetics') show much less migration than the predictions using the rate constants from the 'natural' sample (scenarios A - D). This is expected, since the 'natural' rate constants are significantly lower than for the lab systems. As soon as the humic metal complex enters the start of the column, any radionuclide in the exchangeable fraction is instantaneously removed from the humic and sorbs on the mineral surface, because the exchangeable is unable to compete with the mineral surface. With the exchangeable depleted, radionuclide will start to leave the non-exchangeable and enter the exchangeable, and then will instantaneously sorb onto the surface. For the new calculation scenarios (A - D) it will take longer for the radionuclide to leave the non-exchangeable fraction, because the rate constants are lower. Hence, the radionuclides will travel further before being immobilised. In Figure 8, the 'old kinetic' plot shows more migration than in Figures 6 and 7, because the old rate constants were smaller anyway, and so the switch to the new constants has made much less difference. However, it is important to remember that the 'old kinetics' plots do not include the effects of humic sorption, and so to see the real differences between the HUMICS and HUPA rate constants, we must consider scenario B, and hence, even in Figure 8, the HUPA constants produce significantly more transport.

Out of the scenarios A - D, scenario B shows the most pronounced migration, because it does not include humic sorption, and hence, the humic-radionuclide complex will transport as a conservative tracer. Scenario D shows the least migration out of A - D, because the non-exchangeable fraction here is empty at the start of the column, hence, only the small amount of metal that manages to access the non-exchangeable, once the solution has entered the far field will be transported: note, although D seems close to the others (A,B,C), at least compared to the old predictions, there is in fact a significant difference (note log y-scale).

Figures 9 and 10 show the effect of changing some of the parameters in the calculations. Figure 9 shows the effect of increasing the humic acid concentration by a factor of 10 (lines): for comparison the original results are also shown (points). Similarly, Figure10 shows the effect of dividing the surface interaction equilibrium constant ($K_{SURF}$) by a factor of 10. Both of these changes have no significant effect upon the predicted transport, since the difference in affinity between the humic exchangeable site and the mineral surface is so great that the surface will always strip all metal ion from the exchangeable, even if the conditions are changed significantly. Since, the non-exchangeable is responsible for the transport, it is only the parameters that affect this fraction and its transport that have a significant effect, i.e. $K_{HA,S}$, $k_{HA,Sf}$, $k_{HA,Sb}$, $k_f$, $k_b$ (see Figures 6, 7 and 8). Note, the humic acid concentration does not affect the distribution of metal ion between the exchangeable and non-exchangeable fractions ([HA] does not appear in equation 10).

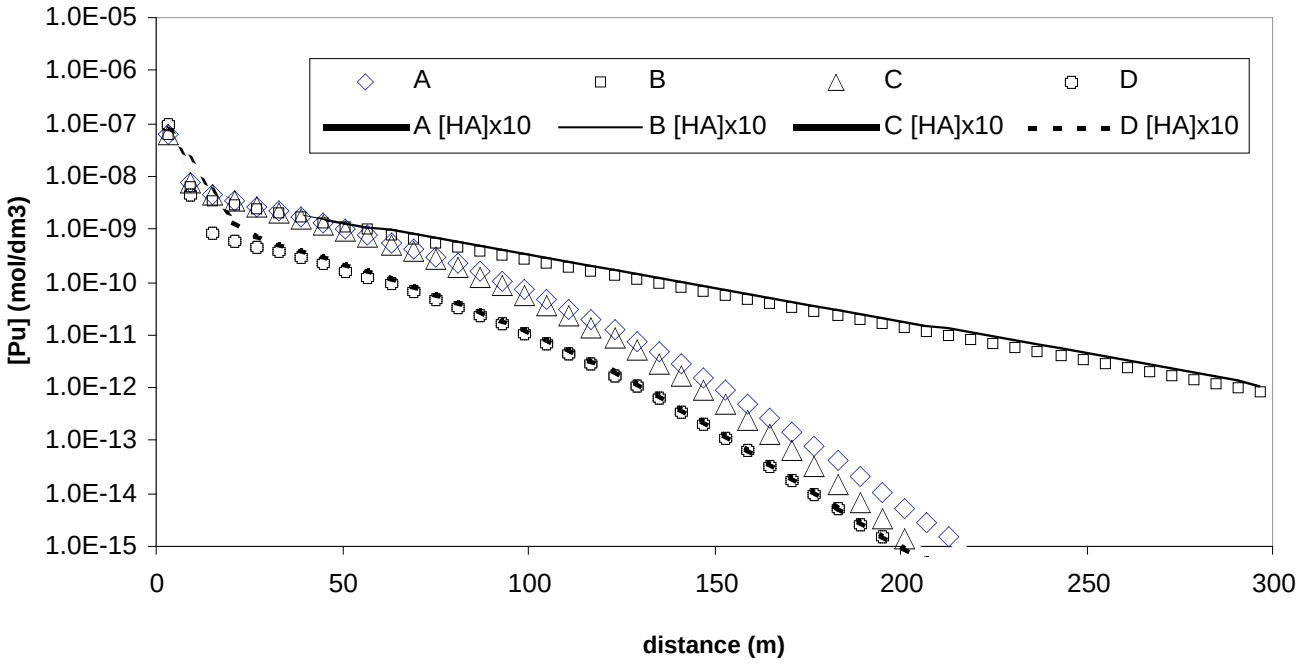


**FIGURE 9: Effect of increasing humic concentration by factor of 10 upon 100 year Pu migration predictions.**

Hence, for all of the radionuclides, humic substances are predicted to promote migration, compared to a humic free system. It is the non-exchangeable that is responsible for the

transport phenomenon. Further, the predictions seem relatively insensitive to the equilibrium parmeters that describe the interaction of the metal ions with the humic exchangeable fraction and the mineral surface.

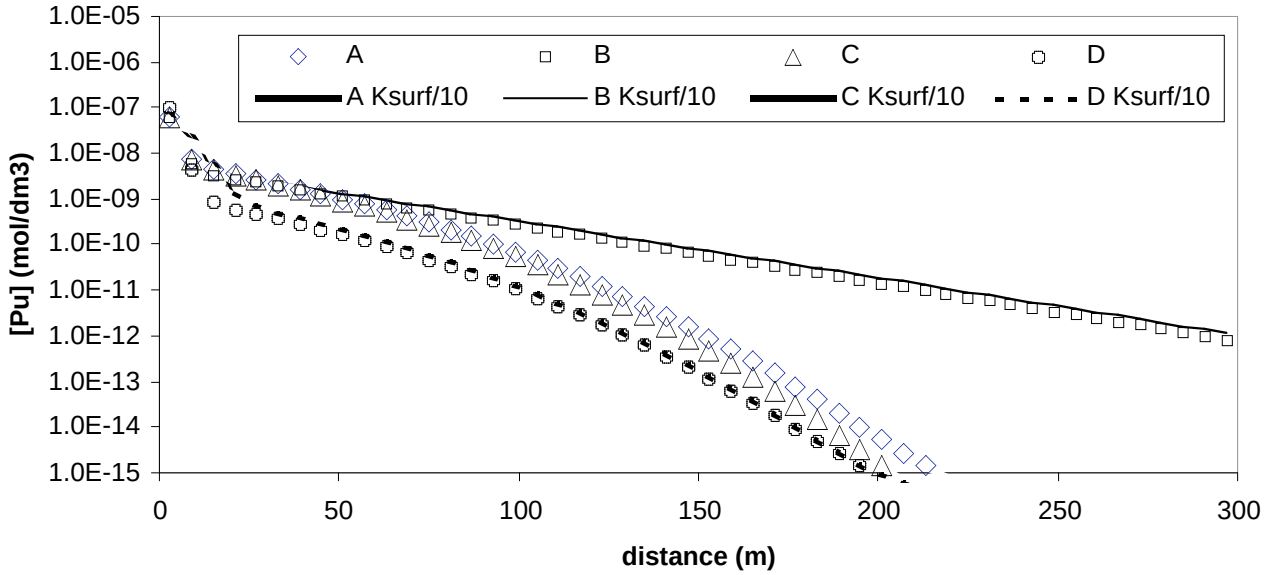


**FIGURE 10: Effect of reducing surface metal ion affinity constant by factor of 10 upon 100 year Pu migration predictions.**

Although the results are relatively insensitive to $K_{Eq}$, and $K_{SURF}$, there is still some uncertainty. Any of the calculation scenarios A - D are plausible. In the case of the non-exchangeable fraction itself, there is little uncertainty about the best way to describe the interaction and the transfer to and from the non-exchangeable, and HUPA work package 5 has provided suitable values for the rate constants. However, in the case of the interaction of the humic itself with the mineral surface, there is more uncertainty, since separate column experiments have been successfully modelled: excluding all humic sorption (Warwick et al 2000), and including humic sorption described with both equilibria and rate constants (Bryan et al 2003). Hence, scenarios A, B and C are all credible. Further, we have no way of knowing what state of equilibrium we would expect between the exchangeable and non-exchangeable at the start of the far field. If humic material enters the near field, and complexes with the radionuclide there, before entry to the far field, then there is a chance that the non-exchangeable fraction could be fully populated. However, if radionuclide and metal only meet at the near/far field boundary, then it is possible that the non-exchangeable will start empty. Hence, scenario D is also possible. Therefore, there is some uncertainty in the predictions, and we have a range of possibilities: note, we may reject the old calculation results, 'old kinetics' and 'no kinetics at all', since these have used data that we now know to be false. Figures 11, 12 and 13 show the range of predictions for Am, Np and Pu, respectively. These ranges of uncertainty include only the humic specific effects.

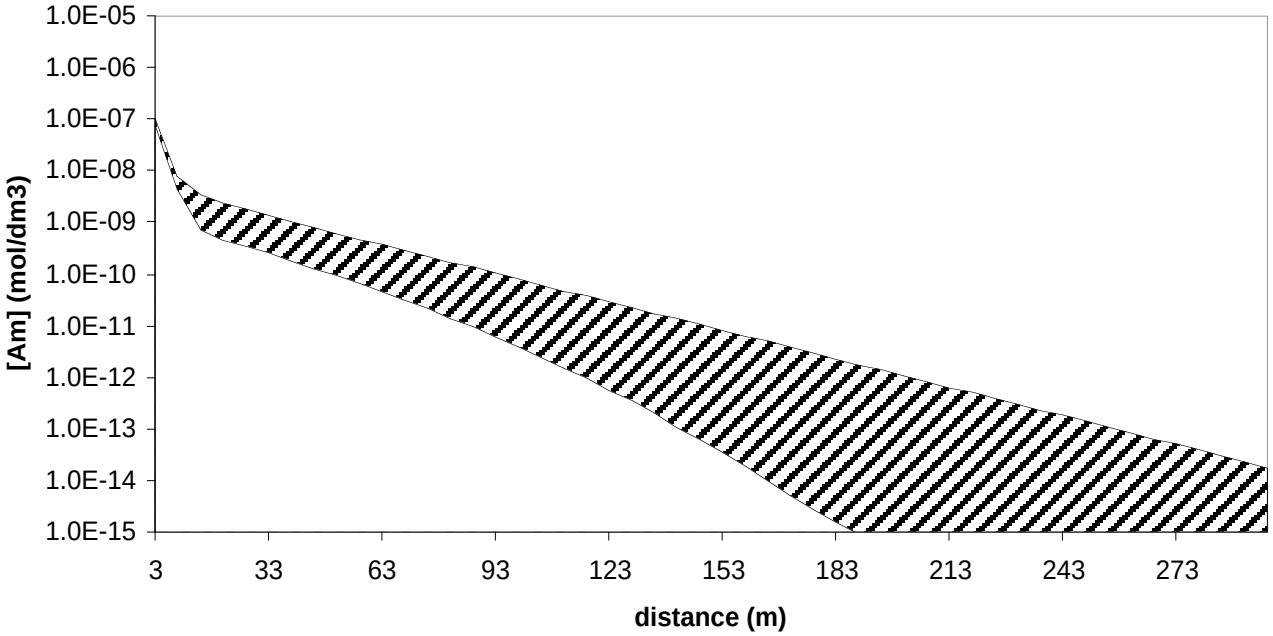


**FIGURE 11: Range of Am predictions for Dukovany case study**

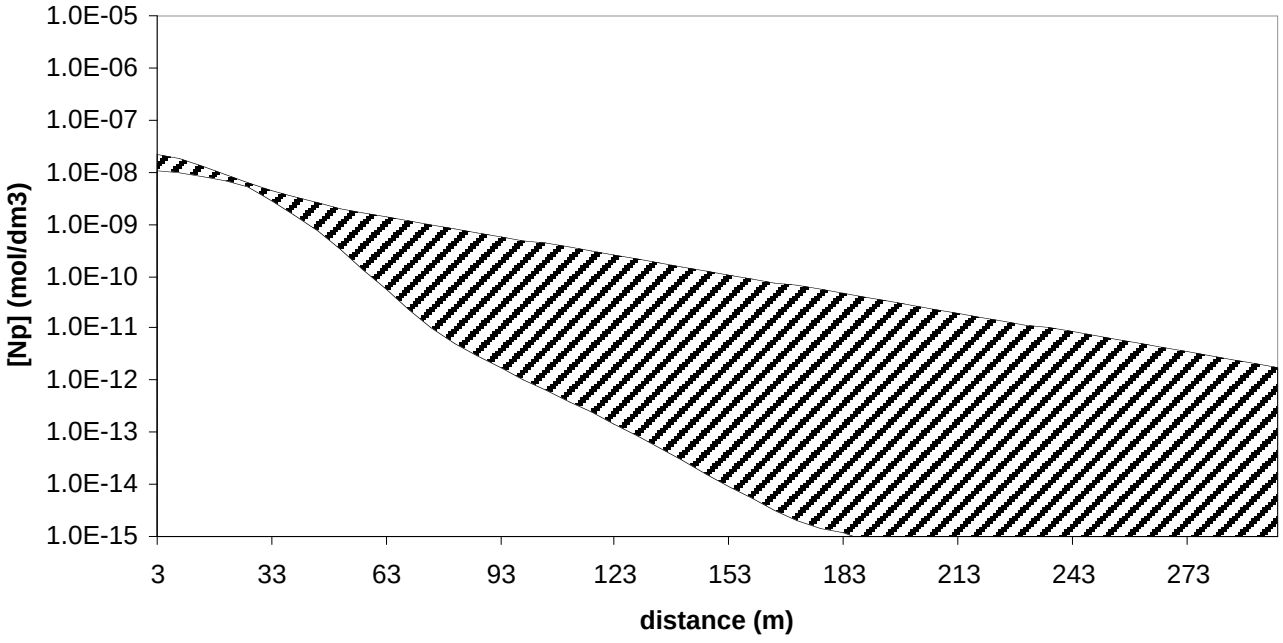


**FIGURE 12: Range of Np predictions for Dukovany case study**

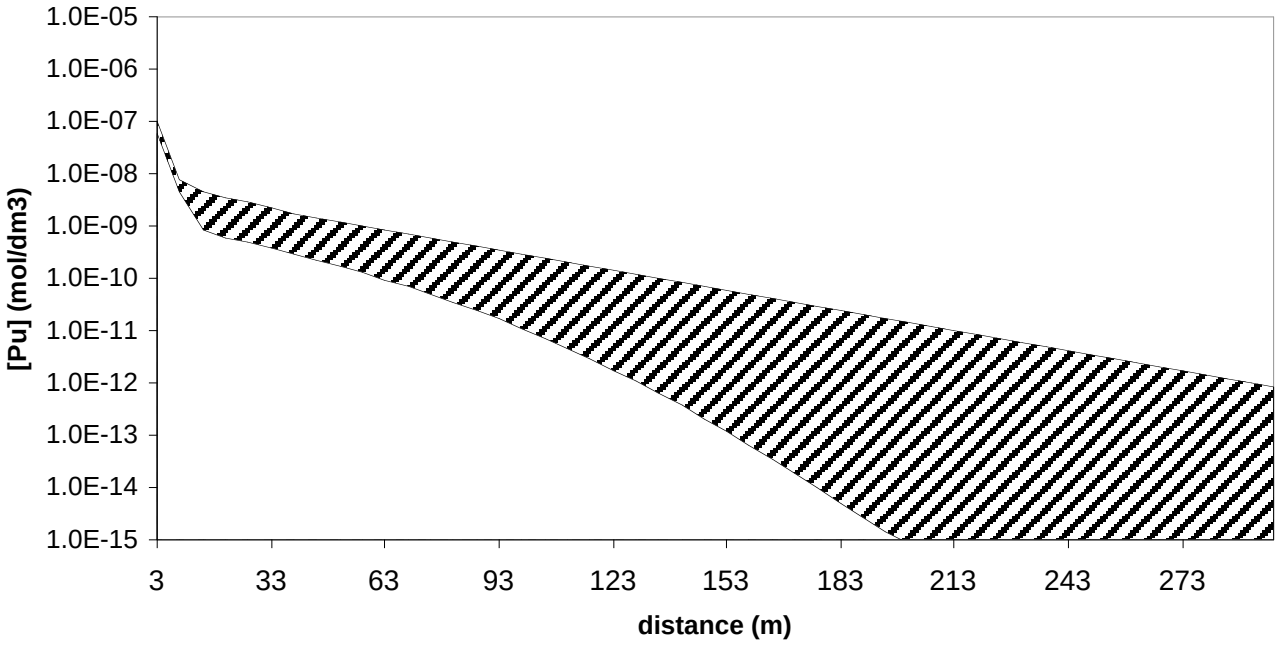


**FIGURE 13: Range of Am predictions for Dukovany case study**

Figure 14 shows the effect of simulation time (100 and 1000 years) upon the Pu predictions for scenarios A and D. There are no changes in the patterns with increased time, and the order of results seen in Figures 6, 7 and 8 are retained.

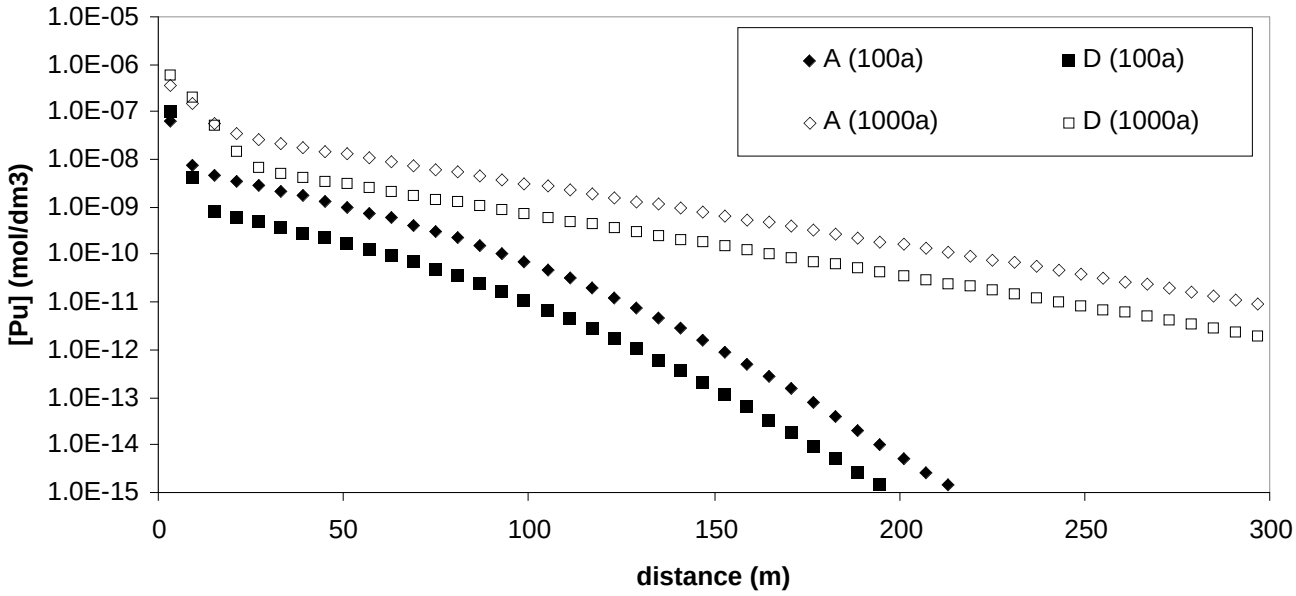


**FIGURE 14: Dukovany 100 and 1000 year predictions for Pu**

## The Gorleben Case Study

### Scenario

The Gorleben case study is based loosely upon the Gorleben proposed nuclear waste repository in Germany. In a number of ways, the scenario is different to that for Dukovany. Instead of horizontal flow, here the flow is vertical away from the repository itself. Rather than the continuous release that was assumed during the Dukovany case, pulsed release is adopted. It is assumed that the activity enters the far field during a period of only 100 years. After 100 years, it is assumed that the repository will become sealed, and no further radionuclide will enter the farfield. Hence, a pulse of activity will travel along the length of the hypothetical column. Calculations were performed for upto 10000 years following the end of the pulsed release.

The hypothetical column was 150m in length with a linear dispersivity of 10m. The linear flow rate was $4.8 \times 10^{-9}$ $ms^{-1}$. A porosity of 0.3 was used, although the results were insensitive to this parameter, providing that the linear flow rate was maintained constant. Molecular diffusion was assumed to be insignificant. These parameters were taken from studies of the geochemistry at the site. The effective humic exchangeable binding site concentration, [HA], is $1 \times 10^{-4}$ mol $dm^{-3}$, equivalent to a D.O.C. concentration of 10 mg $dm^{-3}$.

The four calculation scenarios defined previously for the Dukovany case study (A - D) have also been used here.

Calculations for the Gorleben site were performed as part of the previous HUMICS project, and have been included in some of the plots as a comparison. All of these assumed that both humic and humate complexes could not sorb. These used two approaches to account for the non-exchangeable fraction:

1. using rate constants ($k_f$ and $k_b$, Table 4) measured in short term lab experiments, labelled as 'old lab kinetics' in the figures;

2. treating the non-exchangeably metal fraction as *pseudo-irreversibly* bound to the humic. Here, the distribution between exchangeable and non-exchangeable on entry to the far field (top of column) was calculated using the ratio between the rate constants $k_f$ and $k_b$ (Table 4), but once the material had entered the column, the values of $k_f$ and $k_b$ were both set to zero, isolating the non-exchangeable from all other chemistry. Hence, this fraction transported conservatively (since metal-humic complexes were not permitted to sorb). These results are labelled as 'irrev binding' in the Figures.

### Results

Figure 15 shows the development of the Np distance profile with time for scenario A: unlike the continuous release Dukovany case, a definite peak develops in the profile with time as the activity is swept down the column. The progress is relatively slow, compared to the

Dukovany case, but this reflects the much lower flow rate here, rather than an intrinsic difference in behaviour.

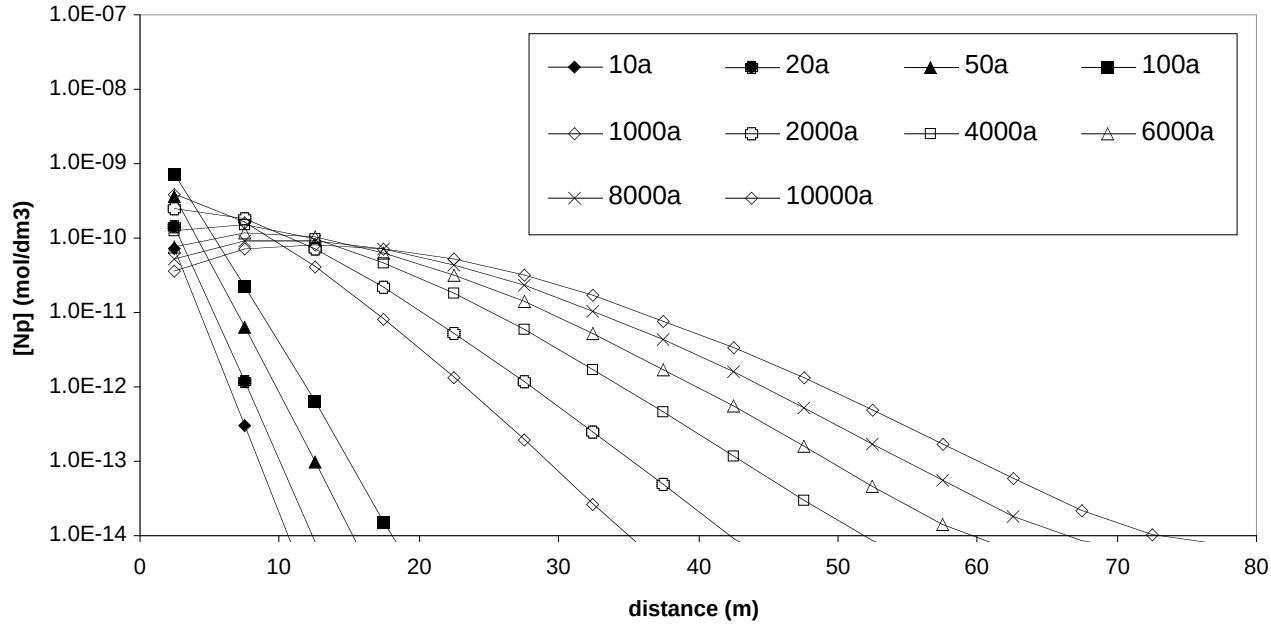


**FIGURE 15: development of Np profile with time, Gorleben calculation, scenario A.**

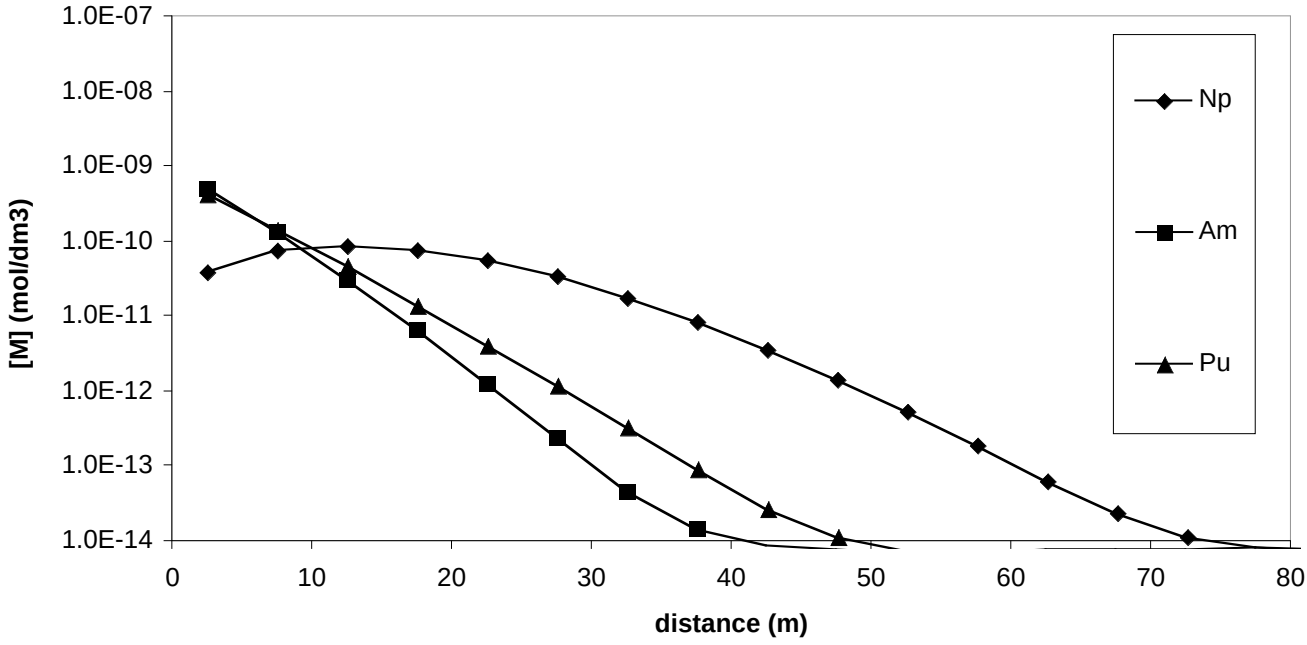


**FIGURE 16: Np, Am and Pu 10000 year profiles, Gorleben calculation, scenario A.**

Figure 16 shows the model predicted profiles for 10000 years for Np, Am and Pu, all using scenario A. The Np has migrated much further than the other two radionuclides. This is due to the fact that the affinity of the mineral surface for this radionuclide is much weaker than for

the other two, because the data are for the $NpO_2^+$ species. In the case of the humic interaction data though, the Np species present in the natural sample (from which $k_f$ and $k_b$ were determined) is unclear, since the amounts concerned are too low to allow determination of speciation. Hence, these data could be for the reduced Np(IV), certainly, the amounts found in the non-exchangeable fraction (Table 2) could be consistent with a highly charged cation.

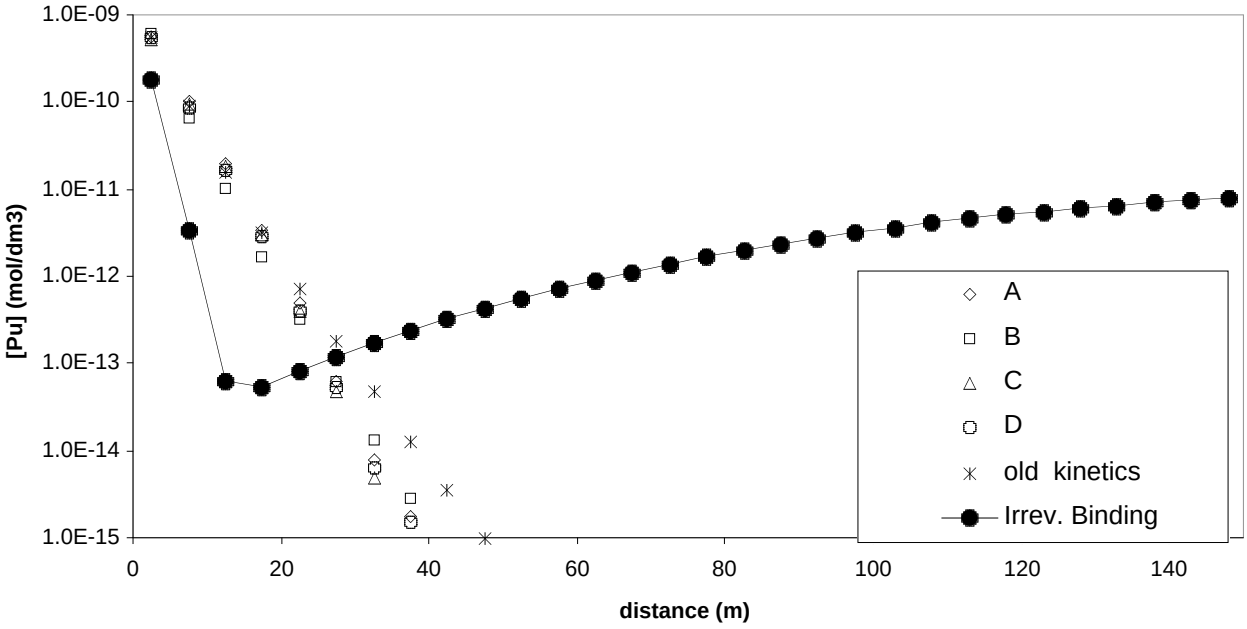


**FIGURE 17: 1000 year prediction for Pu, Gorleben calculation.**

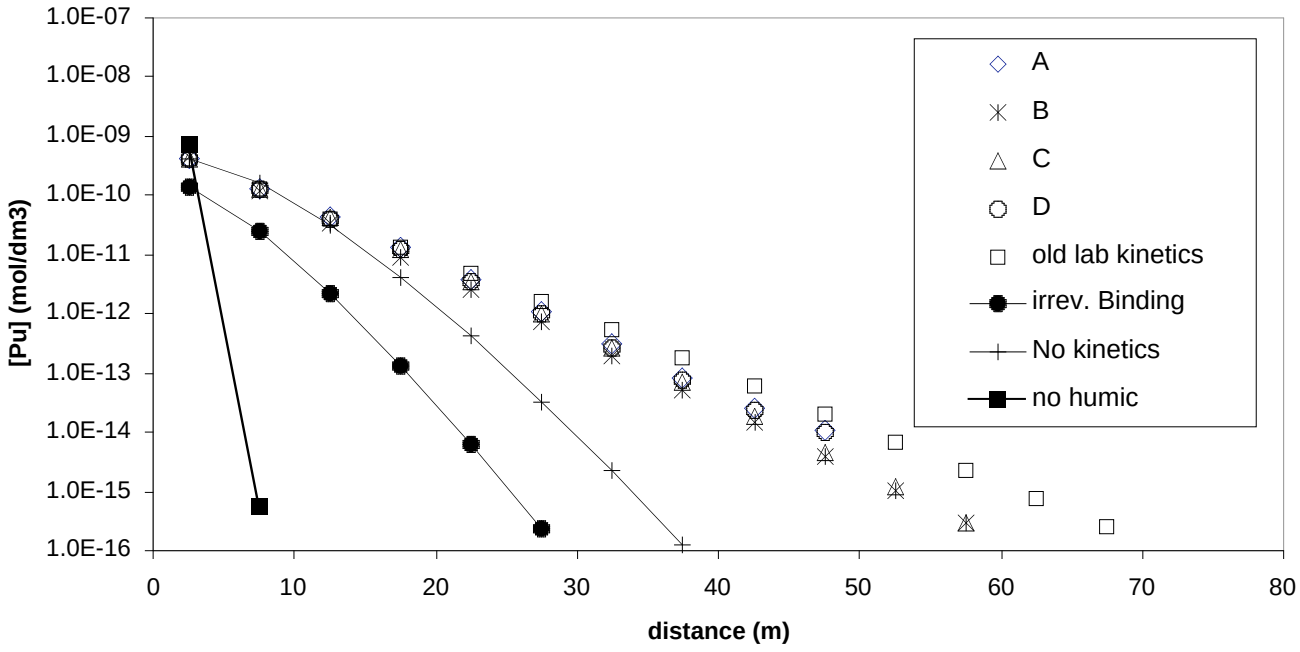


**FIGURE 18: 10000 year prediction for Pu, Gorleben calculation.**

Figures 17 and 18 show the predictions for Pu migration after 1000 and 10000 years, respectively. The behaviour of the plots for the irreversible binding scenarios might seem very odd: after 1000 years, this plot shows the most migration, but some of the lowest after 10000 years. This is because of the radically different behaviour of the non-exchangeable and exchangeable in this scenario. The non-exchangeable moves as a conservative tracer, and moves quickly down the column (responsible for the broad peak beyond 20m in Figure 17). The exchangeable though is easily removed from the humic and sticks at the start of the column (material in 0 - 20m range, Figure 17). After 10000 years, all of the non-exchangeable has been removed from the column, and only that which was bound exchangeably, but is now stuck to the mineral surface, is left (Figure 18). Hence, if pseudo-irreversible binding were to take place, then it would result in the maximum possible migration. However, this behaviour was not observed in the natural anthropogenic sample.

Figure 18 shows that once again, the 'no humic' and 'no kinetics' plots show the least migration, and for the same reasons as before. However, the scenarios A - D are behaving very differently. In the Dukovany cases, there was a significant spread in the results. However, here there is very little difference, and the reason is the much lower flow rate. Considering the treatment of the sorption of the humic and humic-radionuclide complex, the flow rate is so slow that the sorption reaction reaches equilibrium, even when modelled using rate constants, rather than an equilibrium constant, and so we expect scenarios A and C to be coincident. In fact, humic sorption has no effect upon the behaviour of the radionuclide: note that scenario B is also coincident with A and C. The low flow rate also means that even if the humic and its complex transport as conservative tracers, the radionuclide still has ample time to desorb from its humic, before the enhanced migration of the humic makes a difference.

Another difference this time is that the initial distribution between exchangeable and non-exchangeable seems to make virtually no difference. This is because, there is sufficient time for the radionuclide to leave the non-exchangeable before significant migration takes place, and so the distribution at the near/far field boundary makes little difference. Given this, one might ask why there is a difference between the results for the scenarios that include a non-exchangeable interaction and the one that does not. The answer is that at each stage a very small amount of radionuclide will manage to enter the non-exchangeable, and this will be able to migrate slightly further than radionuclide that has remained in the exchangeable. This effect depends only upon the values of $k_b$ and $k_f$ (Figure 8), which are the same for all of the scenarios A - D, and hence they are all coincident.

Perhaps the most surprising result is that the 'old kinetics' plot using the old rate constants actually shows slightly enhanced migration compared to A - D. This is the opposite behaviour to that observed in the Dukovany case. The effect is subtle. The forward and backward rate constants for the 'old kinetic' plot are faster than those for A - D. That might lead us to expect that this plot would show less migration, because the radionuclide would leave the non-exchangeable fraction faster. However, as we have seen, there is sufficient time to deplete the non-exchangeable in this system. The faster rates show slightly more migration, because the

radionuclide finds is 'easier' to access the non-exchangeable, due to the faster forward rate, and this effect counteracts the effect that we expect, because of the faster backward rate (kb).

Another general difference, between the Gorleben and Dukovany cases is the relative importance of the humic kinetics. For Dukovany, the presence of non-exchangeable binding had a very significant effect. There is still an effect here, and we predict that humics and especially the non-exchangeable interaction, will promote migration relative to a humic free system. However, the effect is smaller here.

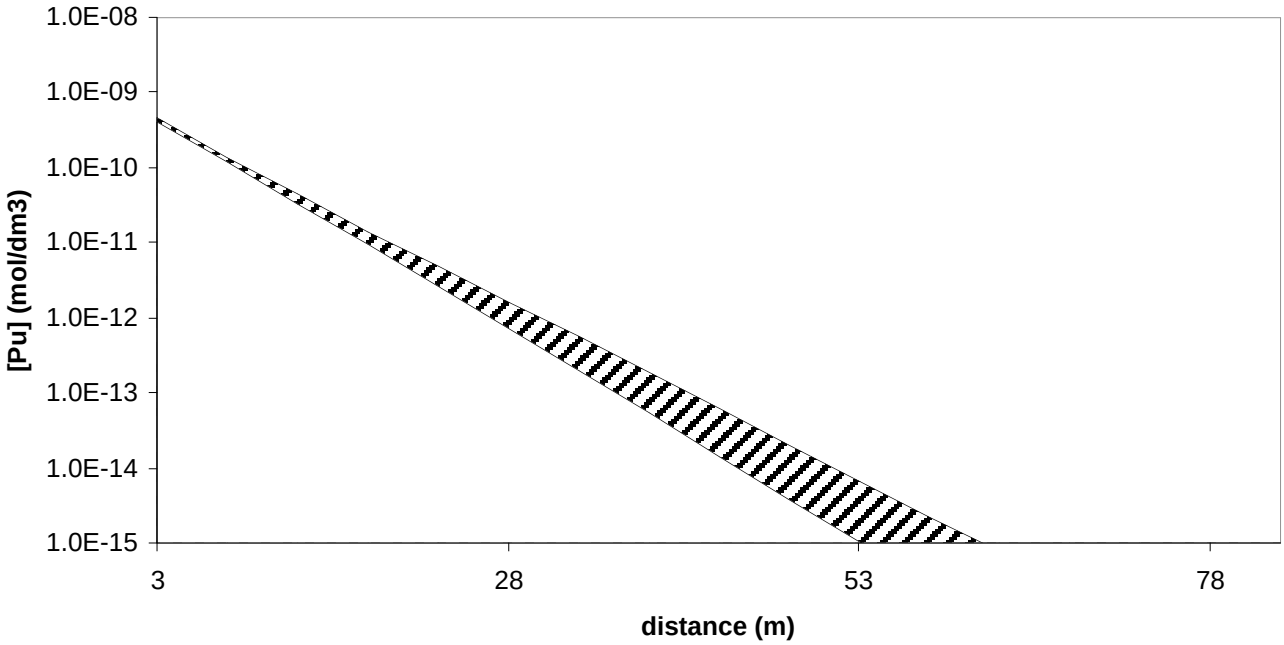


**FIGURE 19: range of predictions for Pu, 10000 years.**

Figure 19, shows the range of Pu predictions, equivalent to the Dukovany plots (Figures 11, 12 and 13). Note that the range of uncertainty is much smaller here, entirely due to the lower flow rate. Similar results were obtained for the other isotopes.

## Conclusions

The results of many column and batch experiments along with the Gorleben and Dukovany migration case studies have shown that humic kinetics are vitally important in controlling the behaviour of metal-humate interactions. All the evidence suggests that it is the non-exchangeable interaction that will be responsible for the movement of metal ions (including radionuclides) in the environment. The U-tailings pile study did suggest that merely as strong ligands, humics might act as transport vectors. However, this reflects the definition of the chemical model for that particular case study, and is almost certainly not applicable to other cases.

There have been a number of significant advances during this project. For example, we now have a greater understanding of the non-exchangeable interaction itself. Before this project, there was uncertainty about the most suitable values for the rate constants, $k_f$ and $k_b$, and the only conservative approach was to assume that the non-exchangeable metal was (pseudo-) irreversibly bound. This assumption has a dramatic effect upon migration (see e.g. Figure 17). However, we now have pairs of values for Np, Am and Pu derived from the 'natural' sample (W.P. 5). Hence, an assumption of irreversible binding is no longer required.

Some uncertainties do remain. Will there be retardation of the humic or humic/radionuclide complex, and if so, will it be a fast or slow process, or will they transport as conservative tracers. Also, what will be the distribution of radionuclide between exchangeable and non-exchangeable on entry to the far field? Of course, this will depend upon whether humics are able to penetrate the near field, how long they would have to equilibrate, and what the chemical conditions were inside the repository, e.g. the strength of any competing sinks/surfaces, pH ,I etc. However, probably the greatest problem at the moment is that the mechanisms responsible for the non-exchngeable interaction are still not understood. In the case of the less important (for transport) exchangeable interaction, some process detail is available, and models exist that explain the origin of the interaction (loss of water from metal ion upon bonding, coupled with double layer relaxation)

**Performance Assessment: Questions and Answers**

Performance assessors have certain questions concerning the role of humic substances in the migration of radionuclides. At an NEA workshop in 1994, several key questions were identified which were unknown at the time, but which required answers before humics could be adequately included within PA (Zuiderma 1994). These questions are still valid today.

***Are natural organics from different origins comparable and can characteristics be generalised?***

The evidence would suggest that, although humic samples from different sites may have certain intrinsic differences, molecular weight, etc., in terms of their interaction with metals, to a first approximation their behaviour is remarkably uniform. This applies to both the exchangeable and non-exchangeable. That said, there are some subtle differences between samples (Monsallier et al 2003).

***Are laboratory studies able to provide suitable parameters for field scale studies and what is the applicability of those parameters to the field scale?***

Laboratory batch and column experiments and associated modelling can provide mechanistic information about the general behaviour of these systems. However, the study of completely synthetic systems, i.e. where metal ions and humic are mixed in the lab and their behaviour monitored, may not provide suitable parameters. It may be that more reliable data are obtained by the study of metal ions that have complexed to the humic under natural conditions. But, once such a 'natural' sample has been obtained, the parameters may be determined in the laboratory.

***Are models for the interpretation and prediction of complexation available and are the simplifications and assumptions made within the models conservative?***

All the evidence suggests that we do have the mathematical tools to allow us to include the effects of humic substances in transport calculations, and that the predictions made with those models can be conservative. More than this, we have experimental methods to provide the input parameters for these models. However, the underlying mechanisms of the crucial non-exchangeable interaction that appears to control transport are completely unknown. Hence, we are able to predict the behaviour of metal ions in transport experiments, but we are not yet able to explain why that behaviour occurs. In those circumstances, it is hard to have confidence in predictions made outside the conditions, and most importantly the time scales, of the laboratory experiments that have been used to calibrate the models. After all, they may be some dramatic effect that becomes very important on a time scale of a few tens of years, but because we do not understand the mechanism, we have no way of knowing. Therefore, work should continue to provide the physicochemical model to describe the system to support the current semi-empirical approach.

One potentially significant uncertainty concerns the state of the humic-radionuclide complex as it enters the far field: will the radionuclide have had chance to access the non-exchangeable interaction, or will all of the metal be bound exchangeably? This can make a significant difference to the degree of transport, depending upon the linear flow rate: at low groundwater flow rates, there is little difference in behviour (e.g. Gorleben case study), but at higher flow rates, the difference can be significant (e.g. Dukovany case study). The answer to this question depends upon whether humic material is able to penetrate the near field and complex the radionuclides before their subsequent entry to the far field. This will depend upon the specific conditions at the repository in question.

***What are the effects of natural organics, including a comparison with competition from other sinks, e g mineral surfaces?***

In the absence of the non-exchangeable interaction, the conclusion of this project would probably have been that humics were of minor importance at most, and that any effects would be small compared to the effects of uncertainty in for example, hydrology. The modelling predicts that the humic exchangeable binding site would not compete effectively with mineral surfaces, or other important sinks. However, those same calculations have demonstrated that metal in the non-exchangeable fraction will migrate regardless of the affinity of the mineral surface for the metal. Rather than the affinity of the mineral surface, it is the groundwater flow rate that is the critical parameter: the extent of migration increasing with flow rate. The non-exchangeably bound fraction transports with the properties of the humic substance, and here there is some uncertainty: column experiments have been modelled that have (1) had humic and humic radionuclide complexes transporting conservatively; (2) undergoing rapid sorption, such that could be described by an equilibrium approach; (3) undergoing sorption, but as a slow process that required a kinetic description. At present, it is unclear which of these approaches is the most appropriate for the real world. Once again, the magnitude of the

flow rate is crucial, if it is sufficiently slow, then humic sorption becomes irrelevant, and the system is dominated by the non-exchangeable backward rate constant ($k_b$, Figure 8), but at higher flow rates, then the differences are significant.

When these questions are addressed, the final question must be:

***Are humics important for the safety of a repository?***

**Are Humics Important?**

This work indicates that humic chemical kinetics are crucially important in controlling the migration behaviour of metals in the environment. Rate constants and methods for determining rate constants now exist

The calculations performed in this work were relatively simple in chemical terms. Apart from the humic/surface/radionuclide ternary system, all other chemical effects have been excluded. It might be possible that one of these other effects might serve to prevent migration. However, the factor that makes this form of mobilisation unique is that the metal appears to be insulated completely from all solution and solid phase chemistry, whilst it is isolated within the non-exchangeable fraction. In the repository type calculations (Dukovany and Gorleben), to a first approximation, any metal which is not within the humic non-exchangeable fraction, is immediately removed by the strong affinity of the solid surface. Hence, it is highly unlikely that any other effects would significantly reduce migration. The only processes that might influence the result are those that cause the destruction of the humic molecule itself. At present, no such mechanisms are known.

In the past, it might have been suggested that the overall influence of humic substances would be benign, since at any site, the vast majority of humic substances remain immobile and therefore, even if humics bind nuclides very strongly, the overall effect would be to retard migration. However, this argument only holds true if the metal-humate interaction is an equilibrium and metal is completely free to 'jump' instantaneously from one humic molecule to another. This would not appear to be the case. If a nuclide starts its journey through the geosphere trapped within the humic, then the chemical affinity of any surfaces or other humic materials will not prevent its movement. Only desorption from the non-exchangeable fraction or the retardation of the humic-radionuclide complex itself will prevent migration.

The general conclusion of this work must be that, given the current state of knowledge, humic substances are expected to have an impact upon the transport of actinides, fission products and other toxic metals in the environment. Their effects should at least be considered in radiological performance assessment studies until there is further evidence to the contrary.

**References**

Bryan N.D., Jones D.M., Keepax R., Warwick P., Stephens S., Higgo J.J.W. (2003) "An Experimental and Modelling Study of Metal Ion/Humate Non-Exchangeable Binding." In: Buckau, G. (Editor) “Humic Substances in Performance Assessment of Nuclear Waste

Disposal: Actinide and Iodine Migration in the Far-Field (First Technical Progress Report)", Report FZKA 6800, Research Center Karlsruhe.

Bryan N., Vopalka D., Benes P, Stamberg K. and Doubravova K. (2004) "Determination of Chemical Parameters for the Schlema-Alberoda Uranium Tailings Pile Migration Case Study.", In: Buckau, G. (Editor) "Humic Substances in Performance Assessment of Nuclear Waste Disposal: Actinide and Iodine Migration in the Far-Field (Second Technical Progress Report)", Report FZKA 6969, Research Center Karlsruhe.

Bryan N.D. (2005) "Accounting for Chemical Kinetics in Field Scale Transport Calculations." In: Buckau, G. (Editor) "Humic Substances in Performance Assessment of Nuclear Waste Disposal: Actinide and Iodine Migration in the Far-Field (Third Technical Progress Report)", Report FZKA, Research Center Karlsruhe.

King, S.J., Warwick, P., Hall, A., Bryan, N.D. (2001) The dissociation kinetics of dissolved metal-humate complexes. Physical Chemistry Chemical Physics, 3, 2080-2085.

Monsallier J.M., Schussler W., Buckau G., Rabung T., Kim J.I., Jones D., Keepax R., Bryan N. Kinetic investigation of Eu(III)-humate interactions by ion exchange resins. *Anal. Chem.*, (2003), 75,3168-3174.

Schmeide K., Geipel G., Heise K.H., and Bernhard G. (2003) "Uranium Mining Waste Rock Pile No. 250 in the Region Schlema/Alberoda (Saxony, Germany)" In: Buckau, G. (Editor) "Humic Substances in Performance Assessment of Nuclear Waste Disposal: Actinide and Iodine Migration in the Far-Field (First Technical Progress Report)", Report FZKA 6800, Research Center Karlsruhe.

Warwick, P., Hall, A., Pashley, V., Bryan, N.D., Griffin, D. (2000) Modelling the effect of humic substances on the transport of europium through porous media: a comparison of equilibrium and equilibrium/kinetic models. Journal of Contaminant Hydrology, 42, 19-34.

Zuiderma P. What a Performance Assessor Would Like to Learn About Natural Organics. In *Binding Models Concerning Natural Organic Substances in Performance Assessment.* (1995), NEA/OECD Report.

## Annex 8:

**Study of Uranium Release From Uranium Waste Rock Pile Material: Column Experiments**

Vopalka D., Doubravova K., Benes P.

# Study of Uranium Release From Uranium Waste Rock Pile Material: Column Experiments

Vopalka D., Doubravova K., Benes P.

Czech Technical University, Department of Nuclear Chemistry, Brehova 7, 115 19 Praha 1, Czech Republic

## Abstract

Uranium release from the waste rock pile material was studied using modelled seepage water with various humic acid contents and flow-through velocities. The dynamic elution experiments using $^{233}$U-spiking, which were prepared on the basis of evaluated batch experiments, were preceded by equilibration of the rock material with solution in which the uranium total concentration was near to equilibrium determined in batch experiments. This type of experiments models real conditions in the waste rock pile for situations in which the release of uranium from the rock layer dominates. The observed influence of the presence humic acid on the release of uranium from the layer of rock pile material was variable and ambiguous, also due to the large retention of humic acid in the rock layer.

## Introduction

The study of environmental impact of uranium mining waste rock piles has a large importance as the piles are often situated, e.g. in Germany or in Czech Republic, in urbanized environment. These wastes can also serve as a geological analogue of other kinds of nuclear waste repositories. Understanding of contaminat migration processes at the basic level in a laboratory study can help to develop models, which may be used with transport codes to predict the fate of pollutants on the field scale. An extensive environmental study was performed in the waste rock piles region at Schlema-Alberoda (Saxony, Germany) mainly between 1990-2000, but, as it was reported (Schmeide et al., 2003), necessary observations and data for performance assessment modelling are still missing. The work performed with waste materials from uranium mining was therefore aimed at better understanding of uranium release/uptake processes and at obtaining suitable input data for modelling of uranium migration.

Waste material from rock pile No. 66 at Schlema-Alberoda was selected for the study. Sampling of the rock material, which included sieving under 1 mm of particle size, and its characterization (elemental composition, mineralogy, total carbon, inorganic carbon and specific surface area) was organized by Research Center Rossendorf (Sachs et al., 2004). Granulometric analysis, determination of exchangeable uranium and sorption/desorption studies by batch and column experiments were performed in our laboratory. Most of these experiments were carried out by radiotracer method using $^{233}U$ as the tracer. Distribution of $^{233}U$ was measured with liquid scintillation counting. Some evaluations were based on determination of $^{238}U$ and $^{233}U$ by means of ICP-MS. The experiments, results of which are presented in this contribution, were performed with the simulated seepage water from the pile No. 66 (0.0175 M $MgSO_4$, 0.0091 M $CaSO_4$, 0.00258 M $NaHCO_3$) aiming to obtain data that could be used in subsequent modelling of uranium migration on the field scale.

## Batch experiments

### *Determination of exchangeable uranium*

First experiments aimed at determination of uranium in the rock sample accessible to leaching with natural water and exchangeable with ions in the water. This so called exchangeable or "labile" (Davis and Curtis, 2003) uranium $U_{ex}$ was determined by isotope exchange with $^{233}U$ in two aqueous media with different initial composition: (i) $10^{-4}$ M $HNO_3$ and (ii) simulated seepage water from the pile No. 66 (Sachs et al., 2004). For the latter medium neither concentration changes of total uranium and concentration of $^{233}U$ nor the change of phase ratio $V/m$ from 20 to 100 mL/g caused a significant change in $U_{ex}$, that with value of 20 μg/g ($8.4\times10^{-5}$ mol/kg) represented approx. 34 % of total uranium in the sample. This stability seemed to be caused by only small changes in total composition of liquid phase in the system due to the changes of phase ratio, as the use of simulated seepage water hindered further leaching of waste rock material.

Additional determination of $U_{ex}$ performed by isotope exchange with $^{233}U$ showed the kinetic character of the complex sorption/desorption and isotope exchange process. One of the

time dependences of $U_{ex}$ measured is presented on the Fig. 2A jointly with two sorption/desorption kinetics of total uranium. A lower $U_{ex}$ value (14 µg/g) was obtained by evaluating of the balance of total uranium in the mentioned couple of experiments that were performed without spiking by $^{233}$U, but higher experimental error was ascertained for this method of the determination of exchangeable amount, as the standard uncertainty of ICP-MS was about 10%.

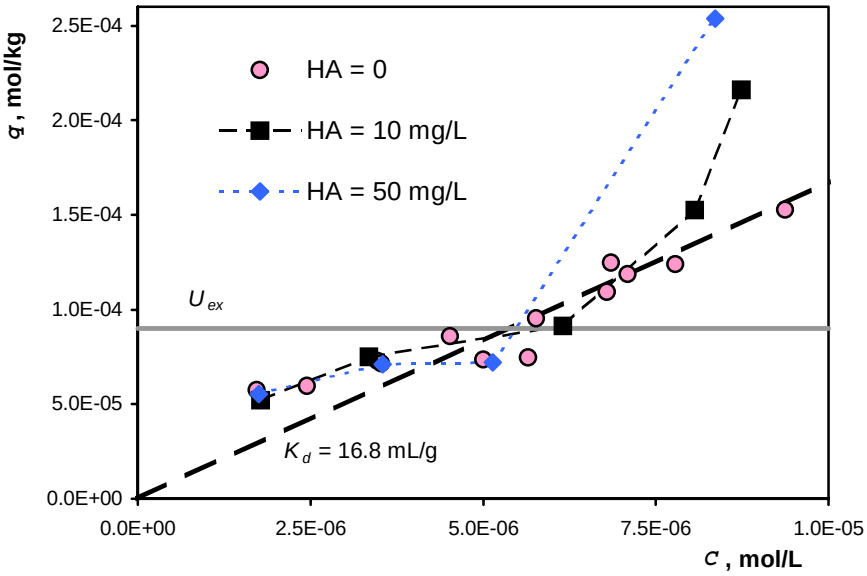


Fig.1: Equilibrium sorption/desorption isotherms for different concentration of added humic acid (HA). The full line shows the value of $U_{ex}$ determined.

*Sorption/desorption equilibrium and kinetics*

Batch experiments carried out with simulated seepage water (pH 8) examined effects of concentration of added uranium and humic acid on uranium distribution and kinetics of uranium sorption and desorption. The near-to-equilibrium distribution data of total uranium (labile + added) corresponded to approximately linear sorption isotherm (Fig. 1), with no significant dependence on the volume to mass ratio ($V/m$ = 10-100 mL/g). The effect of added Aldrich humic acid (HA, 10 and 50 mg/L) was almost negligible with exception of experiments at the highest concentration of added uranium, when the addition of HA caused an increase of $K_d$ to 25-30 mL/g. The small effect of HA could be explained by saturation of added HA by Ca and Mg present in the simulated seepage water.

Slow kinetics of $^{233}$U uptake was found with about two weeks required to obtain a steady-state distribution at $V/m$ = 10-100 mL/g (Bryan et al., 2004). Rather complicated effects of experimental conditions (total uranium added, $V/m$, concentration of HA, the pre-equilibration of phases preceding addition of the spike) on the kinetics were observed. Most of these effects can be explained if the distribution of uranium initially present in the rock material and of uranium added are considered separately. E.g., when very small concentration of labelled uranium is initially present in the solution, uptake of $^{233}$U is measured but the flow of total uranium in the system can be dominated by the release of exchangeable uranium from the

rock. These facts are demonstrated on Fig. 2 by comparison of sorption and desorption kinetics without $^{233}$U added with experime nts in which only uptake of $^{233}$U was measured. By evaluation of experiments that used $^{233}$U spiking one can obtain $K_d$ values, that are not possible for the first type of experiments (if $U_{ex}$ is not known). On the other hand measured kinetics of $^{233}$U uptake always partly represents also isotope exchange $^{233}$U–Unat, which dominates if the initial concentration of total uranium in liquid phase is near to that in equilibrium with $U_{ex}$.

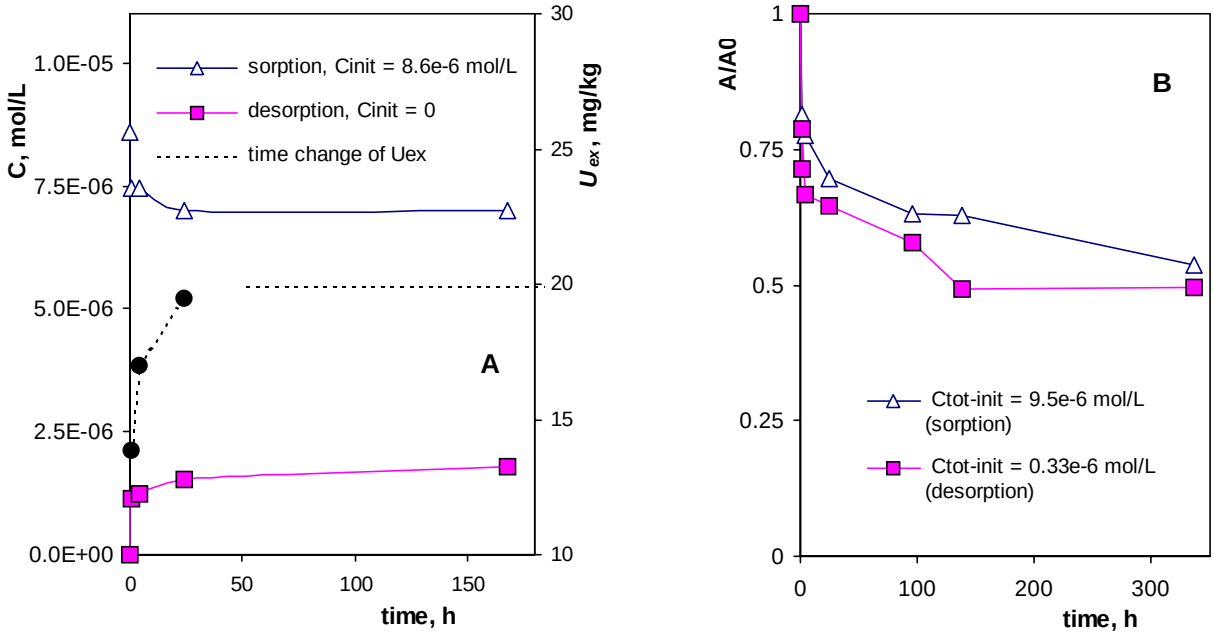


Fig. 2: Kinetics of uranium sorption/desorption from the rock material with simulated seepage water at room temperature and *V*/*m* = 20 mL/g for two experiment types: (A) without spiking by $^{233}$U, and (B) with $^{233}$U – spiking. The time change of $U_{ex}$ corresponded to experiments performed with initial concentration $U_{tot}$ = $9.5\times10^{-6}$ mol/L, *V*/*m* = 20 mL/g or *V*/*m* = 100 mL/g.

Kinetics of uranium release from the rock material was studied both by radiotracer method and by direct (ICP-MS) measurement of released uranium. In the first case, the rock material was pre-equilibrated with $^{233}$U. In order to avoid premature release of uranium, the pre-equilibration was made with $5.6\times10^{-6}$ M solution of uranium (see Fig. 1) labelled with $^{233}$U. The direct measurement of released uranium was also made without pre-equilibration of the rock with the simulated seepage water. Good agreement between the results of the direct U measurement and of the radiotracer method was obtained (Vopalka et al., 2004). This suggests that the radiotracer method used (elution after pre-conditioning of solid phase with spiked solution) is suitable for determination of input data for modelling of uranium release from the pile.

## Column experiments

Humic colloid-mediated uranium migration can be studied by columns experiments that together with batch experiments might provide an insight into U migration in subsurface aquifers (Artinger at al., 2002). Presence of colloids mostly lowers the retardation quality of

porous rock layer (Roy and Dzombak, 1998; Warwick et al., 2000) and the kinetic character of interaction of contaminant with natural colloids requires more complicated techniques of migration modelling (e.g., Zurmühl, 1998). Preparation and accomplishment of our dynamic experiments aimed at simple modelling of dynamic conditions of uranium leaching and migration in waste rock pile using the method developed with use of batch experiments, as well as at testing applicability of batch data and column data for the modelling on larger scale.

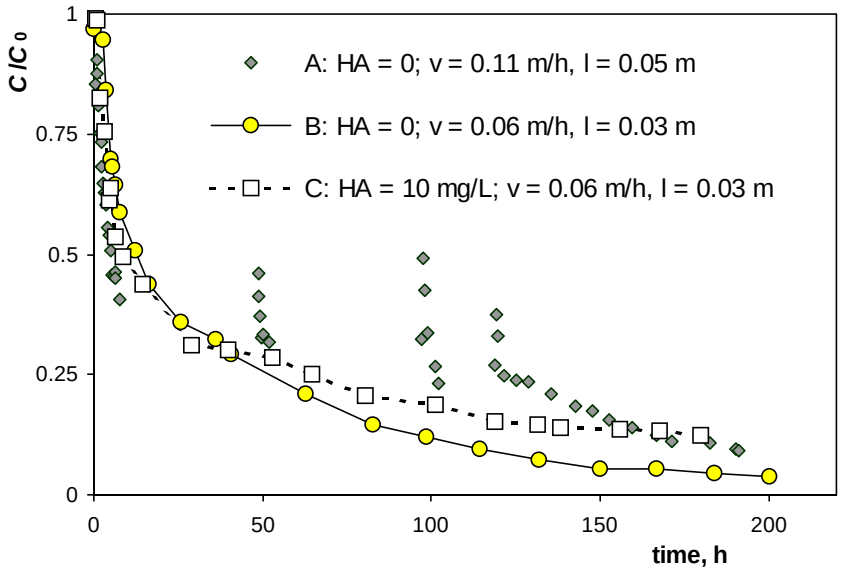


Fig. 3: Dynamics of uranium release from the layer of rock material eluted by simulated seepage water (*l* - height of the sediment layer, *v* - linear flow velocity).

Dynamic experiments were carried out with small columns (inner diameter 0.9 cm, height of rock layer 3 and 5 cm) and linear flow-through velocities between 0.02 and 0.11 m/h. The elution experiments using $^{233}$U-spiking were preceded by equilibration of the rock sample with spiked uranium solution directly in the assembled circuit (column and tubing) unless a steady state, characterized by approx. the same values of input and output activities of the spike ($A_0$), was attained (7-10 days). This procedure was based on method of preliminary equilibration with spiked solution that was verified in kinetic elution experiments. Also here, parallel experiments were run with the non-spiked and non-equilibrated rock and the comparison of results was satisfactory.

The first experiments using flow-interruption technique (e.g. Kookana et al., 1994) showed that non-equilibrium conditions existed during the experiments (Fig. 3, curve A). Some of the column experiments validated the results of batch experiments that showed a small influence of the presence of HA, e.g. beginning of time dependence of uranium outflow presented on Fig. 3 by curves B and C. In contrast to batch experiments, a significant influence of humic acid on U release was observed in other dynamic experiments (see curves B and C on Fig. 4). These results, which are presented in the form of cumulative activities that is more demonstrative with respect to balance considerations and seems to be also convenient for the calibration of transport models, proved the expected enhancement of uranium transport by complexation with HA. The discrepancy found between the different effects of HA presence was not yet explained and therefore the quantification of the effects is not yet

possible. Large retention of humic acid in the waste rock layer was observed, probably aided by the high content of small particles in the sample (33 wt. % of particles with size under 0.1 mm).

Because of the small amount of the waste rock material in the column, used for technical reasons (e.g. to limit duration of the experiment to 7–10 days for both equilibration and elution steps), sorption of uranium on the walls of column and tubings has also to be taken into account. Further discussion and computational modelling of uranium leaching and sorption under dynamic conditions is under way.

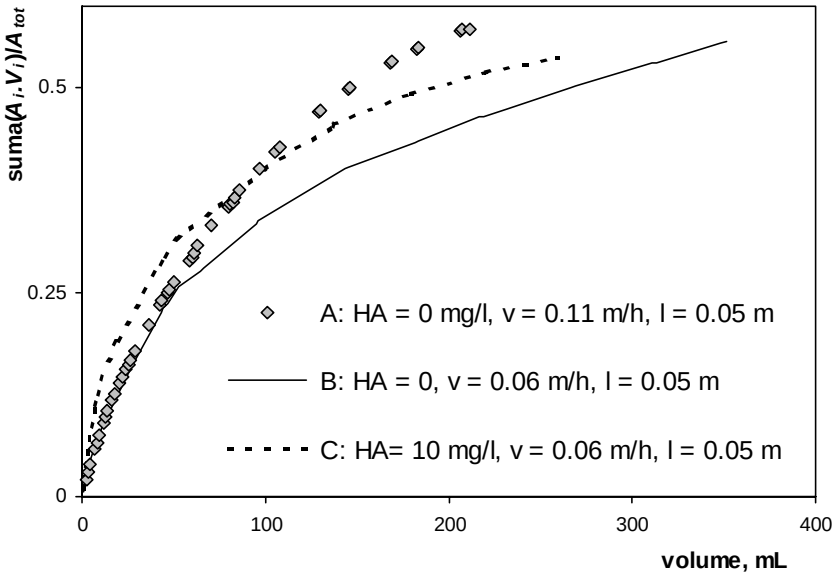


Fig. 4: Influence of experimental conditions on the relative cumulative outflow of uranium from the apparatus (*l* - height of the sediment layer, *v* - linear flow velocity).

## Conclusions

The results of batch experiments enabled the preparation of column experiments that should model real conditions in the waste rock pile:

1. By means of tracer technique using $^{233}U$ in the isotope exchange experiments, the value of exchangeable uranium $U_{ex}$ (about 20 µg/g) and equilibrium release/uptake isotherm were determined. The data obtained were needed for settig of the initial concentration of U in the liquid phase for equilibration that preceded the elution experiments in column arrangement.
2. The good correspondence of release kinetics of naturally present uranium and of $^{233}U$ pre-equilibrated with the studied rock material in conditions near to release/uptake equilibrium enabled to perform a set of dynamic elution experiments in which the release of $^{233}U$ from the layer of rock pile material represented the release of exchangeable uranium.
3. Measured kinetics of $^{233}U$ uptake does not correspond to kinetics of release/uptake of total uranium (labile + added) due to a complex character of the isotope exchange. Therefore radiotracer arrangement using $^{233}U$ is not suitable for dynamic sorption experiments.

The results of dynamic elution experiments proved the kinetic character of uranium release for experimental conditions used. The observed influence of the presence of HA on the release rate of uranium from the layer of rock pile material was variable and ambiguous.

Substantial release of uranium from the layer of rock pile material in near natural conditions was found: 10 days leaching by simulated seepage water that did not contain uranium released about 50% of accessible uranium.

## Acknowledgement

This study was supported by the EC Commission under contract No. FIKW-CT-2001-00128 and by the Grant No. MSM 210000020 of the Czech Ministry of Education.

## References

Artinger R., Rabung T., Kim J.I., Sachs S., Schmeide K., Heise K.H., Bernhard G., Nitsche H. (2002) "Humic colloid-borne migration of uranium in sand columns", *J. Contam. Hydrol.*, 58, 1.

Bryan N., Vopalka D., Benes P., Stamberg K., Doubravova K. (2004) "Determination of chemical parameters for the Schleme-Alberoda uranium tailings pile migration case study", In: *FZKA 6969, Wissenschaftliche Berichte* (Buckau G., ed.), Forschungszentrum Karlsruhe, Karlsruhe, Germany, 215.

Davis J.A., Curtis G.P. (2003) "Application of Surface Complexation Modeling to Describe Uranium (VI) Adsorption and Retardation at the Uranium Mill Tailings Site at Naturita, Colorado", Report NUREG/CR-6820, U.S. Geological Survey, Menlo Park, CA, p. 29.

Kookana R.S., Najdu R., Tiller K.G. (1994) "Sorption non-equilibrium during cadmium transport through soils", *Austral. J. Soil Res.*, 32, 235.

Roy S.B., Dzombak D. A. (1998) "Sorption nonequilibrium effects on colloid-enhanced transport of hydrophobic organic compounds in porous media", *J. Contam. Hydrol.*, 30, 179.

Sachs S., Beneš P., Vopálka D., Štamberg K., Mibus J., Bernhard G., Bauer A. (2004) "Sampling and Characterization of Rock Material from Uranium Mining Waste Rocks for Study and Modeling of Release and Migration of Uranium", In: *FZKA 6969, Wissenschaftliche Berichte* (Buckau G., ed.), Forschungszentrum Karlsruhe, Karlsruhe, Germany, 75.

Schmeide K., Geipel G., Heise K.H., Bernhard G (2003) "Uranium Mining Waste Rock Pile No. 250 in the Region Schlema/Alberoda (Saxony, Germany)", In: *FZKA 6800, Wissenschaftliche Berichte* (Buckau G., ed.), Forschungszentrum Karlsruhe, Karlsruhe, Germany, 79.

Vopalka D., Benes P., Prochazkova S. (2004) "Release and sorption of uranium in the system waste rock from uranium mining – natural water", In: *Advances in Nuclear and Radiochemistry – Extended Abstracts of Papers presented at NRC-6* (Qaim S.M and Coenen H.H., eds.), Schriften des Forschungszentrum Jülich, General and Interdisciplinary, Band 3, 696.

Warwick P., Hall A., Pashley V., Bryan N.D., Griffin D. (2000) "Modelling the effect of humic substances on the transport of europium through porous media: A comparison of equilibrium and equilibrium/kinetic models", *J. Contam. Hydrol.*, 42, 19.

Zurmühl T. (1998) "Capability of convection–dispersion transport models to predict transient water and solute movement in undisturbed soil columns", *J. Contam. Hydrol.*, 30, 101.

## Annex 9:

**Use of Free-Liquid Electrophoresis for Analysis of Thorium Complexation with Humic Acids**

Benes P.

# Use of Free-Liquid Electrophoresis for Analysis of Thorium Complexation with Humic Acids

Benes P.

Czech Technical University, Department of Nuclear Chemistry, Brehova 7, 115 19 Praha 1, Czech Republic

## Abstract

Free-liquid electrophoresis was used for the study of thorium complexation with Aldrich humic acid (HA) with the aim to test applicability of the method under difficult conditions and to obtain missing data on the complexation at low pH values. Electrophoretic mobility $u$ of thorium labelled with $^{234}$Th was measured in aqueous solutions of 0.01M ($HClO_4$ + $NaClO_4$) as a function of pH (2-4), concentration of thorium ([Th] $\leq 10^{-7}$ - $10^{-5}$ M) and concentration of HA (0 – 10 mg/L). It was found that in the absence of HA the mobility ${}_{+}u$ towards cathode decreased with pH and decreasing [Th]. This was due to hydrolysis of $Th^{4+}$ and formation of thorium pseudocolloids by adsorption of thorium ([Th] $\leq 10^{-6}$ M) on colloidal impurities ever present in solutions. The mobility towards anode ${}_{-}u$ was negligible except for that of carrier-free $^{234}$Th. Addition of HA caused decrease in ${}_{+}u$ and increase in ${}_{-}u$ due to formation of negatively charged or neutral complexes ThHA.

Abundance of ThHA (*%ThHA*) was calculated from the decrease of ${}_{+}u$ assuming that only $Th^{4+}$, monomeric products of its hydrolysis and neutral or negatively charged ThHA complexes were present. Accuracy of this assumption and the effects of Th sorption losses were examined. The values of *%ThHA* obtained indicated nearly complete transition of Th to ThHA complexes upon addition of 10 mg/L HA except for $10^{-5}$ M Th at pH 2 and 3, where significant effect of saturation of HA capacity for Th was found. Similar effect was observed with $10^{-7}$ M Th and 0.1 mg/L HA. In these two cases, however, the binding of Th by HA exceeded capacity of dissociated carboxyl groups of HA thus pointing to at least partial displacement of $H^+$ ions from non-dissociated carboxyl groups.

The values of *%ThHA* obtained were used for calculation of mean electrophoretic mobilities of ThHA complexes ${}_{-}u_{\mathrm{ThHA}}$ from the corresponding values of ${}_{-}u$ of Th found in the presence of HA. The values of ${}_{-}u_{\mathrm{ThHA}}$ mostly increased with pH and decreased with [Th]/[HA] ratio. Surprisingly, complete charge neutralization of ThHA complexes was not found even in cases, when these complexes were formed from large excess of positively charged Th ions over dissociated carboxyl groups of HA.

## Introduction

In the frame of HUPA project, applicability of the free-liquid electrophoresis (Benes and Glos 1979, Benes and Majer 1980) for the study of formation and properties of actinide humate complexes was tested with europium and Aldrich humic acid (HA), when data on the abundance of EuHA complexes obtained with the method and three other methods were compared (Benes et al. 2004). It has been found that the method can yield correct data, if carried out and interpreted appropriately. In this paper, additional insight to conditions for the use of the method is provided by the study of formation and properties of thorium humate complexes at pH 2-4.

Use of the method for the purpose is based on several assumptions: First it is assumed that individual physicochemical forms (species) of studied metal migrate independently in electric field, so that the measured electrophoretic mobility of the metal towards cathode ${}_{+}u$ and anode ${}_{-}u$ can be calculated as a sum of the mobilities of individual positively or negatively charged species ${}_{+(-)}u_i$ , multiplied by their abundances $\delta_i$:

$$ {}_{+(-)}u = \Sigma\, {}_{+(-)}u_i \cdot \delta_i. \qquad (1) $$

This need not be true, if separation of species due to electrophoresis is not significantly more rapid than establishment of equilibrium between them. Incorrectness of this assumption causes no problem when the metal migrates only to one electrode (${}_{+}u$ or ${}_{-}u = 0$), since the interaction among only positively (or negatively) charged and neutral species will not change value of ${}_{+}u$ (or ${}_{-}u$). Rapid establishment of equilibrium between positively and negatively charged forms simultaneously present can, however, lead to mutual retardation of migration of these forms and to a decrease in both ${}_{+}u$ and ${}_{-}u$ compared to that calculated from Eq. (1).

The second assumption in the use of the method for analysis of metal humate complexation is that metal humate complexes are negatively charged or neutral, and thus their formation leads to a decrease in ${}_{+}u$ and increase in ${}_{-}u$ of the metal. If no other negatively charged forms of the metal are present, abundance of metal humate complex can be calculated as

$$ \%MeHA = 100\ \delta_{MeHA} = 100\ (1 - {}_{+}u / {}_{+}u_0) \qquad (2) $$

where ${}_{+}u_0$ is metal mobility measured under the same conditions but in absence of HA. An implicit third assumption for the validity of Eq. (2) is that addition of HA does not change mutual ratio of positively charged forms of metal remaining in the solution. This is true when only monomeric cations and neutral complexes of the metal are present ($Me^{n+}$ and mononuclear complexes), but need not be the case if polynuclear complexes, (colloidal) precipitates or pseudocolloids of the metal are formed in the absence of HA.

Free-liquid electrophoresis is unique in that it enables determination of mean electrophoretic mobility of metal humate complexes depending on their charge. It can be used for the study of charge neutralization phenomena in the formation of metal humate complexes. In absence of other negatively charged forms of metal the mean mobility of MeHA complexes is equal to

$$\bar{u}_{MeHA} = \bar{u} / \delta_{MeHA}. \quad (3)$$

In order to obtain correct values of $\delta_{MeHA}$ and $\bar{u}_{MeHA}$, the mobilities used in Eqs. (2) and (3) have to correctly represent metal speciation in analyzed solution. This requirement means that specific conditions for accurate performance of the electrophoresis must be observed (see Benes and Majer 1980) and that the mobilities measured should not be significantly affected by the adsorption of the metal on the walls of mixing vessel and electrophoretic cell. A large adsorption loss of metal from solution prior to (in mixing vessel) and during electrophoresis can change speciation of metal in solution, and the adsorption on central part of electrophoretic cell during electrophoresis can affect the mobility measured. The last mentioned effect is accounted for in the evaluation of mobility and suitable correction is applied (Benes and Glos 1979, Benes and Majer 1980) but the exact correction requires knowledge of the adsorption kinetics, seldom available. Analysis of errors caused by this effect was given by Mizera et al.(2003) for Eu-HA complexation.

In the present paper, applicability of the method was tested for complexation of thorium with Aldrich humic acid. Thorium hydrolyzes already at low pH values (2-3, Neck and Kim 2001, Reiller et al. 2003), readily precipitates as hydroxide (Neck and Kim 2001, Walther 2003) and strongly adsorbs on any available surface from its very dilute solutions (Rydberg and Rydberg 1952). Thus the study of its complexation represents rather difficult problem and an opportunity to analyze different complicating effects. At the same time, speciation of Th in its very dilute solutions and properties of its humate complexes are not well known.

## Experimental

*Reagents and solution preparation*

Ultrapure water (Millipore Milli-Q 50 system) and A.R. reagents were used for preparation of all solutions in this work. Carrier-free $^{234}$Th was prepared by dissolution of $UO_2(NO_3)_2.6H_2O$ crystals in diethylether, purification of $^{234}$Th in the aqueous phase thus formed by extraction with several portions of diethylether saturated with nitric acid and final separation of $^{234}$Th from traces of uranium by anion exchange using Ostion AT 807 resin and solution in 9.5M HCl. For further use, $^{234}$Th was transformed into $Th(ClO_4)_4$ form and stored in 1M $HClO_4$. Purification, characterization and preparation of stock solutions (500 mg/L) of Aldrich humic acid were described in detail previously (Mizera et al. 2003).

Experimental solutions were prepared in 50 mL polypropylene vessels by mixing stock solution of $^{234}$Th with water, 0.1 M NaOH and humic acid (in this order) so as to obtain the desired pH and concentration of humic acid and thorium. Other concentrations of thorium than "carrier-free" ($<< 10^{-7}$ M) were obtained by addition of $^{232}$Th at beginning of the mixing. The ionic strength of the solutions was maintained at 0.01 mol/L. The solutions were used for experiments 24 hours after their preparation. Before the use, pH of each solution was measured and, if necessary, readjusted.

*Apparatus and procedures*

The apparatus and procedure for free-liquid electrophoresis used in this work were described in detail earlier (Benes and Glos 1979, Benes and Majer 1980). The electrophoretic

cell consisted of three parts made of plastic tubings connected with two three-way Teflon stopcocks. The central part of the cell was filled with working solution labelled with $^{234}$Th, the side arms contained a working solution of the same pH and composition except for the label.

The electrophoretic experiments were carried out at a constant current (around 1 mA, with potential difference at the electrodes 230-240 V) at 22 ± 3 °C. The electrophoretic mobilities were calculated from the relationship

$$_{+(-)}u = \frac{\kappa \cdot V}{i \cdot t} \cdot \frac{A_{+(-)} + A'_{+(-)}}{A + kA' + A_{+} + A'_{+} + A_{-} + A'_{-}} \qquad (4)$$

Here $\kappa$ (in S.cm $^{-1}$) is the specific conductivity of the solution, $V$ (in ml) is the volume of the central part of the cell, $i$ (in A) is the mean current during the electrophoresis, $t$ (in s) is duration of electrophoresis. $A_{+(-)}$ stands for the activity of thorium found after the electrophoresis in the side arm close to cathode (anode), $A'_{+(-)}$ is the activity of thorium desorbed from the wall of the corresponding side arm, $A$ is the activity of thorium found in the central part after the electrophoresis and $A'$ is the activity desorbed from the central part. $k$ is coefficient depending on the kinetics of thorium adsorption in the central part during electrophoresis. Its value was set equal to 0.5, corresponding to a linear kinetics of the adsorption.

In all experiments, thorium was desorbed from the cell for 1 h using 1M HCl. Percentage of thorium adsorption loss on the central part of the cell as well as overall activity balance were calculated from all measured activities. The activity balance served as check for unaccounted activity losses during the experiments. In most cases, its values deviated from 100% by less than 5%, but deviations up to 20% were also encountered. Total adsorption loss of thorium on the walls of mixing vessel prior to electrophoresis was calculated from the difference between activity filled into the cell and that added to the mixing vessel (represented by a standard). All activity measurements were made by liquid scintillation counting in glass vials using Triathler Multilaber Tester and Rotiszint eco plus scintillation cocktail. No correction was necessary for the presence of humic acid at concentrations used in this work. Specific conductivity of the solutions was determined with a conductometer OK 102/1 equipped with a bell electrode OK-9023 (Radelkis, Budapest), pH was measured with combined glass electrode and Orion 525A pH meter.

## Results and discussion

Electrophoretic mobilities and sorption data presented in this paper are the mean values obtained by two to four independent experiments carried out with one (two experiments) or two (more experiments) thorium solutions. Their accuracy depends on the concentration of thorium used and on the adsorption of thorium in the electrophoretic cell. Due to the number of data needed for their calculation (Eq. 4) and to the small number of repeated experiments it is difficult to give any exact error for the mobilities presented. However, our long time experience with the method suggests that the total error of mobility determined usually does not exceed $\pm 0.3 \times 10^{-4}$ cm$^2$ s$^{-1}$ V$^{-1}$ and can be due to the inaccuracy of the measurement of

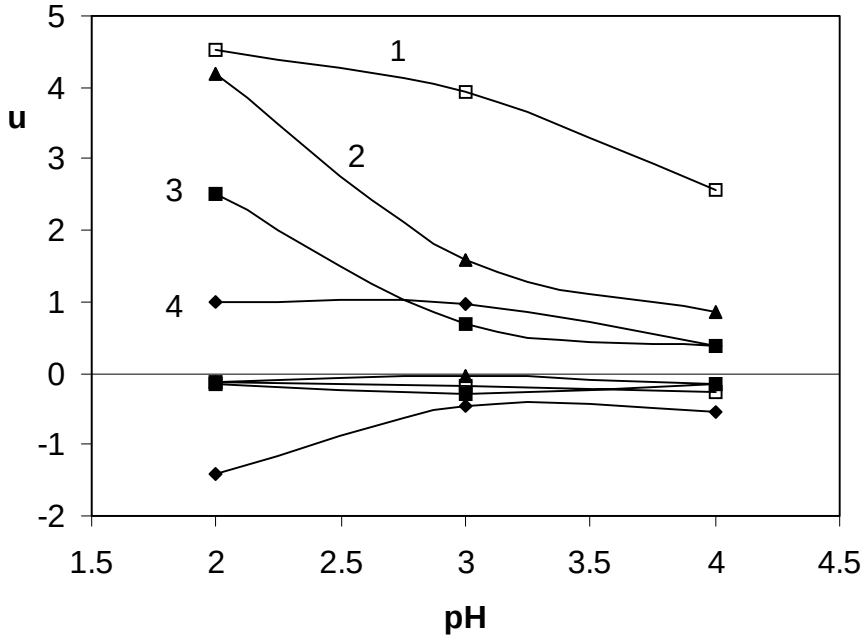


Fig.1: Mobility of thorium (in $10^{-4}$ $cm^2$ $s^{-1}$ $V^{-1}$) in solutions of 0.01 M ($HClO_4$ + $NaClO_4$) as a function of pH and initial concentration of Th: *1* – $1\times10^{-5}$ M , *2* – $1\times10^{-6}$ M, *3* – $1\times10^{-7}$ M, *4* – carrier-free $^{234}$Th.

thorium distribution in the cell (including cross-contamination in filling and sampling of solutions in the cell and errors of activity measurements), to the diffusion of neutral or equipolarly charged species of thorium (e.g. cations towards anode) and to the problems in accounting for thorium adsorption in the central part of the cell.

The first experiments were carried out in absence of humic acid with the aim to obtain the baseline data on the mobility of inorganic thorium species. Electrophoresis of thorium at pH 2-4 was studied as a function of thorium concentration (Fig. 1). It can be seen that thorium migrates predominantly to cathode. Its mobility towards anode is small and with the exception of carrier-free $^{234}$Th it may be within experimental errors ($_{-}u = 0.06 – 0.29\times10^{-4}$ $cm^2s^{-1}V^{-1}$).

The positive mobility decreases with increasing pH and with decreasing concentration of thorium. Similar changes were found by Mizera et al. (2001) for mobilities of europium in the concentration range $3.4\times10^{-8}$ - $1.7\times10^{-3}$ M and at pH 3-6. The authors explained the decrease by a large adsorption of Eu on the central part of electrophoretic cell which was not well corrected for in the calculation of mobility due to lack of knowledge of the adsorption kinetics. This explanation was supported by a similarity of the adsorption increase and of the mobility decrease observed. Rather large adsorption losses were found also for thorium. They are depicted in Figs. 2 and 3 as a function of pH and concentration of thorium. Comparison of the adsorption data with mobilities $_{+}u$ shown in Fig. 1 reveals that no simple correlation exists between them, although some of the partial changes show similar tendency. Moreover, the calculation using method by Mizera et al. (2003) of maximum possible errors caused by an incorrect assumption on the adsorption kinetics has shown that the errors can hardly account for the large $_{+}u$ decrease observed in Fig. 1.

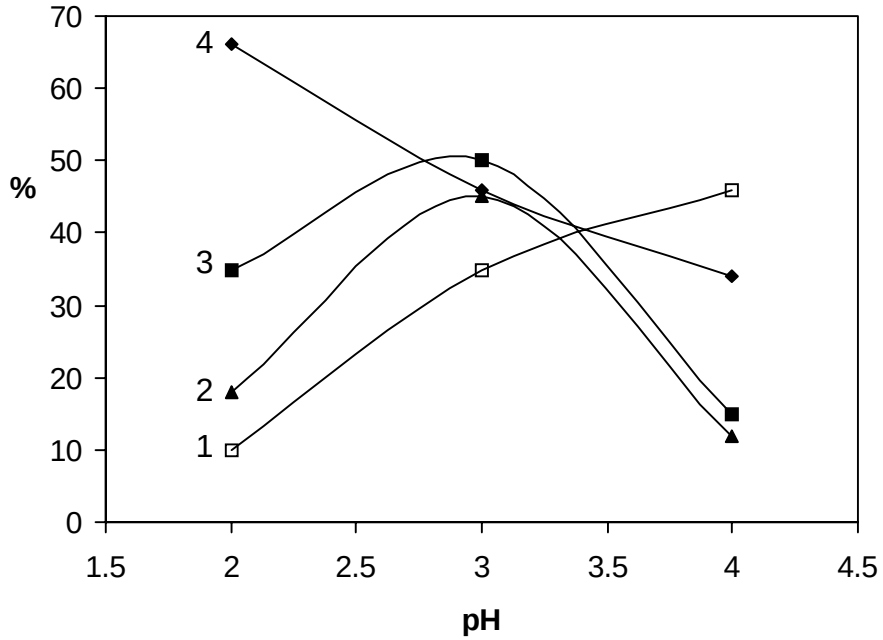


Fig.2: Adsorption loss (in % of introduced activity) of thorium from solutions of 0.01 M ($HClO_4$ + $NaClO_4$) on central part of electrophoretic cell as a function of pH and initial concentration of Th: *1* – $1\times10^{-5}$ M, *2* – $1\times10^{-6}$ M, *3* – $1\times10^{-7}$ M, *4* – carrier-free $^{234}$Th.

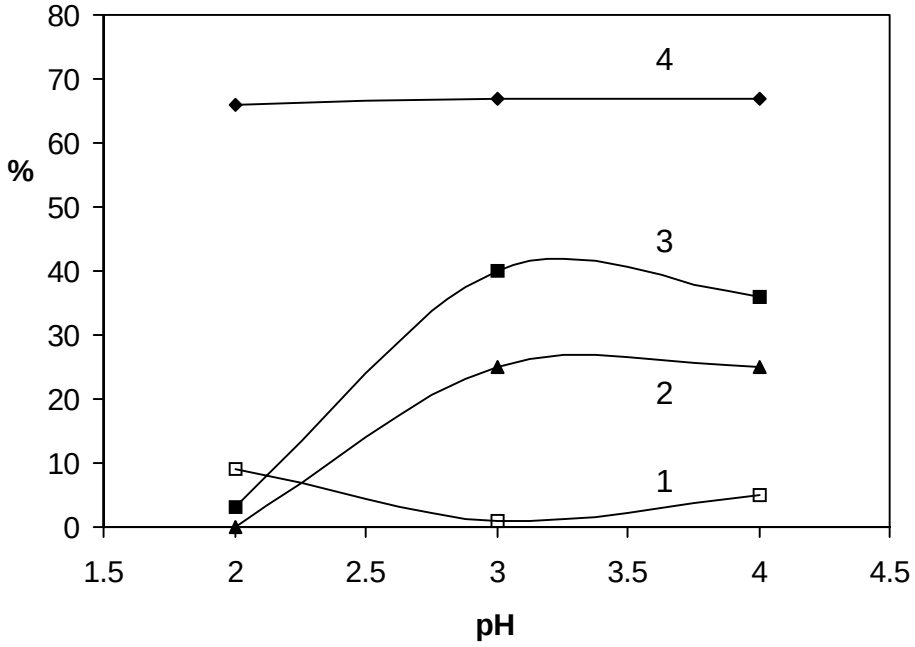


Fig.3: Adsorption loss (in % of introduced activity) of thorium from solutions of 0.01 M ($HClO_4$ + $NaClO_4$) on mixing vessel as a function of pH and initial concentration of Th: *1* – $1\times10^{-5}$ M, *2* – $1\times10^{-6}$ M, *3* – $1\times10^{-7}$ M, *4* – carrier-free $^{234}$Th.

Another effect of the adsorption can be a shift in equilibrium among thorium forms prior to or during electrophoresis accompanied by a decrease in $_{+}u$. However, such a shift cannot

take place between $Th^{4+}$ and mononuclear products of its hydrolysis, where equilibrium establishes rapidly. Polynuclear products of the hydrolysis or colloidal hydroxide with possibly slower formation/dissociation kinetics should not exist under conditions used in this work (Neck and Kim 2001) so that the main reason for the decrease in $_{+}u$ is simple hydrolysis of thorium and formation (at $\leq 10^{-6}$ M Th concentration) of pseudocolloids by adsorption of $Th(OH)_n^{(4-n)+}$ cations (n = 0-3) on colloidal impurities ever present in solution. Existence of pseudocolloids can explain the negative mobility of carrier-free $^{234}$Th and the dependence of $_{+}u$ on the concentration of thorium. Abundance of pseudocolloids is known to decrease with increasing metal concentration and their negative charge can be reversed by adsorption of polyvalent ions (Benes and Majer 1980).

The adsorption on mixing vessel and central part of electrophoretic cell may well bring about shift in ratio between dissolved and pseudocolloidal forms of thorium. This is one of reasons why the electrophoretic data cannot be easily used for analysis of formation and properties of thorium pseudocolloids. On the other hand, formation of pseudocolloids causes problems in the study of speciation of thorium (and other metals) at trace concentrations.

Addition of humic acid brings about decrease in $_{+}u$ and increase in $_{-}u$ of thorium. Extent of these changes depends on the concentration of humic acid (Fig. 4) and thorium (Fig. 5). The changes are mainly due to the formation of negatively charged or neutral ThHA complexes. It was interesting to examine possible effects of thorium adsorption on the changes in $_{+}u$ and $_{-}u$. Therefore the data on thorium adsorption in the absence and presence of humic acid were compared and correlations between the changes in the adsorption and in the mobilities were sought.

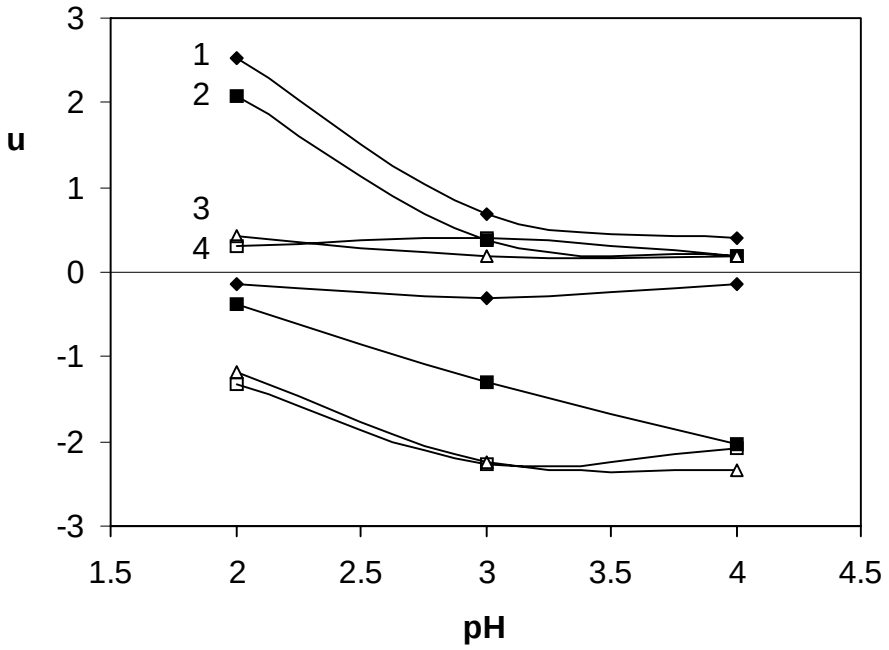


Fig.4: Mobility of $1\times10^{-7}$ M thorium (in $10^{-4}$ $cm^2$ $s^{-1}$ $V^{-1}$) in solutions of 0.01 M ($HClO_4$ + $NaClO_4$) as a function of pH and initial concentration of Aldrich humic acid (in mg/L): *1* – 0, *2* – 0.1, *3* – 1.0, *4* – 10.0.

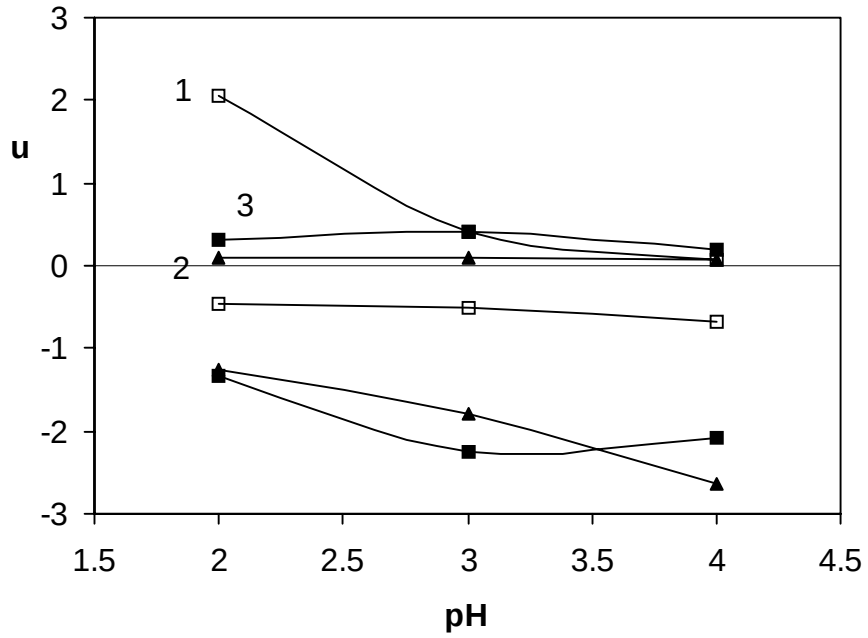


Fig.5: Mobility of thorium (in $10^{-4}$ $cm^2$ $s^{-1}$ $V^{-1}$) in solutions of 0.01 M ($HClO_4$ + $NaClO_4$) and 10 mg/L Aldrich humic acid as a function of pH and initial concentration of Th: *1* – $1\times10^{-5}$ M, *2* – $1\times10^{-6}$ M, *3* – $1\times10^{-7}$ M.

It has been found that addition of humic acid can significantly change the adsorption of thorium due to its bonding into ThHA complex. The changes vary with pH, concentration of thorium and humic acid, but the trends are difficult to identify and interpret. As an example, Fig. 6 presents some data for comparison with those in Fig. 2. Different trends have also been found between adsorption on mixing vessels and central part of the cell. E.g., addition of 10 mg/L HA completely suppressed adsorption of $10^{-5}$ and $10^{-6}$ M Th on the mixing vessel, whereas similar adsorption on the cell increased (cf. curves 1, 2 in Figs. 2 and 6). The difference may be due to different material of the vessel and cell, but also due to different conditions in the adsorption: freshly prepared or aged solution, time of contact, surface area to volume ratio.

The variability of the changes and difficulties in their interpretation make any exact prediction of their effect on $_{+}u$ and $_{-}u$ impossible. It is, however, clear that unless the adsorption is extremely high, errors due to the lack of knowledge of the adsorption kinetics (see above) cannot significantly contribute to the pronounced decrease in $_{+}u$ upon addition of humic acid documented in Figs. 4 and 5. As regards the possible shift in thorium speciation, an increase in the adsorption by the addition of humic acid indicates that ThHA complex is adsorbed more than the (positively charged) inorganic species of thorium. Since the equilibrium between the inorganic species and ThHA complex can re-establish slowly (Choppin and Cacheris 1986, Davis et al. 1999) and thus the original composition of solution prior to the adsorption need not be re-established during the electrophoresis, the higher removal of ThHA complex from the solution can bring about an increase in $_{+}u$ measured. The opposite effect can take place if the inorganic species are more adsorbed than ThHA. Then $_{+}u$ can decrease due to a high adsorption.

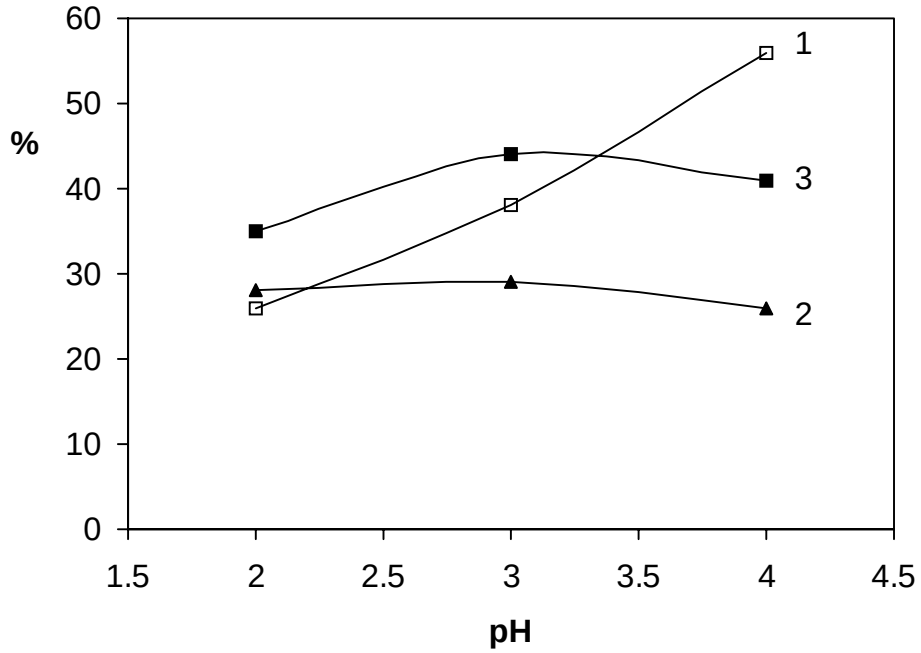


Fig.6: Adsorption loss (in % of introduced activity) of thorium from solutions of 0.01 M ($HClO_4$ + $NaClO_4$) and 10 mg/L Aldrich humic acid on central part of electrophoretic cell as a function of pH and initial concentration of Th: *1* – $1\times10^{-5}$ M, *2* – $1\times10^{-6}$ M, *3* – $1\times10^{-7}$ M.

No significant correlation between the decrease in ${}_{+}u$ and increase in thorium adsorption has been found except for the adsorption of $10^{-5}$ M Th from the solution of 10 mg/L HA on the cell as a function of pH (cf. differences between Figs.1 and 5 with those between Figs.2 and 6) and the adsorption of $10^{-7}$ M Th on the mixing vessel as a function of pH at 0.1 mg/L HA or concentration of humic acid at pH 2 (not shown here). In both the cases, the adsorption increases upon addition of humic acid so that the value of ${}_{+}u$ measured can be higher than the correct one (see below).

Thorium mobilities presented in Figs. 1, 4 and 5 can be used for calculation of the abundance of ThHA complexes using Eq.(2). Basic problem is that pseudocolloids of thorium with unknown mobility and abundance are present in solutions of pH 2-4 with no humic acid added and $\leq 10^{-6}$ M Th, and it can hardly be assumed that their ratio to dissolved cationic forms of thorium will not be affected by addition of humic acid (see Introduction). Thus ${}_{+}u$ mobilities measured in the above solutions are not suitable for use as ${}_{+}u_0$ representing mobility of remaining positive forms of thorium. It is more feasible to assume that the existence of thorium pseudocolloids will be completely suppressed by the addition of HA and to use as ${}_{+}u_0$ for the calculation the values of ${}_{+}u$ measured in the solution of $10^{-5}$ M Th (Fig. 1), where the abundance of thorium pseudocolloids is obviously negligible. Results of such calculation (mode A) are presented in Table1. For comparison, results of calculation using "unsuitable" values of ${}_{+}u_0$ are also shown (mode B). The data in Table 1 represent means of values calculated by combination of all measured values of ${}_{+}u$ and ${}_{+}u_0$ for the given conditions, errors attached are the ranges of variability of the data.

Table1: Abundances of ThHA complexes (in %) calculated using Eq.(2) and mobilities $_{+}u$ from Figs. 4, 5 assuming that the mobility $_{+}u_0$ (in absence of HA, Fig. 1) is equal to the mobility of $1\times10^{-5}$ M Th (mode A) or of the corresponding concentration of thorium (mode B).

| Mode | $[Th]_0$ mol/L | $[HA]$ mg/L | pH 2 | pH 3 | pH 4 |
|---|---|---|---|---|---|
| A | $10^{-7}$ | 0.1 | 53.8 ± 10.0 | 90.3 ± 4.2 | 92.4 ± 1.9 |
| A | $10^{-7}$ | 1.0 | 90.8 ± 1.8 | 95.2 ± 1.7 | 92.5 ± 3.2 |
| A | $10^{-7}$ | 10 | 92.2 ± 0.8 | 89.3 ± 1.9 | 92.6 ± 2.5 |
| A | $10^{-6}$ | 10 | 99.4 ± 0.6 | 97.4 ± 1.2 | 97.2 ± 2.4 |
| AB | $10^{-5}$ | 10 | 54.6 ± 2.5 | 89.4 ± 1.1 | 97.3 ± 1.2 |
| B | $10^{-7}$ | 0.1 | 19.5 ± 19.5 | 43.1 ± 26.7 | 49.7 ± 12.8 |
| B | $10^{-7}$ | 1.0 | 83.2 ± 4.3 | 71.8 ± 11.1 | 50.7 ± 21.8 |
| B | $10^{-7}$ | 10 | 87.5 ± 4.0 | 38.0 ± 13.3 | 50.8 ± 16.6 |
| B | $10^{-6}$ | 10 | 98.0 ± 2.0 | 93.4 ± 3.4 | 91.5 ± 7.4 |

It can be seen that the use of "unsuitable" values of $_{+}u_0$ results in abundances of ThHA whose dependence on pH and partially also on the concentration of humic acid contradicts to the expected trends. Calculation in mode A leads to more consistent and explainable data, inicating predominance of ThHA complexes under the conditions studied. The abundance of ThHA does not depend on pH (2-4) except for conditions when the concentration of thorium approaches saturation of complexing capacity of humic acid present in solution. Practically complete complexation of thorium with humic acid is observed for $10^{-5}$ M Th and 10 mg/L HA at pH 4 as well as for $10^{-6}$ M Th. The small deviation from 100% can be at least partially due to neglecting the small background values of $_{+}u$ caused by diffusion (cf. above). The data obtained in mode A on *%ThHA* for $10^{-7}$ M Th are lower and do not seem to depend on pH and concentration of humic acid (with one exception). This contradicts to the expected trends and can be explained only by an error in their calculation. Very probably the error is due to the high adsorption losses of thorium, which result in incorrectly high values of $_{+}u$ measured (see above).

Of special interest is the saturation of complexing capacity of humic acid with thorium, indicated by the data in Table 1 for $10^{-7}(10^{-5})$ M Th and 0.1(10) mg/L HA. The only other reasons for the observed decrease in *%ThHA* with decreasing pH can be formation of positively charged ThHA complexes, which is very improbable, and large adsorption loss of ThHA. However, neither the pH dependence of thorium adsorption nor the effect of humic acid concentration correlates with that of *%ThHA* (see, e.g. Fig. 6).

The complexation capacity of humic acid can be expressed using concentration of humic acid (*[HA]*, in mg/L), its proton exchange capacity (*PEC*, in mol/kg) and the degree of dissociation of complexing (here carboxyl) sites of the acid ($\alpha$), determined by acidobasic titration of the acid:

$$CC_{HA} = 10^{-6}\ [HA].\ PEC.\ \alpha \qquad (5)$$

In Table 2, complexing capacities calculated using Eq. (5) and data on *PEC* and α taken from Mizera et al. (2003) are compared with the concentrations of ThHA, calculated from $[Th]_0$ and *%ThHA* values given in Table 1. As can be seen, concentrations of ThHA formed in the solution exceed complexation capacities of humic acid for bonding of monovalent cations, represented by the concentration of available dissociated sites ($COO^-$) of the acid. The effect increases with decreasing pH. Considering that thorium cations participating in the complexation under studied conditions carry higher charge than 1 (up to 4+), the exceeding of $CC_{HA}$ is still more pronounced and means that either the complexation proceeds at least partially by displacement of $H^+$ from non-dissociated COOH groups of humic acid or positively charged ThHA complexes are formed. The latter possibility is not supported by data on the negative mobility of ThHA complexes (see below).

Table2: Comparison of complexation capacities $CC_{HA}$ and *[ThHA]* concentrations (both in mol/L) in solutions of $10^{-7}$ M Th + 0.1 mg/L HA and $10^{-5}$ M Th + 10 mg/L HA.

| Compared values | pH 2 | pH 3 | pH 4 |
|---|---|---|---|
| $[ThHA]\times10^7$ | 0.538 | 0.903 | 0.904 |
| $[ThHA]\times10^5$ | 0.546 | 0.894 | 0.973 |
| $CC_{HA}\times10^7$ or $10^5$ | 0.14 | 0.84 | 2.17 |

The negative thorium mobilities $-u$ shown in Figs.4,5 and the values of *%ThHA* given in Table 1 (mode A) were used for calculation of the mean mobilities of ThHA complexes using Eq. (3). Results are presented in Table 3. Here again, errors attached are the ranges of possible values calculated from the corresponding ranges found for $-u$ and *%ThHA*. The results are calculated without consideration (subtraction) of the small mobilities $-u$ found in the absence of humic acid (see Fig.1). Control calculations have shown that subtraction of these mobilities causes only minor deviations from the data shown in Table 3, which mostly lie in the range of attached errors. Moreover, whatever is reason for the negative mobility of thorium in the absence of humic acid, the underlying process (e.g. diffusion or migration of unknown thorium species) will probably be strongly suppressed in the presence of humic acid.

Consideration of possible effects of adsorption losses of thorium on the values of $-u_{\mathrm{ThHA}}$ calculated with Eq.(3) suggests that shift of equilibria due to prevalent adsorption of inorganic (positively charged) forms of thorium over that of ThHA complexes or vice versa will probably not much influence the values. E.g., when the adsorption of ThHA is higher, the resulting increase in $+u$ (causing decrease in *%ThHA*) and decrease in $-u$ measured will compensate each other and the overall effect on $-u_{\mathrm{ThHA}}$ will be small. This is probably the case of data presented in Table 3 for $10^{-7}$ M Th, which can therefore be considered as not much affected by possible errors in the calculation of *%ThHA* (see above). On the other hand, neglecting real kinetics of thorium adsorption on central part of electrophoretic cell (i.e. assuming $k = 0.5$ in Eq.(4) instead of a correct lower value) can result in lower $+u$ and $-u$ values, which will cause even larger decrease in $-u_{\mathrm{ThHA}}$.

Table 3: The mean mobilities of ThHA complexes ($_{-}u_{ThHA}$, in $10^{-4}$ $cm^2$ $s^{-1}$ $V^{-1}$) in solutions of 0.01 M ($HClO_4$ + $NaClO_4$) as a function of pH and initial concentration of thorium and humic acid.

| $[Th]_0$ mol/L | [HA] mg/L | pH 2 | pH 3 | pH 4 |
|---|---|---|---|---|
| $10^{-7}$ | 0.1 | 0.74 ± 0.12 | 1.39 ± 0.11 | 2.21 ± 0.14 |
| $10^{-7}$ | 1.0 | 1.31 ± 0.15 | 2.36 ± 0.27 | 2.52 ± 0.10 |
| $10^{-7}$ | 10 | 1.43 ± 0.04 | 2.53 ± 0.10 | 2.25 ± 0.25 |
| $10^{-6}$ | 10 | 1.26 ± 0.27 | 1.83 ± 0.07 | 2.72 ± 0.20 |
| $10^{-5}$ | 10 | 0.87 ± 0.26 | 0.55 ± 0.08 | 0.69 ± 0.34 |

Data in Table 3 show that the values of $_{-}u_{ThHA}$ generally increase with pH and decrease with increasing $[Th]_0/[HA]$ ratio. These effects can be explained by the higher dissociation of COOH groups of humic acid at higher pH values and by neutralization of negative charge of humic acid with thorium cations bound to ThHA complex, respectively. The former effect does not take place at $10^{-5}$ M concentration of thorium where precipitation of thorium humate was observed. In contrast, it is most pronounced in the solution of $10^{-7}$ M Th and 0.1 mg/L HA with the same ratio $[Th]_0/[HA]$ and the same value of $_{-}u_{ThHA}$ at pH 2. Very probably the precipitation can somehow mask the increase of charge of ThHA with pH. The other two solutions with the same $[Th]_0/[HA]$ ratio, i.e $10^{-6}(10^{-7})$ M Th + 10(1.0) mg/L HA, are characterized by very similar values of $_{-}u_{ThHA}$ (except for pH 3). At pH 4 no obvious effect of $[Th]_0/[HA]$ ratio on $_{-}u_{ThHA}$ is found.

The most important conclusion drawn from Table 3 is that the negatively charged ThHA complexes are formed even in conditions when the complexation capacity of dissociated $COO^-$ groups of humic acid is more than completely saturated with thorium cations (cf. Table 2), i.e. the large surplus of positive charge of thorium cations in the formation of ThHA complexes does not bring about total neutralization of the negative charge of humic acid. Data in Table 3 do not provide any support for possible formation of positively charged ThHA complexes. Such complexes are certainly not formed at pH 4, as the corresponding $_{+}u$ values shown in Figs. 4,5 are very small. Their significant presence at lower pH values should be indicated by higher $_{+}u$ values and should result in a decrease of $_{-}u_{ThHA}$ with decreasing pH, which was observed for $10^{-7}$ M Th but not for $10^{-5}$ M Th. Thus at least for $10^{-5}$ M Th the presence has to be excluded.

The last question to be solved is whether the results obtained and their interpretation are affected by kinetic lability of ThHA complexes, i.e. by dissociation of the complexes and exchange of thorium or its label between ThHA and non-complexed (inorganic) forms of thorium (cf. Introduction). The ensuing mutual retardation of migration of the oppositely charged thorium species would diminish measured mobilities $_{+}u$ and $_{-}u$ and would result in higher *%ThHA* and in lower $_{-}u_{ThHA}$ values. Such effect was found in the study of formation of EuHA complexes (Mizera et al. 2003) under conditions of higher loading of humic acid with europium, when the mobility $_{-}u$ of europium was lower than that of humic acid simultaneously present. Due to this effect, the abundance of metal humate determined by electrophoresis must be regarded as maximum possible value for given conditions, which was

also corroborated by comparison of results of electrophoresis with data obtained by other methods (Benes et al. 2004).

It is not easy to assess importance of the effect only from the electrophoretic data presented and comparison with *%ThHA* obtained by other methods can be recommended. However, the effect can surely be neglected in cases where ThHA complexes predominate and abundance of positively charged thorium species is very low. Analysis of mobility data for $10^{-5}$ M Th (Fig. 5) characterized by a large $_{+}u$ at pH 2 also does not suggest any retardation of thorium migration towards anode as the value of $_{-}u$ is the same at pH 2 and 3, although the corresponding values of $_{+}u$ are very different. The only case where the effect could be pronounced is probably indicated by the decrease in $_{-}u$ with decreasing pH in the solution of $10^{-7}$ M Th and 0.1 mg/L HA, accompanied by the increase in $_{+}u$. Particularly the mobilities measured at pH 2 can be lowered due to the mutual retardation and therefore the corresponding values of *%ThHA* (53.8%, Table 1) and of $_{-}u_{ThHA}$ ($0.74\times10^{-4}$ cm$^2$ s$^{-1}$ V$^{-1}$, Table 3) can be too high or low, respectively. The maximum possible error caused by this effect can be assessed in the following way: The maximum possible value of $_{-}u_{ThHA}$ is undoubtedly limited by the neighbouring values in Table 3 (1.31 or $1.39\times10^{-4}$ cm$^2$ s$^{-1}$ V$^{-1}$) since $_{-}u_{ThHA}$ can hardly increase with decreasing pH or *[HA]/[Th]* ratio. Taking $1.3\times10^{-4}$ cm$^2$ s$^{-1}$ V$^{-1}$ as the maximum possible value, calculation using the measured $_{-}u$ value and Eq.(3) gives 28.5% as the minimum possible value of *%ThHA*. This value still conforms to conclusions drawn above (cf. Table 2).

## Conclusions

The free-liquid electrophoresis can be used for analysis of thorium complexation with humic acids in solutions of pH 2-4 containing $10^{-5}$ M or lower concentration of thorium where thorium migrates to cathode in the absence of humic acid. Abundance of thorium humate complex (*%ThHA*) can be calculated from the decrease in the cathodic mobility of thorium upon addition of humic acid. For this purpose, cathodic mobility of $10^{-5}$ M Th in the absence of humic acid has to represent mobility of mononuclear cationic forms of thorium ($Th^{4+}$ and hydroxocomplexes). At lower concentration of thorium pseudocolloids exist and at higher concentration polynuclear hydroxocomplexes and colloidal hydroxide can be formed, which change the mobility of thorium in the absence of humic acid. Accuracy of determination of *%ThHA* depends on the value of *%ThHA* and on the adsorption of thorium prior to electrophoresis on the mixing vessel and during electrophoresis on the electrophoretic cell.

If *%ThHA* is close to 100%, the large adsorption can exert only minor effect on its value, which can be lowered due to a shift of equilibrium between ThHA complexes and cationic thorium species in favour of the latter, caused by the adsorption. Such effect was probably responsible for the lower values of *%ThHA* found in this work for $10^{-7}$ M Th. A small decrease in calculated *%ThHA* can be also due to neglecting of the diffusion of neutral thorium species towards cathode and cross-contamination during filling and sampling of solution in electrophoretic cell.

The accuracy of *%ThHA* values lower than about 90% is generally worse for several reasons. One of them can be kinetic lability of ThHA complex, which can result in an increase (positive error) of *%ThHA*. Similar but smaller error may be caused by incorrect assumption on the linearity of time dependence of thorium adsorption during electrophoresis ($k$ = 0.5 in Eq.(4)). A shift in equilibrium between ThHA and non-complexed forms of thorium due to a large adsorption can bring about positive or negative errors in *%ThHA* when adsorption of the uncomplexed forms or ThHA prevails, respectively. In this paper, none of these effects was identified with certainty, although the adsorption losses were quite large and adsorption of ThHA prevailed in conditions favourable for existence of the effects. Nevertheless, *%ThHA* values lower than 90% presented in this paper should be considered as maximum possible values for the given conditions.

Anodic mobility of thorium in the presence of humic acid divided with the corresponding *%ThHA* yields the mean mobility of ThHA complexes under given conditions. Accuracy of the value of $-u_{ThHA}$ thus obtained depends on the accuracy of *%ThHA* and on the effects of the adsorption. While shift of the equilibrium in solution due to the adsorption can have only a small effect, an incorrect assessment of the adsorption kinetics can result in a significant decrease in $-u_{ThHA}$. Thus $-u_{ThHA}$ values obtained can be considered as minimum possible values. The error possible can be diminished by neglecting of the contribution of negative "background" mobility of thorium caused by the diffusion and cross-contamination.

Results of this work indicate virtually complete complexation of thorium with Aldrich humic acid when a surplus of total complexation capacity of the acid over thorium concentration exists in the solutions studied. However, some results also prove that the complexation capacity of the acid based on its dissociated $COO^-$ groups can be significantly exceeded in the complexation if $[Th]_0/[HA]$ ratio is large enough. This indicates that under such conditions the complexation proceeds at least partially by displacement of $H^+$ ions from non-dissociated COOH groups. The mean anodic mobilities $-u_{ThHA}$ found mostly increase with pH and decrease with increasing $[Th]_0/[HA]$ ratio. However, complete charge neutralization of humic acid is not found even in cases, when ThHA complexes are formed under large excess of positive charge of thorium cations over dissociated carboxyl groups of humic acid. Although formation of positively charged ThHA complexes cannot be excluded for one set of the conditions studied, no evidence for existence of such complexes has been found.

## Acknowledgement

This study was supported by the EC Commission under contract No. FIKW-CT-2001-00128 and by the Grant No. MSM 210000019 of the Czech Ministry of Education.

## References

Benes P. and Glos J. (1979) „Radiotracer Analysis of the Physico-chemical State of Trace Elements in Aqueous Solutions.II. Electromigration Method", *J. Radioanal. Chem*. **52**, 43.

Benes P. and Majer V. (1980) „Trace Chemistry of Aqueous Solutions", Academia/Elsevier, Prague/Amsterdam.

Benes P., Mizera J., Stamberg K. and Prochazkova S. (2004) „Comparison of dialysis, electrophoresis, ion exchange and ultrafiltration as methods for analysis of complexation of europium with humic acid“. In: Buckau, G. (Editor) “Humic Substances in Performance Assessment of Nuclear Waste Disposal: Actinide and Iodine Migration in the Far-Field (second technical progress report)”, Report FZKA 6969, Research Center Karlsruhe, July 2004, 265.

Choppin G.R and Cacheris W.P. (1986) “Kinetics of Thorium Humate”, *J. Less-Common Met.* **122**, 551.

Davis J.R., Higgo J.J.W., Moore Y. and Milne C. (1999) “The characterisation of a fulvic acid and its interactions with uranium and thorium”. In: Buckau, G. (Editor) “Effects of Humic Substances on the Migration of Radionuclides: Complexation and Transport of Actinides (second technical progress report)”, Report FZKA 6324, Research Center Karlsruhe, June 1999, 61.

Mizera J., Dolansky J. and Benes P. (2001) “Radiotracer Study of the Electrophoretic Behavior of Eu and its Complexes with Humic Acid”, *Radiochim. Acta* **89,** 529.

Mizera J., Benes P. and Masnerova G. (2003) „Electrophoretic Determination of the Degree of Eu Complexation by Humic Acid: Analysis and Assessment of Experimental Error“. In: Buckau G. (Editor) “Humic Substances in Performance Assessment of Nuclear Waste Disposal: Actinide and Iodine Migration in the Far-Field (first technical progress report)”, Report FZKA 6800, Research Center Karlsruhe, April 2003, 191.

Neck V. and Kim J.I. (2001) “Stability and Hydrolysis of Tetravalent Actinides”, *Radiochim. Acta* **89**, 1.

Reiller P., Moulin V., Casanova F. and Dautel Ch. (2003) “On the Study of Th(IV)-Humic Acid Interactions by Competition Studies with Silica and Determination of Global Interaction Constants”, *Radiochim. Acta* **91**, 513.

Rydberg J. and Rydberg B. (1952) “Adsorption on Glass and Polythene from Solutions of Thorium and Thorium Complexes in Tracer Concentrations”, *Svensk Kem. Tidsk.* **64**, 200.

Walther C. (2003) “Comparison of Colloid Investigations by Single Particle Analytical Techniques – a Case Study on Thorium-oxyhydroxides”, *Coll. Surfaces A-Phys. Eng. Aspects* **217**, 81.

## Annex 10:

**The Assessment of Mean Molecular Weight of Aldrich humic Acid (HA) Using MMWM-Model and Experimental Data on Eu-HA Complexation**

Stamberg K., Benes P.

# The Assessment of Mean Molecular Weight of Aldrich humic Acid (HA) Using MMWM-Model and Experimental Data on Eu-HA Complexation

Stamberg K. and Benes P.

Czech Technical University, Department of Nuclear Chemistry, Brehova 7, 115 19 Praha 1, Czech republic

## Abstract

The mean molecular weight model, MMWM (Stamberg et al., 2003), and the results of Eu-HA complexation study by dialysis and ion exchange methods (Benes et al., 2004) were used for assessment of mean molecular weight of Aldrich humic acid, *MHA*. The humic acid was purified/protonated by the procedure described by Kim (Kim et al., 1990). The assessment was made for the following conditions: initial Eu(III) concentration $1.17 \times 10^{-5}$ mol/L, 10 mg/L HA, ionic strength 0.1, pH 4 and 6, HA loading with Eu equal to 50 %. The molecular weight was assessed by comparison of the abundance of Eu humate, *%EuHA*, calculated by the MMWM-model for pH 4 and 6 as a function of *MHA*, with the experimental data obtained as *%EuHA* for the same values of pH, i.e., for pH 4 and 6. The comparison points to the values between approx. 0.6 kDa for pH 4 and 1.6 kDa for pH 6. This interval is in relatively good agreement with the measurements using the AFFFF and TOF-SIM techniques (Wolf et al., 2004) and indicates the influence of pH on the aggregation of HA in the presence of Eu(III).

Linear dependences, calculated by means of MMWM model, exist between charge ($p\{-\}$) of HA molecules and *MHA*; naturally, the charge depends on pH. In the case of low values of the charge, i.e. if valency of the metal $z\{+\} > p\{-\}$, the formation of the larger entities type of $Me_pHA_z$ can be expected.

## 1 Introduction

Many data and informations exist in the literature which support the concept of macromolecular and polydisperse character of humic substances (HS). Depending on the type and origin of HS, on the way of their isolation and pretreatment or purification, their molecular weight was reported to lie in the range approx. from $10^2$ to $10^5$ dalton (see, e.g. Swift, 1989).
Using new techniques such as AFFFF (Asymetrical Flow Field-Flow Fractionation, for size distribution) or TOF-SIMS (Time-of-Flight Secondary Ion Mass Spectrometry, for mass distribution) quite different results were obtained indicating that the mean molecular weight of HS can be much smaller, somewhere between $10^2$ and $10^3$ dalton. Earlier data were explained as due to an aggregation of individual molecules of HS (Wolf et al., 2004). In the last HUPA meeting in Karlsruhe, new results of size distribution measurements conducted by AFFFF with different humic and fulvic acids at different degrees of ligand loading with $Eu^{3+}$ were reported by M. Wolf. For humic acid an increase in size distribution was found for high metal loading. The results may indicate generation of larger entities with complexation at high metal ion ligand loading (Buckau, 2004).
With the aim to contribute to the knowledge of molecular weights of humic acids and of the associated effects of metal ion complexation, we have used the MMWM (Mean Molecular Weight Model) model (Stamberg et al., 2003) and the experimental results of Eu-humic acid complexation study by dialysis (DIA) and ion exchange (IEX) methods (Benes et al., 2004) for assessment of mean molecular weight of Aldrich humic acid (*MHA*). The approach employed consisted in two steps: (1) the calculation of *%EuHA* = f(*MHA*) for pH 4 and 6 using MMWM model, (2) the comparison of the calculated results with experimental data expressed as *%EuHA* for pH 4 and 6 and deduction of *MHA* values. The main goal was to compare the values of *MHA* assessed for pH 4 and 6 and for HA loading with Eu(III) equal to 50 %, with the above mentioned results of AFFFF and TOF-SIMS techniques.

## 2 MMWM-model and the description of Eu-HA complexation

At first, let the MMWM be briefly described (Stamberg et al., 2003). For the sake of simplicity it is assumed that the complexation takes place at pH < 8 - 8.5, i.e., only with dissociated carboxylic groups of humic acid, namely with so called strong carboxylic groups ($HAS^{n-}$, more acidic) and so called weak carboxylic groups ($HAW^{m-}$, less acidic); this classification is based on the evaluation of titration curve of Aldrich HA (Stamberg et al., 2003). In accordance with the results of electrophoretic measurements (Mizera et al., 2001), the complexation reactions can be written as

$$a.Me^{z+} + HAS^{n-} = Me_aHAS^{(n-a.z)-} \qquad a = 1,2,3,\ldots..,a_{max}; \quad a_{max} = |n/z| \qquad (1a)$$

$$b.Me^{z+} + HAW^{m-} = Me_bHAW^{(m-b.z)-} \qquad b = 1,2,3,\ldots..,b_{max}; \quad b_{max} = |m/z| \qquad (1b)$$

If both the reactions occur simultaneously (probably above pH 4), then

$$(a + b).Me^{z+} + (HAS^{n-} + HAW^{m-})^{p-} = (Me_aHAS^{(n-a.z)-} + Me_bHAW^{(m-b.z)-})^{(p-a.z-b.z)-} \qquad (2)$$

$(HAS^{n-} + HAW^{m-})^{p-}$ in Eq. (2) denotes one mole of $HA^{p-}$ with total charge $p- = n- + m-$ where $n-$ is contributed by dissociated carboxylic groups of type "S" ($HAS^{n-}$) and $m-$ by dissociated carboxylic groups of type "W" ($HAW^{m-}$). Similarly the sum $(Me_aHAS^{(n-a.z)-} + Me_bHAW^{(m-b.z)-})^{(p-a.z-b.z)-}$ denotes

one mole of HA whose carboxylic groups HAS + HAW are occupied by cations $(a + b)Me^{z+}$. In Eqs. (1a, 1b and 2), polyanionic molecule HA represents central ion in the complex formation, in contrast to the classical concept of complex formation where this role is played by a cation. The maximum values of stoichiometric coefficients, $a_{max}$ and $b_{max}$, should correspond to the zero charge of the complex for a given pH. This is, however, valid only if *n*- and *m*- are divisible by *z* (leaving no remainder), otherwise the "last" complex can be positively charged with maximum charge equal to (*z-1*)+. Symbol $Me^{z+}$ in Eqs. (1a,b) and (2) stands for any cationic form taking part in the complexation including, e.g., hydroxocomplexes.

Stability constants for reactions (1a) and (1b) are defined as

$$KS_a = \frac{\left[Me_a HAS^{(n-a.z)-}\right]}{\left[Me^{z+}\right]^a \left[HAS^{n-}\right]} \quad (3) \qquad KW_b = \frac{\left[Me_b HAW^{(m-b.z)-}\right]}{\left[Me^{z+}\right]^b \left[HAW^{m-}\right]} \quad (4)$$

The charges *n* (= mol $LS^-$/mol HA) and *m* (= mol $LW^-$/mol HA) can be calculated from

$$n = MHA \,.\, Q_{LS} = MHA \,.\, Q\Sigma_{LS} / (1 + K_{LS} \,.\, [H^+]) \quad (5)$$

$$m = MHA \,.\, Q_{LW} = MHA \,.\, Q\Sigma_{LW} / (1 + K_{LW} \,.\, [H^+]) \quad (6)$$

where: $LS^-$ and $LW^-$ denote the dissociated carboxylic groups of strongly and weakly acidic type, respectively; $Q_{LS}$ and $Q_{LW}$ are their concentrations, in mol $COO^-$ /kg HA; $Q\Sigma_{LS}$ and $Q\Sigma_{LW}$ are the total concentrations, i.e. dissociated + nondissociated, in mol/kg HA; and $K_{LS}$ and $K_{LW}$ are the protonation constants of these groups.

As for the stoichiometric coefficients, for example in the Eu(III) - HA system, $a_i$ is equal to the molar ratio of Eu and HAS in the *i*-th complex $Eu_{ai}HAS$, whereas the experimentally determined ratio [*Eu*]/[*HA*] i.e. its average value $([Eu]/[HA])_{mean}$ represents the ratio of total molar concentrations [*Eu*] and [*HA*] in solution for given conditions. Therefore $(a_i)_{mean}$ is defined as

$$(a_i)_{mean} = \left( \frac{[Eu] - [Eu]_{free}}{[HA] - [HA]_{free}} \right)_{mean} \quad (7)$$

where $[Eu]_{free}$ (e.g., $[Eu^{3+}]$, $[EuOH^{2+}]$) and $[HA]_{free}$ are the equilibrium molar concentrations of noncomplexed forms in solution. In addition, it holds that $a_i \leq a_{max}$ and $b_i \leq b_{max}$ , i.e. that these coefficients depend on pH and *MHA*, too. Consequently, the assessment of $a_i$ (or $b_i$) based on [*Eu*]/[*HA*] is the more accurate the higher is the extent of complexation between Eu and HA. The exact determination of stoichiometric coefficients is not, however, crucial for the regression of experimental data, as several coefficients are usually used in the computing (*a1 – a3*, or *b1 – b3*)) and their suitability is judged (or the coefficients are corrected) by the quality of the fit.

As shown above, the values of constants $KS_a$ and $KW_b$ depend on the values of stoichiometric coefficients. From this point of view, there are two important equations in the paper (Stamberg et al., 2003) derived for I = 0.1 on the basis of evaluation of experimenal data, namely:

$$\log KS_a = 5.911\, a_i + 1.621 \quad (8) \quad \text{and} \quad \log KW_b = 7.342\, b_i + 1.261 \quad (9)$$

## 3 Results and discussion

In the first step, the new speciation code based on MMWM model was constructed and then the abundances of individual species, i.e., $Eu^{3+}$, $Me_aHAS^{(n-a.z)-}$, $Me_bHAW^{(m-b.z)-}$, $(Me_aHAS^{(n-a.z)-} + Me_bHAW^{(m-b.z)-})^{(p-a.z-b.z)-} \equiv$ EuHA, for different values of *MHA* were calculated as a function of pH. In the course of iteration calculations, it was also looked for the values of stoichiometric coefficients $a_1$, $a_2$, $a_3$ and $b_1$, $b_2$, $b_3$, and for the values of corresponding stability constants (see equations (8) and (9)). In addition, the charges of HA molecules for pH 4 and 6 as a function of *MHA* were computed using equations (5) and (6) .

The following input data were used:

$K_{LS}$ = 1.99x10$^3$; $K_{LW}$ = 6.3x10$^5$; $K_{LPh}$ = 9.52x10$^{10}$ (protonisation constant of phenolic groups);

$Q\Sigma_{LS}$ = 2.41 mol/kg HA; $Q\Sigma_{LW}$ = 2.14 mol/kg HA; $Q\Sigma_{LPh}$ = 2.45 mol/kg HA;

$PEC = Q\Sigma_{LS} + Q\Sigma_{LW} + Q\Sigma_{LPh}$ = 7 mol/kg HA;

$CEu_0$ = 1.17x10$^{-5}$ mol/L Eu(III); $CHA_0$ = 10 mg/L Aldrich HA;

HA *Loading* with Eu(III) = 50 %; $I$ = 0.1;

*MHA* = 0.6 - 1.25 - 2.5 - 5 - 10 kDa.

The parameters characterizing the humic acid purified by the procedure described by Kim et al. (1990) were taken from Stamberg et al. (2003). Conditions ($CEu_0$, $CHA_0$, HA *Loading* and $I$) were the same as used in obtaining experimental data (Benes et al., 2004).The values of *%EuHA*, calculated for pH 4 and 6 as a function of *MHA*, are shown in Fig. 1 together with the corresponding charges $p- = n- + m-$.

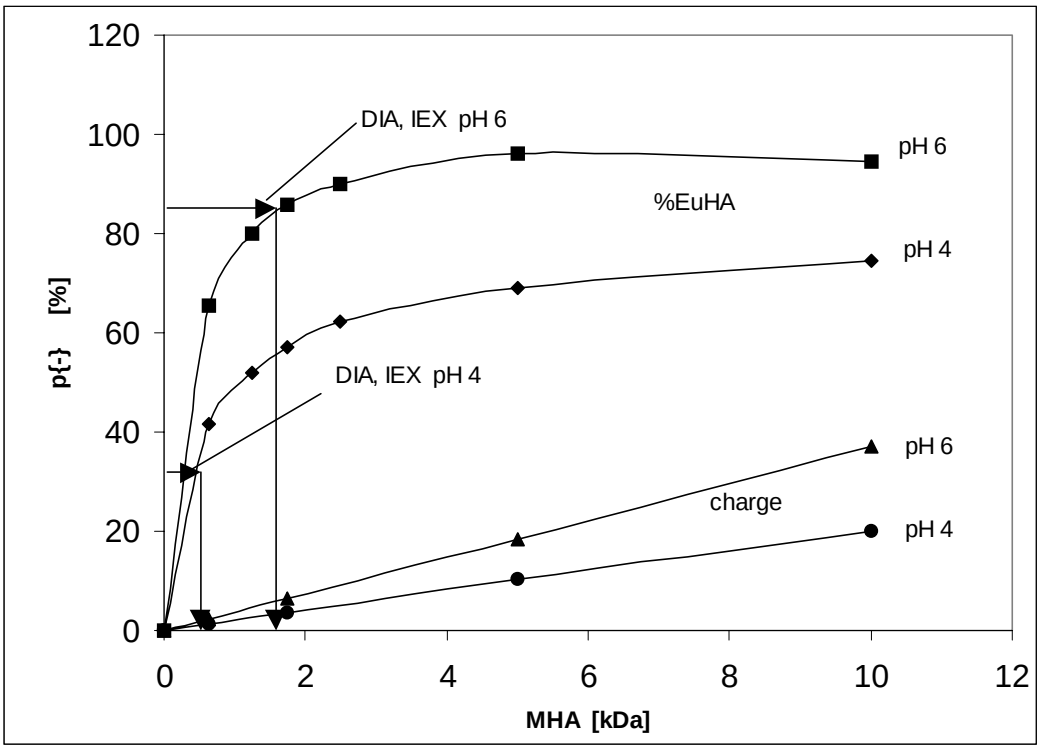


Fig. 1: a) *%EuHA* = f(*MHA*) and charge *p*{-} = f(*MHA*) calculated by MMWM model;
b) *%EuHA* determined by DIA and IEX methods

In the second step, the calculated values were compared with experimental data obtained by dialysis and ion exchange (Benes et al., 2004). *%EuHA* determined for $I$ = 0.1 and *Loading* = 50 % amounted to 35 % at pH 4 and 84.5 % at pH 6. As can be seen in Fig. 1, molecular weight derived from the comparison is approximatelly 0.6 kDa for pH 4 and 1.6 kDa for pH 6.
Furthermore, data in Fig. 1 show that linear dependences exist between the charge and *MHA*. The charge also depends on pH due to increase of dissociation of carboxylic groups with growing pH. The charge/valency $p\{-\}$ of HA molecules can attain very low values, especially at pH < 4 and when the size decreases below 1 kDa. As an example, the selected values of pH, *MHA* and $p\{-\}$ are summarized in Tab. 1.

Tab. 1: The values of the charges $p\{-\}$ of HA molecules for the given pH and *MHA*

| pH | MHA [kDa] | $p\{-\}$ | pH | *MHA* [kDa] | $p\{-\}$ |
|---|---|---|---|---|---|
| 4 | 0.5 | 1.02 | 6 | 0.5 | 1.85 |
| 4 | 1.0 | 2.04 | 6 | 1.0 | 3.71 |
| 4 | 1.5 | 3.06 | 6 | 1.5 | 5.56 |
| 4 | 2.0 | 4.08 | 6 | 2.0 | 7.42 |
| 4 | 3.0 | 6.12 | 6 | 3.0 | 11.12 |
| 4 | 5.0 | 10.20 | 6 | 5.0 | 18.54 |

The large span of charges $p\{-\}$ can have interesting implications. Depending on the ratio of valencies of the cation $M^{z+}$ and anion $HA^{p-}$, different mechanisms can be considered for the complexation, where the cation and the anion play role of either central ion or ligand. The boundary between these two possibilities can depend on pH and size of HA molecules (*MHA*), particulary at high loading of HA with the metal. If $z\{+\} > p\{-\}$, the complexation could result in formation of larger entities of $Me_pHA_z$ type consisting of several $HA^{p-}$ molecules and at least one ion $Me^{z+}$. These entities may be responsible for the changes in size distribution of EuHA molecules observed by AFFFF method (see Introduction).

## 4 Conclusions

1. Mean molecular weight (*MHA*) of Aldrich HA was assesed using MMWM model and experimental data obtained by DIA and IEX methods.
2. At first, the *%EuHA* values were calculated as a function of pH for given values of *MHA*; it was found out that *%EuHA* depends not only on pH but also on *MHA*, especially if *MHA* < 5 kDa.
3. As a result of comparison with calculated data, the values of *%EuHA* obtained with DIA and IEX methods point to the molecular weight of Aldrich HA between approx. 0.6 (for pH 4) and 1.6 (for pH 6) kDa. This interval seems to be in relatively good agreement with measurements of Wolf et al. (2004) ($M_n$ = 445 Da, $M_w$ = 626 Da, size range = 150 - 3000 [5000] Da), especially if the influence of Eu(III), resulting in sligth increase in size distribution (Buckau , 2004), is taken into account.
4. Linear dependences exist between charge, $p\{-\}$, of HA molecules and *MHA*; furthermore, the charge logically depends on pH. In the case of low values of *MHA* and/or charge, the formation

of the entities of $Me_pHA_z$ type can be expected in the course of complexation of $Me^{z+}$ with $HA^{p-}$ if $z\{+\} > p\{-\}$.

## References


Benes P., Stamberg K., Mizera J., Prochazkova S. (2004) "Comparison of Dialysis, Electrophoresis, Ion Exchange and Ultrafiltration as Methods for Analysis of Complexation of Europium with Humic Acid". In: Buckau, G. (Editor) "Humic Substances in Performance Assessment of Nuclear Waste Disposal: Actinide and Iodine Migration in the Far-Field (second progress report)", Report FZKA 6969, Research Center Karlsruhe, July 2004, p. 265.

Buckau G. (2004), Minutes of Karlsruhe HUPA Meeting.

Kim J. I., Buckau G., Li H., Duschner H., Psarros N. (1990) "Characterization of Humic and Fulvic Acids from Gorleben Groundwater", Fresenius J. Anal. Chem., 338(1990)245.

Mizera J, Dolansky J., Benes P., (2001) "Radiotracer Study of the Electrophoretic Behaviour of Eu and Its Complexes with Humic acid", Radiochimica Acta, 89(2001)529.

Stamberg K., Benes P., Mizera J., Dolansky J., Vopalka D., Chalupska K. (2003) "Modeling of Metal-Humate Complexation Based on the Mean Molecular Weight and Charge of Humic Substances: Application to Eu(III) Humate Complexes Using Ion Exchange", J. Radioanal. Nucl. Chem., 256, 2, 329.

Swift R. S. (1989), in Humic Substances II, Hayes M. H. B. (Ed.), John Wiley and Sons Ltd., New York, 1989, p. 449.

Wolf M., Szymczak W., Chanel V., Buckau G. (2004), "Molecular Size and Mass Distributions of Humic Substances Measured by AFFFF and TOF-SIMS". In: Buckau, G. (Editor) "Humic Substances in Performance Assessment of Nuclear Waste Disposal: Actinide and Iodine Migration in the Far-Field (second progress report)", Report FZKA 6969, Research Center Karlsruhe, July 2004, p. 95.

## Annex 11:

**IR (DRIFT) Spectroscopic Studies on Temperature Impact of Humic Acid**

Pashalidis I., Colocassidou C., Costa C.N., Efstathiou A.M., Buckau G.

# IR (DRIFT) spectroscopic studies on temperature impact of humic acid

Pashalidis I.[1)]*, Colocassidou C. [1)], Costa C.N. [1)], Efstathiou A.M. [1)], Buckau G. [2)]

1) University of Cyprus, P.O. Box 20537, 1678 Nicosia, Cyprus

2) Institut für Nukleare Entsorgung, Forschungszentrum Karlsruhe, P.O. Box 3640, 76021 Karlsruhe

## Abstract

The impact of temperature on the stability of the humic acid Gohy-573(HA) is studied. The studies are made both in order to add general knowledge about humic acid but also in order to provide the basis for experimental setup of studies, and judgment of published data, on the metal ion humate complexation as a function of temperature. Methods applied are IR(DRIFT) spectroscopy as a function of temperature elevation up to 200 °C, and thermogravimetric analysis (TGA). Both methods are conducted under inertgas atmosphere in order to avoid burning with air oxygen. The reversibility of changes is also studied by IR-DRIFT spectroscopy after subsequent storage at room temperature. The results of the IR(DRIFT) measurements agree with the results obtained from corresponding studies based on Temperature-Programmed Desorption (TPD) experiments by means of MS analysis. Heating of dried humic acid leads to gradual degradation of the product. From room-temperature up to 110 °C the water released corresponds to sorbed water (up 60 °C) and to structural water (60 °C to 110 °C) as well as to water produced by condensation of carboxylic acids. Above 110 °C the decomposition and autoxidation of humic acid starts resulting in the production of $CO_2$, $H_2O$ and CO. According to TGA measurements the water released up to 110 °C is about 7% of the total mass of the dried humic acid. Out of this water less than 50% corresponds to sorbed water. The total amount of $CO_2$, $H_2O$ and CO released up to 800 °C is about 90% of total mass of the dried humic acid.

*pspasch@ucy.ac.cy

## Introduction

Humic and fulvic acids consist mainly of carbon, oxygen and hydrogen. In addition small varying quantities of nitrogen and sulfur are found. Disregarding the latter, the sum formula is approximately $CO_{0.5}H$ (Buckau 2004). The thermal stability of humic acid is of interest for general understanding of the nature of humic acid. Furthermore, deduction of thermodynamic data ($\Delta H$ and $\Delta S$) requires studies over a temperature interval. In this context, response of humic acid to elevated temperature needs to be known. For these reasons, initial studies on the response of humic acid to thermal treatment are conducted. The release of water, carbon monoxide and carbon dioxide of humic acid in response to temperature elevation under inert-gas atmosphere is studied by IR(DRIFT) spectroscopy. Furthermore, the change in mass as a function of temperature is studies by thermogravimetric measurements.

## Experimental

The humic acid Gohy-573(HA) is used. The groundwater is isolated from 140 m depth in the Gorleben aquifer system. The humic acid originates from microbiologically mediated conversion of Miocene brown coal sand under simultaneous reduction of sulfate dissolving from the underlying Gorleben salt dome. Details on origin, preparation and characteristic properties of this humic acid can be found in (Artinger et al. 2000, Buckau et al. 2000a, Buckau et al. 2000b, Kim et al. 1990).

IR spectroscopic analysis of water and carbon dioxide released from humic acid under temperature elevation up to 200 °C under inert gas was performed by Diffuse Reflectance Infrared Fourier Transform Spectroscopy (DRIFTS). The DRIFTS spectra were recorded on a Perkin-Elmer GX FTIR spectrophotometer at a resolution of 1 $cm^{-1}$ and using a high-temperature/high-pressure temperature controllable DRIFTS cell (Spectra Tech) equipped with ZnSe IR windows. About 30 mg of humic acid sample in powder form was used for each experiment. The experiments were carried out under pure argon atmosphere and the total flow rate was kept constant at 50 scc/min. Spectra collection was performed after thermal pre-treatment at the appropriate temperature of the experiment to be followed for 30 min. For FTIR single-beam background subtraction, the spectrum of the background was taken in Ar flow. FTIR spectra were collected at the rate of 1 scan/s at 1 $cm^{-1}$ resolution in the 800-3000 $cm^{-1}$ range and the averaged spectrum was then recorded. All spectra were analyzed by using the instrument's Spectrum for Windows® software provided.

TGA measurements were performed under inertgas atmosphere ($N_2$) using a Shimadzu Thermogravimetric Analyzer (TGA 50). About 20 mg of humic acid sample in powder form was used for each experiment and the temperature gradient was 5 °C/min. Three different types of TGA measurements have been performed: a) temperature increase up to 800 °C with a constant gradient of 5 °C/min, b) stepwise increase of the temperature from 80 to 130 °C and thermal treatment of the sample for 0.5 h at each temperature, and c) temperature increase up to 110 °C and thermal treatment of the sample for 5h at this temperature

## Results and discussion

In Fig. 1, IR-DRIFT spectra of the of Gohy-573(HA) are shown as a function of temperature elevation up to 240 °C. The spectra in Fig.1 can be distinguished into three groups, namely the first which includes the spectrum at 25 °C, the second including the spectrum at 100 and 110 °C and the last group consisting of the spectra from 120 to 200 °C.

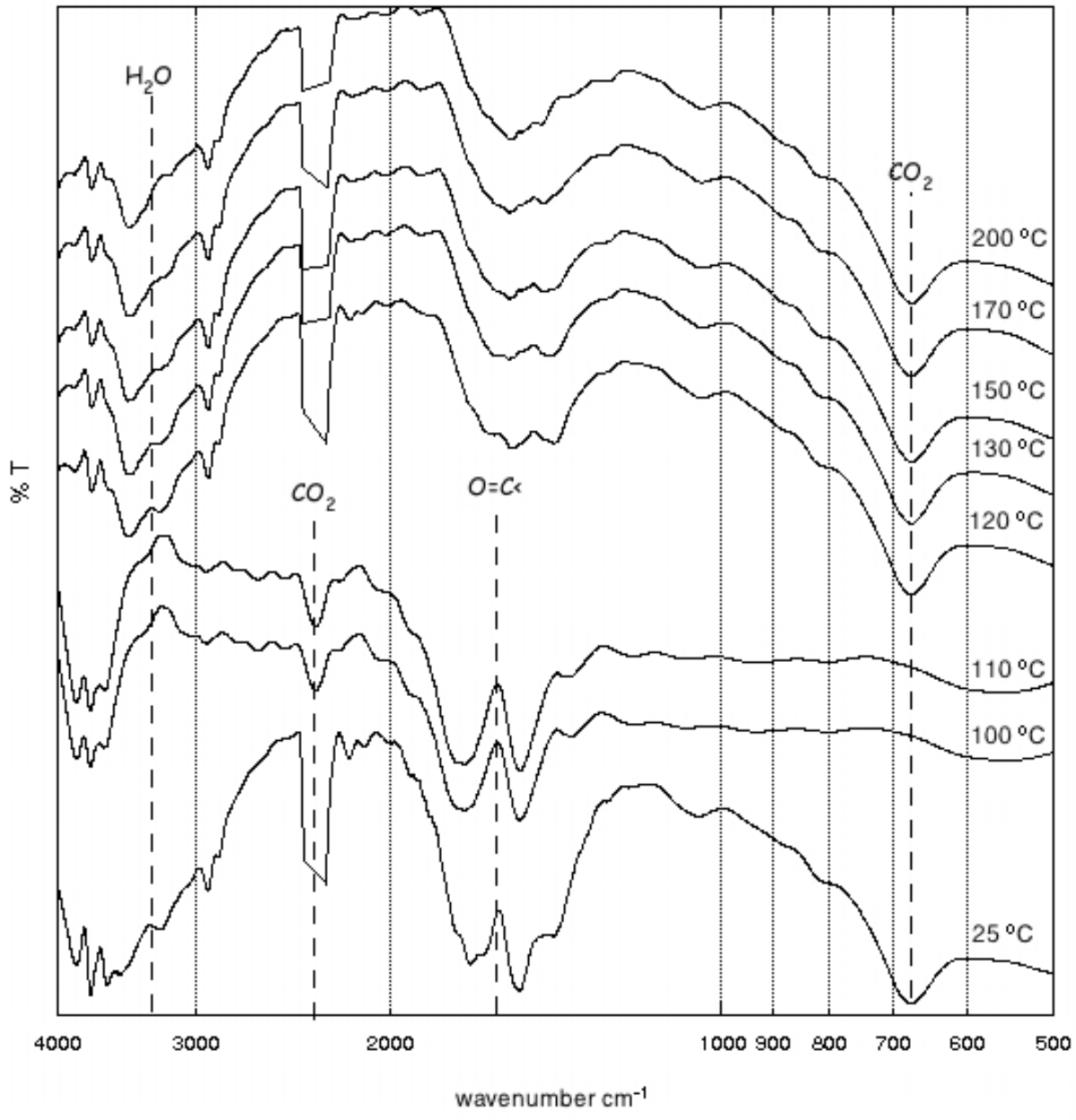


Fig. 1: Release of water and carbon dioxide monitored by IR-DRIFT spectrometry upon thermal treatment of Gohy-573(HA) under inertgas atmosphere.

The spectrum at 25 °C shows the characteristic absorption bands of water ($H_2O$) at 3455 $cm^{-1}$, of carboxy groups (O=C<) from 1670 to 1500 $cm^{-1}$ and carbon dioxide ($CO_{2(g)}$) at 2341 and 670 $cm^{-1}$. In the spectra at 100 and 110 °C the bands for water and $CO_{2(g)}$ are significantly

diminished indicating that carbon dioxide and water molecules are removed from the sample because of temperature elevation . The carbon dioxide, which couldn't be observed by the corresponding MS measurements, is most probably carbon dioxide adsorbed at the supporting material (silica) that was used in order to elevate the level of humic acid in the DRIFT cell. The removed water molecules correspond not only to adsorbed water but also to structural water as well as to water produced by the condensation of carboxylic acids, since the adsorption bands from 1670 to 1500 $cm^{-1}$, are reshaped to a double peak, which is characteristic for carboxylic acid anhydrites.

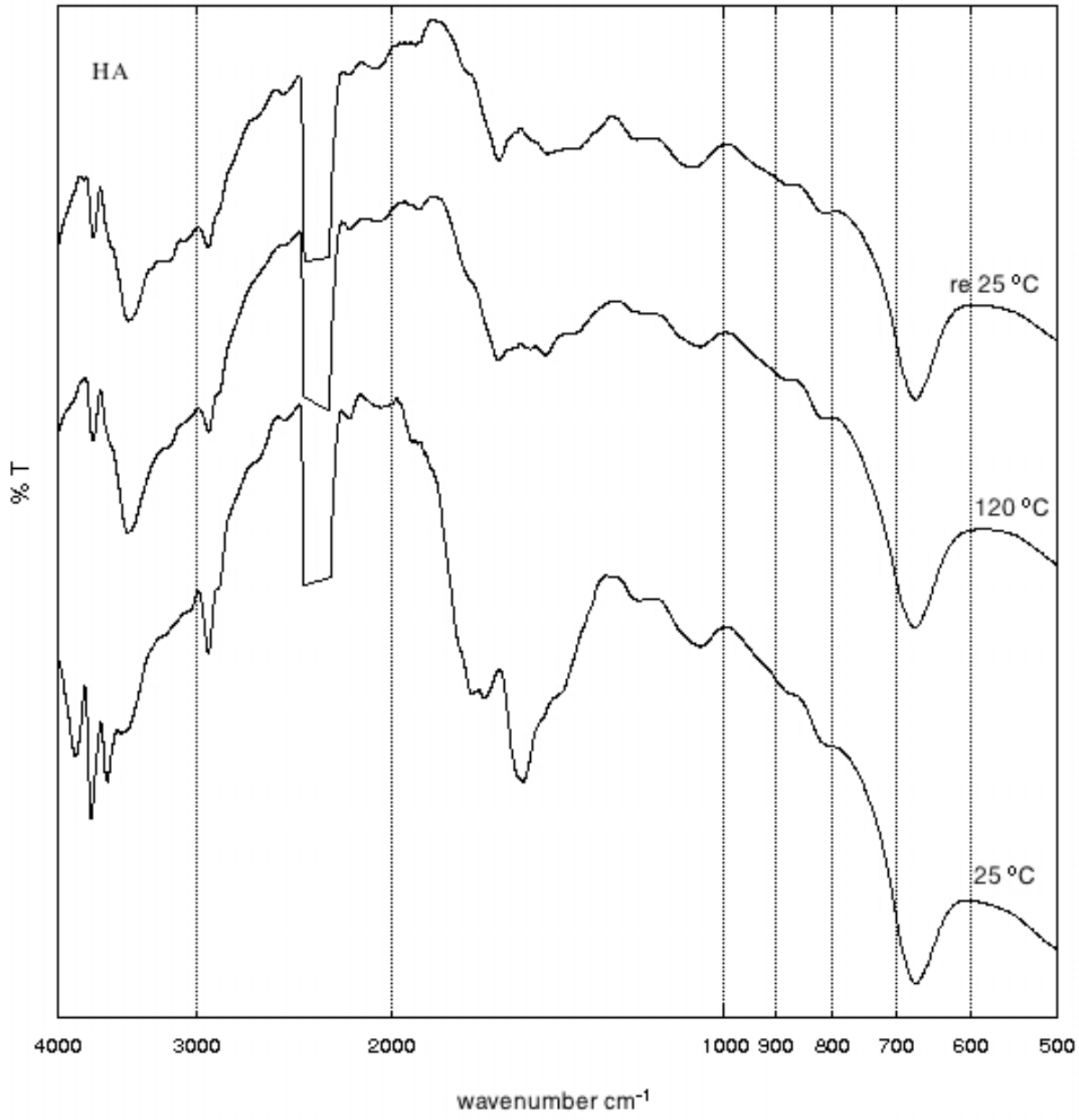


Fig. 2: IR-DRIFT spectra of Gohy-573(HA) under inertgas atmosphere prior, during and after thermal treatment.

According to the spectra of the third group temperature elevation above 110 °C results in production of water and carbon dioxide molecules which are produced by the decomposition of the carboxylic groups and at higher temperatures the auto-oxidation of the humic acid. The corresponding spectra include the characteristic bands for both, water and carbon dioxide molecules at 3455 and 2341 $cm^{-1}$ and 670 $cm^{-1}$, respectively. Moreover, the adsorption bands from 1670 to 1500 $cm^{-1}$ diminish gradually with increasing temperature, indicating on the decomposition of the carboxylic groups. The IR DRIFTS data are in agreement with the corresponding MS data obtained by previous experiments and clearly show that the thermal decomposition of humic acid is a stepwise process starting with dehydration, followed by decarboxylation and ending up with auto-oxidation reactions.

Figure 2 shows the spectra of the same humic acid prior thermal treatment at 25 °C, during thermal treatment at 120 °C and after keeping the thermally terated sample for 1 h under normal atmospheric conditions. The similarities between the two last spectra and their differences from the spectrum of the non-treated sample indicate that the decarboxylation process of the humic acid is an irreversible process.

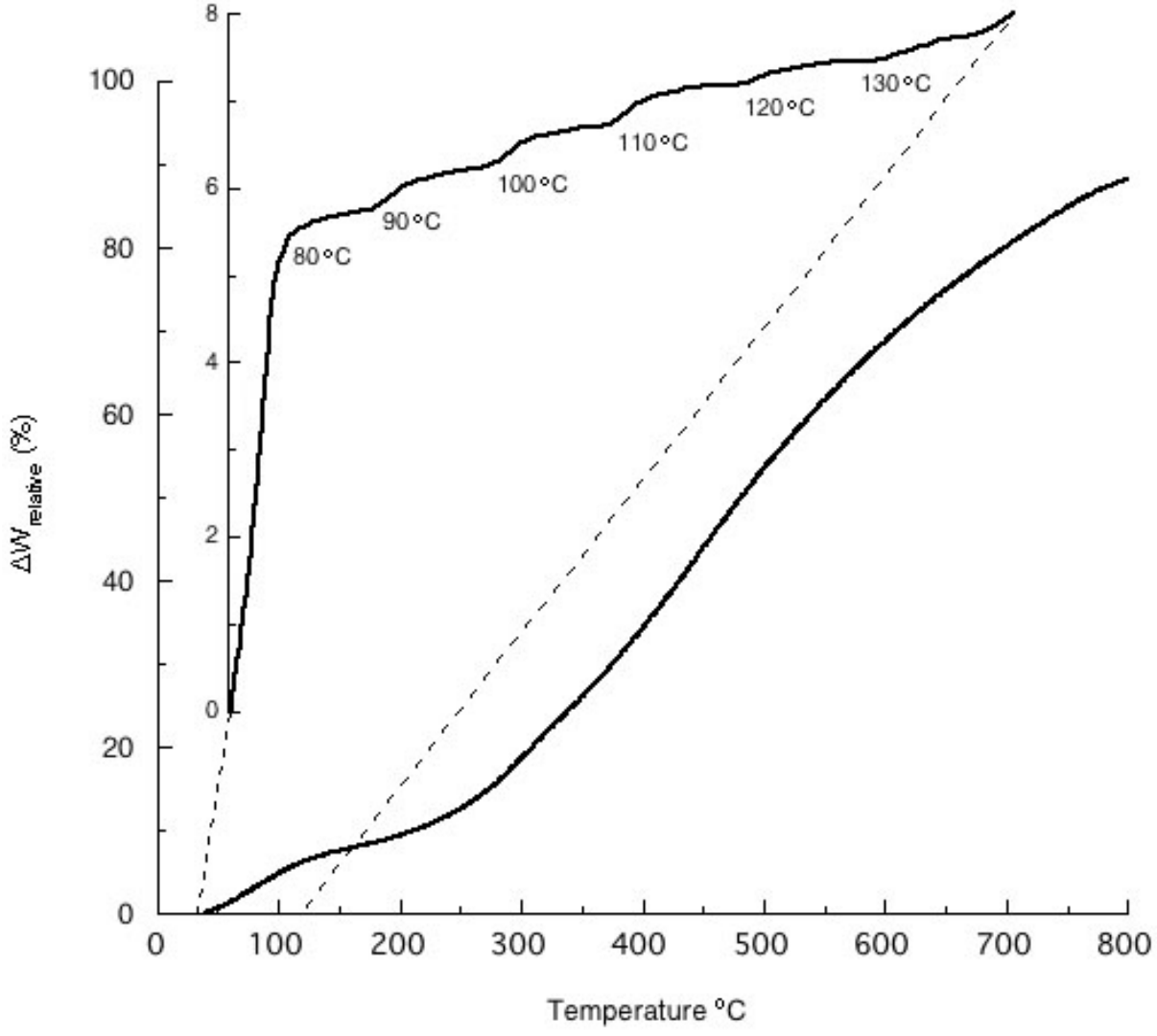


Fig. 3: Thermogravimetric analysis of Gohy-573(HA) under inertgas atmosphere.

In order to quantify the amounts of water, carbon dioxide and carbon monoxide released TGA measurements of humic acid samples (about 20 mg) have been performed under pure nitrogen atmosphere and variable thermal treatment times. Fig.3 shows two thermogravimetric lines corresponding one to a measurement carried out from 25 to 800 °C with a temperature gradient of 5 °C /min and another (inserted line) to a measurement between 25 to 130 °C with a temperature gradient of 5 °C /min and thermal treatment of the sample for 1 h at each temperature level. According to Fig. 3 the weight loss of the sample up to 110 °C, that corresponds to water release is about 7%. Thermal treatment of the sample under inert gas atmosphere up to 800 °C results in a weight loss of about 80% and corresponds to water, carbon dioxide and carbon oxide produced by the decomposition and auto-oxidation of the humic acid.

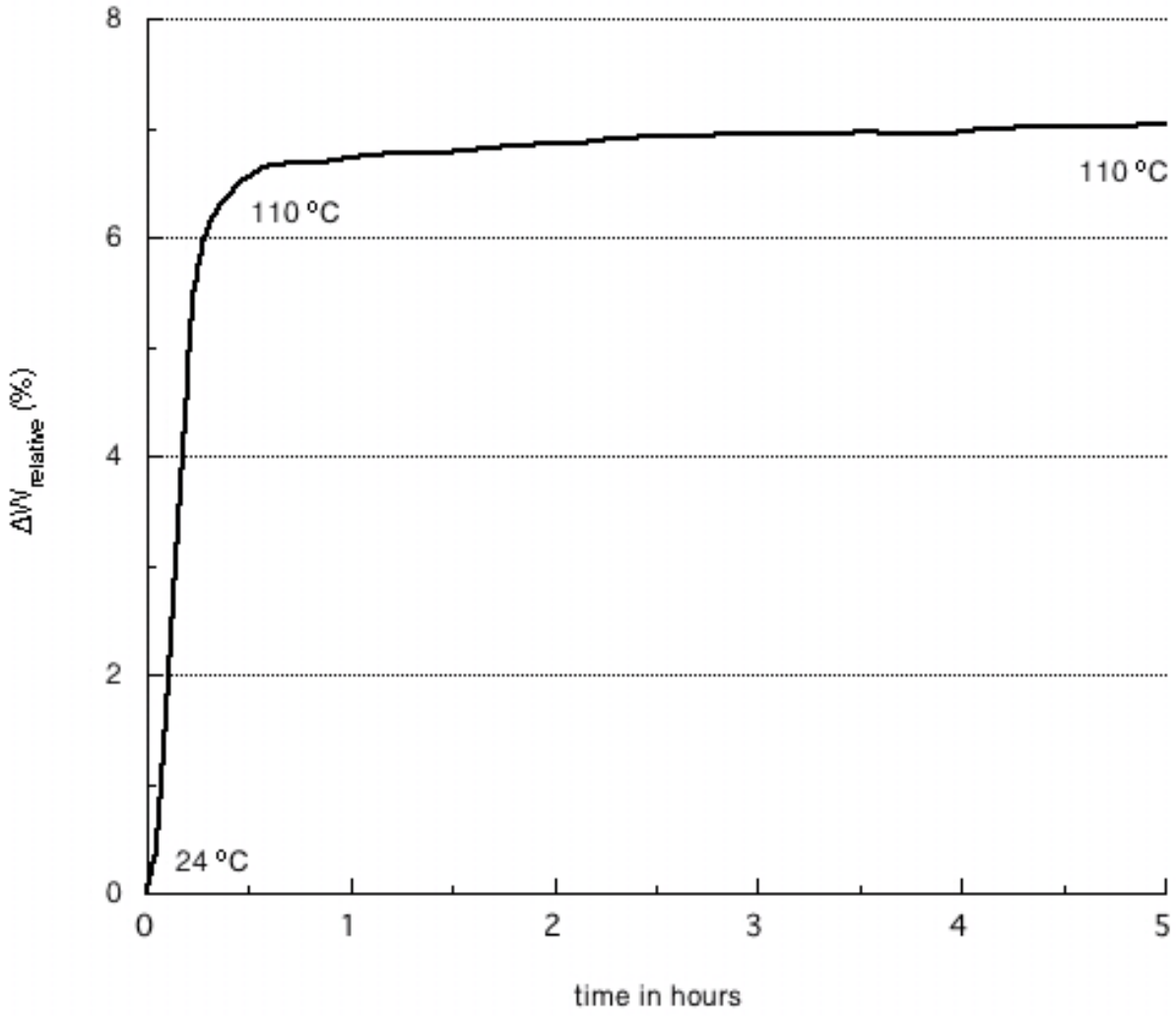


Fig. 4: Thermogravimetric analysis of Gohy-573(HA) at constant temperature and under inertgas atmosphere.

Fig. 4 shows the thermogravimetric graph obtained by thermal treatment of the sample at 110 °C which according to the MS measurements is the upper limit for the removal of adsorbed and structural water without further decomposition of the sample (e.g. decarboxylation).

According to Fig. 4, even after 5 h thermal treatment at 110 °C the relative amount of water released is about 7 % of sample mass.

## Conclusions

The results obtained from the FTIR-DRIFTS studies at various temperatures up to 200 °C are in good agreement with the corresponding results obtained by TPD-MS studies and clearly indicate that up to 110 °C only water is released from thermally treated humic acid. This water corresponds to both physically adsorbed water and structural water or water produced by condensation processes taking place among carboxylic and phenolic groups. The amount of physically adsorbed water on dried humic acid is estimated to be about 3%.

Above 110 °C starts the decomposition of humic acid. Under inert gas conditions the first step is the decarboxylation and the second step the auto-oxidation process, which results apart from $CO_2$ also in the production of CO and $H_2O$.

Qualitative evaluation based on TGA measurements results in about 7% weight loss corresponding to water released up to 110 °C and almost 70% weight loss up to 800 °C corresponding to the decarboxylation and autoxidation products.

## References


Artinger R., Buckau G., Geyer S., Wolf M., Kim J.I., Fritz P. "Characterization of Groundwater Humic Substances: Influence of Sedimentary Organic Carbon", *Applied Geochemistry*, **15/1**, 2000, 97-116.

Buckau G., Artinger R., Fritz P., Geyer S., Kim J.I., Wolf M. (2000a) "Origin and Mobility of Humic Colloids in the Gorleben Aquifer System", *Applied Geochemistry*, **15/2**, 171-9.

Buckau G., Artinger R., Geyer S., Wolf M., Kim J.I., Fritz P. (2000b) "Groundwater in-situ Generation of Aquatic Humic and Fulvic Acids and the Mineralization of Sedimentary Organic Carbon", *Applied Geochemistry*, 15/6, 819-32.

Buckau G. (2004) "Approach for Physico-Chemical Interpretation of An(III) and An(VI) Humate Complexation.", Annex 3, same report.

Kim J.I., Buckau G., Li G.H., Duschner H., Psarros N. (1990) "Characterization of Humic and Fulvic Acids from Gorleben Groundwater", Fresenius J. Anal. Chem., **338**, 245.

## Annex 12:

**Photodynamic Processes of Cm(III) with different Fulvic Acids**

Claret F., Rabung Th., Schäfer Th., Buckau G.

# Photodynamic Processes of Cm(III) with different Fulvic Acids

Claret F., Rabung Th., Schäfer Th., Buckau G.

Institut für Nukleare Entsorgung, Forschungszentrum Karlsruhe, P.O. Box 3640, 76021 Karlsruhe

## Summary

Photodynamic processes of the $Cm^{3+}$ ion complexed with four different fulvic acids are discussed. The four different fulvic acids of different origins have different optical properties, reflected in the fluorescence intensity of the complexed Cm(III) fulvate. The fluorescence intensity of fulvate complexed curium ion is enhanced relative to the non-complexed aqueous $Cm^{3+}$ ion. This enhanced fluorescence intensity is shown to be related to the fluorescence intensities of the different fulvic acids. Contrary to this, the fluorescence intensity from direct excitation of the fulvate complexed Cm(III) show no significant trend with the fluorescence properties of the fulvic acids. The study is of somewhat preliminary nature because of the small number of substances used and the complexity of the involved photodynamic processes. In order to delineate individual process contributions, organic model ligands will need to be studied.

## Introduction

Time-resolved laser fluorescence spectroscopy provides different information in relation to photodynamic processes. Excitation (related to the population of fluorescent states), emission (release of energy in the form of light from fluorescent states) and the time function of the emission is the directly accessible information by this analytical method. Indirect information is obtained also over quenching, i.e. entropy driven loss of energy at lower energies than observed as light emission. The processes related to complexes of fluorescent ions with fluorescent ligands is schematically described in Fig. 1, on the example of fulvate complexed Cm(III). In addition to excitation, emission and quenching, energy transfer takes place between the two fluorescent centers, namely the complexed Cm(III) ion and the fulvic acid ligand. Applying time resolved fluorescence spectroscopy with time resolution in the microsecond range, direct emission information is only obtained on the emission from Cm(III). As a consequence, individual processes cannot be resolved. This leads to a situation where for example the coordination of the complexed ion cannot be directly determined. In Annex 1, the replacement of the water solvent by heavy water ($D_2O$) results in two separate time functions of the fluorescence decay mainly differing with respect to the quench impact of Cm(III) coordinated water. This difference is used for quantification of the number of water quenchers on the fulvate complexed Cm(III) ion.

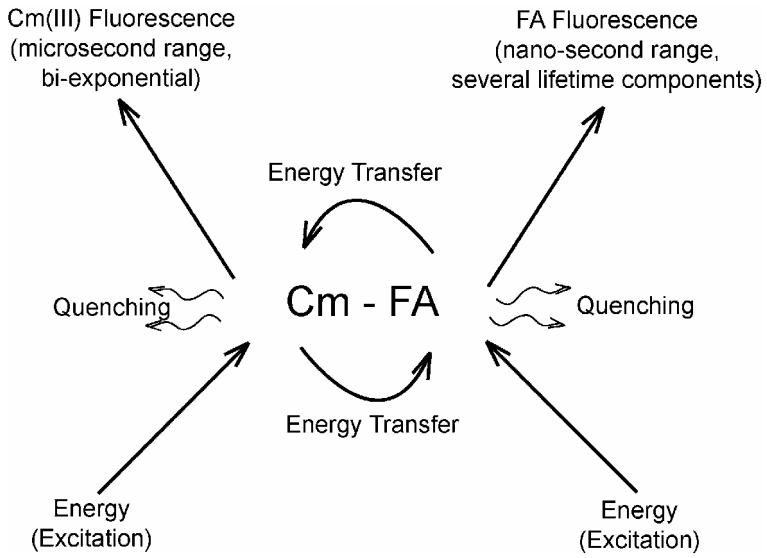


Fig. 1: Photodynamic processes of Cm(III) fulvic acid complexes.

In the present study another issue is studied, namely the impact of photodynamic properties of the organic fulvate ligand on the Cm(III) fluorescence. For this purpose, four different fulvic acids are used that are isolated from groundwater of the Gorleben aquifer system (see Table 1 and Artinger et al. 2000).

Table 1: Origin of fulvic acids used in the study, including the groundwater that the fulvic acids are isolated from (for details, see Artinger et al. 2000).

| | Origin of groundwater | Depth (m) | Predominant origin of fulvic acid |
|---|---|---|---|
| Gohy-411(FA) | Young recharge | 17-20 | Soil zone |
| Gohy-421(FA) | Young recharge | 10-13 | Soil zone |
| Gohy-711(FA) | Young recharge | 6-9 | Soil zone |
| Gohy-573(FA) | Old mixed water | 134-137 | Microbial lignite conversion |

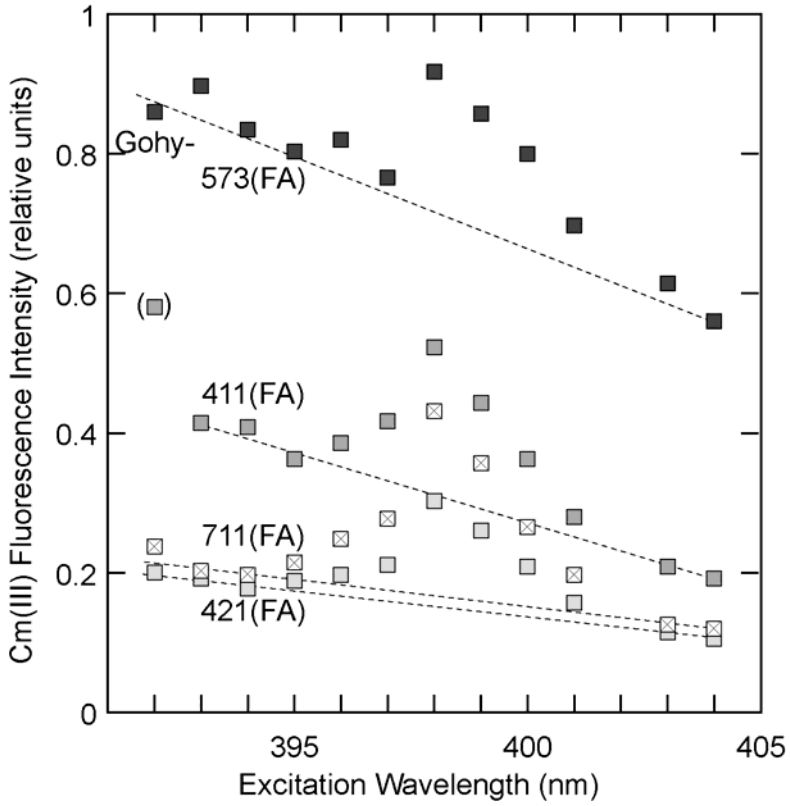


Fig. 2: Cm(III) fluorescence intensity as a function of the excitation wavelength.

## Results and discussion

Fig. 2 shows the fluorescence intensity (emission band with maximum around 600 nm) of Cm(III) fulvate complexes at pH 6.0 in 0.1 $NaClO_4$ as a function of the excitation wavelength. These excitation spectra have some common characteristics between the different fulvic acids, but also some distinct differences. All excitation spectra can be described as increasing fluorescence intensity with increasing excitation energy (decreasing wavelength) in combination with a separate Cm(III) excitation peak. The interpretation is that the separate Cm(III) excitation peak is that of Cm(III) itself, with a slight redshift resulting from fulvate complexation. The dotted line in Fig. 2 indicates indirect excitation via energy transfer from the fulvate

ligand. Both these observations show that the two fluorescent centers (Cm(III) and fulvic acid) are coupled. The coupling results in energy shuffling between these two centers, however, the individual identity of the Cm(III) electronic system remains clearly visible.

The next question arising is which electronic states of fulvic acid results in the energy transfer to the complexed Cm(III) ion. The Cm(III) fluorescent state is a multiplet, indicating the importance of phosphorescent states of fulvic acid. Such states, however, are expected to be populated via singlet fluorescent states of the fulvic acid. In this case the Cm(III) fluorescence originating from indirect excitation, i.e. via energy transfer from the fulvic acid ligand, should follow the principle trend of the fulvic acid excitation spectrum. As seen in Fig. 3, this is the case. The respective contributions to excitation of the complexed Cm(III) ion from fluorescent and phosphorescent states of fulvic acid will depend on their population densities and energy transition probabilities.

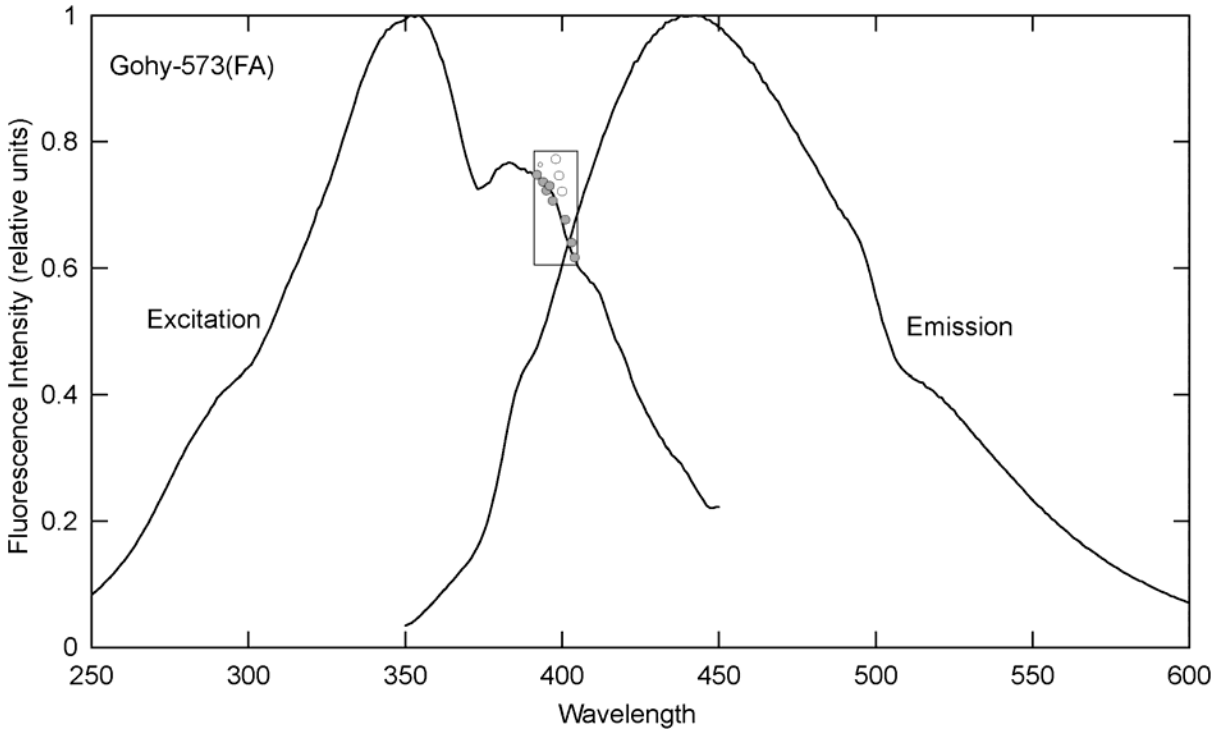


Fig. 3: Comparison of excitation and emission intensities of the fulvic acid Gohy-573(FA) with the Cm(III) fluorescence intensity of that fulvate complex. Data points from Figure 2 with open circles including fluorescence from direct Cm(III) excitation.

From Fig. 2, the contributions from direct Cm(III) excitation and its excitation via energy transfer are determined. They are quantified as follows: The contribution up to the dotted line is allocated to indirect excitation (energy transfer from the fulvate ligand) and the contribution from the dotted line to the total fluorescence intensity is allocated to direct excitation of the complexed Cm(III) ion. The results for 398 and 404 nm excitation wavelengths are shown in Fig. 4. For 404 nm excitation wavelength there is no significant contribution from direct excitation. At 398 nm, both direct and indirect excitations contribute significantly. As shown in Fig. 3, the Cm(III) fluorescence intensity from indirect excitation should be related to the fluorescence intensity of the fulvic acid itself. Therefore, the results in Fig. 4 are shown as a function of the fulvic acid fluorescence intensity. The direct excitation of Cm(III) does not

show a dependency of the fulvic acid fluorescence intensity. Contrary to this, this seems to be the case for the indirect excitation.

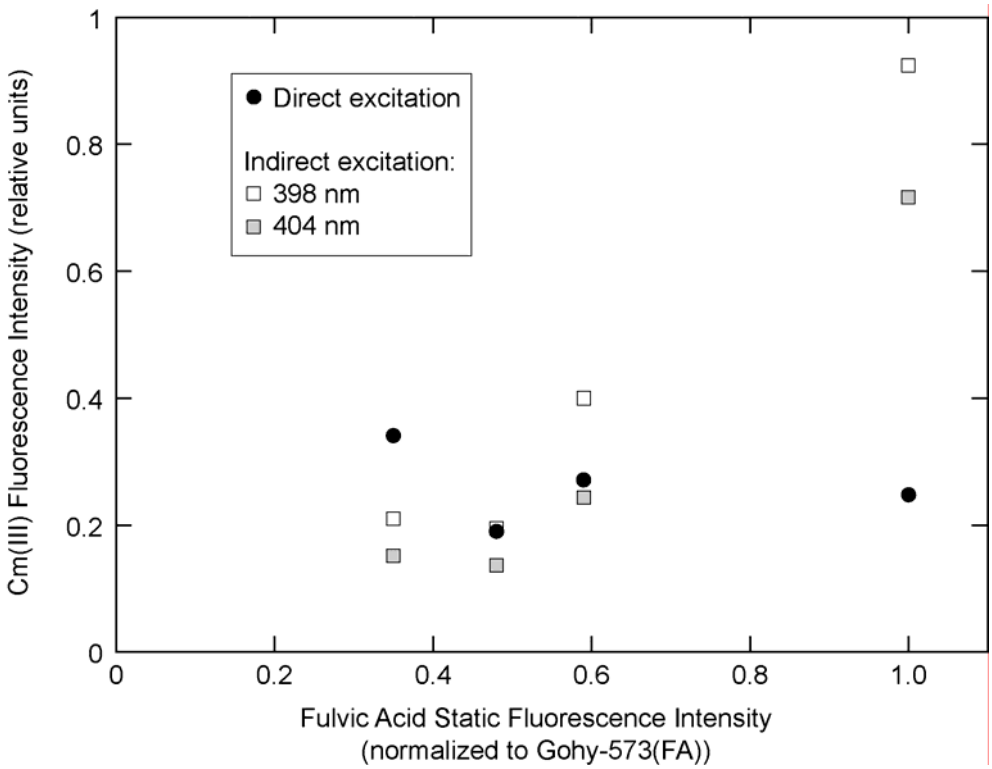


Fig. 4: Cm(III) fluorescence intensity evaluated as direct and indirect excitation for different excitation wavelengths(cf. text).

## Conclusions

This study shows that the fluorescence intensity of fulvate complexed Cm(III) is strongly related to the fluorescence properties of fulvic acid itself. This shows that the energy transfer to the fulvate complexed Cm(III) ion proceeds via population of fluorescent states of fulvic acid. The results also show that despite coupling of the electronic systems of the reacting components, the individual character of the Cm(III) electronic system is retained to a large extent. The present results are of preliminary nature. Reasons are that the number of accessible fulvic acids with significantly different properties is relatively low and scatter of data is considerable. More important, the fluorescence intensity of fulvic acid referred to is that of non-complexed fulvic acid and is measured at low energy density, i.e. presumable far away from saturation of fluorescent sites. Contrary to this, the Cm(III) fluorescence measured is exclusively from the small fraction of complexed fulvic acid molecules, and saturation is approached when applying pulsed laser excitation (Morgenstern 1997).

Natural humic and fulvic acids of different origins show a spectrum of differences in composition and properties. A single indicator is not sufficient for an exhaustive description of individual differences. Therefore, in order to delineate different contributors to the overall photodynamic behavior, organic model ligands will need to be studied. Because of the complexity of the system, involvement of several research groups will be required.

## References

Artinger R., Buckau G., Geyer S., Wolf M., Kim J.I., Fritz P. (2000) "Characterization of Groundwater Humic Substances: Influence of Sedimentary Organic Carbon", *Applied Geochemistry*, **15/1**, 97-116.

Morgenstern A. (1997) “Humat- und Phosphatkomplexierung von Actinidionen im Grundwasser-relevanten pH-Bereich”, PhD Thesis, Technical University of Munich.